Branched-Chain Amino Acid Catabolism: Regulation and Effect on Insulin Resistance

Gagandeep Mann

A DISSERTATION SUBMITTED TO THE FACULTY OF GRADUATE STUDIES IN PARTIAL FULFILLMENT OF THE REQUIREMENTS FOR THE DEGREE OF DOCTOR OF PHILOSOPHY

GRADUATE PROGAM IN KINESIOLOGY AND HEALTH SCIENCE YORK UNIVERSITY, TORONTO, ONTARIO, CANADA

© Gagandeep Mann 2024

Abstract

Insulin resistance is the reduced responsiveness of a target tissue to insulin. Insulin resistance is an underlying cause of Type 2 diabetes mellitus (T2DM) and cardiovascular diseases, two debilitating diseases. Therefore, targeting insulin resistance can help prevent the development of T2DM and cardiovascular diseases.

Dietary protein, and in particular branched-chain amino acids (BCAAs; leucine, valine and isoleucine) stimulate muscle protein synthesis, and regulate body weight and glucose homeostasis. However, despite these benefits, circulating levels of BCAAs and BCAA metabolites, branched-chain α-ketoacids (BCKAs) are upregulated in insulin-resistant states like T2DM. This raises the question if upregulated levels of BCAAs and BCKAs cause insulin resistance or are a symptom of insulin resistance. Numerous studies have also shown how insulin resistant states can regulate the BCAA catabolic pathway and the enzymes involved, and how targeting this pathway can provide benefits in regards to insulin resistance and its sequalae. Thus, the purpose of this dissertation is to examine the link between BCAAs and their metabolism, and insulin resistance.

Previous *in vitro* studies have showed that depletion of branched-chain ketoacid dehydrogenase (BCKD), the enzyme responsible for the catabolism of BCKAs, suppressed insulin-stimulated glucose uptake in L6 myotubes and the metabolite of leucine, ketoisocaproic acid (KIC) worsens it. Thus, I demonstrated that interventions that increased BCKD activity improved insulin sensitivity and attenuated the suppressive effect of KIC on insulin sensitivity in L6 myotubes.

We have previously shown that KIC reduces insulin-stimulated glucose transport in muscle cells. However, contributions from other tissues aside from skeletal muscle in BCAA

metabolism emphasize the importance of studying the effect of KIC gavage *in vivo* as well. Whereas KIC alters insulin signaling in the liver, it did not affect whole-body insulin tolerance.

Finally, since BCAA catabolism is implicated in many chronic conditions like insulin resistance, and age is a major risk factor in insulin resistance, we assessed how aging affects BCAA catabolism in both sexes. There was an increase in plasma BCAAs of old male mice, but changes in BCAA levels in plasma/tissues were not largely consistent with any changes in metabolic enzyme abundance/activity and did not correlate with changes in insulin sensitivity with sex or aging. Taken together, this thesis shows that although KIC suppresses glucose transport *in vitro* and its effect is attenuated by increasing BCAA oxidation, it does not affect insulin sensitivity *in vivo* likely due to contributions of the liver to catabolize KIC. Also, increases in plasma BCAAs seen in older male mice does not correlate with increased insulin resistance, suggesting that greater BCAAs in plasma may only be present in disease states. Together these studies suggest that altered BCAA levels do not cause insulin resistance but are a result of insulin resistance.

Acknowledgments

Thank you first and foremost to Dr. Adegoke, without your guidance and help throughout this journey, this would not have been possible.

Thank you to my committee members Dr. Riddell, Dr. Cheng and Dr. Tsushima for their support as well.

Next, thank you to my lab mates for all the help. Special shoutout to Stephen, we started this PhD together and now we're ending it in the same week. I will always appreciate all the help, but the laughs and life talks as well, we really built a great friendship along the way.

Thank you to all my other lab mates, Armita, Miriam, Termeh, Glory, Lilia, and Logan. Thank you for the help, and the countless laughs.

Finally thank you to my parents, siblings and friends for their support throughout this process.

Table of Contents:

List of Tables

Chapter 4

Chapter 5

Chapter 6

List of Figures

Chapter 2

Chapter 4

Chapter 5

Chapter 6

List of Supplementary Figures

List of Abbreviations

3-hydroxyisobutyrate 3-HIB

4E-BP1 eukaryotic translational initiation factor 4E-binding protein 1

Akt protein kinase B

α-KG alpha ketoglutarate

AMPK AMP activated protein kinase

aPKC atypical protein kinase C

AS160 Akt substrate of 160 kDa

BAIBA beta-aminoiso-butyric acid

BCAA branched chain amino acid

BCAT branched-chain aminotransferase

BCAT1 cytosolic BCAT

BCAT2 mitochondrial BCAT

BCKA branched chain α-keto acid

BCKD branched chain α-keto acid dehydrogenase complex

BDK branched chain α-keto acid dehydrogenase kinase

DAG diacylglycerol

EDL extensor digitorum longus

ERK extracellular signal-regulated kinase

EIF Eukaryotic initiation factor

FFA free fatty acids

GATOR1/2 GAP activity Towards Rags Complex 1 (GATOR1)

GLUT4 glucose transporter type 4

HFD high fat diet

IL-6 interleukin-6

IRS Insulin receptor substrate

JNK c-jun N-terminal kinase

KIC alpha-ketoisocaproic acid

KIV alpha-ketoisovaleric acid

KMV alpha-keto-beta-methylvaleric

mTORC1 mammalian/mechanistic target of rapamycin complex 1

mTORC2 mammalian/mechanistic target of rapamycin complex 2

Nox2 NADPH oxidase 2

PDK1 3-phosphoinositide-dependent protein kinase 1

PGC-1α peroxisome proliferator-activated receptor gamma coactivator 1-alpha

PH pleckstrin homology

PI3K phosphoinositide 3-kinase

PIP2 phosphatidylinositol 4,5-bisphosphate

PIP3 phosphatidylinositol (3,4,5)-triphosphate

PKC protein kinase C

PPA2A protein phosphatase 2A

Pp2Cm protein phosphatase 2Cm

PRAS40 proline-rich Akt substrate 40 kDa

PKC protein kinase C

PTB phosphotyrosine binding

PTEN phosphatase and tensin homolog

PTP1B protein tyrosine phosphatase 1B

ROS reactive oxygen species

S6K1 ribosomal protein S6 kinase-1

Ser serine

T2DM type 2 diabetes mellitus

TBC1D1 TBC1 domain family 1

TBC1D4 TBC1 domain family 4

Thr threonine

TNF-α tumor necrosis factor alpha

TSC1/2 tuberous sclerosis complex protein 1/2

Chapter 1: Introduction

Insulin resistance is an underlying cause of type 2 diabetes mellitus (T2DM) (1) and cardiovascular diseases (2). This has resulted in a growing importance in the study of insulin resistance and how it is implicated in chronic disease. Insulin resistance is the suppressed response to insulin by a target tissue (3). Genetics can play a role in the onset of insulin resistance, but lifestyle choices can also reduce the risk of developing insulin resistance (4). A sedentary lifestyle is associated with an increased risk of insulin resistance (5,6). The increasing prevalence of insulin resistance is also linked to the rise in obesity rates, as obese individuals experience insulin resistance (6). The overconsumption of energy is also major risk factor in obesity induced insulin resistance (7).

Calorie restriction is a strategy applied for weight loss, but this can lead to loss of muscle mass. High protein diets or branched-chain amino acid (BCAAs; leucine, valine, isoleucine) supplements are recommended to counter these losses (8,9). Dietary protein, and in particular, BCAAs stimulate muscle protein synthesis, and regulate body weight and glucose homeostasis (10). However, despite these benefits, increased circulating levels of BCAAs and BCAA metabolites, branched-chain α-ketoacids (BCKAs; alpha-ketoisocaproic acid (KIC), alpha-keto-beta methylvaleric acid (KMV), and alpha-ketoisovaleric acid (KIV)) are seen in insulin-resistant states like T2DM (11–13). Thus, although BCAAs may protect against muscle mass loss, it might contribute to reduced insulin sensitivity. This raises the question if upregulated BCAA and BCKA levels seen in insulin resistance are correlative or causative.

Many studies have shown that BCAAs can act as anabolic signals like insulin. BCAAs activate mammalian/mechanistic target of rapamycin complex 1 (mTORC1) and p70 ribosomal protein S6 kinase-1 (S6K1) leading to increased protein synthesis. Increased activation of

mTORC1/S6K1 leads to the phosphorylation of inhibitory serine residues of the insulin receptor substrate-1 (IRS-1) by S6K1, and thus hindering downstream insulin signaling (14,15).

We have previously shown that leucine (16) and KIC (16,17) suppressed insulin-stimulated glucose uptake in L6 myotubes, along with the activation of the S6K1-IRS-1 mechanism. We have also shown that leucine gavage in rats worsened insulin tolerance, and this is seen with a consistent increase in S6K1 phosphorylation (18). The effect of BCAAs/BCKAs can also be attributed to the muscle fiber type, as BCAAs did not phosphorylate mTOR (Ser2448) in the soleus but did in the extensor digitorum longus (EDL) muscle (19). However, some studies have shown improved insulin sensitivity with leucine supplementation *in vivo* (20–22).

This discrepancy of BCAA supplementation on insulin sensitivity and insulin signaling suggests that perhaps the increase in BCAAs during insulin resistance might be a product of altered BCAA metabolism. One study shows a reduction in branched-chain aminotransferase 2 (BCAT2) mRNA expression, the enzyme responsible for the catabolism of BCAAs into BCKAs, in patients with T2DM. That study also showed reduction in the beta subunit of branched-chain ketoacid dehydrogenase (BCKD) mRNA expression, the enzyme responsible for the irreversible oxidation of BCKAs into their acyl-CoA derivatives (23), in patients with T2DM. In our previous work, we showed that depletion of BCKD in L6 myotubes leads to reduced insulin sensitivity in starved conditions (17), suggesting a connection between skeletal muscle BCAA catabolism and insulin sensitivity.

Altered BCAA metabolism is implicated in many human diseases like diabetes (23,24), cardiovascular disease (25,26), chronic kidney disease (27,28), liver disease (29,30) and cancer (31–33). Age is an important risk factor (34–37) for these diseases. However, there are no studies

that have investigated BCAAs and their metabolism in aging. Interestingly, aged men exhibit significantly lower circulating BCAA levels (38–40). This complicates the relationship between BCAAs and their metabolism, and insulin resistance, as insulin resistance is more prevalent in older individuals (41), and BCAAs are upregulated in insulin resistance (12,13). Also, sex hormone estrogen inhibits the BCKD complex by activating branched-chain ketoacid dehydrogenase kinase (BDK), a negative regulator of BCKD, decreasing BCAA catabolism (42,43). Males have greater leucine oxidation compared to women following endurance exercise (44). This emphasizes the importance of studying BCAA and their metabolism in two underrepresented groups (females and old populations), as this could have major implications in understanding disease development and potential treatment, as most intervention studies target young male animals.

Here we aim to answer, firstly, does depleting/inhibiting BDK improve insulin sensitivity, and can it attenuate BCAA/BCKA induced suppression of insulin-stimulated glucose uptake in L6 myotubes. Also, we will analyze how mTORC1 signaling is implicated in the link between BCAA catabolism and insulin sensitivity. Secondly, what is the effect of KIC gavage on whole-body insulin sensitivity and insulin signaling in various tissues, and if different muscle fiber types respond differently to KIC gavage. Lastly, what is the effect of aging and sex on BCAA metabolism. This thesis will help elucidate potential mechanisms involved in the pathogenesis of insulin resistance. It will also give insight on how targeting BCAA metabolism can provide therapeutic benefits against the development and management of insulin resistance.

Chapter 2: Literature Review

Here I will review the insulin signaling pathway, with a focus on proteins in the insulin signaling pathway that may be affected by BCAAs (IRS-1/Protein kinase B (Akt)/mTORC1/S6K1). I will then discuss the causes and molecular mechanisms of insulin resistance. Next, I will discuss BCAAs, and how they are metabolized and regulated. Finally, I will discuss the link between BCAAs and their metabolism with insulin signaling and insulin resistance.

2.1 Insulin Signaling

2.1.1 Insulin Receptor and Insulin Receptor Substrates

The first step in insulin signaling involves the insulin receptor. The insulin receptor is a heterotetrametric glycoprotein comprising of two α and two β subunits (45,46). The subunits are linked by disulfide bonds in an α-β-β-α arrangement. The α subunits are on the extracellular side of the membrane, which has the insulin binding site. The β subunits are on the intracellular side of the membrane to transmit the insulin signal downstream (45). Insulin binds to the α subunit, resulting in a conformational change in the insulin receptor, leading to the phosphorylation of the Tyr960 residue of the β subunit (45) (Figure 2.1). This further activates the β subunit and its kinase activity, allowing for propagation of the signal downstream.

The insulin receptor propagates this signal to the insulin receptor substrate (IRS), which is recruited to the insulin receptor through pleckstrin homology and phosphotyrosine binding domain (46). IRSs are a family of proteins, from IRS-1 through to IRS-6. For activation of IRSs they are phosphorylated on tyrosine residues by the insulin receptor (47). The insulin receptor and IRS tyrosine phosphorylation is transient and are dephosphorylated by protein tyrosine

phosphatase 1B (PTP1B) (48). Muscle specific knockout of PTP1B results in improved insulin sensitivity (49).

IRS-1 also has inhibitory serine/threonine residues, which hinder the propagation of the insulin signal downstream, and triggers the degradation of IRS-1 when phosphorylated (47). IRS-1 is necessary for glucose uptake in L6 myoblasts (50), while IRS-2 is not required for glucose uptake (51,52). IRS-3 is present in adipocytes, liver and lung in rodents, while IRS-3 is not present in humans (53). IRS-4 mRNA is present in skeletal muscle, liver, heart, brain, and kidney (53). IRS-5 and IRS-6 have limited tissue expression and are relatively poor insulin receptor substrates (54). The importance of IRS-1 in insulin signaling has been emphasized with IRS-1 knockout mice exhibiting peripheral insulin resistance and decreased growth (55).

2.1.2 IRS-1/PI3K/Akt Pathway

IRS-1 transmits the insulin signal to two pathways, the phosphoinositide 3-kinase (PI3K)-protein kinase B (Akt) pathway (Fig 2.1) and the extracellular signal-regulated kinase (ERK) pathway (56). We will focus on the PI3K-Akt pathway, as this pathway is implicated in BCAA-induced insulin resistance.

PI3K is a heterodimer comprising of a catalytic and a regulatory subunit (57). The regulatory domain binds to activated IRS-1 through two SH2 domains, activating the catalytic subunit of PI3K. When PI3K is activated, it phosphorylates phosphatidylinositol 4,5-bisphosphate (PIP_2) to generate a lipid second messenger phosphatidylinositol (3,4,5)-triphosphate (PIP_3). Phosphate and tensin homolog deleted on chromosome 10 (PTEN) is a phosphatase that antagonizes PI3K. It converts PIP3 into PIP2 to inhibit further insulin signaling (58). The loss and mutation of PTEN leads to hyperactive PI3K signaling (58). Hyperactive

PI3K has been implicated in tumor progression (59), emphasizing the importance of PTEN in regulating insulin signaling.

Ultimately, PIP_3 activates 3-phosphoinositide-dependent protein kinase 1 (PDK1) by interacting with the PH domain of PDK1. Once PDK1 is activated, it phosphorylates Akt at Thr308 (60) (Fig 2.1). For full activation, Akt requires Ser473 phosphorylation as well, which is catalyzed by mammalian/mechanistic target of rapamycin complex 2 (mTORC2) (61). Akt has three different isoforms (62). Akt2 is the most predominant isoform in insulin-sensitive tissues. Akt2 knockout mice develop insulin resistance, while knockout of Akt1 and Akt3 do not (63).

PDK1 is also important in the activation of atypical protein kinase C (aPKC) (Fig 2.1). aPKC is critical in both the translocation and docking/fusion of glucose transporter type 4 (GLUT4) to the plasma membrane (64) and is required for insulin-mediated glucose uptake in skeletal muscle (65). aPKC is activated by the allosteric binding of PIP_3 and phosphorylation at the Thr410 residue by PDK1 (66–68).

Phosphorylated Akt plays an important role in insulin-stimulated glucose uptake as it also regulates the translocation of GLUT4 from intracellular vesicles to the plasma membrane (69). Constitutively active Akt results in the translocation of GLUT4 to the plasma membrane (70), while inhibition of Akt blocks insulin-mediated translocation of GLUT4 (71,72), emphasizing the role of Akt in glucose transport.

Akt regulates GLUT4 translocation through Akt substrate of 160 kDa (AS160) (Fig 2.1). Phosphorylated Akt phosphorylates AS160, also called TBC1 domain family 4 (TBC1D4) at Thr642, and its homolog TBC1D1 at Thr596 (73–75). Phosphorylated AS160/TBC1D1 binds

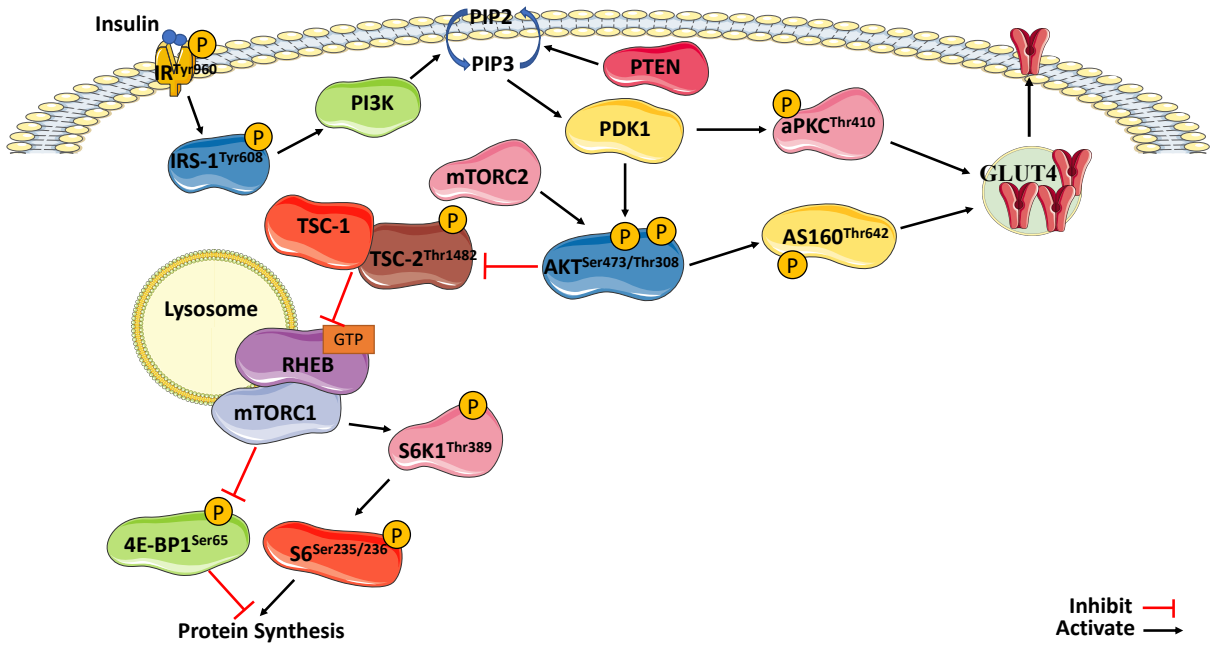

Figure 2.1: Simplified overview of insulin signaling pathway and proteins involved in glucose transport, and protein synthesis. Insulin activates the insulin receptor and IRS-1 leading to the activation of the PI3K pathway and PIP_3 synthesis. PIP_3 activates PDK1, which phosphorylates Akt. Activated Akt phosphorylates and inactivates the TSC complex, allowing RHEB to remain GTP loaded to activate mTORC1. Activated mTORC1 phosphorylates 4E-BP1 and S6K1, and S6K1 phosphorylates S6, ultimately leading to an upregulation of protein synthesis. Figure modified from (440).

to 14-3-3, which leads to the inhibition of GTPase activity (hydrolysis of GTP to GDP) by Rab-GTPase-activating protein (GAP) toward Rab proteins, as Rab proteins need to be GTP loaded to facilitate GLUT4 translocation and fusion to the plasma membrane (76). AS160 deficient mice exhibit reduced basal and insulin-stimulated glucose uptake in skeletal muscle, highlighting the importance of AS160 in glucose transport (77).

2.1.3. Akt/mTORC1 Pathway

Along with AS160, Akt is also crucial in the activation of mammalian/mechanistic target of rapamycin complex 1 (mTORC1). mTORC1 is important in the regulation of processes involved in growth, glucose and lipid metabolism, and protein synthesis. Activated Akt phosphorylates Thr1462 of tuberous sclerosis complex protein 2 (TSC-2) (Fig 2.1). This results in the degradation of a complex formed between TSC-2 and TSC-1, leading to activation of mTORC1 (78). Degradation of TSC-2 prevents its GTPase activity to inhibit Ras homologue enriched in brain (Rheb), as GTP loaded Rheb activates mTORC1 (78,79). Activated Akt also phosphorylates proline-rich Akt substrate 40 kDa (PRAS40), an inhibitor of mTORC1, alleviating the inhibition on mTORC1 (80).

2.2 Mammalian Target of Rapamycin Complex 1 (mTORC1)

mTOR is a serine/threonine protein kinase that forms the catalytic subunit of complexes, mTORC1 and mTORC2. mTORC1 is sensitive to extracellular and intracellular signals like stress, energy status, and amino acids, and controls many biological processes (81). Activated mTORC1 is implicated in cell growth, proliferation, survival, and metabolism. Once it is activated by insulin it can promote protein synthesis, lipid metabolism, and inhibit autophagy. It is also linked to numerous disease states, such as cancer, insulin resistance and type 2 diabetes mellitus (T2DM) (81,82).

It has six components: mTOR, the catalytic subunit of the complex; regulatory-associated protein of mTOR (Raptor); mammalian lethal with Sec13 protein 8 (mLST8, also known as G protein beta subunit-like (GbL)); PRAS40; FK506 binding protein 12 (FKBP12) and DEP-domain-containing mTOR-interacting protein (Deptor) (83,84). PRAS40, and FKBP12 are

negative regulators of just mTORC1, while Deptor is a negative regulator of both mTORC1 and mTORC2 (83,85). The function of mLST8 seems unclear as its deletion does not affect mTORC1 activity (86). Raptor is a scaffolding protein that plays an important role in the regulation of mTORC1. Raptor interacts with upstream regulators like Rheb (87) and RagB (88) and downstream substrates like ribosomal protein S6 kinase 1 (S6K1) and eukaryotic translation initiation factor *4E* (eIF4E)-binding protein 1 (4E-BP1) (89). Once mTOR is activated, it phosphorylates PRAS40 and Deptor, reducing the physical interaction of these negative regulators with mTORC1, leading to enhanced mTORC1 activity (83,90).

2.2.1 Downstream Substrates of mTORC1

Two downstream substrates of mTORC1, S6K1 and 4E-BP1 (Fig 2.1), are involved in regulating protein synthesis (78) (Fig 2.1). These two are amongst the best characterized substrates of mTORC1. mTORC1 phosphorylates the Thr389 site of S6K1 leading to its activation. Activated S6K1 activates key substrates involved in mRNA translation initiation, like eukaryotic initiation factor (eIF) 4B, a positive regulator of the 5'cap binding to the eIF4F complex (91). S6K1 also phosphorylates programmed cell death 4 (PDCD4), an inhibitor of mRNA translation, which results in its degradation, relieving its interaction with eIF4A (92,93). The best characterized substrate of S6K1 is ribosomal protein S6 (S6) (Fig 2.1). S6K1 activates S6 by phosphorylating it at its 5 serine residues, Ser235, Ser236, Ser240, Ser244 and Ser247. Activated S6 is a ribosomal protein involved in the initiation of mRNA translation (94,95).

4E-BP1 is another substrate of mTORC1 involved in protein synthesis. 4E-BP1 is a negative regulator of protein synthesis (96). 4E-BP1 inhibits translation by binding and

sequestering eIF4E to prevent assembly of the eIF4F complex. mTORC1 phosphorylates 4E-BP1 at Ser65 resulting in its dissociation from eIF4E, allowing for mRNA translation to occur (97).

2.2.2 Upstream Regulators of mTORC1

As stated above, mTORC1 is involved in numerous anabolic processes. mTORC1 is regulated by upstream stimuli. It is positively regulated by growth factors like insulin and insulin-like growth factor-1, inflammation, and amino acids. It is negatively regulated by cellular energy status, and stressors like hypoxia.

2.2.2.1 Energy Status

Low energy levels activate AMP activated protein kinase (AMPK) (98), which phosphorylates TSC-2 (99) to inhibit mTORC1. AMPK can also phosphorylate Raptor, resulting in its binding to 14-3-3 to inhibit mTORC1 (100). During glucose starvation, tumor suppressor protein 53 can also inhibit mTORC1 (101).

2.2.2.2 Stress

Certain stressors like hypoxia and inflammation can regulate mTORC1. During hypoxia, DNA damage and development 1 (REDD1) can inhibit mTORC1 through TSC-2 activation (102,103). In certain cancers IkB kinase A (IKKA), an important protein in inflammation signaling, can directly phosphorylate mTORC1 (Ser 1415), activating it, and leading to proliferation of cancer cells (104). IkB kinase b (IKKB) can also phosphorylate TSC-1, resulting in the activation of mTORC1 (105).

2.2.2.3 Amino Acids

Amino acids are important for synthesis of proteins, but they can also act as nutrient signals to induce cell growth. Cells can stimulate anabolic processes like protein synthesis based on the availability of amino acids (106). Specifically, BCAAs can activate mTORC1 signaling, which has been implicated in insulin resistance (14,15,21,107–114).

Availability of amino acids leads to the translocation of mTORC1 to the late endosomal/lysosomal membranes resulting in its activation by Rheb, while absence of amino acids results in the translocation to the cytosol away from the late endosomal/lysosomal membranes preventing activation of the complex (88,115).

Sestrins are proteins that negatively regulate mTORC1. Sestrin1 and sestrin2 negatively regulate Gap activity towards Rags 2 (GATOR2), a positive regulator of mTORC1. GATOR2 inhibits the GAP activity of GATOR1 on RagA/B. RagA/B need to be GTP loaded for mTORC1 activation (116). When deprived of leucine, sestrin1 and sestrin2 bind to GATOR2 (116,117), leading to reduced activation of mTORC1. When leucine is present, sestrin2 disassociates from GATOR2 (118,119), allowing for the translocation of mTORC1 to the lysosome to be active.

2.3 Insulin Resistance

Insulin resistance is the suppressed response to insulin by a target tissue (3) and is the underlying cause of T2DM. Insulin resistance impairs glucose disposal resulting in a compensatory increase in the production of insulin, ultimately resulting in hyperinsulinemia (120). Insulin resistance is characterized by hyperglycemia, and can cause an array of metabolic issues including hypertension, dyslipidemia, hyperuricemia, elevated inflammatory markers, endothelial dysfunction, and a prothrombotic state (120). Understanding how insulin resistance

affects the insulin signaling pathway is imperative. Below I will discuss the different causes of insulin resistance, which include genetics, lack of physical activity and obesity, and nutrition. Then I will highlight the molecular mechanisms of insulin resistance and how they impact the insulin signaling cascade explained above. This will lead me into the focus of my thesis, BCAAs and their metabolism, and how they are linked to insulin resistance and the insulin signaling pathway.

2.3.1 Causes of Insulin Resistance

2.3.1.1 Genetics

Leprechaunism Rabson-Mendenhall syndrome is autosomal recessive condition where both alleles in the insulin receptor are mutated leading to elevated insulin resistance. Patients with this disease only partially respond to insulin (121). Type A insulin resistance syndrome is another autosomal recessive or dominant genetic disease affecting the insulin receptor (122,123). Patients with both of these diseases need significantly more insulin than even a typical diabetic patient (124). A single nucleotide polymorphism in IRS-1 (Gly972Arg) can lead to insulin resistance (125). A Thr608Arg missense mutation in IRS-1 also results in decreased insulin signaling (126).

2.3.1.2 Lack of Physical Activity and Obesity

Physical activity is commonly prescribed in response to insulin resistant states like in obesity and T2DM. Daily physical activity is a major determinant of insulin sensitivity (127), as exercise training increases glucose uptake, and GLUT4 protein expression in skeletal muscle (128–130), even in T2DM patients (131,132). An acute bout of exercise reduces blood glucose

levels in T2DM patients similar to non-diabetic individuals (133). GLUT4 translocation from intracellular vesicles to the plasma membrane in skeletal muscle was similar in both nondiabetic and diabetic subjects in response to exercise (68). Exercise-induced glucose uptake can take place independent of insulin action (134), and this can persist for 48-hours post exercise (20).

Epidemiological studies reveal that the risk of insulin resistance increases as body fat content increases (135) and intra-abdominal depots compared to peripheral fat depots are more strongly linked to insulin resistance (136) and physical inactivity directly leads to an increase in intra-abdominal fat depots (137).

Mechanistically, physical inactivity promotes insulin resistance in many ways. A lack of exercise is associated with islet cell insufficiency (138), and exercise improves beta cell function in type 2 diabetes (139). Exercise also suppresses the apoptosis of beta cells seen in T2DM, increasing the functional mass of beta cells (140).

Physical inactivity and sedentary behaviours can have a negative effect on mitochondrial function (141,142). Limb immobilization downregulates mitochondrial proteins abundance (143). Trained individuals had greater mitochondrial function than sedentary individuals (144). Physical inactivity also increases oxidative stress (145,146), and promotes inflammation (147,148), which will be discussed further below on how they mechanistically induce insulin resistance.

2.3.1.3 Nutrition

Chronic overconsumption of energy coupled with physical inactivity leads to intra-abdominal fat, leading to insulin resistance (149). In mice, a normocaloric diet also attenuates the effect of a high fat diet (HFD) and improves insulin sensitivity, suggesting that it is imperative to

maintain energy balance (150), however even during bed rest and when energy intake is reduced, glycemia is still increased (151). High lipid, protein and carbohydrate diets have been implicated in insulin resistance, and I will discuss each below.

2.3.1.3.1 High Lipid Intake

A HFD contributes to obesity and insulin resistance. Epidemiological studies (152,153) and cross sectional studies (154,155) display a link between a HFD and obesity. However, energy intake may also have implications on the effect of a HFD on insulin sensitivity. A high fat hypocaloric diet did not differ from a high carbohydrate hypocaloric diet in terms of insulin sensitivity, but a high fat hypocaloric diet reduced lipids in the blood and systemic inflammation (156). T2DM patients fed a calorie unrestricted diet with high fat and low carbohydrates exhibited improvements in glycemic control and weight loss (157).

Mechanistically, GLUT4 activity was reduced in response to a HFD in rat skeletal muscle (158). A HFD has shown to worsen insulin and glucose tolerance (159). Saturated fatty acid, palmitate, induces hepatic insulin resistance by stimulating reactive oxygen species (ROS), leading to reduced tyrosine phosphorylation of IRS-2 (160). Interestingly, acute supplementation of palmitate to L6 muscle cells led to increased Akt phosphorylation and glucose uptake (161), but chronic exposure to palmitate in beta cells led to decreased Akt phosphorylation through the activation of mTORC1/S6K1 (162). Interestingly, in rats a HFD impairs the central nervous system ability to regulate food intake and body weight regardless of obesity. The inability to reduce food intake was consistent with reduced insulin signaling in the hypothalamus (163). Another study showed that a diet high in saturated fat decreased insulin sensitivity in overweight/obese with normal glucose tolerance without changes in intra-abdominal fat (164).

Typically in rodents, diets consisting of 45-60% fat are considered an HFD, and have both shown to induce obesity (165), and exhibit reduced insulin sensitivity (166). Ketogenic diets are high in fats and low in carbohydrates. Ketogenic diets differ from typical high fat diets as ketogenic diets must be low in carbohydrates to induce ketosis (167), unlike typical high fat diets, which do not need to limit carbohydrates. Ketogenic diets help against obesity and improve insulin sensitivity (168,169).

2.3.1.3.2 High Carbohydrate Intake

Regarding insulin resistance, high carbohydrate diets get less attention in the literature compared to an HFD. High fructose and sucrose diets result in reduced insulin sensitivity in rats (170), but the effect of sucrose in humans is not as convincing (171). Compared to a high saturated fat diet, a high carbohydrate diet improved insulin sensitivity in young subjects (172). A high carbohydrate and fiber diet increased peripheral insulin sensitivity (173). One study showed no change in whole-body insulin sensitivity in response to high carbohydrate feeding and high fat feeding, but a high carbohydrate diet increased tyrosine phosphorylation of IRS-1 in skeletal muscle, with increased PI3K activity, while a HFD increased inhibitory serine phosphorylation of IRS-1 in skeletal muscle (174). Interestingly, A high carbohydrate hypocaloric diet worsened insulin sensitivity (175). However, in another study, obese men fed a hypocaloric diet consisting of high carbohydrate exhibited improved insulin sensitivity (176), suggesting that total energy intake may have greater impacts than specific macronutrient intake on insulin sensitivity.

2.3.1.3.3 High Protein Intake

High protein diets are often recommended against obesity (177). Increasing absolute protein intake to 1.5-2g/kg of body weight has been suggested for overweight/obese individuals with T2DM (178), with normal kidney function, as it promotes insulin secretion (179) and reduces hemoglobin A1C (180). Dietary protein promotes insulin release and glucose uptake by the tissues (181). Overweight humans on a high protein diet for 6 weeks had reduced insulin sensitivity, along with increased S6K1 phosphorylation. However, the reduced insulin sensitivity was attenuated with individuals on the high protein diet for longer periods (18 weeks) (182). Arginine is another amino acid implicated in insulin resistance, as arginine supplementation in rats for 4 weeks reduced insulin sensitivity (183). However, another study showed that arginine supplementation for 6 days increased glucose uptake in L6 myotubes, consistent with enhanced Akt phosphorylation (184). Additionally, methionine restricted mice are resistant to diet-induced obesity and insulin resistance, with enhanced phosphorylation of Akt in liver (185,186). BCAAs are recommended for weight management (187) and the literature suggests a link between BCAAs supplementation and insulin resistance (21,107,112–114).

Interestingly, a high protein hypocaloric diet further increased weight loss and insulin sensitivity compared to just a hypocaloric diet (188). Another study showed that a high protein hypocaloric diet improved insulin sensitivity (175). As touched on in the high lipid and carbohydrate intake sections, energy intake may play the biggest role in treatments against obesity and insulin resistance.

2.3.2 Molecular Mechanisms of Insulin Resistance

2.3.2.1 Chronic Inflammation

During insulin resistance (189) and obesity (190), pro-inflammatory cytokine levels are increased. Pro-inflammatory cytokines can activate c-jun N-terminal kinase (JNK), which then phosphorylates IRS-1 (Ser302/307), which in turn hinders insulin signaling (191). Knockdown of JNK protects against obesity induced insulin resistance (192).

Pro-inflammatory cytokines like tumor necrosis factor-alpha (TNF-α) released from adipose tissue can trigger insulin resistance by activating serine residues of IRS-1 in skeletal muscle (191,193). Interleukin-6 (IL-6) is another pro-inflammatory cytokine that activates Janus kinase-signal transducer and activator of transcription (JAK-STAT) signaling pathway and increases the expression of suppressor of cytokine signaling 3 (SOCS3). This results in reduced expression of GLUT4 and IRS-1 (194,195).

2.3.2.2 Accumulation of Lipid Intermediates

Diacylglycerol (DAG) levels are increased in many organs of obese individuals (196). Increases in DAG levels can activate protein kinase C (PKC) and JNK (197,198) leading to increases in IRS-1 (Ser302/307/1101) phosphorylation (191). Ceramides are another type of lipid molecule that can activate JNK and PKC to induce insulin resistance (199,200). One study shows that reduced insulin sensitivity and Akt phosphorylation was consistent with increased ceramide levels in C2C12 myotubes. Inhibiting ceramide synthesis attenuated this reduction of Akt phosphorylation and insulin sensitivity (201).

2.3.2.3 Oxidative Stress

High fat feeding activates ROS production before the onset of inflammation or insulin resistance (202). Excess ROS is produced in response to mitochondrial dysfunction (203). Oxidative stress induces insulin resistance in both adipose tissue (204) and skeletal muscle (205). Like inflammation, ROS activates JNK and PKC to phosphorylate serine residues of IRS-1 to hinder downstream insulin signaling (206). Thus, the upregulation of ROS might be the key event in triggering HFD-induced insulin resistance (202). Another study supports this as mice deleted of NADPH oxidase 2 (Nox2), a ROS generating enzyme, show an attenuation of insulin resistance from an HFD. Nox2 knockdown also attenuated glucose and palmitate induced insulin resistance, but not H_2O_2 induced insulin resistance (207). Interestingly, some studies have shown ROS can also promote insulin sensitivity (208). ROS can inhibit PTEN and PTP1B (209,210), which are negative regulators of the insulin signaling pathway.

2.4 Branched Chain Amino Acids (BCAAs)

BCAAs activate mTORC1 and muscle protein synthesis. BCAA-rich diets or BCAA supplementation stimulate muscle protein synthesis (211–213), regulate body weight (214,215), and reduce protein breakdown (211,216).

Despite the benefits of the BCAAs, they have been implicated in insulin resistance. Plasma BCAA levels are increased in insulin resistant states like obesity and T2DM (11,108,217,218). In clinical studies, BCAA levels in the blood positively correlate with insulin resistance (218–220). BCAA levels are also predictive of future insulin resistance or T2DM (218,221,222). Questions remain if increased levels of BCAAs in insulin resistance is causative

or correlative. Here I will discuss the BCAAs, their metabolism and regulation, and then finally how BCAAs are linked with insulin resistance.

2.4.1 BCAA Catabolism

BCAAs share the initial two steps in their catabolism (Fig 2.2). The first step is a transamination reaction catalyzed by branched-chain aminotransferase 2 (BCAT2). This first step is reversible, and it yields branched-chain alpha-ketoacids (BCKAs; α-ketoisocaproate/4-methyl-2-oxopentanoic acid (KIC) from leucine, α-keto-methylvalerate/3-methyl-2-oxopentanoate, (KMV) from isoleucine, and α-ketoisovalerate/3-methyl-2-oxobutanoic acid (KIV) from valine). During the transamination reaction, the amino group released from the BCAAs reacts with α-ketoglutarate (α-KG) to produce glutamate (223).

The next step of BCAA catabolism is the irreversible oxidative decarboxylation of BCKAs. This reaction is catalyzed by branched chain α-keto acid dehydrogenase complex (BCKD). The products of BCKA decarboxylation are acyl CoA derivates (isovaleryl-CoA from KIC, 2-methylbutyryl-CoA from KMV, and isobutyryl-CoA from KIV) (Fig 2.2). Then the acyl-CoAs are catabolized in separate pathways.

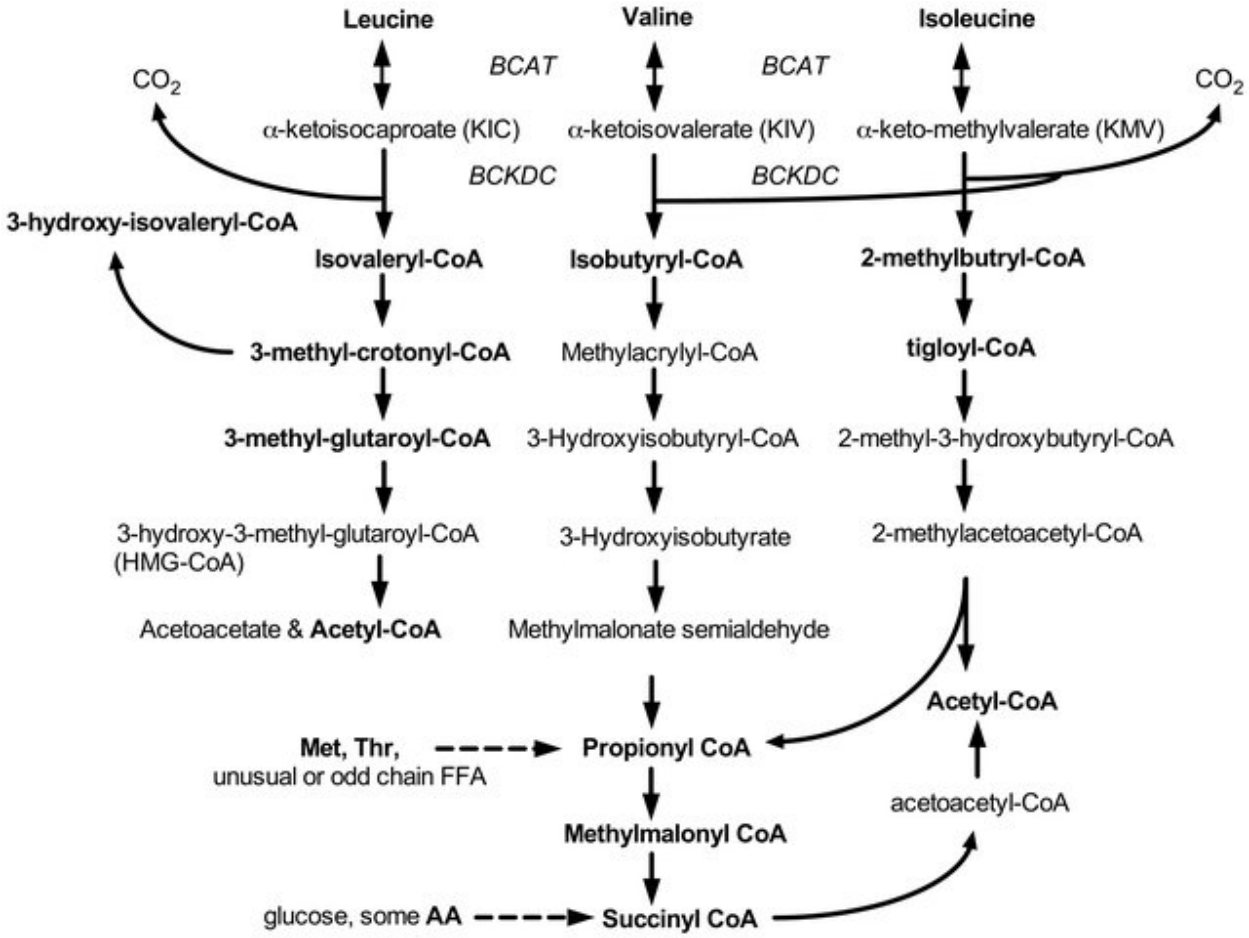

Figure 2.2: Schematic of the overview of BCAA Catabolism. BCAAs (leucine, isoleucine, and valine) undergo reversible transamination, catalyzed by BCAT producing BCKAs (KIC, KIV and KMV). BCKAs are irreversibly decarboxylated by BCKD to yield respective CoA compounds, which divide into their respective metabolic pathways. Taken from reference (382).

Isovaleryl-CoA produced from leucine is catabolized to acetyl-CoA and acetoacetate in multiple steps. Acetoacetate can be further broken down into two molecules of acetyl CoA, which can enter the TCA cycle. 2-methylbutyryl-CoA produced from isoleucine ultimately produces acetyl-CoA and succinyl-CoA. Isobytyryl-CoA produced from valine produces propionyl-CoA (224) (Fig 2.2). Valine and isoleucine are both glucogenic amino acids. Their metabolites, propionyl-CoA and succinyl-CoA can be converted into glucose by

gluconeogenesis. On the other hand, acetyl-CoA produced from isoleucine and leucine can produce fatty acids, so leucine is known as a ketogenic amino acid, while isoleucine is both glucogenic and ketogenic (225,226).

Numerous tissues are involved in BCAA metabolism. One study analyzed the relative contributors of isoleucine disposal into protein synthesis. Liver (27%) is the largest contributor following with skeletal muscle (24%), pancreas (24%), the kidneys (9%), brown adipose tissue (6%) and other tissues (10%) (227). In terms of whole-body BCAA oxidation, skeletal muscle (59%) plays the biggest role, and then the brown adipose tissue (19%), liver (8%), kidneys (5%), heart (4%) and other tissues (5%) play smaller roles. The majority of BCAA catabolism takes place in skeletal muscle mostly due to the fact that 65% of BCAA transamination occurs in the skeletal muscle (228).

2.4.1.1 Branched-chain amino acid transaminase (BCAT)

As stated above, BCAT is responsible for the transamination of BCAAs into their respective BCKAs, and α-KG receives the amino group producing glutamate. However, this reaction is reversible, as in the opposite direction, BCKAs react with the amino group of glutamate to produce their respective BCAA and α-KG. Pyridoxal 5′-phosphate (PLP), a coenzyme of vitamin B6 acts as the amino group carrier. It binds to the amino group of the BCAA producing the respective BCKA and the pyridoxamine 5′-phosphate (PMP)-bound forms of the enzyme. PMP then transfers the amino group to α-KG to produce glutamate, which then restores BCAT-PLP conformation (223) (Fig 2.3). There are two isoenzymes of BCAT, the *BCAT1* gene encodes the cytosolic BCAT (BCAT1), and the *BCAT2* gene encodes the mitochondrial BCAT (BCAT2) (229). BCAT2 is found in many tissues including skeletal

muscle, kidney, cortex, heart, subcutaneous adipose tissue, stomach, colon, ileum, and liver, while BCAT1 is only present in the brain, ovary and placenta (229). BCAT prefers isoleucine, then leucine and then valine (230–232). As explained above, BCAA catabolism and transamination especially, largely occurs in skeletal muscle and this is due to the fact that BCAT2 is mostly abundant in the skeletal muscle, and least in the liver (228).

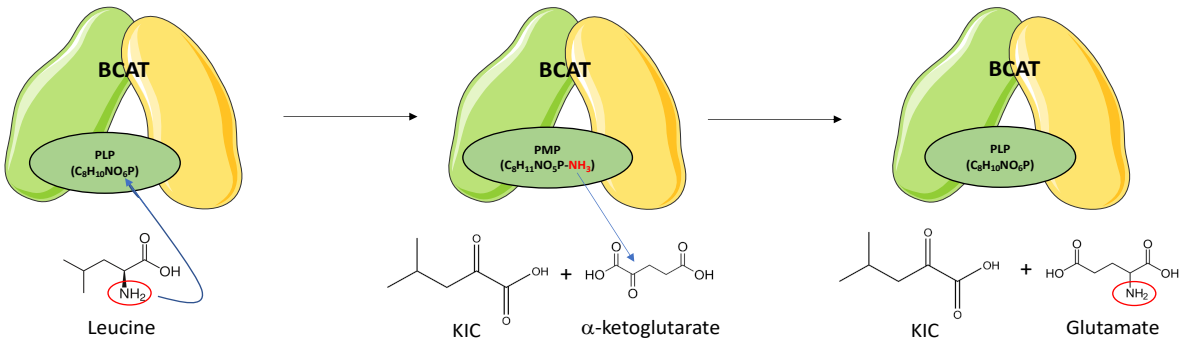

Figure 2.3. Schematic of the BCAA Transamination Reaction. BCAT catalyzes the reversible transamination of BCAAs into their respective BCKAs. Leucine is transaminated to α-ketoisocaproic acid (KIC), isoleucine to α-ketomethylvaleric acid (KMV), and valine to α-ketoisovaleric acid (KIV). BCAT-pyridoxal phosphate (PLP) transfers the α-amino group from the BCAA yielding BCAT-pyridoxamine phosphate (PMP) and the respective BCKA. BCAT-PMP transfers the α-amino group to α-ketoglutarate producing glutamate and restoring BCAT-PLP. Leucine transamination is shown as representative of transamination reactions of the other BCAAs. Taken from reference (376).

The importance of BCAT2 is evident as BCAT2 knockout mice are smaller (214), and have reduced endurance in response to exercise (233). Gene expression of protein degradation, apoptosis, and necrosis are also increased in BCAT2 knock out animals (234). Knockdown of BCAT2 in L6 cells impaired myotube differentiation (235). BCAT2 is also implicated in diabetes, as its mRNA expression is reduced in diabetic patients (23), highlighting its importance.

2.4.1.2 Branched-chain α-ketoacid dehydrogenase (BCKD)

BCKD is a complex that has three proteins, heterodimeric branched-chain α-keto acid decarboxylase (E1), dihyrolipoyl transacylase (E2) and homodimeric dihydrolipoyl dehydrogenase (E3) (Fig 2.4). BCKD is responsible for the irreversible oxidative decarboxylation of BCKAs yielding respective branched-chain acyl-CoA derivates (isovaleryl-CoA from KIC, 2-methylbutyryl-CoA from KMV, and isobutyryl-CoA from KIV), producing CO_2 and NADH as well.

The E1 protein is a tetramer consisting of two α and two β subunits (α2β2). The *BCKDHA* gene encodes the α subunits of E1 and the *BCKDHB* gene encodes the β subunits. Thiamine pyrophosphate (TPP) is an important cofactor in the BCKD reaction (236). The E2 protein, at the centre of the complex, attaches to E1 and E3. The *dihydrolipoamide branched-chain transacyclase* gene (DBT) gene encodes for E2. E2 has three domains: the core domain, the binding domain and the lipoyl domain. The core domain is the active site of the enzyme. The binding domains attach to E1 and E3 (237) through ionic interactions (238). The lipoyl domain is responsible for channelling the substrate within the complex (239). *Dihydrolipoamide dehydrogenase* (DLD) gene encodes for E3. It is a homodimeric flavoprotein that contains a bound flavin adenine dinucleotide molecule (240) (Fig 2.4).

The oxidative decarboxylation by BCKD is a multistep process. E1 decarboxylates the BCKAs, producing the respective branched-chain acyl intermediate and CO_2. The lipoyl domain of the E2 subunit transfers the respective BCKA to the core of the E2 subunit, attaching to coenzyme A, producing branched-chain acyl-CoA ester. Lipoate is reduced to dihydrolipoic acid in the process. E3 reoxidizes the dihydrolipoic acid using NAD+ to produce NADH and lipoate again (224) (Fig 2.4).

Unlike BCAT2, BCKD activity is highest in the liver (241). The heart and kidney have intermediate activity. Skeletal muscle, adipose tissue, and brain exhibit the lowest BCKD activity (241). Despite low activity of BCKD in skeletal muscle, knockdown of BCKD in L6 myotubes has shown to reduce insulin sensitivity (17), and impair myotube differentiation (242).

BCKAs also have other pathways responsible for their metabolism. Cytosolic dioxygenase can convert a small percentage of KIC to beta-hydroxy-beta-methylbutyrate (HMB) (243) (Fig 2.2). This enzyme is largely present in the liver, with a small abundance in the skeletal muscle (244). HMB has been used as an ergogenic aid to promote exercise performance and skeletal muscle hypertrophy (245). In that sense it is similar to BCAAs, as it has shown to increase mTORC1 signaling (246,247), muscle protein synthesis (248), and suppress proteolysis (246). BCKAs can also be reduced at the α-carbon, producing branched chain α-hydroxy ketoacids in metabolic disorders like maple syrup urine disease, propionic acidaemia and ketoacidosis (249,250).

The action of BCKD is irreversible, thus BCKD activity is tightly regulated by two proteins (Fig 2.5). Branched-chain ketoacid dehydrogenase kinase (BDK) is a negative regulator of BCKD. BDK inactivates BCKD by phosphorylating it at Ser293 and Ser303 of the E1 subunit (148, 149). Protein phosphatase 2Cm (pp2Cm) dephosphorylates BCKD, activating it (255,256).

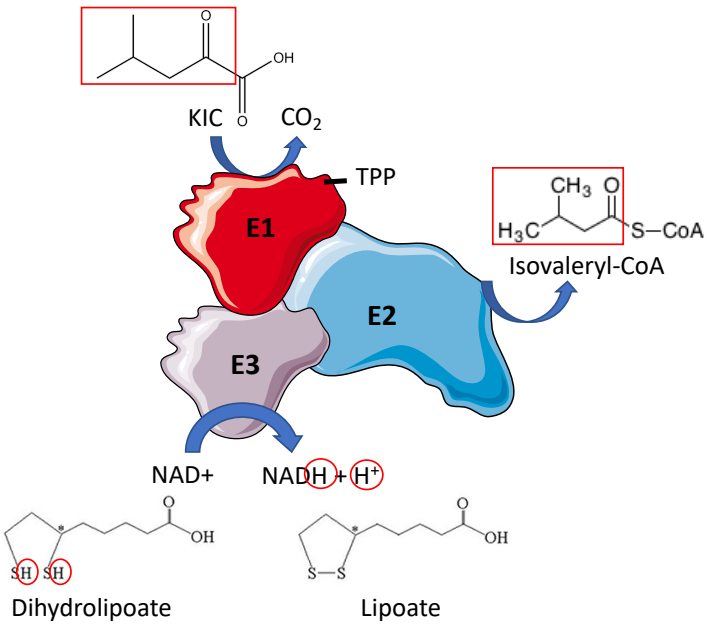

Figure 2.4: Schematic of the BCKD Reaction. Firstly, BCKD binds TPP on the E1 subunit initiating oxidative decarboxylation of the BCKA (shown here for ketoisocaproic acid). The acyl group that is formed (both red boxes) is transferred to E2, attaching to coenzyme A (CoA) forming its respective CoA derivative (isovaleryl-CoA in this instance). Lipoate is oxidized in the process, producing dihydrolipoate. Then, E3 reduces dihydrolipoate producing lipoate and NADH + H^+. Taken from reference (376).

2.4.1.3 Branched-chain α-ketoacid dehydrogenase kinase (BDK)

BDK contains a nucleotide-binding domain and a four-helix bundle domain (253,257). BDK mRNA expression is highest in skeletal muscle, explaining why BCKD activity is low in skeletal muscle and why BCKAs produced in the skeletal muscle go to the liver to be oxidized (228). However, BDK depletion in L6 myotubes rescued the defects in myotube formation from BCAT2 depletion (235), highlighting its importance in skeletal muscle as well. In the brain and kidney it has intermediate activity, and then it is the lowest in the liver and small intestine (228). BDK exists in the mitochondrial matrix of a cell in two forms: a free form and bound form (29,254,258). BDK binds to BCKD when it is catalytically active and promotes the

phosphorylation and inactivation of BCKD. BCKAs induce conformational change of BDK, removing the attachment of it to the BCKD complex, and thus activating the BCKD complex (259).

Mice with muscle-specific deletion of BDK have reduced skeletal muscle BCAA concentrations, and increased BCKD activity in the heart and kidney. This is consistent with decreased phosphorylation of S6K1 and 4E-BP1 when fed a low protein diet (260), but in BCAA supplementation, the BDK depleted mice exhibited greater S6K1 phosphorylation compared to wild-types. They also exhibit reduced myofibrillar protein content in a low protein diet, but this was rescued when BCAAs were supplemented (260). Thus, greater BCKD activity by BDK depletion leads to greater mTORC1 sensitivity in response to amino acids.

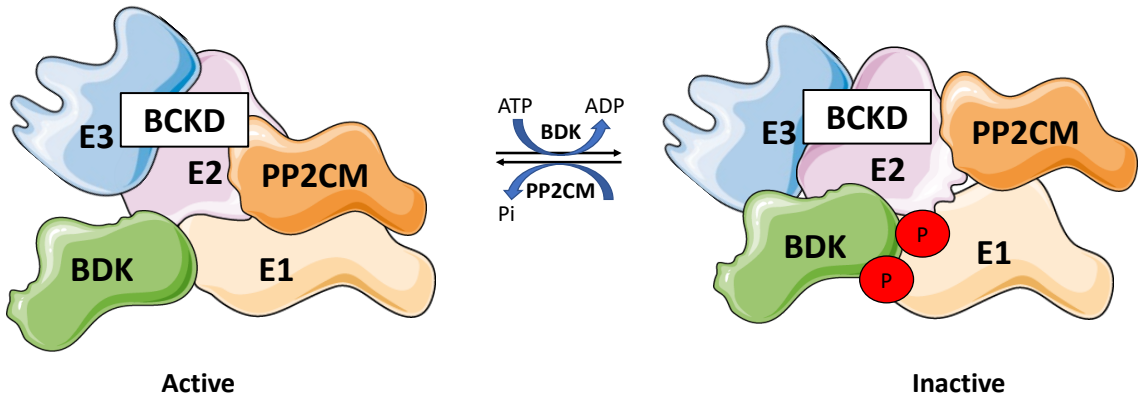

Figure 2.5. Schematic of BCKD Regulation. BCKD is regulated by a kinase, BDK, and a phosphatase, pp2Cm that interact with the E1 subunit. BDK phosphorylates BCKD at Ser293 and Ser303 inhibiting BCKD, while pp2Cm dephosphorylates BCKD, reactivating the complex. Taken from reference (376).

2.4.1.4 Protein phosphatase 2Cm (pp2Cm)

As stated above, pp2Cm dephosphorylates BCKD, leading to its activation (255,256). It is encoded by the *PPM1K* gene (261,262). It is highly expressed in the liver, brain, heart, kidney and diaphragm (263). There is low expression of pp2Cm in skeletal muscle (263), which also partly explains the low activity of BCKD in skeletal muscle. The enzyme physically interacts with BCKD to dephosphorylate it at the Ser293 residue. Mutation of the Ser293 residue of BCKD, but not the Ser303 residue affects this interaction (262). The interaction of BCKD and pp2Cm is disrupted by BDK, suggesting that both enzymes compete to interact with the BCKD complex (263). Pp2Cm knockout mice demonstrate a 3–4-fold increase in circulating BCAAs and a 5–10-fold increase in liver BCKAs (264), which led to reduced glucose oxidation and made the heart more vulnerable to ischemia-reperfusion injury, but this was rescued by increasing BCAA catabolism or by the overexpression of GLUT1. Increased BCAA and BCKA levels have been linked to numerous diseases including insulin resistance, obesity, T2DM (12,265), highlighting the importance of pp2Cm activity towards BCKD.

2.4.2 Physiological Regulation of BCAA Metabolism

2.4.2.1 Effect of Sex on BCAA Metabolism

Very few studies have assessed sex differences in BCAA catabolism. Sex hormone estrogen inhibits the BCKD complex by activating BDK, decreasing BCAA catabolism (42,43). Males exhibit higher plasma BCAA concentrations compared to females (266), but have greater leucine oxidation compared to women following endurance exercise (44). However, very little work has been done examining the effect of sex on BCAA levels and BCAA catabolic enzyme activity and abundance in relevant tissues.

2.4.2.2 Effect of Aging on BCAA Metabolism

Aged men show significantly lower circulating BCAA levels compared to young men (38,39). However, one study showed no age related loss in serum BCAA levels or total amino acid levels, and greater serum BCAA levels in males compared to females in young and aged individuals (267). One study did show increased serum BCAAs in an old male population compared to old females, which could be explained due to reduced energy and protein intake in the female population (268). There are no studies examining the change in BCAA concentrations or BCAA catabolic enzymes in any of the major tissues responsible for BCAA metabolism (skeletal muscle, liver, adipose tissue or heart) with age, but one could speculate that because insulin resistance is more prevalent with age (41), the activity and abundance of these enzymes may be lower like in insulin resistant states. However, one study found that insulin treatment to type 1 diabetic patients reduced leucine oxidation (269), but improved KIC oxidation. This suggests that in an insulin resistant aged population, there is an increased breakdown of leucine, but an accumulation of KIC. Another study showed endogenous insulin treatment reduced BCAA levels (270), suggesting increased BCAA oxidation in response to insulin, which would ultimately lead to decreased BCAA catabolism in aging as insulin resistance increases. Also many parameters of mitochondrial health is reduced with aging (271), which could impact BCAA catabolic enzymes as they are mitochondrial proteins.

2.4.2.3 Effect of Exercise on BCAA Metabolism

Numerous studies have examined the effect of exercise on BCKD activity (272–274). Endurance exercise upregulates BCAA catabolism and BCKD activation in skeletal muscle of humans (273) and rats (272,274). Also, endurance training reduces the amount of BDK bound to

the BCKD complex in rat skeletal muscle and liver (43,272,275,276). Roberson et al. demonstrate an increase in *BCAT2* mRNA expression in endurance trained individuals compared to resistant trained individuals (277). This is consistent with the fact endurance exercise typically promote mitochondrial adaptations, while resistance exercise promote myofibrillar adaptations (277), as BCAT2 is a mitochondrial protein. There is also an increase in the KIC to leucine ratio post exercise implying an increase in BCAT2 activity (278,279). Increases in KIC after exercise could contribute to increased BCKD activity as KIC inhibits BDK (280). Enhanced BCAT2 activity in the muscle could also be to produce glutamate for ammonia detoxification, as plasma ammonia levels are increased post exercise (281).

2.5 The link between BCAAs and Insulin Resistance

There is an increase in plasma BCAA levels in insulin resistant states like obesity and T2DM (11,108,217,218). In clinical studies, BCAA levels in the blood positively correlate with insulin resistance (218–220). BCAA levels are also predictive of future insulin resistance or T2DM (218,221,222). Older men exhibit significantly lower circulating BCAA levels (38,39). This is interesting, as insulin resistance is more prevalent in older individuals (41), so you would expect higher BCAA levels in old age, as BCAA levels have been found to be correlated with the degree of insulin resistance (218). Thus, questions persist if elevated levels of BCAAs cause insulin resistance or are a symptom of insulin resistance. Therefore, I will review the effect of BCAAs and their metabolites on insulin sensitivity. I will also discuss how insulin resistant states like obesity and T2DM may regulate BCAA catabolic enzyme activity/abundance, which may explain the increase in BCAA levels in insulin resistance. Finally, I will review studies that

have targeted BCAA catabolism and how manipulating the regulation of this pathway may affect insulin sensitivity.

2.5.1 Effect of BCAAs and their Metabolites on Insulin Sensitivity

High levels of BCAAs lead to an increase in the activation of mTORC1. This results in the increased activation of S6K1 as well. Increased mTORC1/S6K1 activation leads to the phosphorylation of inhibitory serine residues, Ser636, Ser312, Ser616 of IRS-1 in humans, and Ser632, Ser307 and Ser612 of IRS-1 in mice (109–111), ultimately leading to reduced insulin sensitivity. Numerous studies show the link between BCAAs and reduced insulin sensitivity through the activation of this mTORC1/S6K1-IRS-1 feedback loop (21,107,112–114) (Fig 2.6).

In vitro, physiological levels (150 μM) and supraphysiological levels (350 μM and 600 μM) of leucine treatment in starved L6 myotubes suppressed insulin-stimulated glucose uptake, which was consistent with an increase in S6K1 phosphorylation (16). However, higher concentrations of leucine (800 μM and 1600 μM) did not. Another study showed that supraphysiological concentrations of leucine (400 μM and 800 μM) increased basal and insulin-stimulated glucose uptake with no change in S6K1 phosphorylation in starved L6 myotubes (282).

In vivo, some studies have showed leucine to stimulate glucose uptake and improve insulin sensitivity in rat skeletal muscle (22,283), however these studies used supraphysiological levels of leucine (2 mM), while leucine concentrations in the plasma are often around 0.12-0.15 mM (214,284). In another study, deletion of BCAT2 improved insulin sensitivity, implying increased levels of BCAAs may not impair insulin sensitivity in mice (214). BCAAs-fed mice in their drinking water showed activated mTORC1 without affecting insulin sensitivity (285). This

could be due to the fact they were given BCAAs for 3 months, while studies that find reductions in insulin sensitivity are acute interventions (18,286). Weickert et al. showed that a high protein diet for 6 weeks activated S6K1, and this was consistent with a reduction in whole-body insulin sensitivity in humans. However, when the high protein diet persisted for 18 weeks, despite an even greater activation of S6K1, whole-body insulin sensitivity returned to control levels (182). This suggests the length of treatment may affect the variability in the results seen in literature.

The physiological context of these animals may influence the outcome of BCAA treatment. One study showed increased insulin sensitivity in rats on a HFD in response to chronic (17-24 weeks) leucine supplementation, while this had no effect on animals fed normal chow (20,287). However, an acute gavage of leucine to obese rats showed increased blood glucose levels compared to rats gavaged water (18). Leucine (12 weeks) and BCAA treatment (34 weeks) improved insulin sensitivity in db/db mice (288,289). However, Newgard et al. show worsening insulin sensitivity in rats fed a HFD supplemented with leucine for 12-16 weeks (108). This is interesting as BCAA restriction in Zucker-fatty rats improved skeletal muscle insulin sensitivity, along with enhanced fatty acid oxidation (290). Despite increased insulin sensitivity, restriction of BCAAs also leads to suppressed immune function (291). Additionally, dietary restriction of BCAAs improves insulin sensitivity in rodent models (290,292–294). On the other hand, another study showed improved insulin sensitivity in rats fed a HFD given leucine for 24 weeks and 32 weeks (295). They do mention that leucine has different effects at different timepoints of insulin resistance. At 32 weeks, leucine enhanced mitochondrial function and lipid oxidation, while at 24 weeks, leucine supplementation led to incomplete oxidation of lipid species and mitochondrial dysfunction in rats, reinforcing that time of treatment may play a

role in the effects of leucine. Further investigation is required to understand the complex relationship between BCAAs, mTORC1 and insulin sensitivity.

In humans, leucine-mediated activation of mTORC1 did not alter leg glucose uptake (296) and BCAA supplementation did not alter arterial blood glucose during and after exercise (297). In another study, 1 or 5 g of BCAA did not influence blood glucose levels in young men (298). From the studies above it is evident that BCAA supplementation in rats, mice and humans are similar, but in muscle cells the suppressive effect is the greatest. This could be due to the fact other tissues aside from muscle in rodents and humans help in catabolizing BCAAs.

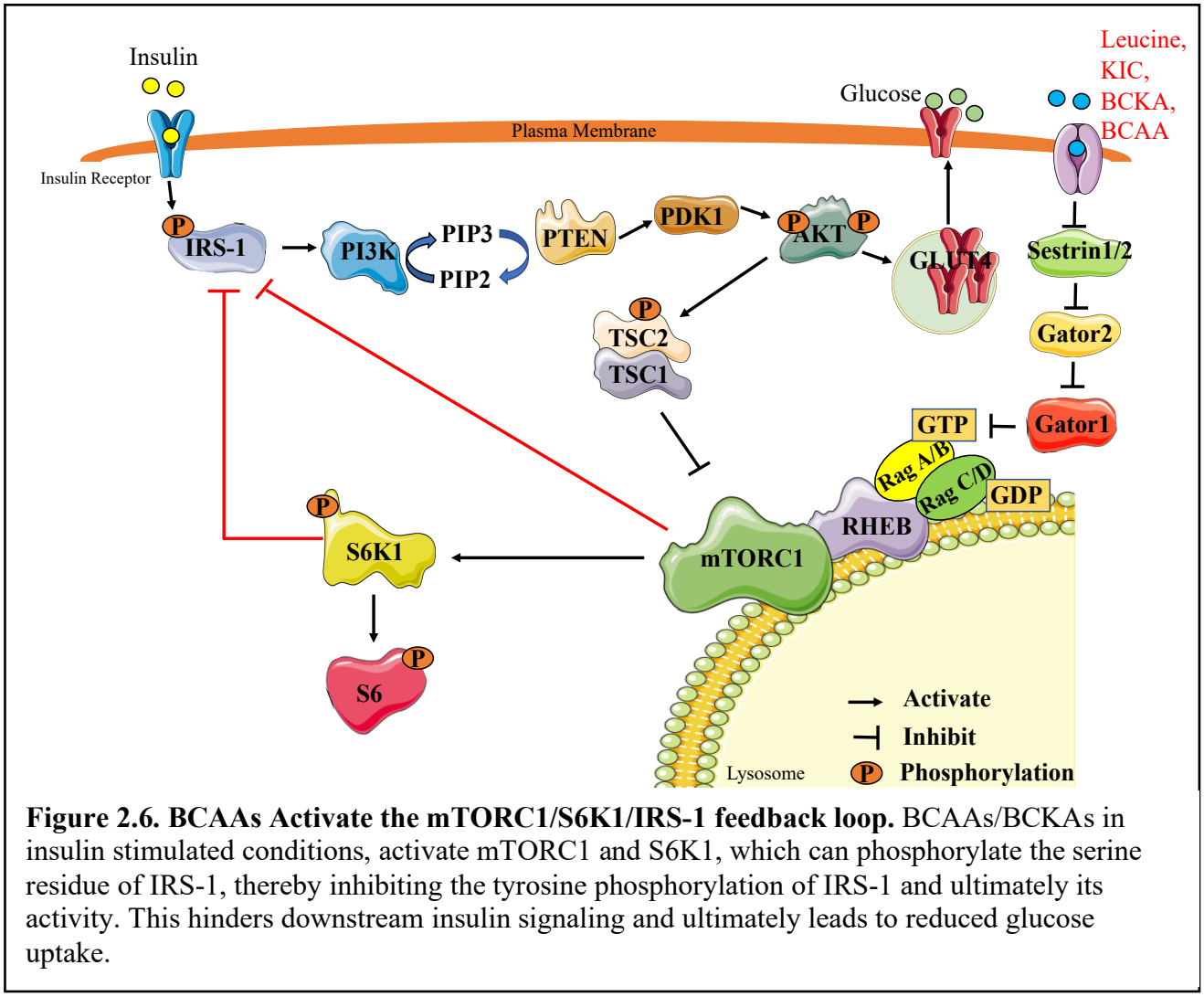

Figure 2.6. BCAAs Activate the mTORC1/S6K1/IRS-1 feedback loop. BCAAs/BCKAs in insulin stimulated conditions, activate mTORC1 and S6K1, which can phosphorylate the serine residue of IRS-1, thereby inhibiting the tyrosine phosphorylation of IRS-1 and ultimately its activity. This hinders downstream insulin signaling and ultimately leads to reduced glucose uptake.

Individual BCAAs can have different effects on insulin sensitivity. Despite the activation of the mTORC1/S6K1-IRS-1 signaling axis, one study showed that although ingesting a leucine drink activated mTORC1, there was no change in Akt activation or leg glucose uptake. On the other hand, whey-protein increased mTORC1 activation and reduced leg glucose uptake with no change in Akt activation, suggesting an alternative pathway in reducing insulin sensitivity than the inhibition of Akt by leucine-mediated mTORC1 signaling (296). In contrast, as discussed above, studies show that chronic leucine supplementation had no effect on insulin sensitivity in mice fed a standard chow diet (20) and protected against HFD induced insulin resistance by increasing fatty acid oxidation (20,21,299,300). One study compared this effect of leucine protecting against HFD-induced insulin resistance with valine and saw that valine supplementation worsened it (301). This correlated with increased valine induced BCKD inhibition (301). This is interesting as dysregulations of BCAA catabolic enzymes are implicated in insulin resistant states (13,23,24,302).

Isoleucine restriction improved insulin sensitivity in normal chow fed mice (303), but reintroducing isoleucine attenuated this effect. The benefits of isoleucine restriction is independent of mTORC1 activation in the liver (303), suggesting mechanisms other than the S6K1-IRS-1 signaling axis may be at play. Isoleucine and valine restriction, but not leucine restriction, improved the metabolic health of obese mice (303), as isoleucine supplementation in mice fed a HFD show increased insulin resistance, along with increased intramuscular lipid droplet accumulation and mitochondrial dysfunction (304).

The effects of BCAAs may also be muscle fiber type dependent. BCAAs had a greater effect on attenuating angiotensin induced muscle atrophy in the extensor digitorum longus (fast twitch, type II fibers) compared to the soleus (slow twitch, type I fibers) (19). BCAAs also had a

greater rescuing effect on angiotensin induced reduction in cross sectional area in type IIb fibers compared to type I fibers. Furthermore, BCAAs significantly increased mTOR (Ser2448) phosphorylation in extensor digitorum longus with and without angiotensin, but not in the soleus (19). Also after exercise, BCAA concentrations were reduced significantly in type II fibers, but not type I fibers suggesting perhaps increased BCAA catabolism in response to exercise in type II fibers (305). The differences in the effects of BCAA across different muscle fiber types may contribute to the variability seen in the literature with changes in mTORC1 signalling and insulin sensitivity.

Circulating levels of BCKAs are elevated in insulin resistant states as well (12,218,220). In particular, high concentrations of KIC has been associated with insulin resistance in humans (265) and animals (12). KIC supplementation has shown to activate mTORC1 (107) and reduce insulin-stimulated glucose uptake in L6 myotubes (17,107). However, this effect was attenuated when BCAT2 was depleted. KIC also could not activate mTORC1 in the presence of an amino transaminase inhibitor in pancreatic β-cells (306). These studies suggest KIC is converted back to leucine to activate mTORC1 and suppress glucose uptake. Another study shows that supraphysiological levels of KIC (5 mM) can activate protein phosphatase 2A (PP2A), a negative regulator of Akt. PP2A dephosphorylates Akt, and KIC prevents insulin-mediated inhibition of PP2A. In fact, an inhibitor of PP2A attenuated the reduction of Akt activation by KIC, confirming that supraphysiological KIC levels reduce Akt phosphorylation by activating PP2A (307).

Studies suggest 3-hydroxyisobutyrate (3-HIB), a metabolite of valine may also play a role in eliciting insulin resistance. Diabetic subjects have increased serum 3-HIB levels (12,308,309). Diabetic mice show a decrease in the enzyme that catabolizes it (310).

Supplementation of 3-HIB increases trans-endothelial fatty acid transport by increasing peroxisome proliferator-activated receptor gamma coactivator 1-alpha (PGC-1α), while knockdown of upstream enzymes blocking its formation attenuates trans-endothelial fatty acid uptake. Knockdown of downstream enzymes preventing 3-HIB catabolism resulted in increased triglyceride levels in mice (309). Increased fatty acid uptake leads to increased DAG levels, thus activating PKC-θ, and ultimately leading to reduced Akt phosphorylation (309). Mice treated for two weeks with 3-HIB become insulin resistant, correlating with an increased lipid signature in skeletal muscle, and reduced Akt phosphorylation (308). These data emphasize the potential role of 3-HIB in eliciting insulin resistance.

Whether BCAA ingestion/supplementation induces insulin resistance is still complicated and there is controversy in the literature. Interestingly, body builders and athletes that consume BCAA supplements are not insulin resistant (311,312). A combination of resistance exercise and consumption of protein/amino acids results in a synergistic effect on muscle protein synthesis (313). The effect of amino acids on muscle protein synthesis are not due to changes in hormones like insulin but the effect of those amino acids themselves (313,314). Leucine activates muscle protein synthesis but needs the presence of the other essential amino acids (315). Muscle protein synthesis plateaus at about 20 g of protein with no difference compared to 40 g of protein. Additional protein did not result in increased protein synthesis, but only increased amino acid oxidation (316), suggesting that higher consumption of BCAAs by body builders does not cause insulin resistance.

There have been no reports of BCAAs induced insulin resistance in athletes as reviewed by Shou et al (312). As stated above, exercise improves BCAA oxidation (272–274), which may offset increased levels of BCAAs and dysregulations in their metabolism in insulin resistant

states. This is emphasized by the increased production of valine metabolite beta-aminoiso-butyric acid (BAIBA) in response to exercise. BAIBA levels are inversely correlated with insulin resistance, promoting hepatic fatty acid oxidation and browning of white adipose tissue (317). This suggests that other factors like physiological context and underlying comorbidities affect BCAA consumption on insulin sensitivity.

2.5.2 Effect of Type 2 Diabetes/Insulin Resistance on BCAA Metabolism

Altered levels of BCAA/BCKAs in insulin resistant states are likely increased due to dysregulated levels of the enzymes responsible for their metabolism. In insulin resistant states, expression of genes encoding for the BCAA catabolic enzymes are downregulated in muscle (318), liver (319) and adipose tissue (13). One study found that a genetic predisposition to impaired BCAA metabolism is implicated in patients with T2DM (320). Knock-in mice expressing the T2D-human ankyrin-B rare variant exhibited reduced expression of BCAA catabolic enzymes in white adipose tissue, with minimal changes in liver, skeletal muscle and brown adipose tissue (321). Insulin resistant mice show blunted BCAA oxidation in adipose tissue and liver, shifting the BCAA oxidation to skeletal muscle. This also leads to increased lipid uptake and muscle lipotoxicity, further contributing to insulin resistance in skeletal muscle (227).

Skeletal muscle *BCAT2* mRNA level is reduced in T2DM patients compared to body mass index-matched controls (23). In skeletal muscle of db/db mice, BCAT2 protein level is increased, while BCAT2 mRNA expression in db/db mice were unchanged (23). However, db/db mice exhibit significantly increased plasma levels of valine, suggesting reduced BCAT2 activity (227). In skeletal muscle of ob/ob mice, there is no change in *BCAT2* mRNA or protein levels

compared to control (23). In skeletal muscle of obese Zucker rats there is no change in BCAT2 protein level compared to lean counterparts (284). Fructose induced insulin resistant rats showed reductions in muscle BCAT2 activity, even though activities of the enzyme in liver and adipose tissue were not affected (322).

In skeletal muscle of db/db mice, *BCKDα* or *BCKDβ* mRNA levels were unchanged, but there was a decrease in the BCKDα protein expression and an increase in BCAT2 protein levels (23). Liver BCKD activity, and adipose tissue BCKDα and BCAT2 protein levels were also reduced in db/db mice (23). Concomitantly, in ob/ob and type 2 diabetic mice, BDK protein expression was increased in skeletal muscle, liver, and adipose tissue (24). There is a decrease in liver and adipose tissue pp2Cm protein expression, but not in skeletal muscle (24). Phosphorylation of BCKD (Ser293) was increased, and BCKD activity was reduced in ob/ob and type 2 diabetic mice (24). Additionally, BCAA levels were elevated in the hearts of diabetic mice due to reduced pp2Cm expression and BCKD activity in the heart (323). These effects seem exclusive to diabetic rodents, as obese mice do not exhibit changes in mRNA or protein expression of BCAT2 or BCKD in skeletal muscle (23). However, in another study, ob/ob mice exhibited significant decreases in *BCAT2*, *BDK*, *pp2Cm,* and *BCKD* mRNA expression in adipose tissue (294). This is not seen in skeletal muscle, but similar effects are seen in liver, except *BDK* mRNA expression is increased (294). This suggests that obesity affects BCAA catabolism in adipose tissue and liver but not in skeletal muscle.

It is evident from the review of the literature that in obesity and type 2 diabetes, BCAA metabolic enzymes are dysregulated, which lead to altered blood/tissue BCAA levels. However, there are other mechanisms in which insulin resistance manifests. One study showed that inflammation and ER stress reduced BCAA metabolic enzyme abundance in adipose tissue,

which lead to an increase in serum BCAA levels (324). Fructose feeding causes insulin resistance by promoting inflammation in the liver and hepatic de novo lipogenesis (325). Fructose feeding has shown to increase BDK protein activity, leading to enhanced lipogenesis and contributing to insulin resistance (326). Ultimately, in various mechanisms of insulin resistance, enzymes involved in the metabolism of BCAAs are dysregulated, which explains the upregulation of BCAA/BCKAs in plasma and tissues in insulin resistant states. As explained below, studies aiming at increasing BCAA catabolic flux have shown improvements in insulin sensitivity, while decreasing BCAA catabolic flux has shown to worsen insulin sensitivity.

2.5.3 Effect of Altered Regulation of BCAA Metabolism on Insulin Sensitivity

Impairments in BCAA catabolism also can contribute to insulin resistance. BCKD depleted L6 myotubes showed a reduction in insulin-stimulated glucose uptake in starved conditions (17). This is interesting as discussed above, BCAT2 knockout mice exhibit better insulin sensitivity despite reduced catabolism of BCAAs (214). Mice heterozygous for the downstream BCAA catabolic enzyme methylmalonyl-CoA mutase are insulin resistant and have reduced fatty acid oxidation (327). Reduced BCAA oxidation leads to reduced availability of BCAA-derived anaplerotic TCA intermediates (propionyl-CoA), ultimately leading to reduced fatty oxidation and the accumulation of acylcarnitines that can activate proinflammatory pathways (328), contributing to insulin resistance. The link between BCAA catabolism and fatty acid oxidation is emphasized, as a study shows that KIC treatment enhances fatty acid oxidation (327). It also shows how defects in BCAA catabolism affect lipid metabolism (327). Also, adiponectin, an adipokine, activates BCKD activity, with AMP-activated protein kinase (AMPK) and pp2Cm both being necessary for adiponectin induced activation of BCKD (24). However,

another study shows AICAR, an activator of AMPK, increased the inhibitory phosphorylation of BCKD, while compound C, an inhibitor of AMPK, reduced BCKD phosphorylation in primary mouse hepatocytes (329). Additionally, long-chain fatty acids are raised in insulin resistant states (330), and they can impair BCKD activity, increasing BCKA levels (331,332).

Zucker fatty rats treated with a BDK inhibitor showed improved insulin sensitivity (326). Conversely, hepatic overexpression of BDK phosphorylates ATP-citrate lyase, enhancing its activity and resulting in increased de novo lipogenesis acids (326). Also in a high fructose diet, the transcription factor Carbohydrate-Response Element Binding Protein (ChREBP) inhibits pp2Cm, resulting in activation of ATP-citrate lyase, and shuttling pyruvate from glucose metabolism to produce fatty acids (326), emphasizing the link between fatty acid oxidation and BCAA catabolism. It is important to note that this ChREBP transcription factor only affects BCAA metabolism in rats and humans, and not in mice (326). Blair et al. also speculate that differences in studies in response to upregulating BCAA oxidation may be dependent on species as rats may have greater liver handling of BCAAs compared to mice (333). Despite the benefits of increased BCAA catabolism on insulin sensitivity, *PP1MK* knockdown mice exhibit an increase in BCKAs that inhibit gluconeogenesis in the liver, which could be a compensatory mechanism, as insulin sensitivity was surprisingly improved in these *PP1MK* knockdown mice fed a HFD (334).

Furthermore, inhibition of BDK or the overexpression pp2Cm, lowers circulating BCAAs, resulting in reduced hepatic steatosis and improved glucose tolerance in the absence of weight loss in Zucker fatty rats. Inhibiting BDK, with BDK inhibitor BT2 attenuates the decrease in insulin sensitivity associated with elevated BCAA/BCKAs, suggesting that targeting BCAA catabolism may help against obesity-induced insulin resistance (294). Vanweert et al. show that treatment with sodium phenylbutyrate, an activator of BCKD activity, improved whole-body

insulin sensitivity in patients with T2DM (335), which could be through enhanced mitochondrial function (336). In one study where BT2 improved glucose tolerance, it also reduced inflammation and steatosis, but liver specific knockdown of BDK did not have the same effects. This emphasizes the importance of the regulation of BCAA catabolism in other tissues like skeletal muscle on insulin sensitivity (337).

A recent paper by Blair et al. demonstrated that muscle specific knockdown of BDK in skeletal muscle and liver lowers plasma BCAAs but had no effect on whole-body insulin sensitivity. However, BT2 treatment at the whole-body level did improve insulin sensitivity (333), suggesting the role of other tissues or that BT2 has effects on other pathways. A recent study has found that BT2 lowers mitochondrial ROS (338), which could contribute to improved insulin sensitivity.

Interestingly, there is an increase in *BCAT2* mRNA expression in response to 12-hour supraphysiological treatment of metformin, a prescribed drug for T2DM, but a significant reduction in *BCAT2* and *BCKDH*α mRNA expression 24 hours post drug treatment in C2C12 myotubes. Protein levels of BCAT2 were also decreased 24 hours post treatment (339). Additionally, metformin treatment in mice limits its own therapeutic potential by reducing BCAA catabolism. Metformin improved insulin sensitivity as expected, but this led to decreased BCAA catabolism (329). The effect of metformin on BCAA catabolism was mediated by a decrease in BCKD activity through the increase in AMPK activation. When metformin was combined with BT2, this potentiated the effect of metformin on insulin sensitivity (329), emphasizing the importance of targeting this pathway in T2DM, but also examining how AMPK may be related in the link between BCAAs and insulin resistance.

Endurance exercise increases BCKD level/BCAA catabolism (273,340,341), and this may contribute to the increased insulin sensitivity seen in trained individuals (342–344), further emphasizing the importance of BCAA catabolic flux. However, like stated earlier BCAT2 depletion in mice improved insulin sensitivity (214) and increased muscle glycogen (233), which poses the question if the dysregulation of BCAA catabolic enzymes and BCAA levels elicit insulin resistance.

2.6 Concluding Remarks

In summary, questions persist whether dysregulations in BCAA levels and their metabolism are a product of insulin resistance or cause insulin resistance. Numerous studies have shown an increase in mTORC1 signaling concurrently with reduced insulin sensitivity in response to BCAA treatment. However, in obese and diabetic mice leucine seems to improve insulin sensitivity, complicating the link. Additionally, mice depleted of BCAT2 that have increased BCAA levels show improved insulin sensitivity. Key factors contributing to the variability in the outcomes of BCAAs on insulin sensitivity are the concentration of BCAAs used, and the duration of treatment. This suggests that perhaps increased BCAA levels may be a result of insulin resistance affecting BCAA catabolic enzyme abundance/activity. Numerous studies have shown reduced activity and abundance of these enzymes in insulin resistant states. Additionally, studies have also shown that targeting this pathway may contribute to altered insulin sensitivity, as upregulating the catabolism of BCAAs has shown to improve insulin sensitivity.

Also, it is important to consider other mechanisms/tissues that may be involved, as even though mTORC1 signaling is at the forefront of BCAA induced insulin resistance, recent studies

have implicated the AMPK pathway as well. Further studies are warranted to fill in gaps in the link between BCAAs, their metabolism and insulin resistance.

Chapter 3 Rationale, Objective, and Hypothesis

3.1 Overview of Thesis

Insulin resistance is an underlying cause for diseases like T2DM and cardiovascular diseases. BCAAs, BCKAs and their metabolism are implicated in insulin resistance. A better understanding of the link between BCAAs, BCKAs and their metabolism with insulin resistance is required due to conflicting reports on BCAA/BCKA supplementation on the induction of insulin resistance. Although BCKAs are upregulated in insulin resistance, it is important to note if this is causative. Also, upregulated levels of plasma BCAA/BCKAs can be due to changes in catabolic enzyme abundance/activity in insulin resistant states like obesity and T2DM. Thus, manipulating the regulation of enzymes involved in BCAA catabolism can help determine their role in the pathogenesis of insulin resistance and their therapeutic potential against it. Although BCAA/BCKAs are elevated in insulin resistant states, they are reduced in plasma of old men, a demographic more susceptible to insulin resistance. This complicates the link between BCAA/BCKA levels and their metabolism and insulin resistance. Female animals have also shown differences in BCAA metabolism, emphasizing the importance of including this underrepresented group.

3.2 Objectives and Hypothesis for study 1 (Chapter 4)

Rationale: Increased circulating levels of BCAAs and BCKAs are seen in insulin-resistant states like T2DM (11–13). This raises the question if increased BCAA and BCKA levels cause insulin resistance or are a symptom of insulin resistance. *BCAT2* and *BCKDHβ* mRNA levels are significantly decreased in diabetic patients, which could explain the increase in BCAA levels (23). BCKD activity is also decreased in T2DM and obesity (24). BCAA transamination

predominantly takes place in the skeletal muscle, but complete oxidation of the BCKAs takes place in the liver (241), as BCKD is predominantly abundant and active in the liver (241). Thus, most studies aim to manipulate BCKD activity in the liver. However, BCKD activity is vital for muscle cell formations and functions (17,235,260). Previous work in our lab has shown that L6 myotubes depleted of BCKD suppressed insulin-stimulated glucose uptake in the starved state (17).

Objective: To examine the effect of inhibiting/depleting BDK on insulin-stimulated glucose uptake with and without BCAA/BCKA supplementation in L6 myotubes.

Hypothesis: Depleting/inhibiting BDK will increase insulin-stimulated glucose uptake and attenuate the suppression of insulin-stimulated glucose uptake from BCAA/BCKA supplementation in L6 myotubes.

3.3 Objectives and Hypothesis for study 2 (Chapter 5)

Rationale: Increased circulating levels of BCAAs and BCKAs are seen in insulin-resistant states like T2DM (11–13). Our lab has previously shown that leucine (150 μM) and KIC (200 μM) significantly suppress insulin-stimulated glucose uptake in starved L6 myotubes (17,107). They significantly increased S6K1 (Thr389) phosphorylation, leading to increased IRS-1 (Ser612) phosphorylation, and thus reducing insulin-stimulated glucose uptake. BCAAs also only phosphorylate mTOR (Ser2448) in fast twitch muscle fibers like the extensor digitorum longus muscle, but not in slow twitch muscle fibers like the soleus (19). Despite the effect of leucine and KIC in muscle cells, other tissues aside from skeletal muscle contribute to whole-body

BCAA catabolism. Thus, we want to explore the effect of KIC *in vivo* and its effects on various tissues and muscle fiber types involved in BCAA metabolism.

Objective: To measure the effect of KIC gavage on whole-body insulin sensitivity and insulin signaling in rats in various tissues and muscle fiber types.

Hypothesis: KIC will suppress insulin sensitivity, along with an increase in phosphorylated S6K1 and IRS-1 (Ser612) in liver, heart, and skeletal muscle, with the greatest effect in fast twitch fibers like the extensor digitorum longus compared to slow twitch fibers like the soleus.

3.4 Objectives and Hypothesis for study 3 (Chapter 6)

Rationale: For many of the human conditions, including diabetes, cardiovascular disease, insulin resistance and cancer, age is the most important risk factor (34,35). BCAA metabolism is modified in many of these conditions (345). Aged men exhibit significantly lower circulating BCAA levels (38,39). This is interesting, as BCAA levels are upregulated in insulin resistance (12,13), but insulin resistance is more prevalent in older individuals (41), complicating the relationship between BCAA levels and insulin resistance. Protein levels of enzymes involved in BCAA catabolism are reduced in insulin resistant states (23,227). There are no studies examining the effect of aging on BCAA metabolism, specifically the activities/abundance of BCAT2, BCKD, BDK and pp2Cm in relevant tissues is an area that needs to be further explored. Sexual dimorphisms may also contribute to changes in BCAA metabolism in young and old mice, and thus female groups must be included.

Objective: To examine the effect of aging and sex on BCAA metabolism in mice.

Hypothesis: BCKD activity will be reduced in old mice compared to young counterparts. Also, BCAT2, BCKD, pp2Cm protein levels will be reduced, while BDK protein levels will be increased in old mice compared to younger counterparts regardless of sex.

3.5 Additional Contributions

The following work includes significant contributions that I made during my PhD that are not included in my dissertation.

Co-Author: Published

Dhanani, Z. N., Mann, G., and Adegoke, O. A. J. (2019) Depletion of branched-chain aminotransferase 2 (BCAT2) enzyme impairs myoblast survival and myotube formation. *Physiol. Rep.* **7**, 1-15

Mann, G., and Adegoke, O. A. J. (2021) Effects of ketoisocaproic acid and inflammation on glucose transport in muscle cells. *Physiol. Rep.* **9**, e14673

Mann, G., Mora, S., Madu, G., and Adegoke O. A. J. (2022) Branched-chain Amino Acids: Catabolism in Skeletal Muscle and Implications for Muscle and Whole-body Metabolism. *Front. Physiol*. **12**, 1-25

Mann, G., Riddell, M.C., and Adegoke, O. A. J. (2022) Effects of Acute Muscle Contraction on Key Molecules in Insulin and Akt Signaling in Skeletal Muscle in Health and in Insulin Resistant States. *Diabetology*. **3**, 423-446.

Co-Author: In Submission

Mora, S., Mann, G., and Adegoke, O. A. J. Sex Differences in Cachexia and BCAA Metabolism following Chemotherapy. Submitted to American Journal of Physiology.

Co-Author: In progress

Mora, S., Mann, G., and Adegoke, O. A. J. Sex-related Differences in Cachexia Outcomes and Branched-Chain Amino Acid Metabolism following Chemotherapy in Old Animals.

Chapter 4: Upregulating BCAA Catabolism Attenuates BCKA-Induced Suppression of Glucose Transport

Gagandeep Mann and Olasunkanmi Adegoke*

School of Kinesiology and Health Science and Muscle Health Research Centre, York University, Toronto, ON, Canada M3J 1P3

***Corresponding Author: Olasunkanmi A. J. Adegoke** Muscle Health Research Centre, School
of Kinesiology and Health Science, York University, 4700 Keele Street, Toronto, ON, Canada.
Tel: 416-736-2100 ext. 20887 Fax: 416-736-5774. Email: oadegoke@yorku.ca

4.1 Abstract

Plasma levels of branched-chain amino acids (BCAAs) and their metabolites, branched-chain ketoacids (BCKAs) are increased in insulin resistance, a condition that can lead to type 2 diabetes mellitus (T2DM). We previously showed that leucine and ketoisocaproicacid (KIC) suppressed insulin-stimulated glucose uptake in L6 myotubes, especially in myotubes with depleted level of branched-chain ketoacid dehydrogenase (BCKD), the enzyme that decarboxylates BCKAs, suggesting that interventions that increase BCKD activity might improve insulin sensitivity. Thus, the objective of this study was to analyze the effect of upregulating BCAA catabolism on measures of insulin sensitivity. We hypothesized that upregulating BCAA catabolism increases insulin-stimulated glucose transport and attenuates BCKA induced insulin resistance.

L6 myotubes were depleted of branched-chain ketoacid dehydrogenase kinase (BDK) or treated with or without a BDK inhibitor BT2. Then myotubes were supplemented with or without either KIC (200μM), leucine (150μM), BCKAs (200μM), or BCAAs (400μM) for 30 minutes. After, cells were incubated with or without insulin (100 nM) for 20 minutes. They then underwent a glucose transport assay or BCKD activity assay, and harvested for immunoblotting and HPLC for the level of BCAA/BCKA.

BDK depletion rescued KIC induced suppression of insulin-stimulated glucose uptake. Consistent with this, BT2 treatment rescued BCKA- and KIC-induced suppression of insulin-stimulated glucose uptake with the attenuation of KIC/BCKA-induced IRS-1 (Ser612) and S6K1(Thr389) phosphorylation but had no effect on Akt (Ser473) phosphorylation. BCAA and leucine supplementation showed a trend for reduced insulin-stimulated glucose uptake and increased S6K1 and IRS-1 phosphorylation, but BT2 did not influence this. Inducing S6 (Ser235/6) and IRS-1 (Ser612) phosphorylation with an mTORC1 activator, abolished effect of BT2 treatment on glucose transport in cells treated with KIC. Conversely, inhibiting mTORC1 with rapamycin significantly lowered glucose uptake.

Our data suggests that the suppression of insulin-stimulated glucose transport by KIC/BCKA in muscle is mediated by mTORC1/S6K1 signaling. This was attenuated by upregulating BCAA catabolic flux, suggesting that interventions targeting BCAA catabolism may provide benefits against insulin resistance and its sequalae.

4.2 Introduction

Branched-chain amino acids (BCAAs; leucine, valine, isoleucine) are essential amino acids required in a human's diet. BCAAs stimulate muscle protein synthesis, and regulate body weight and glucose homeostasis (10). However, despite these benefits, increased circulating levels of BCAAs and BCAA metabolites, branched-chain α-ketoacids (BCKAs), are seen in insulin-resistant states like T2DM (11–13). Whether or not these BCAAs/BCKAs directly cause insulin resistance still requires further investigation. Previous studies have showed a causative role of BCAAs and metabolites (17,21,107,113,114). Numerous studies have also shown how insulin resistant states can regulate the BCAA catabolic pathway and the enzymes involved (23,24,326,327), and how potentially targeting this pathway can improve insulin sensitivity (24,326).

BCAAs are catabolized by branched-chain aminotransferase 2 (BCAT2) predominantly in skeletal muscle, producing BCKAs. These BCKAs are then funnelled to the liver as the enzyme responsible for BCKA catabolism, branched-chain ketoacid dehydrogenase (BCKD) is predominantly abundant and active in the liver (241). Thus, most studies investigate BCKD and its activity in the liver. However, we have shown that depletion of the E1 alpha subunit of BCKD in L6 myotubes reduced insulin-stimulated glucose uptake, suggesting a connection between skeletal muscle BCAA catabolism and insulin signaling. Here, we investigated the effect of upregulating BCAA catabolism at the level of BCKD on insulin sensitivity and insulin signaling in L6 myotubes alongside BCAA/BCKA supplementation. We also analyzed if the effects of upregulating BCAA catabolism on insulin signaling is mediated by mTORC1 activity.

4.3 Methods

Reagents

Alpha modification of Eagle's medium (AMEM, #310-010-CL), phosphate-buffered saline (PBS, #311-010-CL), trypsin (#325-043-CL), and antibiotic–antimycotic (ab-am, #15240-062) preparations were purchased from Wisent (St Bruno, Quebec, Canada). Fetal bovine serum (FBS, #12483-020), horse serum (HS, #26050088), Lipofectamine RNAiMAX (#13778-150), Opti-MEM 1X Reduced Serum Medium (#31985070) and antibody against BDK (#PA5-31455) were purchased from Thermo Fisher Canada (Burlington, Ontario Canada). Amino acid-free RPMI 1640 medium (R8999-04A) was purchased from US Biologicals (Salem, Massachusetts, United States). L-leucine (#L8912), L-isoleucine (#I7403), L-valine (#V0513), sodium 4-methyl-2-oxovalerate (sodium salt of KIC, #K0629), 3-methyl-2-oxovaleric acid (sodium salt of KMV, #K7125), 3-methyl-2-oxobutyrate (sodium salt of KIV, #198994), 2-deoxyglucose, protease (#P8340) and phosphatase (#P5726), inhibitor cocktails, anti-gamma tubulin antibody (#T6557), siRNA oligonucleotides, amino acid standard (#AAS-18), dimethyl sulfoxide (DMSO, #D5879-100ML), O-phthalaldehyde (OPA, #P1378), 4,6-dimorpholino-*N*-(4-nitrophenyl)-1,3,5-triazin-2-amine (MHY1485, #SML0810), 1,2-diamino-4,5-methylenedioxybenzene (DMB, #66807), trypan blue dye (#T8154), and 3-Chloro-benzo[*b*]thiophene-2-carboxylic acid (BT2, #592682) were purchased from Sigma Aldrich (Oakville, Ontario, Canada). Rapamycin (#Rap004) was purchased from BioShop (Burlington, Ontario, Canada). Antibodies against phosphorylated (ph) S6K1 (Thr389, #9234), S6 (Ser235/6, #4858), Akt (Ser473, #4060), BCKDH-E1α (Ser293, #40368), ACC (Ser79, #3661) and IRS-1 (Ser612, #3203), as well as horseradish peroxidase (HRP)-conjugated anti-rabbit (#7074) and anti-mouse (#7076) secondary antibodies were purchased from Cell Signaling Technology (Danvers, Massachusetts, United States). Antibody

against BCAT2 (#16417-1-AP) was purchased from ProteinTech (Rosemont, Illinois, United States). [^{3}H]-2-deoxyglucose (NET549) was purchased from Perkin Elmer (Markham, Ontario, Canada), U-^{14}C labelled valine (ARC0678) was purchased from American Radiolabeled Chemicals (St. Louis, Missouri, United States of America), while chemiluminescence substrate (#WBKLS0500) was purchased from Millipore (Etobicoke, Ontario, Canada).

Cell Culture

L6 rat skeletal muscle myoblasts (L6 cells are derived from male rats) were purchased from American Type Culture Collection. Cells were cultured in 10-cm plates with growth medium (GM: AMEM supplemented with 10% FBS and 1% ab-am preparations). Cells were seeded (2×10^{5}cells/well) in six-well plates for western blot experiments or (10^{5} cells/well) in 12-well plates for glucose transport experiments. They were allowed to proliferate for 48 h or until they became 90–100% confluent. They were then shifted into differentiation medium (DM: AMEM, 2% HS, 1% ab-am preparations) and replenished with fresh DM every 48 h. Myotubes were used on day 5 (D5) of differentiation.

BCAA and BCKA Treatment

Myotubes were treated with BCAAs or BCKAs for 30 min. They were then treated with or without 100 nM of insulin and the treatment of BCAA/BCKAs continued with insulin for 20 minutes. For KIC (Fig 4.1-4.2, 4.4-4.6, 4.8-4.10), the concentration used was 200 μM, as shown previously to reduce glucose transport (16). For leucine (Fig 4.7), the concentration was 150 μM, as shown previously to reduce glucose transport (16). For the BCKA treatment (Fig 4.8), like for the KIC treated group we used 200 μM, made up of 76 μM of KIC, 62 μM of KMV and 62 μM

of KIV. Like for the BCAA treatment (Fig 4.7), we used 150 μM of leucine, and 175 μM of valine and 75 μM isoleucine, for a total of 400 μM, as in the literature valine levels is typically the highest in plasma, while isoleucine is the lowest (346).

BT2 Treatment

BT2 is an inhibitor of BDK, a protein kinase that is a negative regulator of BCKD (227,347). On D5 of differentiation, L6 myotubes were treated with 250 μM of BT2 in complete starvation medium, free of amino acids and serum for 3 h. Incubation then continued in starvation medium with BT2 or vehicle (VEH) that was also supplemented with or without KIC for 30 min. Incubation then continued in starvation medium with BT2 or vehicle that was also supplemented with or without KIC for 30 min and with or without 100 nM insulin for 20 min followed by glucose transport assay, BCKD activity assay or harvesting for immunoblotting. These treatments were done similarly in control (SCR) and BDK depleted conditions (Fig 4.6). The schematic for the experimental design is outlined in Appendix A.

Trypan Blue

Cell viability in response to BT2 treatment was measured using a trypan blue dye (348). L6 myotubes were incubated for 3 h in 250μM of BT2 in a starvation medium that lacked amino acids and serum. After, cells were trypsinized and then resuspended in trypan blue. Then using a hemocytometer, viable cells (black arrow) and non-viable cells (red arrow) were counted.

MHY1485 Treatment

4,6-dimorpholino-*N*-(4-nitrophenyl)-1,3,5-triazin-2-amine (MHY1485) is an mTOR activator (349). MHY1485 is dissolved in DMSO. Since insulin treatment already diminishes TSC-2's inhibition on mTORC1, we combined TSC-2 knockdown and MHY1485 treatment to produce a greater activation of mTORC1. On D5 of differentiation, L6 myotubes depleted of TSC-2 were treated with vehicle or 10μM of MHY1485 in complete starvation medium, free of amino acids and serum for 3 h. Incubation then continued in starvation medium with MHY1485 or vehicle that was also supplemented with or without KIC for 30 min. After, incubation then continued in starvation medium with MHY1485 (10 μM) or vehicle that was also supplemented with KIC (200 μM) and with 100 nM insulin for 20 min followed by glucose transport assay and harvesting for immunoblotting. Schematic of experimental design outlined in Appendix B.

Rapamycin Treatment

Rapamycin was used as an mTORC1 inhibitor (350), as done previously in our work (107). Cells were starved with or without BT2 (250 μM) for 3 h. Incubation then continued in starvation medium with BT2 or vehicle that was also supplemented with or without KIC (200 μM) and with or without rapamycin (50 nM) for 30 min. After, incubation then continued in starvation with or without BT2 (250 μM), KIC (200 μM) and rapamycin (50 nM), and with or without 100 nM insulin for 20 min. Then cells were used for glucose transport assay or harvested for immunoblotting. Schematic of experimental design outlined in Appendix C.

Glucose transport

Following treatments, myotubes cultured in 12-well plates were washed twice with HEPES [4-(2-hydroxy-ethyl)piperazine-1-ethanesulfonic acid]-buffered saline]. They were then incubated

in 300 μL of transport solution (HEPES buffer, pH 8, 10 μM 2-deoxyglucose, 0.5 μCi/ml [^{3}H]-2-deoxyglucose) for 5 min at 37°C and 2-deoxyglucose transport was performed as described previously (107,351). Following the 5-min incubation, plates were placed on ice and cells were washed with ice-cold saline 3 times. They were then lysed with 1 mL of cold 0.05 M NaOH. An aliquot of the lysate was used to determine protein concentration while another aliquot was counted. Glucose transport was calculated by dividing the radioactivity counts by the specific activity of the transport solution to obtain pmol of deoxyglucose transported. This value was then divided by the protein concentration in each well to obtain pmol of deoxyglucose transported per μg protein. Then this data was normalized to the non-insulin group. Full protocol outlined in appendix D.

BCKD Activity Assay

BCKD catalyzes the irreversible oxidative decarboxylation of the BCKAs. Cells were seeded into a 6-well plate. Cells were supplemented with a 1-^{14}C labelled valine. CO_2 released from the oxidative decarboxylation of valine's ketoacid α-ketoisovalerate (KIV) is collected in 2 M NaOH soaked filter paper wicks. This radiolabelled bicarbonate on the filter paper wick is transferred into a 20 ml scintillation vial (Perkin-Elmer, #6008118) containing 3.5 ml of scintillation fluid (Ecoscint A, National Diagnostics, #LS-273). Cells are harvested to correct for protein content. Relative values are counts per minute (CPM)/μg of protein. Full protocol outlined in Appendix E. We used valine instead of leucine, as valine-derived KIV is the preferred substrate for BCKD (352).

Amino Acid Concentrations

Following treatments, myotubes were washed 2× in PBS, then harvested with 10% trichloroacetic acid. Lysates were centrifuged at 2.3 ***g*** for 15 min. Supernatant containing free amino acids were diluted in a 1:2:1:8 ratio (sample: potassium phosphate buffer: 0.1 N hydrochloric acid: HPLC grade water, respectively). Diluted samples were pre-column derivatized with a 1:1 ratio of sample to o-Phthalaldehyde (29.28 mM). They were then injected into a YMC-Triart C18 column (C18, 1.9 µm, 75 × 3.0 mm) fitted onto an ultra-high-pressure liquid chromatography system (Nexera X2, Shimadzu, Kyoto, Japan) that was connected to a fluorescence detector (excitation: 340 nm; emission: 455 nm). Amino acids were eluted with a gradient solution derived from 20 mM potassium phosphate buffer (6.5 pH) mobile phase (mobile phase A) and a solution made from 45% acetonitrile, 40% methanol and 15% HPLC grade water (mobile phase B) at a flow rate of 0.8 mL/min. A gradient of 5%–100% of mobile phase B over 21 min was used. Amino acid concentrations were calculated using amino acid standard curves and were normalized to total protein. Full protocol outlined in Appendix G.

BCKA Concentrations

Following treatments, myotubes were washed 2× in PBS, then harvested with lysis buffer (1 mM EDTA, 2% sodium dodecyl sulfate (SDS), 25 mM Tris-HCl, pH 7.5, 1 mM DTT, and 10 µl/ml of each of protease inhibitor and phosphatase inhibitor cocktails). Lysates were centrifuged at 10000 ***g*** for 10 min. Supernatant containing free BCKAs were diluted in a 1:2:1:8 ratio (sample: potassium phosphate buffer: 0.1 N hydrochloric acid: HPLC grade water, respectively). Diluted samples were treated with a 1:1 ratio of DMB solution. DMB solution was prepared by adding 1.6 mg of DMB to 1.0 mL of solution, which contained 4.9 mg of sodium sulfite, 70 µL of 2-

mercaptethanol, and 58 µL of 12 M HCl in 0.87 mL of ddH_2O. Once samples were treated with DMB, this solution was heated at 85°C for 45 minutes then cooled on ice for at least 5 min. They were injected into an Inertsil ODS-4 column (2 µM, 100 × 2.1 mm; GL Sciences, Torrance, CA, USA) fitted onto an ultra-high-pressure liquid chromatography system (Nexera X2, Shimadzu, Kyoto, Japan) that was connected to a fluorescence detector (excitation: 367 nm; emission: 446 nm). Mobile phases were: (A) HPLC-grade methanol/ddH_2O (30/70, v/v) and (B) HPLC-grade methanol. Gradient elution was performed as follows: 0 min 0% B, 3.33 min 0%B, 5 min 50%B, 17.34 min 50%B. The flow rate was 0.2 mL/min, and the column temperature was maintained at 40°C. Full protocol outlined in Appendix H.

Gene Silencing

On D3 of differentiation cells were transfected with 50 nM of BDK (Sigma Aldrich, #NM019244) (sense 5'-CUAUGCAUGGCUUUGGCUU, anti-sense 5'-GAUACGUACCGAAACCGAA) or TSC-2 (Sigma Alrdich, #NM_012680) (sense 5'-GAGAUUGUUCUGUCCAUAA, anti-sense 5'-CUCUAACAAGACAGGUAUU) or BCAT2 (sense 5′-GAGUGCAUCCGCCAGCUCA, anti-sense 5′-UGAGCUGGCGGAUGCACUC) siRNA oligonucleotides or 50 nM of scrambled siRNA (Sigma Aldrich, #SIC-001) oligonucleotides using Lipofectamine RNAiMAX reagent according to the manufacturer's instructions into 1mL of AMEM containing 2% HS and no ab-am. Twenty-four hours following transfection, 1mL of AMEM containing 2% HS, 1% ab-am was added to the transfected cells on top of the existing media. Full protocol described in Appendix I.

Protein Assay and Western Blot

Following treatments, cells were harvested in lysis buffer (1 mM EDTA, 2% sodium dodecyl sulfate (SDS), 25 mM Tris-HCl, pH 7.5, 1 mM DTT, and 10 µl/ml of each of protease inhibitor and phosphatase inhibitor cocktails). Then the Pierce BCA Protein Assay Kit (Thermo Scientific, #23225) was used to determine protein concentration. The KC4 plate reader software (Bio-Tek Instruments Inc., Winooski, Vermont, United States) was used to acquire an absorbance reading of each well at a wavelength of 550 nanometers. A standard curve was used to estimate the volume needed to load 25 µg of protein into each well of a polyacrylamide gel. The proteins were separated on 10% SDS-polyacrylamide gel electrophoresis (SDS-PAGE). Following gel electrophoresis, they were transferred onto polyvinylidene difluoride (PVDF) 0.2 µm pore sized membranes (Bio-RAD, #1620177). Transfer efficiency was checked with a ponceau dye treatment to the membranes to check the protein was transferred. This dye was then washed off with 3 5-minute washes of Tris Buffered Saline with Tween (TBST). Next, membranes were incubated for one hour in 5% non-fat milk in TBST at room temperature to block non-specific antigen binding. Subsequently, they were quickly washed 3 times, 5 minutes each with TBST at room temperature and then incubated overnight at 4°C with the primary antibody of interest.

Table 4.1: List of Antibodies used.

Primary Antibody	Dilution	Company Purchased From	Secondary Antibody Used
ph-S6K1 (Thr389)	1:1000	Cell Signaling (CST) #9205	Anti-rabbit (CST #7074)
BDK	1:1000	Thermo Fisher #PA5-31455	Anti-rabbit (CST #7074)
ph-Akt (Ser473)	1:1000	CST #9271	Anti-rabbit (CST #7074)
γ-Tubulin	1:10000	Sigma Aldrich #T6557	Anti-mouse (CST #7076)
ph-IRS-1 (Ser612)	1:1000	CST #3203	Anti-rabbit (CST #7074)

ph-BCKD (Ser293)	1:1000	CST #40368	Anti-rabbit (CST#7074)
ph-S6 (Ser235/6)	1:2000	CST #4858	Anti-rabbit (CST#7074)
BCAT2	1:1000	ProteinTech #16417-1-AP	Anti-rabbit (CST #7074)
ph-ACC (Ser79)	1:1000	CST #3661	Anti-rabbit (CST #7074)

Following the overnight incubation in primary antibody, membranes were washed 3 times for 5 minutes each with TBST and were incubated in a secondary antibody for three hours at room temperature. Secondary antibodies were diluted into a 5% milk with TBST solution before incubation with the membranes. Secondary antibodies; anti-rabbit (CST # 7074) or anti-mouse (CST #7076) antibodies were used with the dilution of 1:10000. Subsequently, membranes were washed 3 times for 5 minutes each with TBST before HRP chemical luminescent substrate was applied to them. Bio-RAD ChemiDoc XRS+ was used for signal visualization and the images were quantified with Image Lab software (version 8; Bio-RAD, Hercules, California, United States).

Statistical Analysis and Data Presentation

Glucose transport data are presented as pmol of 2-deoxyglucose per μg protein and normalized to the basal group (without insulin) as control. BCKD activity data are presented as CPM per μg protein. Proteins for western blots were adjusted for loading using γ-tubulin values. Statistical analyses were performed using GraphPad Prism 8 software (GraphPad, Massachusetts, United States). Data are presented as mean ± SEM. Two-way analysis of variance (ANOVA)

was used and Tukey's post-hoc tests were done to measure statistically significant differences among means. Significance was determined as $p < 0.05$.

4.4 Results

BDK knockdown resulted in significantly reduced BDK protein (Fig 4.1A, $p<0.0001$). BDK depletion increased insulin-stimulated glucose uptake (Fig 4.1B, $p<0.05$). There was a trend ($p=0.054$) for KIC-induced suppression of insulin-stimulated glucose uptake in control cells (SCR). This effect was attenuated in BDK depleted cells (Fig 4.1B).

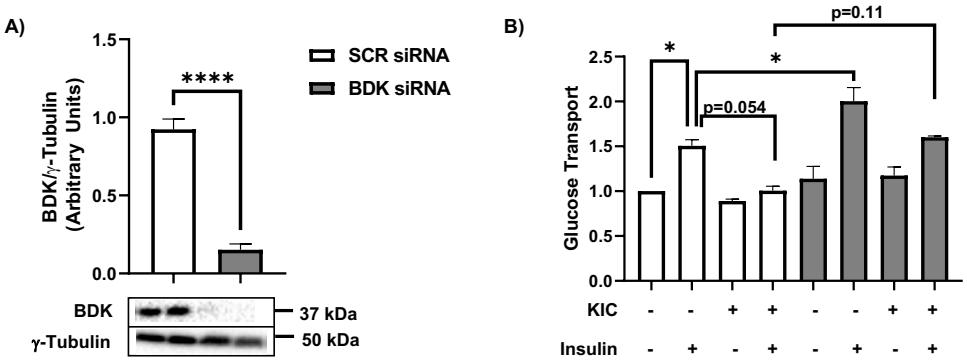

Figure 4.1: BDK depletion attenuates the suppressive effect of KIC on insulin-stimulated glucose uptake.
Cells were transfected with control (SCR) or BDK siRNA oligonucleotides. Forty-eight h later, cells were starved in a medium lacking amino acids and serum for 3 hours. They were then treated without (−KIC) or with 200 μM KIC (+KIC) for 30 min. After, cells were incubated with or without 100 nM insulin for 20 min. Proteins in lysates were immunoblotted against BDK (A). Glucose uptake assay was performed (B). Glucose uptake, expressed as picomole of 2-deoxyglucose transported into the cell/μg protein and normalized to the no insulin (-insulin), in the SCR condition. n = 3 biological replicates with three technical replicates per experiment. Data presented as Means ± SEM. * $p<0.05$, **** $p<0.0001$.

Next, we examined the effect of BDK depletion and KIC supplementation on components of insulin/mTORC1 signaling, as the effects of KIC on glucose transport is mediated through mTORC1 signaling (16,17). There was no effect of BDK depletion or KIC supplementation on Akt (Ser473) phosphorylation (Fig 4.2A-B). There was a trend for increased insulin-stimulated S6K1 (Thr389) phosphorylation in response to KIC treatment (Fig 4.2A, 4.2C, $p=0.055$), but this effect was attenuated in BDK depleted cells (Fig 4.2A, 4.2C). Similarly, KIC increased insulin-stimulated IRS-1 (Ser612) phosphorylation ($p<0.05$), a negative regulator of insulin signaling that is phosphorylated by S6K1, but this effect was attenuated in BDK depleted cells (Fig 4.2A, 4.2D). These data suggest BDK depletion attenuates KIC-induced suppression of insulin-stimulated glucose uptake by attenuating the increase in S6K1/IRS-1 phosphorylation.

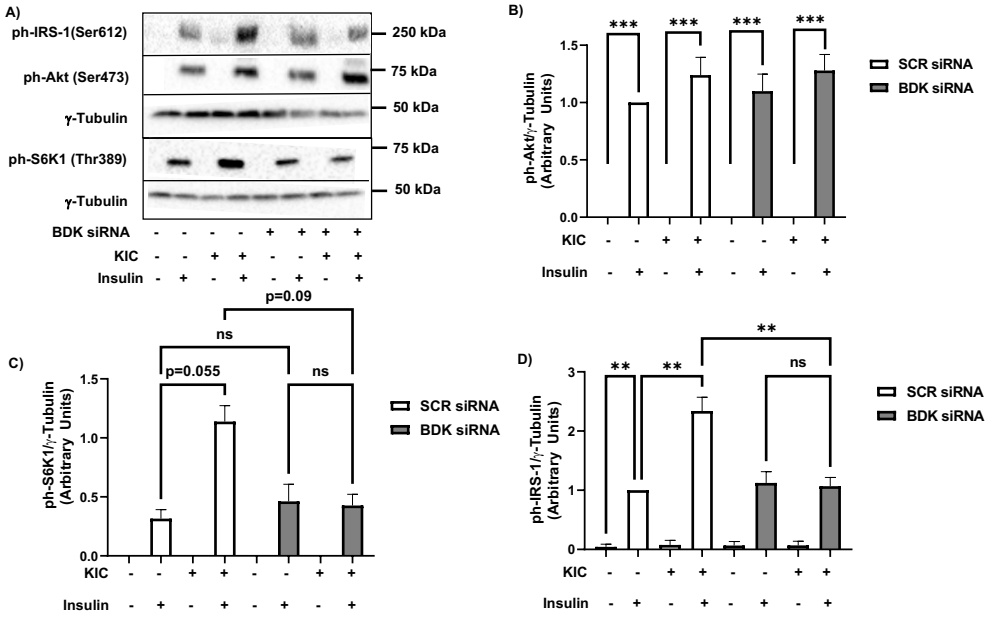

Figure 4.2: BDK depletion attenuates phosphorylation of S6K1/IRS-1 induced by KIC
Cells were treated as described in Fig 4.1. Proteins in lysates were immunoblotted against phosphorylated (ph)-Akt (Ser473) (A, B), ph-S6K1 (Thr389) (A, C), and ph-IRS-1 (Ser612) (A, D). n=3 biological replicates with 3 technical replicates per experiment. Data presented as Means ± SEM. ns = not significant, * $p<0.05$, ** $p<0.01$, *** $p<0.001$.

The above experiments involve genetic alterations to increase BCAA oxidation. In addition to BDK knockdown experiments, we used a relatively more acute pharmacological approach to increase BCKD activity, by treating the cells with BT2, a BDK inhibitor. First, we examined the effect of BT2 on myotube morphology and cell cytotoxicity to ensure myotubes were not compromised with drug treatment. BT2 did not have any effect on myotubes morphology or on cell viability (Fig 4.3A-C). There was also no effect of BT2 on protein concentration (Fig 4.3D).

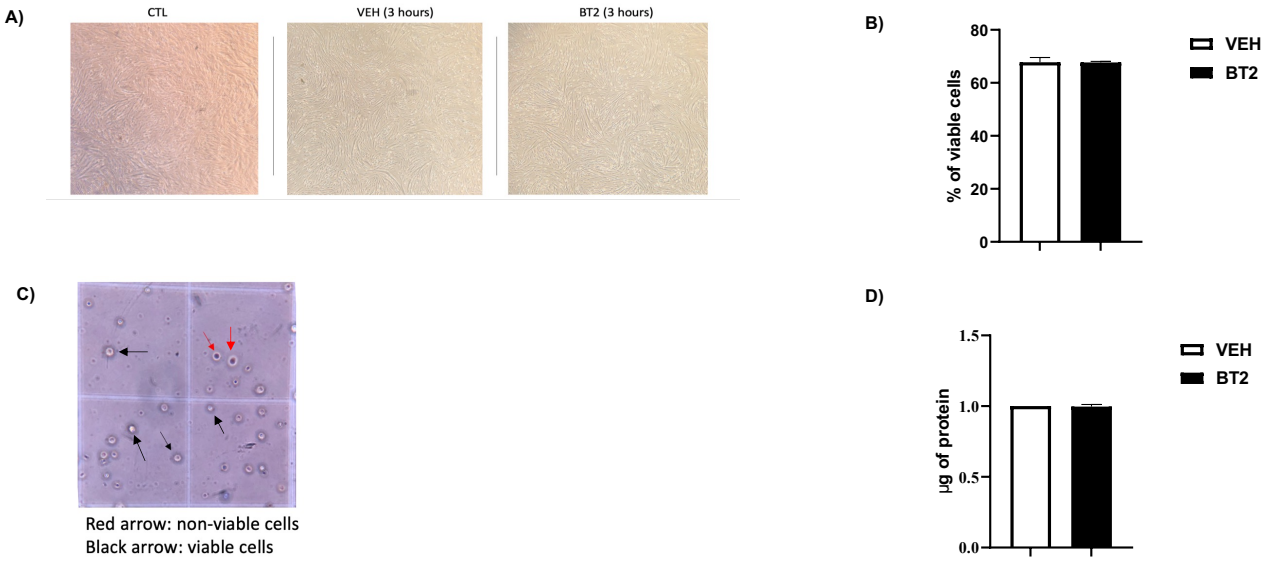

Figure 4.3: BT2 does not affect cell morphology or viability cells.
L6 myotubes were incubated for 3 h in 250µM of BT2 in a starvation medium that lacked amino acids and serum. After, cells were trypsinized and then resuspended in trypan blue. Then using a hemocytometer, viable cells (black arrow) and non-viable cells (red arrow) were counted. Light microscope image of the cells following drug/vehicle treatment at 4x magnification (A), and percentage of viable cells counted using trypan blue dye (B). Microscope image of cells with trypan blue dye at 40x magnification (C). Protein concentration following VEH and BT2 treatment (D). n=3 biological replicates with 3 technical replicates per experiments. Data presented as Means ± SEM.

KIC reduced phosphorylation of BCKD (Ser293) and phosphorylation of BCKD was not detected in BT2 treated conditions (Fig 4.4A-B, $p<0.05$). Since KIC can activate BCKD (280,353), we wanted to ensure BCKD was activated to a greater extent in BT2 treated

conditions. BT2 increased BCKD activity in control ($p<0.01$) and KIC treated conditions BT2-treated cells (Fig 4.4C, $p=0.07$). KIC reduced insulin-stimulated glucose uptake, but this effect was attenuated in BT2-treated cells (Fig 4.4D, $p<0.05$). It has previously been shown that KIC is converted back to leucine to elicit its effects on insulin-stimulated glucose uptake (17). Here we showed that BT2 treatment reduced accumulation of leucine in KIC-treated cells (Fig 4.4E), potentially explaining why KIC-induced suppression of insulin-stimulated glucose uptake was attenuated. BT2 did not affect myotube isoleucine, valine, or glutamate (Fig 4.4F-H) levels with or without KIC treatment.

As shown in our BDK depleted experiments (Fig 4.2A-B), there was no effect of KIC or BT2 treatment on insulin-stimulated Akt (Ser473) phosphorylation (Fig 4.4A, 4.4I). Like the BDK experiments (Fig 4.2A, 4.2C-D), insulin or insulin plus KIC increased insulin-stimulated S6K1 (Thr389) and IRS-1 (Ser612) phosphorylation, however, this was attenuated in BT2 treated cells (Fig 4.4A, 4.4J-K).

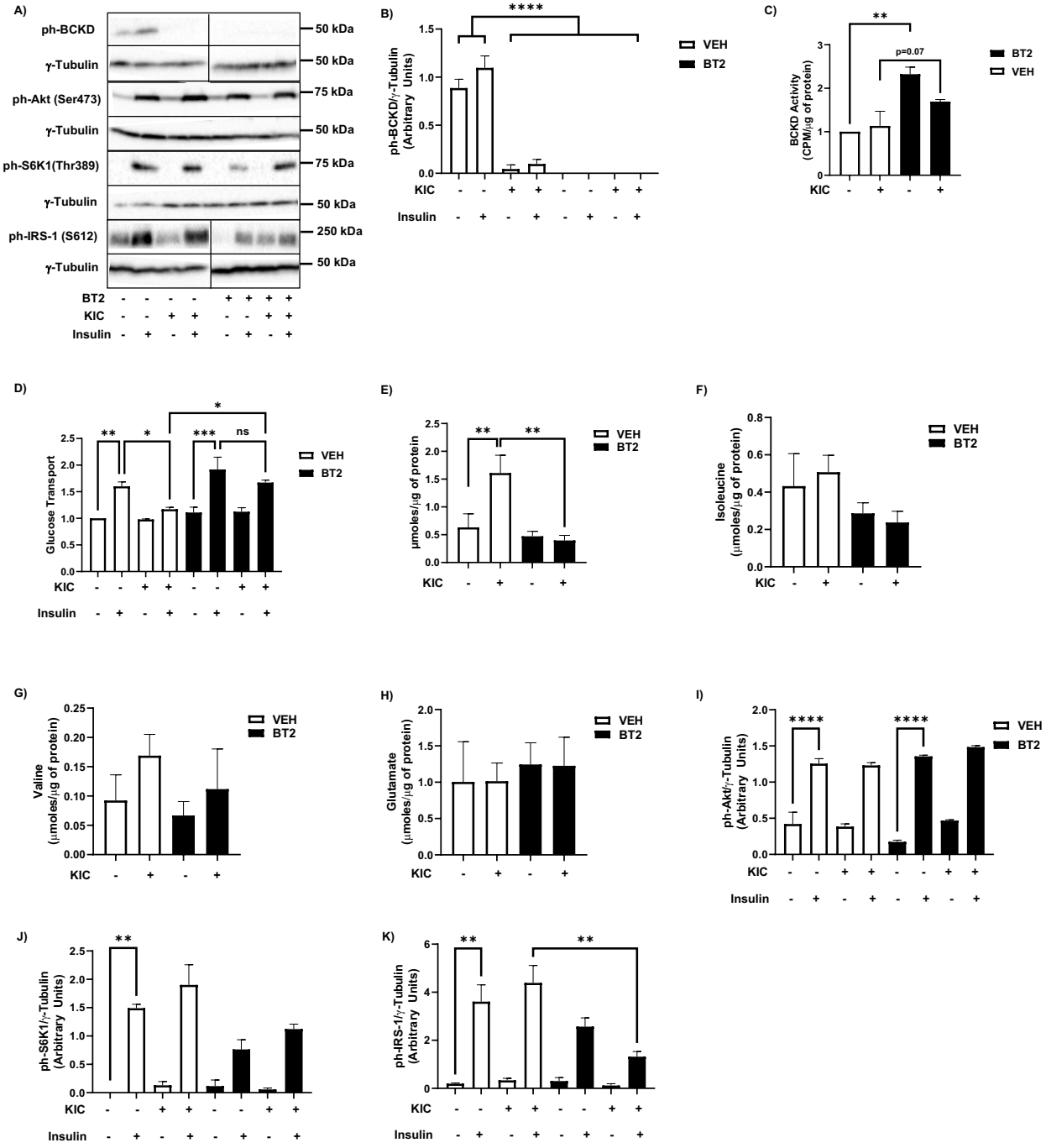

Figure 4.4: BDK inhibition attenuates the suppression of KIC on insulin-stimulated glucose uptake.

L6 myotubes were incubated for 3 h in 250μM of BT2 in a starvation medium that lacked amino acids and serum. Incubation then continued in the medium with BT2 that was also supplemented with or without KIC (200 μM) for 30 min. After, cells were incubated with or without 100 nM insulin for 20 min. Proteins in lysates were immunoblotted against ph-BCKD (Ser293) (A, B).

BCKD assay (C), glucose uptake assay (D) and measurement of intracellular leucine (E), isoleucine (F), valine (G), and glutamate (H) concentrations were performed. Proteins in lysates were also immunoblotted against ph-Akt (Ser473) (A, I), ph-S6K1 (Thr389) (A, J) and ph-IRS-1 (Ser612) (A, K). Glucose uptake, expressed as picomole of 2-deoxyglucose transported into the cell/µg protein and normalized to the no insulin (-insulin), in the VEH condition. n=3 biological replicates with 3 technical replicates per experiment. Data presented as Means ± SEM. ns = not significant, * $p<0.05$, ** $p<0.01$, *** $p<0.001$, **** $p<0.0001$.

Since, BT2 prevented the accumulation of leucine from KIC treatment (Fig 4.4E), as shown in our previous study (107), we wanted to confirm BCAT2 was responsible for the conversion of KIC to leucine. Here we show that the conversion of KIC to leucine requires BCAT2 (Fig 4.5A-B). We also show that the effect of BT2 on glucose transport in cells treated with KIC was more pronounced with BDK depletion (Fig 4.6A-B). BDK inhibition does not attenuate KIC-induced suppression of insulin-stimulated glucose uptake as well as BDK depletion.

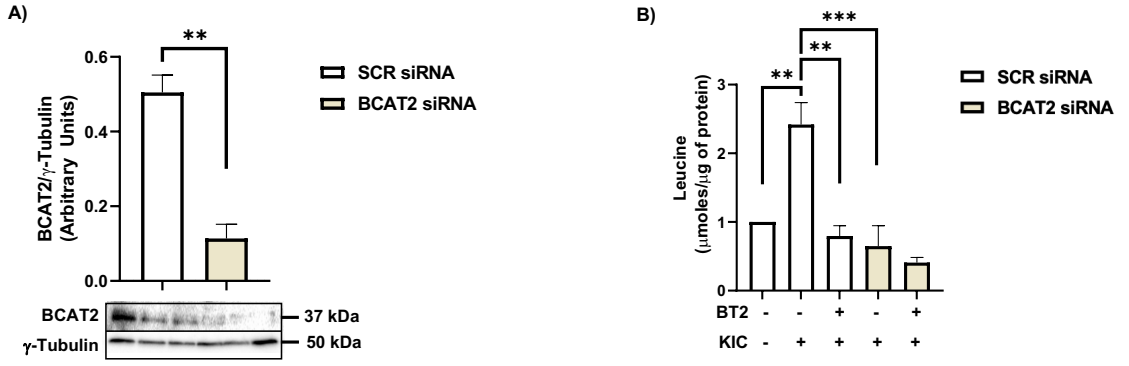

Figure 4.5: BCAT2 knockdown prevents conversion of KIC to leucine.
Cells were transfected with control (SCR) or BCAT2 siRNA oligonucleotides. Forty-eight h later L6 myotubes were incubated for 3 h in 250 μM of BT2 in a starvation medium that lacked amino acids and serum. Incubation then continued in the medium with BT2 that was also supplemented with or without KIC (200 μM) for 30 min. Proteins in lysates were immunoblotted against BCAT2 (A) and intracellular leucine concentrations were determined by HPLC (B). n=3 biological replicates with 3 technical replicates per experiments. Data presented as Means ± SEM. ** p<0.01.

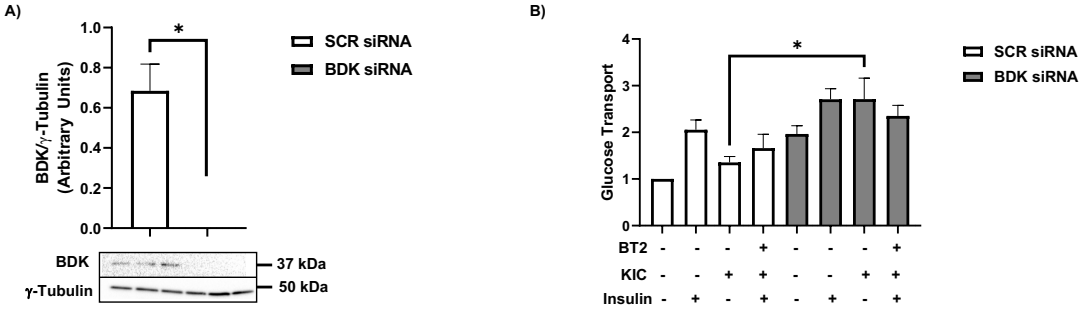

Figure 4.6: BDK depletion has a greater effect that BT2 on insulin-stimulated glucose transport
Cells were transfected with control (SCR) or BDK siRNA oligonucleotides. Forty-eight h later L6 myotubes were incubated for 3 h in 250 μM of BT2 in a starvation medium that lacked amino acids and serum. Incubation then continued in the medium with BT2 that was also supplemented with or without KIC (200 μM) for 30 min. After, cells were incubated with or without 100 nM insulin for 20 min. Proteins in lysates were immunoblotted against BDK (A). Glucose transport assay was performed (B). Glucose transport was expressed as picomole of 2-deoxyglucose transported into the cell/μg protein and normalized to the no insulin (-insulin) in SCR condition. n=3 biological replicates with 3 technical replicates per experiment. Data presented as Means ± SEM. * p<0.05

Next, we wanted to assess the effect of BT2 with BCAAs or BCKAs on insulin resistance, as leucine and KIC exist in the presence of the other BCAAs and BCKAs. Leucine or the BCAAs had no effect on BCKD activity (Fig 4.7B) or insulin-stimulated glucose transport (Fig 4.7C). Insulin-stimulated increase in Akt (Ser473) phosphorylation was not modified by leucine, BCAA or BT2 treatment (Fig 4.7A, 4.7D). There was a trend for increased S6K1 (Thr389) phosphorylation (40% increase relative to insulin only, Fig 4.7A, 4.7E), in response to BCAA and leucine treatment, but these effects were not statistically significant. BT2 treatment also tended to suppress the effects of leucine/BCAAs on S6K1 (~32% decrease relative to vehicle treated cells; Fig 4.7A, 4.7E) and IRS-1 (Ser612) phosphorylation (~70% decrease relative to vehicle treated cells; Fig 4.7A, 4.7F). There was no effect on the phosphorylation of another downstream substrate of BDK, acetyl-CoA carboxylase (ACC) (Ser79) (Fig 4.7A, 4.7G) in any of the treatments, although the effect of insulin on ACC phosphorylation tended to be lower (~50%) in BT2-treated cells.

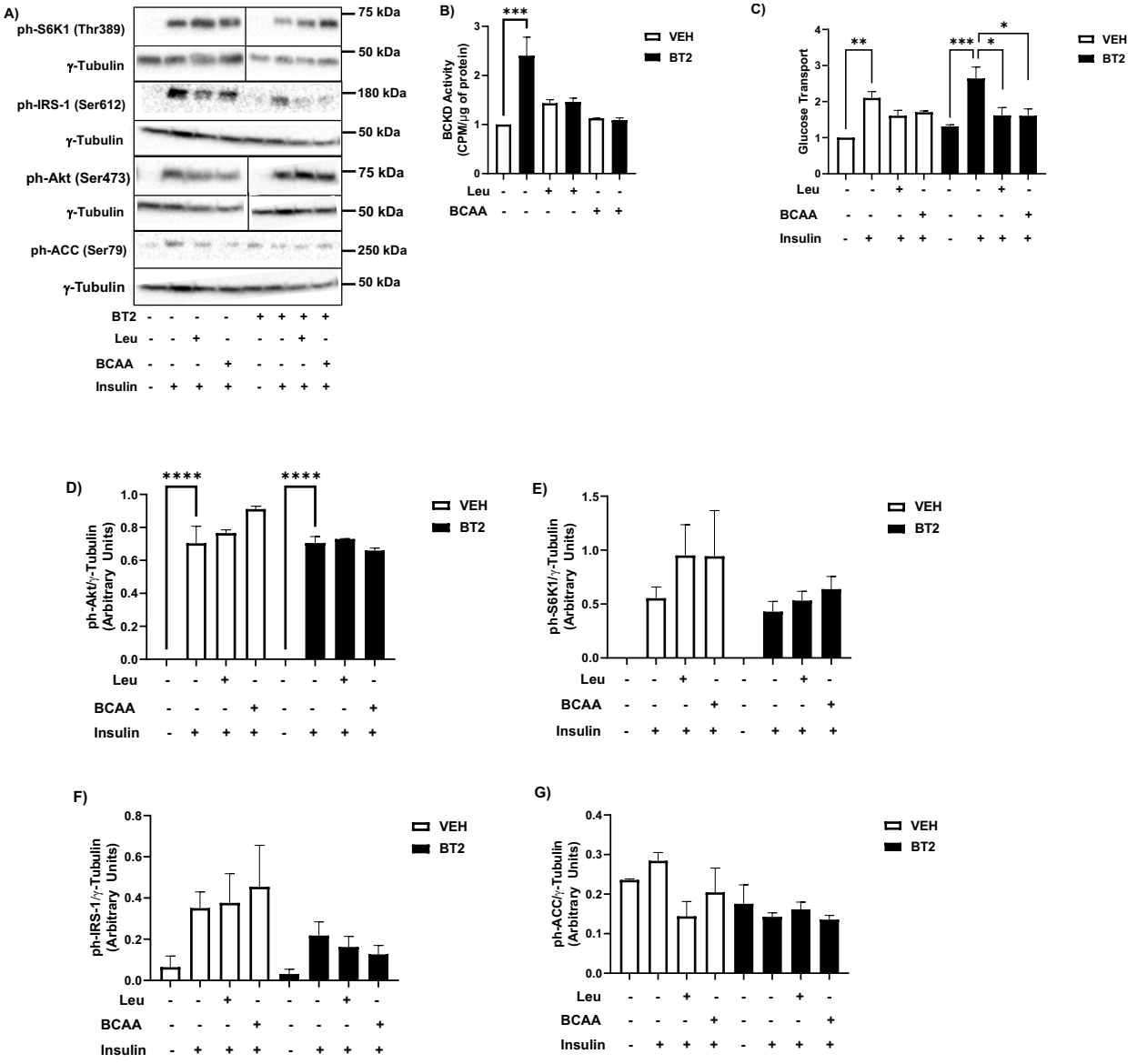

Figure 4.7: Inhibition of BDK did not modify the suppression of BCAA on insulin stimulated glucose uptake.

L6 myotubes were incubated for 3 h in 250µM of BT2 in a starvation medium that lacked amino acids and serum. Incubation then continued in starvation medium with BT2 along with the addition of leucine (150 µM) or BCAA (total 400 µM: consisting of 175 µM of valine, 150 µM of leucine and 75 µM of isoleucine) for 30 min. After, cells were incubated with or without 100 nM insulin for 20 min. After treatments, BCKD activity assay (B) and glucose uptake (C) were performed. Proteins in lysates were immunoblotted against ph-Akt (Thr389) (A, D), ph-S6K1 (Thr389) (A, E), ph-IRS-1 (Ser612) (A, F), and ph-ACC (Ser79) (A, G). Glucose uptake, expressed as picomole of 2-deoxyglucose transported into the cell/µg protein and normalized to the no insulin (-insulin), in the VEH condition. n=3 biological replicates with 3 technical replicates per experiment. Data presented as Means ± SEM. * $p<0.05$, ** $p<0.01$, *** $p<0.001$, **** $p<0.0001$.

KIC supplementation led to increased levels of leucine (Fig 4.8A, $p<0.05$) and KIC (Fig 4.8B, $p<0.001$), which was attenuated by BT2 treatment. BCKA treatment only marginally increased leucine (Fig 4.8A), KIC (Fig 4.8B), KIV (Fig 4.8C), and KMV (Fig 4.8D) levels, but they were reduced with BT2 treatment. BCKAs and KIC decreased BCKD phosphorylation (Fig 4.8E-F, $p<0.05$). There was also a slight increase in BCKD activity when BCKAs and KIC were supplemented with BT2 (Fig 4.8G), but this was not statistically significant. Unlike for BCAAs and leucine, KIC and BCKA supplementation significantly reduced insulin-stimulated glucose uptake (Fig 4.8H, $p<0.01$). The effect of KIC and BCKAs on insulin-stimulated glucose uptake was attenuated with BT2 treatment. KIC/BCKAs, with or without BT2, did not modify Akt (Ser473) phosphorylation (Fig 4.8E, 4.8I). BCKAs and KIC increased insulin-stimulated S6K1 (Thr389) phosphorylation (Fig 4.8E, 4.8J, $p<0.001$), which was attenuated with BT2 treatment. There was no effect of KIC and BCKAs with or without BT2 on IRS-1 (Ser612) phosphorylation, although the values in BT2 groups were less in groups treated with KIC/BCKAs (Fig 4.8E, 4.8K). KIC/BCKA, with or without BT2, did not modify ACC (Ser79) phosphorylation (Fig 4.8E, 4.8L).

Figure 8

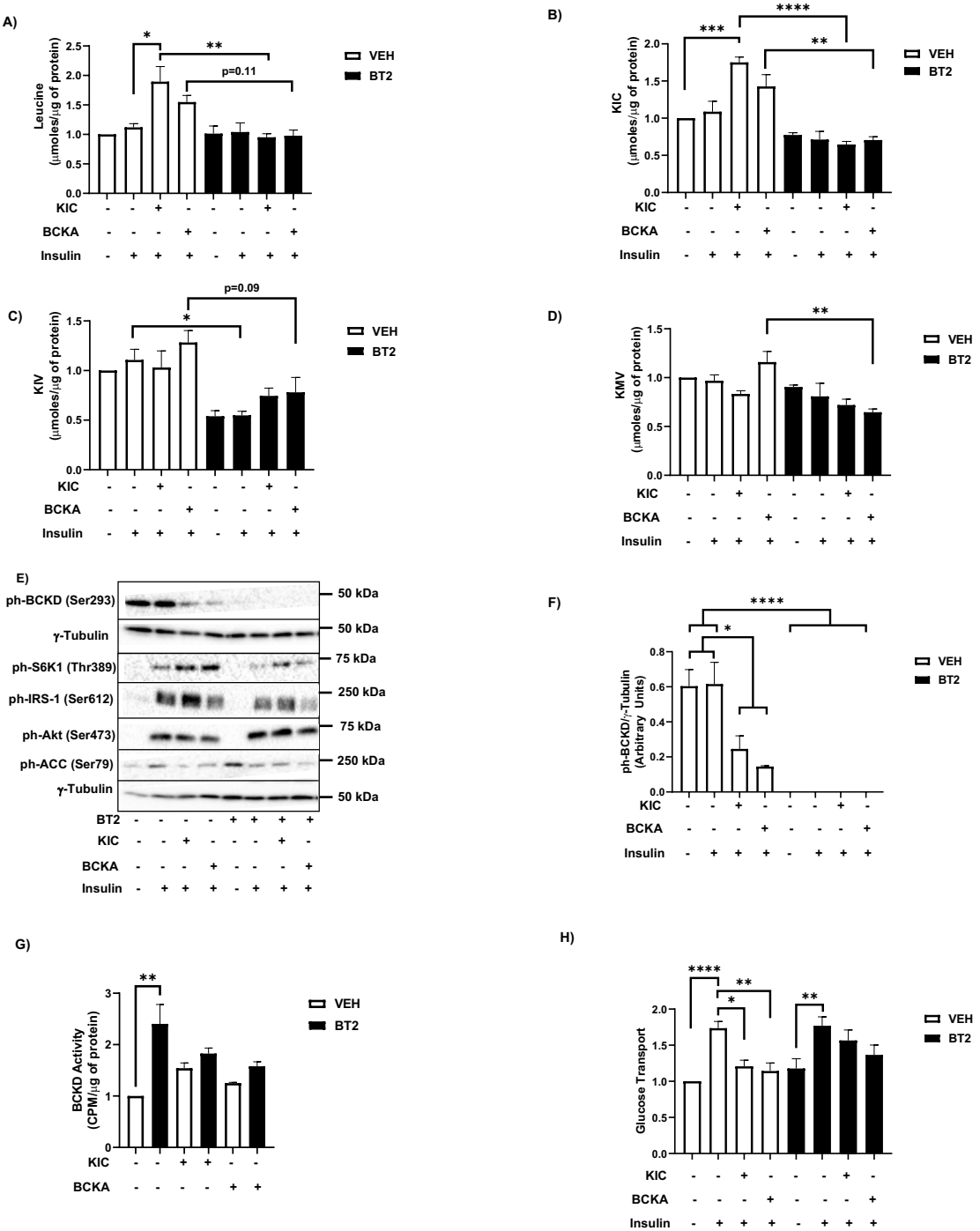
A)
Leucine (µmoles/µg of protein)
VEH
BT2
p=0.11
KIC
BCKA
Insulin
B)
KIC (µmoles/µg of protein)
C)
KIV (µmoles/µg of protein)
p=0.09
D)
KMV (µmoles/µg of protein)
E)
ph-BCKD (Ser293)
γ-Tubulin
ph-S6K1 (Thr389)
ph-IRS-1 (Ser612)
ph-Akt (Ser473)
ph-ACC (Ser79)
50 kDa
75 kDa
250 kDa
BT2
F)
ph-BCKD/γ-Tubulin (Arbitrary Units)
G)
BCKD Activity (CPM/µg of protein)
H)
Glucose Transport

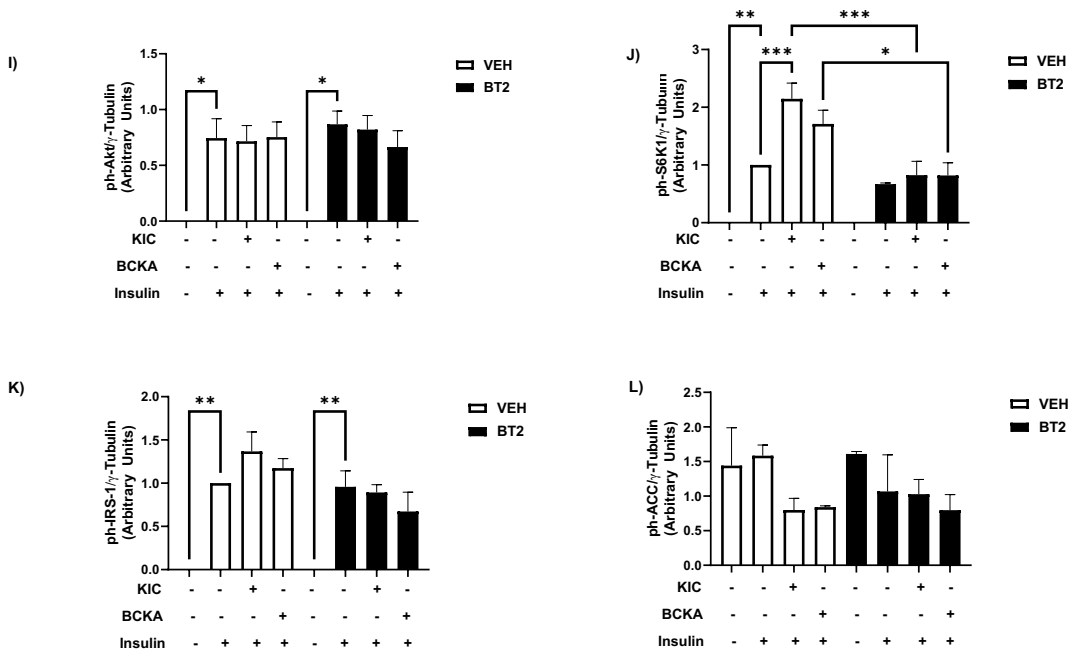

Figure 4.8: BDK inhibition attenuates the suppression of glucose uptake by BCKA.
L6 myotubes were incubated for 3 h in 250μM of BT2 in a starvation medium that lacked amino acids and serum. Incubation then continued in starvation medium with BT2 along with the addition of KIC (200 μM) or BCKA (total 200 μM: consisting of 76 μM of KIC and 62 μM for each of KMV and KIV) for 30 min. After, cells were incubated with or without 100 nM insulin for 20 min. After treatments, cells were harvested and measurement of intracellular leucine (A), KIC (B), KIV (C), and KMV (D) were performed. Protein in lysates were immunoblotted against ph-BCKD (Ser293) (E, F). BCKD activity assay (G) and glucose uptake assay (H) were performed. Protein in lysates were also immunoblotted against ph-Akt (Ser473) (E, I), ph-S6K1 (Thr389) (E, J), ph-IRS-1 (Ser612) (E, K), and ph-ACC (Ser79) (E, L). Glucose uptake, expressed as picomole of 2-deoxyglucose transported into the cell/μg protein and normalized to the no insulin (-insulin), in the VEH condition. n=3 biological replicates with 3 technical replicates per experiment. Data presented as Means ± SEM. * $p<0.05$, ** $p<0.01$, *** $p<0.001$, **** $p<0.0001$

Based on our data in Fig 4.2, the relationship between suppressed insulin-stimulated glucose transport and the activation of S6K1/IRS1 is apparent. Depleting or inhibiting BDK also suggests a link between attenuating the effect of KIC-induced suppression of insulin-stimulated glucose uptake and the S6K1/IRS1 signaling pathway. To mechanistically confirm that this signaling pathway is necessary for KIC to elicit its effects, we combined TSC2 deletion and

treatment with MHY1485, an mTOR activator to re-establish mTORC1/S6K1/IRS-1 signalling in the presence of BT2 and KIC treatment. With TSC-2 knockdown and MHY1485 treatment combined, we showed greater S6 (Ser235/6) phosphorylation (Fig 4.9A-B, $p<0.05$) and IRS-1 (Ser612) phosphorylation (Fig 4.9A, 4.9C, $p<0.05$). As shown before, KIC suppressed insulin-stimulated glucose uptake, which was attenuated by BT2. However, this attenuation is absent when mTORC1/S6K1/IRS-1 signaling is restored (Fig 4.9D), showing that the inhibitory mTORC1/S6K1/IRS-1 pathway contributes to the suppression of insulin-stimulated glucose uptake from KIC supplementation in myotubes.

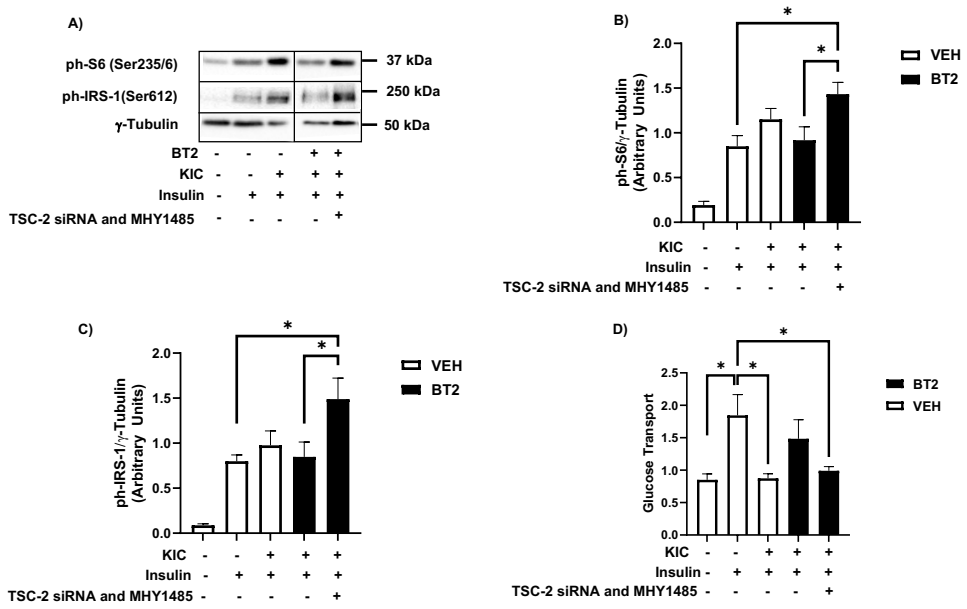

Figure 4.9: Suppression of mTORC1 is required for the attenuating effect of BT2 on the impairment in glucose uptake by KIC.

Cells were transfected with control or TSC-2 siRNA oligonucleotides. Forty-eight h later, they were treated with or without 250μM of BT2 and with or without 10μM of MHY1485 in serum- and amino acid-free medium for 3 h. Afterwards, the cells were supplemented without (−KIC) or with 200 μM KIC (+KIC) for 30 min followed by incubation with or without 100 nM insulin for 20 min. After treatments, proteins in lysates were immunoblotted against ph-S6 (Ser235/6) (A, B) and ph-IRS-1 (Ser612) (A, C). Glucose transport assay was performed (D). Glucose uptake was expressed as picomole of 2-deoxyglucose transported into the cell/μg protein and normalized to the no insulin (-insulin), in the VEH condition. Mean ± SEM; n = 3 biological replicates with 3 technical replicates per experiment. * $p<0.05$, ** $p<0.01$.

In our previous work, we showed that the suppressive effect of KIC was dependent on mTORC1, as rapamycin treatment attenuated the suppressive effect of KIC on insulin-stimulated glucose uptake (107). Thus, we were curious and wanted to examine if this suppression held true with BT2 co-treatment. Rapamycin co-treatment with BT2 and KIC further reduced S6K1 (Fig 4.10A-B, $p<0.05$) and S6 phosphorylation (Fig 4.10A, 4.10C, $p<0.01$), which led to a consistent further suppression of insulin-stimulated glucose uptake (Fig 4.10D, $p<0.01$). Based on our results, this suggests that although increased mTORC1 activation reduces glucose transport, some mTORC1 activation is required for glucose uptake, emphasizing the complexity of mTORC1 signalling and its link to glucose transport.

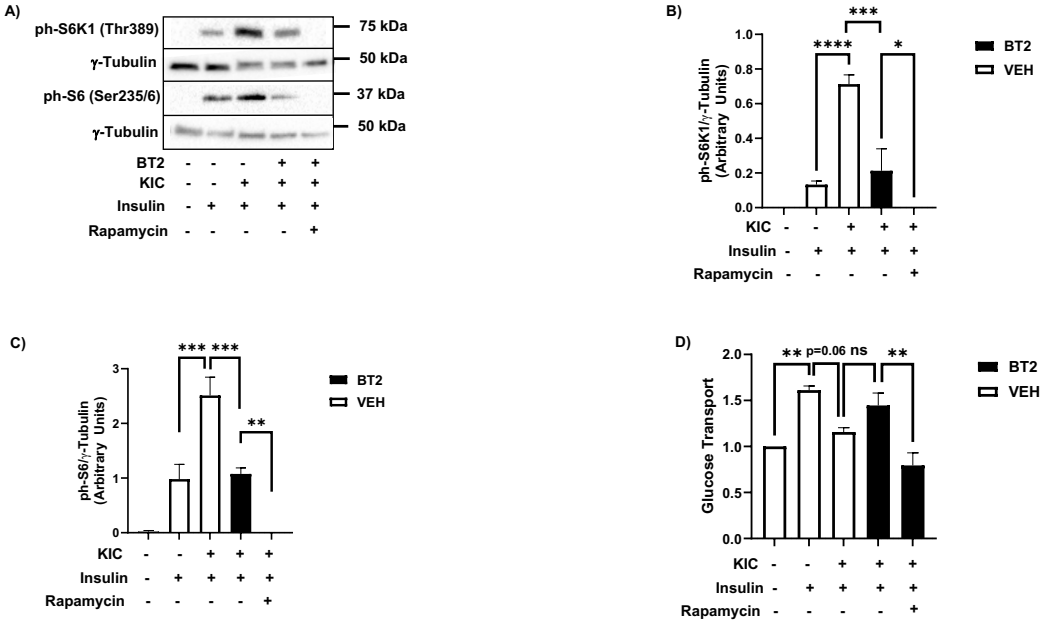

Figure 4.10: The BT2 mediated attenuation of suppressed insulin-stimulated glucose uptake by KIC requires mTORC1 activity.

L6 myotubes were incubated for 3 h in 250μM of BT2 in a starvation medium that lacked amino acids and serum. Incubation then continued in the medium with BT2 or vehicle that was also supplemented with or without KIC (200 μM) for 30 min and with or without rapamycin (an mTORC1 inhibitor, 50 nM). After, cells were incubated with or without 100 nM insulin for 20 min. After treatments, proteins in lysates were immunoblotted against ph-S6K1 (Thr389) (A, B) and ph-S6 (Ser235/6) (A, C). Cells underwent a glucose transport assay (D). Glucose transport was expressed as picomole of 2-deoxyglucose transported into the cell/μg protein and normalized to the no insulin (-insulin), in the VEH condition. n=3 biological replicates with 3 technical replicates per experiment. Data presented as Means ± SEM. ns = not significant, * $p<0.05$, ** $p<0.01$, **** $p<0.0001$.

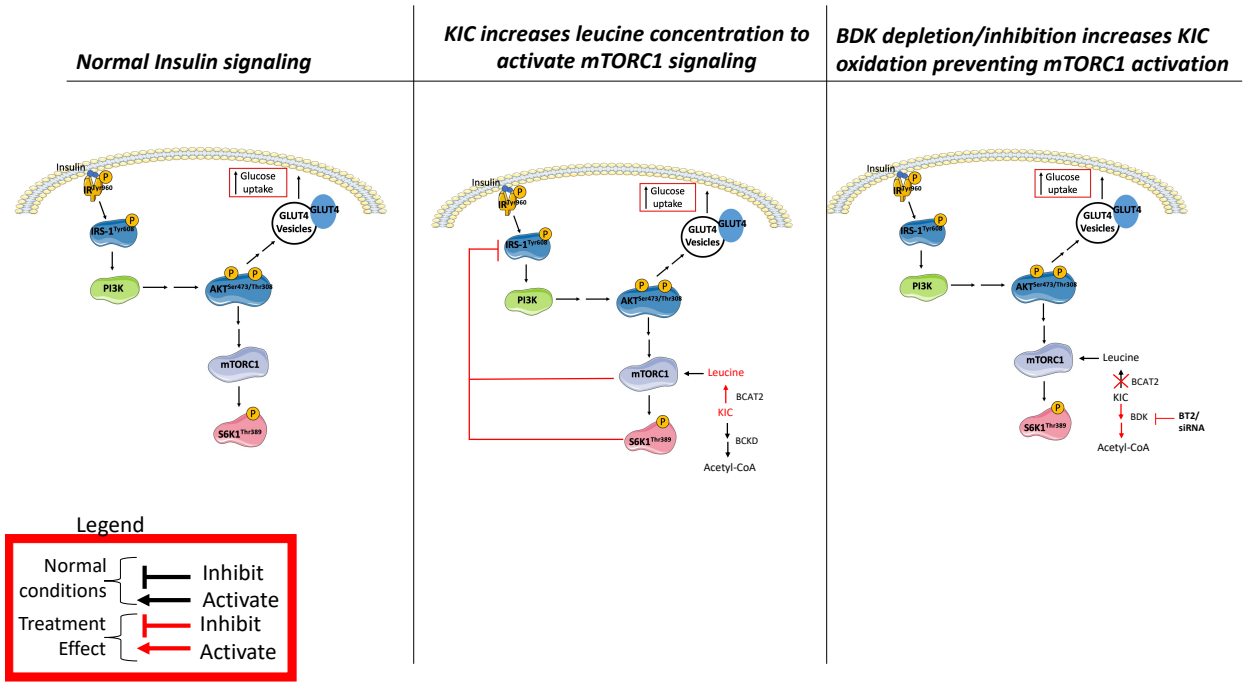

Figure 4.11: Schematic showing how BCAA catabolic enzyme activity affects BCKA induced insulin resistance.

In the first panel, a simplified insulin signaling pathway is shown. In the second panel, with KIC supplementation, KIC is converted back to leucine by BCAT2. Leucine then activates mTORC1/S6K1, leading to the phosphorylation of IRS-1 (Ser612) and thus hindering IRS-1 signaling downstream. In the third panel, with BDK depletion or BT2 treatment, BCKD activity is increased leading to reduced leucine levels, and corresponding attenuation of mTORC1 activation and rescuing of insulin-stimulated glucose uptake.

4.5 Discussion

In this study, we demonstrated a suppression in insulin stimulated glucose uptake by KIC and BCKAs. We also demonstrated that using genetic and pharmacological interventions regulating proteins involved in KIC/BCKA metabolism attenuates their effect on insulin stimulated glucose uptake and related insulin signaling proteins. We also confirmed the role of the mTORC1/S6K1/IRS-1 signaling pathway in KIC-induced insulin resistance (Fig 4.11). Data presented here suggests that increasing BCAA oxidation through enhanced BCKD activity can be a potential therapeutic strategy against insulin resistance in skeletal muscle. Since insulin resistance in skeletal muscle is the primary cause for T2DM (354), our data also suggests that enhanced BCAA oxidative flux may provide benefits for the management and prevention of T2DM and its sequelae.

Elevated levels of BCAA and BCKA show high associations with future diabetes (221), which is mediated by insulin resistance (222). Lotta et al. showed that a genetic predisposition to impaired BCAA metabolism is implicated in T2DM (320). Consistent with this BCAA oxidation and BCAA catabolic enzymes are reduced in insulin resistant states in skeletal muscle (23,24). We have also demonstrated that BCKD depletion reduces insulin-stimulated glucose uptake (17). Consistent with these findings, activating BCKD via BT2 treatment improves whole-body insulin sensitivity, liver steatosis and fatty acid oxidation in the liver of obese mice. However, liver specific knockdown for BDK in these obese mice did not yield similar results, suggesting other tissues like skeletal muscle may play a role in BT2-mediated benefits on insulin sensitivity (337). Studies on BCKD activity have focused on the liver where BCKD activity is the highest. Our previous study (17) and data presented here clearly implicate muscle BCKD regulation in contributing to insulin resistance.

The role of activating BCKD activity in improving insulin sensitivity is consistent with the literature (294,326,337). Vanweert et al, show activating BCKD by sodium phenylbutyrate treatment for two weeks improved insulin sensitivity in T2DM patients (335). Blair et al. also demonstrate BT2 treatment improved insulin sensitivity in mice, but specific activation of BCKD activity in only skeletal muscle, and in liver and skeletal muscle together did not improve insulin sensitivity, but did reduce plasma BCAAs, suggesting contribution of more tissues than just skeletal muscle and liver (333). Additionally, Zhao et al. show that metformin improved insulin sensitivity, but worsened BCAA catabolism (329). They did show that AMPK phosphorylation was increased with consistent decreases in BCKD activity and increased BCAA/BCKA levels (329), This is interesting as AMPK opposes mTORC1 signaling (355), which could be preventing BCAA induced mTORC1 activation. This shows how other mechanisms may impact the mTORC1 mediated effects of BCAAs on insulin sensitivity.

Previous studies have shown that mTORC1 mediates the suppressive effects of BCAAs and BCKAs on insulin resistance (108,356,357). Activated mTORC1/S6K1 phosphorylates inhibitory serine residues of IRS-1 (Ser612) (358), hindering signaling downstream (10,15). Past studies have focused on BCAAs, so it was not clear how the effects of KIC and the other BCKAs could be mediated. However, BCAA supplementation in mice with muscle specific BDK knockout mice have increased S6K1 phosphorylation (359), suggesting that despite enhanced BCKD activity, the role of BCAT2 to provide substrates for BCKD is important and may limit BCAA catabolism. The importance of BCAT2 is evident in our previous work, as BCAT2 knockdown reduces the conversion of KIC back to leucine (17), attenuating the effect of KIC on insulin-stimulated glucose. Here we showed that KIC activated this S6K1-IRS-1 signaling, but BDK depletion or inhibition attenuated this, most likely by increasing the catabolism of KIC to

prevent it from activating this mechanism, as leucine concentration was reduced in cells in which BDK was inhibited. While rapamycin (mTORC1 inhibitor) attenuated the effect of KIC on insulin-stimulated glucose transport (107) in our past work, here we show that activating mTORC1 in the presence of KIC and BT2 re-establishes the suppression of glucose uptake. However, rapamycin treatment in BT2 and KIC treated cells suggests that the action of BT2 requires some mTORC1 activity, as completely abolishing mTORC1 activity back to basal levels reduced insulin-stimulated glucose uptake. Muscle specific ablation of raptor in mice showed increased blood glucose levels via glucose tolerance test (360), and an increase in glucose levels via an insulin tolerance test (361). Both studies are consistent with our data that rapamycin reduces insulin-stimulated glucose transport.

Our data clearly demonstrates that the activation of mTORC1/S6K1/IRS-1 pathway is vital for the effect of KIC on insulin stimulated glucose transport in myotubes in both control and BDK depleted/inhibited conditions.

It is interesting that both increased and reduced activation of mTORC1 reduces glucose transport. As discussed above, increased mTORC1 activation results in phosphorylation of inhibitory serine residues of IRS-1. Interestingly, rapamycin reduces insulin-stimulated glucose transport by reducing insulin-stimulated GLUT4 translocation (362). Furthermore, rapamycin is known to inhibit FKBP12, a protein part of mTORC1, and FKBP12 protein is also necessary for ryanodine receptor function, which are intracellular calcium channels involved in excitation-contraction coupling (363). Loss of FKBP12 proteins leads to calcium leak, which is seen in myopathies and heart failure (364), and an increase in calcium leak suppresses insulin sensitivity in skeletal muscle *in vitro* and *in vivo* (365). Thus, reductions in glucose transport from rapamycin could be due to off-target effects. To prevent off-target effects of a drug, it would be

better to knock down raptor to inhibit mTORC1, but as stated above, muscle specific raptor ablation in mice worsened insulin sensitivity (360,361). Ultimately this suggests that mTORC1 activation must be kept between a certain threshold and any divergence from this may impact insulin sensitivity.

Akt plays a critical role in insulin-stimulated glucose transport (69). However, while there was an effect of insulin on Akt Ser473 phosphorylation, neither KIC nor BT2 influenced Akt Ser473 phosphorylation. However, Zhou et al. demonstrated that BCAA treatment in ob/ob mice given a low protein diet reduced Akt (Thr308) phosphorylation in skeletal muscle, and BT2 increased Akt (Thr308) phosphorylation in ob/ob mice (294). They also demonstrated that BCKA (500 μM) treatment in 3T3-L1 reduced Akt (Thr308) phosphorylation, and this was dependent on mTORC1 (294). On the other hand, whey-protein increased mTORC1 activation and reduced leg glucose uptake with no change in Akt phosphorylation of either residue, suggesting that the effect of protein ingestion is not due to inhibition of Akt by leucine-mediated mTORC1 signaling (296). Even though reduced Akt activation may suggest reduced glucose transport, this is not always the case. Akt phosphorylation is also increased in leg muscle insulin resistance (366–368). Inflammation also has shown to increase Akt phosphorylation (369). This suggests the complex relationship between Akt phosphorylation and insulin stimulated glucose transport is context dependent.

Interestingly, BCKAs treatment exhibited a significant reduction in insulin-stimulated glucose transport, while BCAAs did not. Also, it is evident that BT2 attenuated the effect of BCKAs on insulin-stimulated glucose transport, while it did not improve insulin-stimulated glucose transport in BCAA supplemented conditions. Although not significant, we do see minor increases in BCKD activity in co-incubation of BT2 and BCKAs compared to BCKAs alone,

while no change in BCKD activity in response to BT2 and BCAA co-incubation compared to BCAAs alone. The effects of valine on reducing insulin sensitivity in obese rats seem to be linked with increased valine induced BCKD inhibition (301). Thus there seems to be a link between increasing BCKD activity and improving insulin sensitivity, as supported by the literature (294,307). Since our cells were cultured in starvation medium prior to BCAA treatment, the differences seen between the effects of BCAAs and BCKAs may be due to the fact that BCAAs are not being catabolized to prevent fasted-state protein degradation (370).

A limitation of this work is that it is an *in vitro* study. It is important to determine if these results can be reproduced in skeletal muscle of intact animals, although it may be difficult to analyze mechanistic links involved in the effect of upregulating BCKD activity on insulin sensitivity in a single tissue. To determine the effects of BCAAs/BCKAs on insulin resistance, we did so in amino acid starved conditions. Presence of other amino acids may influence results acquired. Normalizing the groups to the non-insulin group is a limitation as well, which may make the power artificially higher. Cell culture experiments were run on separate days, so different cell lines and passages were used. Also, each biological replicate had different myotube integrity as well. These factors may contribute to the variability in the raw values of pmol of glucose up taken by the myotubes. However the percent change between groups were similar, so we normalized it to the control.

Another limitation may be the sample size, as for example in figure 4.1B, it was very close to significance, but we did not want to chase a specific p-value. Power calculations were not done before the start of this study, but using previous research that showed KIC suppressed insulin stimulated glucose transport by 34% (means of ~175±15 vs ~115, power value was 80%, and the alpha value was 0.05), (16) power calculations showed that a sample size of 1 per group

would suffice. Here we did 3 biological replicates with 3 technical replicates per experiment for all measures, as typically done in cell culture studies.

In conclusion, we show that inhibition/depletion of BDK in L6 myotubes improves insulin sensitivity and attenuates BCKA induced suppression of insulin-stimulated glucose uptake and that the mTORC1/S6K1-IRS-1 signaling pathway is in part responsible for these changes. Our data suggests that interventions that upregulate BCAA catabolic flux may provide therapeutic potential for the management/prevention of insulin resistance and associated diseases.

4.6 Author Contributions

GM and OAJA conceived and designed the experiments. GM performed the experiments. GM drafted the initial version of the manuscript. OAJA reviewed and edited the manuscript. Both authors approved the final version of the manuscript.

Acknowledgements

We acknowledge the Muscle Health Research Centre at York University for their help with HPLC.

Funding

This work is supported by funds from the Natural Science and Engineering Research Council of Canada and from the Faculty of Health, York University.

Disclosure

The authors declare no conflict of interest.

Chapter 5: Leucine, but not ketoisocaproic acid (KIC) gavage alters insulin signaling but not whole-body insulin tolerance in rats

Gagandeep Mann[1], Stephen Mora[1] and Olasunkanmi Adegoke*

School of Kinesiology and Health Science and Muscle Health Research Centre, York University, Toronto, ON, Canada M3J 1P3[1]

***Corresponding Author: Olasunkanmi A. J. Adegoke** Muscle Health Research Centre, School
of Kinesiology and Health Science, York University, 4700 Keele Street, Toronto, ON, Canada.
Tel: 416-736-2100 ext. 20887 Fax: 416-736-5774. Email: oadegoke@yorku.ca

5.1 Abstract:

Plasma levels of branched-chain amino acids (BCAAs) and their metabolites, branched-chain ketoacids (BCKAs) are increased in insulin resistance, a condition that can lead to type 2 diabetes mellitus. Our previous *in vitro* studies showed that leucine and its metabolite KIC suppress insulin-stimulated glucose uptake in L6 myotubes along with the activation of the S6K1-IRS-1 signaling axis. However, due to contributions of various tissues and differences in muscle fiber types to whole-body BCAA metabolism, we analyzed the effect of KIC gavage on whole-body insulin sensitivity and insulin signaling *in vivo.* We hypothesize that KIC gavage will reduce whole-body insulin sensitivity, and increase S6K1-IRS-1 phosphorylation in various tissues.

Five-week-old male Sprague-Dawley rats were fasted for 24 hours and then gavaged with 0.75ml/100g of body weight of water, leucine (22.3g/L) or KIC (30g/L) twice, ten minutes apart. They were then sacrificed at different time points post-gavage (0.5-3h) and muscle, liver, and heart tissues were dissected. Another set of rats were fasted 6 hours and then gavaged with either water, leucine, or KIC and underwent an insulin tolerance test.

Phosphorylation of S6K1 (Thr389) in gastrocnemius, soleus, and EDL, and S6 (Ser235/6) in gastrocnemius, soleus, EDL, liver, and heart were increased after 30 minutes of leucine gavage, but were back to control levels by 60 minutes, while KIC increased S6 (Ser235/6) phosphorylation in only the liver. IRS-1 (Ser612) phosphorylation was increased 30 minutes after leucine gavage in the liver and skeletal muscles irrespective of fiber type, but not in the heart. This effect was alleviated by the 60-minute mark. Leucine and KIC did not affect insulin tolerance. Neither leucine nor KIC modified ph-Akt (Ser473) in skeletal muscle and heart. There were no differences in the expression of enzymes involved in BCAA catabolism across the different muscle fibers.

Our data suggests that leucine but not KIC activates the S6K1-IRS-1 signaling axis in various tissues. KIC only alters this pathway in the liver, suggesting it is predominantly up taken by the liver. KIC and leucine also does not affect insulin tolerance and therefore, the effect of leucine and KIC on the S6K1-IRS-1 signaling pathway is also uncoupled from whole body insulin tolerance.

5.2 Introduction:

Dietary protein and, in particular, branched-chain amino acids (BCAAs; leucine, valine, isoleucine) stimulate muscle protein synthesis, and regulate glucose homeostasis and body weight (10). However, despite these benefits, elevated levels of plasma BCAAs and BCAA metabolites, branched-chain α-ketoacids (BCKAs; alpha-ketoisocaproic acid (KIC), alpha-keto-beta methylvaleric acid (KMV), and alpha-ketoisovaleric acid (KIV)) are seen in insulin-resistant states like T2DM (11–13,221,222). This poses the question if increased BCAA and BCKA levels cause insulin resistance or are a consequence of insulin resistance.

Rats require ~1.2 g of BCAAs per kg of body weight in a day, compared to humans who require ~68 mg of BCAAs per kg of body weight (371). The discrepancy in required intake between humans and rats is because protein consumption per kg of body weight is tenfold higher in rats than in humans (372,373). Also, the enzymes involved in BCAA metabolism is similar in humans and in rats (228), making the rat an appropriate model for studying BCAA metabolism. In terms of comparing BCAA transport across different species, only one study has examined the whole-body distribution of isoleucine oxidation and disposal into protein synthesis, and this was done in mice, but not in rats and humans (227). However, since BCAAs metabolism is less active in primates than rats, primates may be an even better model for future studies (374).

Many studies have shown that BCAAs increase the activation of mammalian/mechanistic target of rapamycin complex 1 (mTORC1) and p70 ribosomal protein S6 kinase-1 (S6K1). This results in the phosphorylation of inhibitory serine residues of IRS-1 (Ser636, Ser312, Ser616 in humans, and Ser632, Ser307 and Ser612 in mice) (109,110) by S6K1. This ultimately leads to the degradation of IRS-1 (47), and thus hindering downstream insulin signaling (14,15). We have shown that leucine treatment *in vitro* and *in vivo* reduces insulin sensitivity, and this is seen with

a consistent increase in S6K1 phosphorylation (16,18). We have also shown that KIC (16,17), the BCKA of leucine, suppressed insulin-stimulated glucose uptake in L6 myotubes along with increases in the S6K1-IRS-1 signalling axis. However, due to the contributions of other tissues aside from just skeletal muscle in BCAA metabolism and that the fact that BCAAs do not phosphorylate mTOR (Ser2448) in the soleus but do in the extensor digitorum longus (EDL) muscle (19), we analyzed the effect of KIC and leucine gavage on insulin tolerance and insulin signaling in various tissues and different muscle fiber types involved in BCAA metabolism. This will help us gain a deeper understanding of the pathogenesis of insulin resistance and potential interventions against it.

5.3 Methods:

Ethics Statement:

All animal experiments were approved by the York University Animal Care Committee in accordance with the recommendations of the Canadian Council on Animal Care.

Reagents and Materials

KIC (#0629), leucine (#L8912), anti-gamma tubulin antibody (#T6557), amino acid standard (#AAS-18), and protease (#P8430) and phosphatase #P5726) inhibitor cocktails were purchased from Sigma Aldrich (Oakville, Ontario, Canada). Water, KIC and leucine were gavaged using feeding tubes (FTP-18-75) purchased from Instech Laboratories, (Plymouth Meeting, Pennsylvania, United States). Insulin (Humulin R, DIN#00586714, short acting insulin) was purchased from Eli Lilly Canada Inc., (Toronto, Ontario, Canada). The glucometer (#71675) and glucose strips (#71681) were purchased from AlphaTrak, (Cleveland, Ohio, United States).

Animals

Young male Sprague–Dawley rats (150–200 g) were purchased from Charles River Laboratories Inc. (Senneville, Quebec, Canada). They were acclimatized for 1 week in the animal care facility at York University while being maintained at the standard 12:12-h light–dark cycle at 22–23°C. They had access to rat chow (product #D12450B, Research Diets, New Brunswick, New Jersey, United States) and water. Animals were handled 2–3 times per week to reduce stress of handling them on the day of the experiment.

Rats were food deprived for 24 h but had access to water. They were then divided into three groups. The first group was gavaged with double distilled water (ddH_2O) at a dose of 1.5

mL/100 g body weight in two halves 10 minutes apart. The second group was gavaged with leucine (1 g/44.84 mL ddH_2O (0.170 mM), 1.5 mL/100 g body weight) in two halves 10 minutes apart. This is equivalent to 0.33 g leucine/kg of body weight, which represents ~30% of a rats daily leucine consumption (375). The third group was gavaged with KIC (1 g/33.33 mL ddH_2O (0.197 mM), 1.5 mL/100 g body weight) in two halves 10 minutes apart. Rats were euthanized at different times (0.5–3 h) after gavage, and blood was taken and soleus, tibialis anterior, EDL, gastrocnemius, liver, and heart were dissected, flash-frozen in liquid nitrogen and stored at -80^{o}C for further analyses. For analysis of fiber type differences in response to KIC/leucine gavage, the soleus was used for type I fibers, the EDL for type II fibers, and gastrocnemius for a mixed muscle fiber.

Insulin Tolerance Test

Following a 6 h food deprivation, rats were gavaged with either water, leucine or KIC, twice, 10 minutes apart as stated above. One hour following the first gavage, glucose readings and blood was collected through the saphenous vein. Then an intraperitoneal insulin injection was administered (1 U/kg body weight). Like basal glucose readings, blood glucose post insulin (10-120 min) was measured and collected through the saphenous vein.

Tissue Homogenization

Gastrocnemius, soleus, EDL, liver, and heart were weighed and homogenized in 7 volumes of homogenization buffer (in mM: 20 mM HEPES pH 7.4, 2 mM EGTA, 50 mM NaF, 100 mM KCl, 0.2 mM EDTA, 50 mM glycerolphosphate) supplemented with 1 mM DTT, 1 mM benzamidine, 0.5 mM sodium vanadate, and protease (10 μl/ml of homogenization buffer) and

phosphatase (10 µl/ml of homogenization buffer) inhibitor cocktails while on ice. This homogenate was then centrifuged 3 min at 1000 *g* and 4°C. The supernatant was collected and centrifuged 30 min at 10000 g and 4°C. These samples were then used for western blotting, and ultra-high-pressure liquid chromatography.

Western Blotting

The Pierce BCA Protein Assay Kit (Thermo Scientific, #23225) was used to determine protein concentration. The KC4 plate reader software (Bio-Tek Instruments Inc., Winooski, Vermont, United States) was used to acquire an absorbance reading of each well at a wavelength of 550 nanometers. A standard curve was used to estimate the volume needed to load 40 µg of protein into one well of a polyacrylamide gel. Proteins were separated on a 10% SDS-polyacrylamide gel electrophoresis (SDS-PAGE). They were then transferred overnight onto 0.2 µm-pore sized polyvinylidene difluoride membranes. Membranes were then treated with a ponceau S dye to check the protein was transferred. This dye was then washed off with 3 5-minute washes of tris buffered saline with tween (TBST). Membranes were then incubated for one hour in 5% non-fat milk in TBST at room temperature to block non-specific antigen binding. Next, they were washed 3 times for 5 minutes each with TBST at room temperature and then incubated with the primary antibody of interest overnight at 4°C.

Table 5.1: List of antibodies used.

Primary Antibody	**Dilution**	**Company Purchased From**	**Secondary Antibody**
Ph-S6K1 (Thr389)	1:1000	Cell Signaling (CST) #9234	Anti-Rabbit (CST #7074)
Ph-S6 (Ser235/6)	1:2000	CST #4858	Anti-Rabbit (CST #7074)
Ph-Akt (Ser473)	1:2000	CST #4060	Anti-Rabbit (CST #7074)

Ph-IRS-1 (Ser612)	1:1000	CST #3203	Anti-Rabbit (CST #7074)
γ-Tubulin	1:10000	Sigma Aldrich #T6557	Anti-Mouse (CST #7076)
BCAT2	1:1000	ProteinTech #16417-1-AP	Anti-Rabbit (CST #7074)
BCKD	1:1000	Sigma Aldrich #90198	Anti-Rabbit (CST #7074)
Ph-BCKD (Ser293)	1:1000	Sigma Aldrich #40368	Anti-Rabbit (CST #7074)
BDK	1:1000	Thermo Fisher #PA5-31455	Anti-Rabbit (CST #7074)
Pp2cm	1:1000	ProteinTech #14573-1-AP	Anti-Rabbit (CST #7074)

Following the overnight incubation in primary antibody, membranes were washed 3 times for 5 minutes each with TBST and then incubated in a secondary antibody (diluted in 5% milk with TBST) for three hours at room temperature. Secondary antibodies, anti-rabbit (CST #7074) or anti-mouse (CST #7076) were diluted in 1:2000-10000. After incubation with the secondary antibody, membranes were washed 3 times for 5 minutes each with TBST before HRP chemical luminescent substrate (Millipore, #WBKLS0500) was applied to them. Bio-Rad ChemiDoc XRS+ was used for signal visualization and the images were quantified with Image Lab software (version 8; Bio-RAD, Hercules, California, United States).

Amino Acid Concentrations

This was done as previously described (17). Homogenized muscle, liver, heart, and plasma samples containing free amino acids were diluted in a 1:2:1:8 ratio (sample: potassium phosphate buffer: 0.1 N hydrochloric acid: HPLC grade water, respectively). Diluted samples were pre-column derivatized with a 1:1 ratio of sample to o-Phthalaldehyde (29.28 mM) (Sigma Aldrich, #P1378). They were injected into a YMC-Triart C18 column (C18, 1.9 μm,

75 × 3.0 mm; YMC America, Allentown, PA, USA) fitted onto an ultra-high-pressure liquid chromatography system (Nexera X2, Shimadzu, Kyoto, Japan) that was connected to a fluorescence detector (Shimadzu, Kyoto, Japan; excitation: 340 nm; emission: 455 nm). Amino acids were eluted with a gradient solution derived from mobile phase A (20 mM potassium phosphate buffer (6.5 pH)) and mobile phase B (45% HPLC-grade acetonitrile, 40% HPLC-grade methanol and 15% HPLC-grade water) at a flow rate of 0.8 ml/min. We used a gradient of 5%–100% of mobile phase B over 21 min. Amino acid concentrations were calculated using amino acid standard curves and for muscle, liver, and heart were normalized to total protein of the respective sample. Detailed procedure is outlined in Appendix G.

KIC Concentrations

Homogenized muscle, liver, and heart samples, and plasma samples were diluted in a 1:2:1:8 ratio (sample: potassium phosphate buffer: HPLC-grade water/homogenization buffer: HPLC-grade water, respectively). Diluted samples were treated with a 1:1 ratio of a 1,2-diamino-4,5-methylenedioxybenzene (DMB) (Sigma Aldrich, #66807) solution. DMB solution was prepared by adding 1.6 mg of DMB to 1.0 mL of solution, which contained 4.9 mg of sodium sulfite, 70 μL of 2-mercaptethanol, and 58 μL of concentrated 12 M HCl in 0.87 mL of ddH_2O. Once samples were treated with DMB, this solution was heated at 85^{o}C for 45 minutes then cooled on ice for at least 5 min. They were injected into an Inertsil ODS-4 (2 μM, 100 × 2.1 mm; GL Sciences, Torrance, CA, USA) fitted onto an ultra-high-pressure liquid chromatography system (Nexera X2, Shimadzu, Kyoto, Japan) that was connected to a fluorescence detector (Shimadzu, Kyoto, Japan; excitation: 367 nm; emission: 446 nm). Mobile phases were (A) HPLC-grade methanol/ddH_2O (30/70, v/v) and (B) HPLC-grade methanol. Gradient elution was

performed as follows: 0 min 0% B, 3.33 min 0%B, 5 min 50%B, 17.34 min 50%B. The flow rate was 0.2 mL/min, and the column temperature was maintained at 40ºC. Detailed procedure is outlined in Appendix H.

Branched Chain Ketoacid Dehydrogenase (BCKD) Assay

We measured BCKD activity using a modified version of a previous assay (21). Frozen gastrocnemius, soleus, EDL, heart, or liver were crushed in liquid nitrogen and homogenized (Bio-Gen PRO200 Homogenizer) in 250 µL of ice-cold buffer 1 (30 mM KPI, 3 mM EDTA, 5 mM DTT, 1 mM valine, 3% FBS, 5% Triton X-100, 1 µM leupeptin) and centrifuged at 10000 ***g*** for 10 minutes. Then, 50 µL of the supernatant was added to 300 µL of buffer 2 (50 mM HEPES, 30 mM KPI, 0.4 mM CoA, 3 mM NAD+, 5% FBS, 2 mM thiamine, 2 mM magnesium chloride and 7.8 µM ^{14}C-labelled valine (Perkin Elmer, #NEC291EU050UC)). This reaction took place in a 1.5 mL Eppendorf tube, which had a 2 M NaOH wick taped to inside surface of the lid. Each Eppendorf tube was capped and sealed tight using tape, before being placed in an incubator at 37°C for 30 min. The radiolabeled $^{14}CO_2$ released from the BCKD reaction reacted with NaOH on the wick. The wick was counted in a liquid scintillation counter to measure BCKD activity. Then 50 µL of the reaction mix was counted in a liquid scintillation counter to measure total radioactivity. Protein levels were also measured, and BCKD activity measured from the wick was adjusted for the total radioactivity and protein levels of the respective sample. We used valine instead of leucine, as valine-derived KIV is the preferred substrate for BCKD (352). Detailed procedure is outlined in Appendix F.

Statistical Analysis and Data Presentation

BCKD activity data are presented as CPM of the CO_2 released and bound to the wick corrected for total radioactivity and μg of protein of each respective sample. Proteins for western blots were adjusted for loading using γ-tubulin values. Statistical analyses were performed using GraphPad Prism 8 software (GraphPad, Massachusetts, United States). This software also provided area under the curve data for the insulin tolerance test. Data are presented as mean ± SEM. One-way analysis of variance (ANOVA) was used and Tukey's post-hoc tests were done to measure statistically significant differences among means. Significance was determined as $p < 0.05$.

.

5.4 Results:

Plasma leucine concentrations were increased 30 ($p<0.0001$) and 60 min ($p<0.001$) post leucine gavage but these levels dropped by 120 min. KIC had no effect on plasma leucine concentrations (Fig 5.1A). Plasma KIC levels were significantly increased 30 minutes post leucine and KIC gavage (Fig 5.1B). Neither Leucine nor KIC gavage influenced plasma valine (Fig 5.1C), isoleucine (Fig 5.1D), or glutamate (Fig 5.1E) levels. Neither leucine nor KIC gavage affected insulin tolerance compared to control (Fig 5.2A-B), although leucine gavage did have greater glucose AUC than KIC (Fig 5.2B, $p<0.05$).

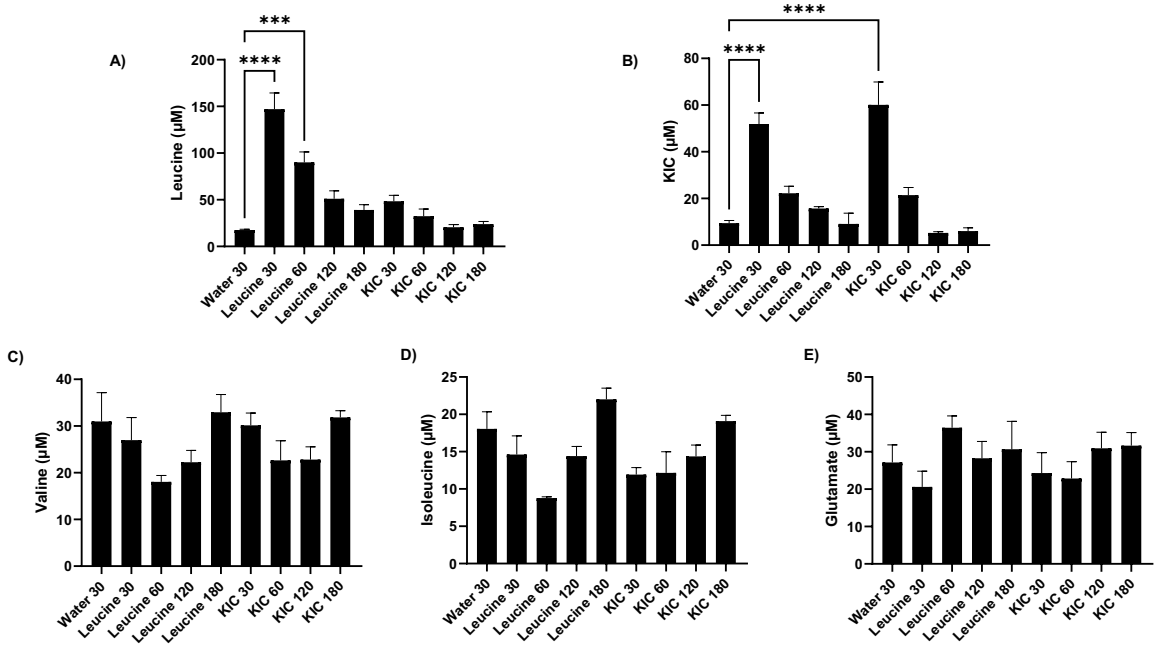

Figure 5.1: Leucine gavage increases plasma leucine and KIC concentration, while KIC gavage increases plasma KIC concentrations
Rats were gavaged 0.75 mL/100 g body weight, twice with water, leucine (0.170 mM), or KIC (0.197 mM) 10 minutes apart. Rats were euthanized at different timepoints (30-180 min), then HPLC was performed to measure plasma leucine (A), KIC (B), valine (C), isoleucine (D), and glutamate (E) concentrations. Data are means ± SEM, N=8 each group; * $p<0.05$, *** $p<0.001$, **** $p<0.0001$.

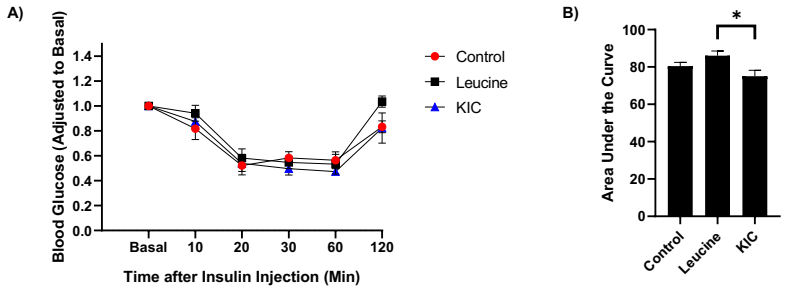

Figure 5.2 Neither Leucine nor KIC affects whole-body insulin tolerance.
Rats were gavaged 0.75 mL/100 g body weight, twice with water, leucine (0.170 mM), or KIC (0.197 mM) 10 minutes apart. Blood glucose (basal) was taken right before insulin injection. Insulin was injected one hour after the first gavage, and then blood glucose was measured at different timepoints. These blood glucose values at each timepoint were adjusted to basal values of the respective rat (F). Area under the curve of the blood glucose curve was analyzed (G). Data are means ± SEM, N=8 each group; * $p<0.05$.

Leucine concentrations in the gastrocnemius were increased 30 min post leucine gavage ($p<0.001$), but these levels dropped by 60 min. KIC had no effect on skeletal muscle leucine concentrations (Fig 5.3A). Thirty minutes post leucine gavage showed no increase in gastrocnemius KIC concentrations, and 30 minutes post KIC gavage increased gastrocnemius KIC concentrations (Fig 5.3B, $p<0.01$). Neither leucine nor KIC gavage had an effect on gastrocnemius valine (Fig 5.3C) and isoleucine (Fig 5.2D) levels, but leucine gavage did significantly increase glutamate (Fig 5.3E, $p<0.01$) levels, as glutamate is produced when leucine is catabolized by branched chain aminotransferase 2 (BCAT2) (376).

In vitro, we see that leucine and KIC activate the S6K1-IRS-1 signaling axis (17,107). Even though insulin tolerance was unchanged from leucine or KIC gavage (Fig 5.2A-B), S6K1 (Thr389) (Fig 5.3F-G, $p<0.001$), S6 (Ser235/6) (Fig 5.3F, H, $p<0.0001$) and IRS-1 (Ser612) (Fig

5.3F, I, p<0.0001) phosphorylation were higher 30 min post leucine gavage compared to animals 30 min post water gavage. KIC had no effect on S6K1 (Thr389) (Fig 5.2F-G), S6 (Ser235/6) (Fig 5.3F, 5.3H) and IRS-1 (Ser612) (Fig 5.3F, 5.3I) phosphorylation. Next, we looked at the phosphorylation of Akt, a marker of insulin signaling. Neither leucine nor KIC gavage modified Akt (Ser473) phosphorylation (Fig 5.3F, 5.3J).

Next we looked at branched-chain ketoacid dehydrogenase (BCKD) activity, as reduced skeletal muscle BCKD activity has been implicated with insulin resistance (294). BCKD is phosphorylated when it is inhibited. Neither leucine nor KIC affected BCKD phosphorylation (Ser293) (Fig 5.3F, 5.3K), but there was a trend for significance 30 min post leucine gavage for BCKD activity (Fig 5.3L, p=0.08).

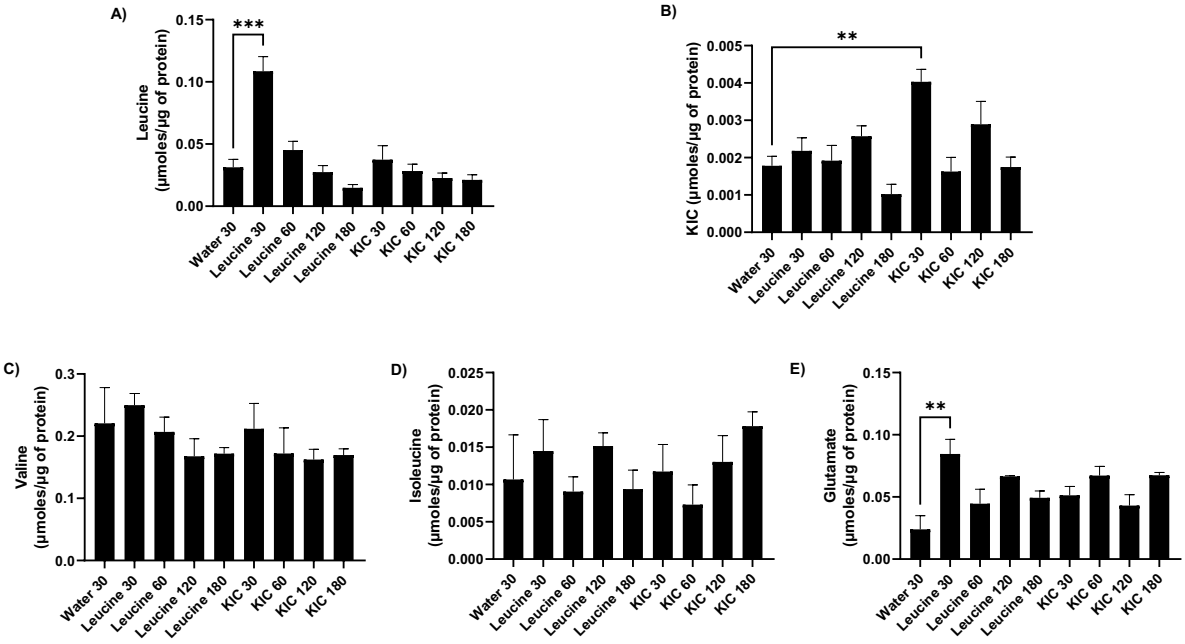

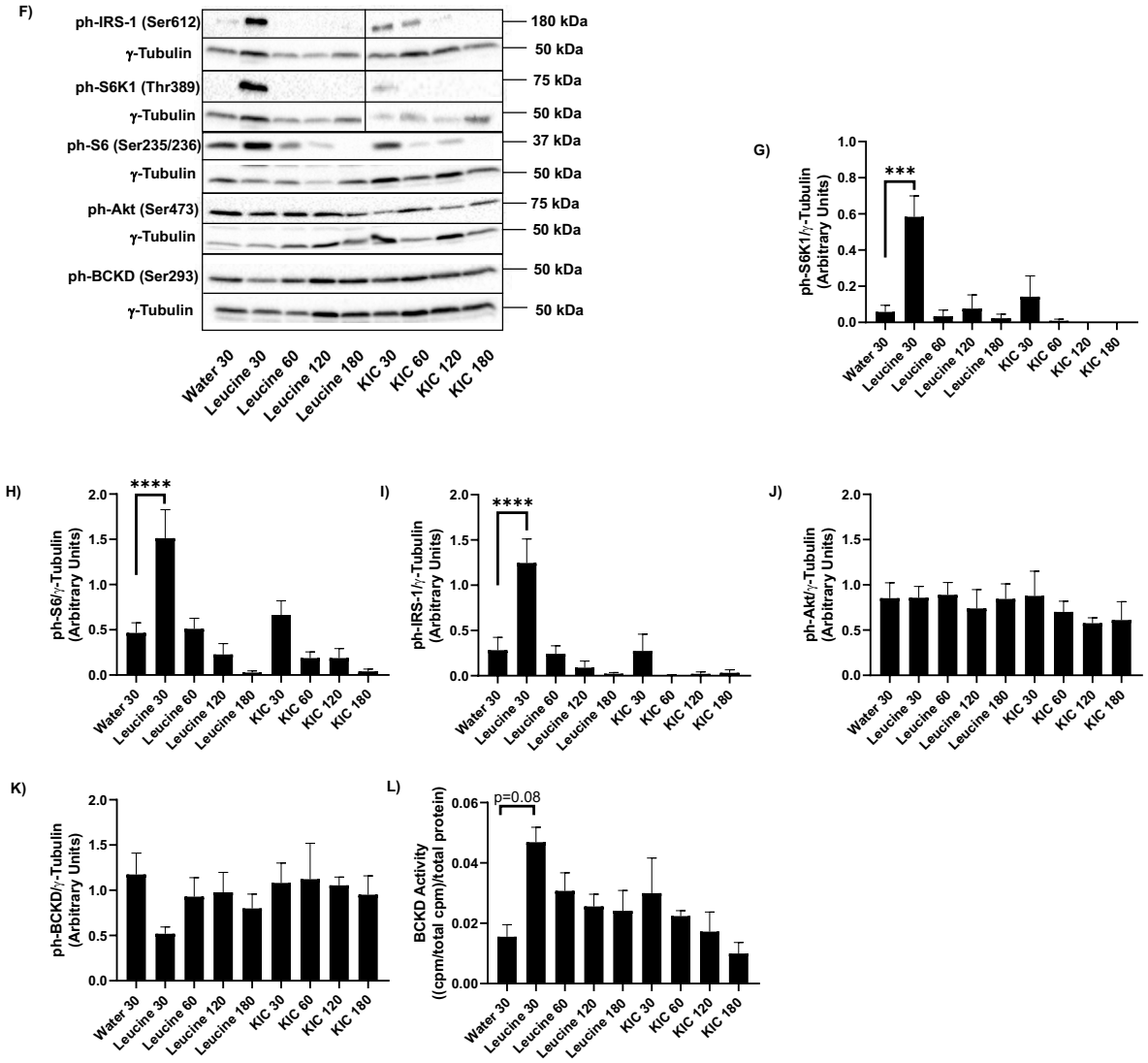

Figure 5.3: Leucine, but not KIC activates S6K1-IRS-1 signalling in the gastrocnemius.

Rats were gavaged and euthanized as explained in Fig 5.1. HPLC was then performed to measure leucine (A), KIC (B), valine (C), isoleucine (D) and glutamate (E) concentrations in the gastrocnemius. Proteins were immunoblotted against phosphorylated (ph)-S6K1 (Thr389) (F-G), ph-S6 (Ser235/6) (F, H), ph-IRS-1 (Ser612) (F, I), ph-Akt (Ser473) (F, J), and ph-BCKD (Ser293) (F, K). BCKD activity assay was performed (L). Data are means ± SEM. N=8 each group; ** $p<0.01$, *** $p<0.001$, **** $p<0.0001$.

BCAA supplementation increased mTOR phosphorylation (Ser2448) in fast twitch fibers like in the EDL, but not in slow twitch fibers like the soleus (19). Thus, we wanted to compare the effect of leucine and KIC gavage on the signalling pathways analyzed above in the soleus and EDL.

In the soleus, leucine levels were increased only 30 min post leucine gavage (Fig 5.4A, $p<0.0001$). We also demonstrated an increase in KIC levels only 30 min post KIC gavage (Fig 5.4B, $p<0,05$). Neither leucine nor KIC gavage influenced soleus valine (Fig 5.4C), isoleucine (Fig 5.4D) or glutamate (Fig 5.4E) levels.

Like the gastrocnemius, S6K1 (Thr389) (Fig 5.4F-G, $p<0.001$), S6 (Ser235/6) (Fig 5.4F, 5.4H, $p<0.0001$) and IRS-1 (Ser612) (Fig 5.4F, 5.4I, $p<0.0001$) phosphorylation were significantly increased 30 min post leucine gavage in the soleus. KIC had no effect on S6K1 (Thr389) (Fig 5.4F-G), S6 (Ser235/6) (Fig 5.4F, 5.4H) or IRS-1 (Ser612) (Fig 5.4F, 5.4I) phosphorylation. Neither leucine nor KIC modified Akt (Ser473) phosphorylation (Fig 5.4F, 5.4J). There was no effect of KIC or leucine on the phosphorylation of BCKD (Ser293) (Fig 5.4F, 5.4K). There was a significant increase in BCKD activity 30 min post leucine gavage compared to 120 min post leucine gavage (Fig 5.4L).

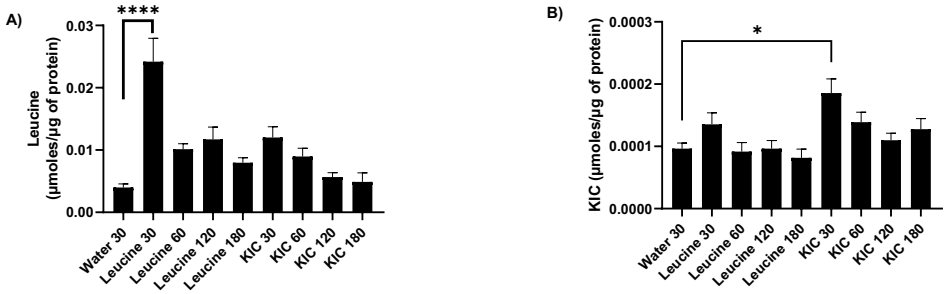

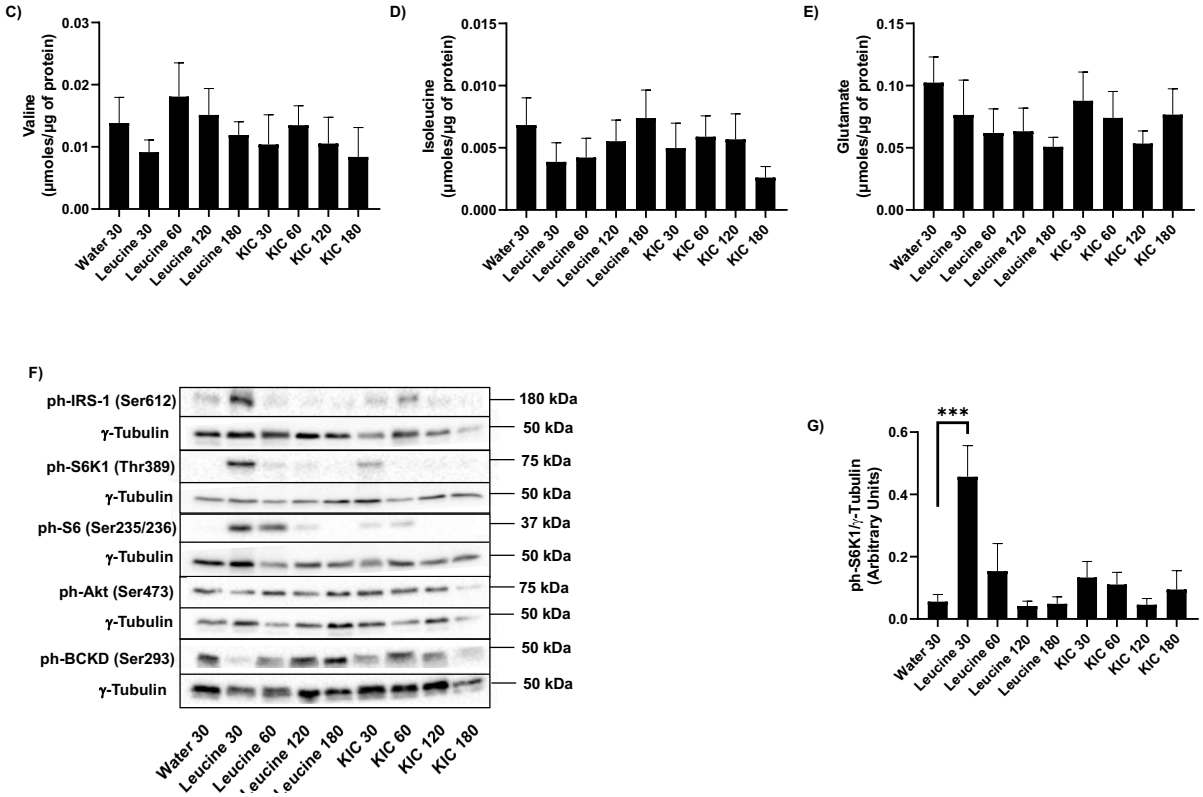
C)
Valine (µmoles/µg of protein)
0.03
0.02
0.01
0.00
D)
Isoleucine (µmoles/µg of protein)
0.015
0.010
0.005
0.000
E)
Glutamate (µmoles/µg of protein)
0.15
0.10
0.05
0.00
Water 30
Leucine 30
Leucine 60
Leucine 120
Leucine 180
KIC 30
KIC 60
KIC 120
KIC 180

F)
ph-IRS-1 (Ser612)
γ-Tubulin
ph-S6K1 (Thr389)
γ-Tubulin
ph-S6 (Ser235/236)
γ-Tubulin
ph-Akt (Ser473)
γ-Tubulin
ph-BCKD (Ser293)
γ-Tubulin
180 kDa
50 kDa
75 kDa
50 kDa
37 kDa
50 kDa
75 kDa
50 kDa
50 kDa
50 kDa
Water 30
Leucine 30
Leucine 60
Leucine 120
Leucine 180
KIC 30
KIC 60
KIC 120
KIC 180

G)
***
ph-S6K1/γ-Tubulin (Arbitrary Units)
0.6
0.4
0.2
0.0
Water 30
Leucine 30
Leucine 60
Leucine 120
Leucine 180
KIC 30
KIC 60
KIC 120
KIC 180

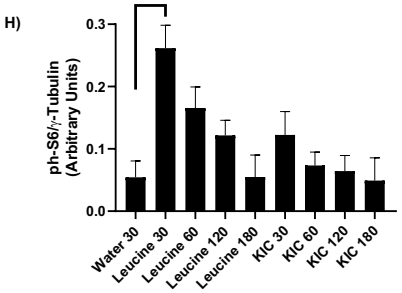
H)
**
ph-S6/γ-Tubulin (Arbitrary Units)
0.3
0.2
0.1
0.0
Water 30
Leucine 30
Leucine 60
Leucine 120
Leucine 180
KIC 30
KIC 60
KIC 120
KIC 180

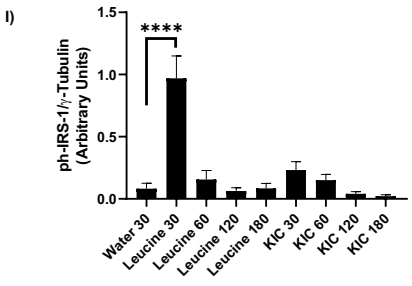
I)
****
ph-IRS-1/γ-Tubulin (Arbitrary Units)
1.5
1.0
0.5
0.0
Water 30
Leucine 30
Leucine 60
Leucine 120
Leucine 180
KIC 30
KIC 60
KIC 120
KIC 180

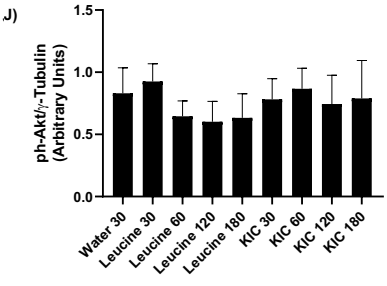
J)
ph-Akt/γ-Tubulin (Arbitrary Units)
1.5
1.0
0.5
0.0
Water 30
Leucine 30
Leucine 60
Leucine 120
Leucine 180
KIC 30
KIC 60
KIC 120
KIC 180

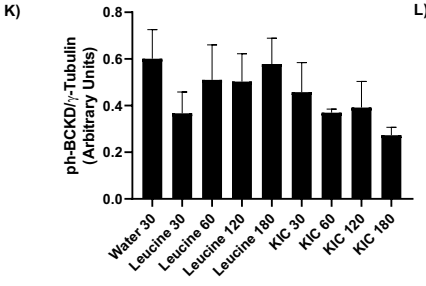
K)
ph-BCKD/γ-Tubulin (Arbitrary Units)
0.8
0.6
0.4
0.2
0.0
Water 30
Leucine 30
Leucine 60
Leucine 120
Leucine 180
KIC 30
KIC 60
KIC 120
KIC 180

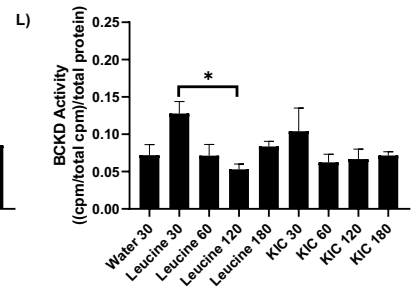
L)
*
BCKD Activity ((cpm/total cpm)/total protein)
0.25
0.20
0.15
0.10
0.05
0.00
Water 30
Leucine 30
Leucine 60
Leucine 120
Leucine 180
KIC 30
KIC 60
KIC 120
KIC 180

Figure 5.4: Leucine, but not KIC activates S6K1-IRS-1 signalling in the soleus.
Rats were gavaged and euthanized as explained in Fig 5.1. HPLC was then performed to measure leucine (A), KIC (B), valine (C), isoleucine (D), and glutamate (E) concentrations in the soleus. Proteins were immunoblotted against ph-S6K1 (Thr389) (F-G), ph-S6 (Ser235/6) (F, H), ph-IRS-1 (Ser612) (F, I), ph-Akt (Ser473) (F, J), and ph-BCKD (Ser293) (F, K). BCKD activity assay was performed (L). Data are means ± SEM. N=8 each group; * $p<0.05$, ** $p<0.01$, *** $p<0.001$, **** $p<0.0001$.

Like the gastrocnemius, in the EDL, leucine levels are increased 30 min ($p<0.001$), 60 min ($p<0.01$) and 120 min ($p<0.05$) post leucine gavage (Fig 5.5A). KIC gavage increased KIC levels 30 min post gavage, but this dropped by 60 min (Fig 5.5B, $p<0.0001$). Neither leucine nor KIC influenced EDL valine (Fig 5.5C) levels, but reduced isoleucine (Fig 5.5D, $p<0.05$) levels 60 min post leucine gavage. Leucine gavage post 60 ($p<0.05$) and 120 min ($p<0.001$) increased glutamate (Fig 5.5E) levels.

Like the gastrocnemius and soleus, S6K1 (Thr389) (Fig 5.5F-G, $p<0.001$), S6 (Ser235/6) (Fig 5.5F, 5.5H, $p<0.0001$) and IRS-1 (Ser612) (Fig 5.5F, 5.5I, $p<0.0001$) phosphorylation were significantly increased 30 min post leucine gavage. KIC had no effect on S6K1 (Thr389) (Fig 5.5F-G), S6 (Ser235/6) (Fig 5.5F, 5.5H) and IRS-1 (Ser612) (Fig 5.5F, 5.5I) phosphorylation. Neither leucine nor KIC modified Akt (Ser473) phosphorylation (Fig 5.5F, 5.5J). There was no effect of leucine on the phosphorylation of BCKD (Ser293) (Fig 5.5F, 5.5K). There was also no effect of leucine or KIC on BCKD activity in the EDL (Fig 5.5L).

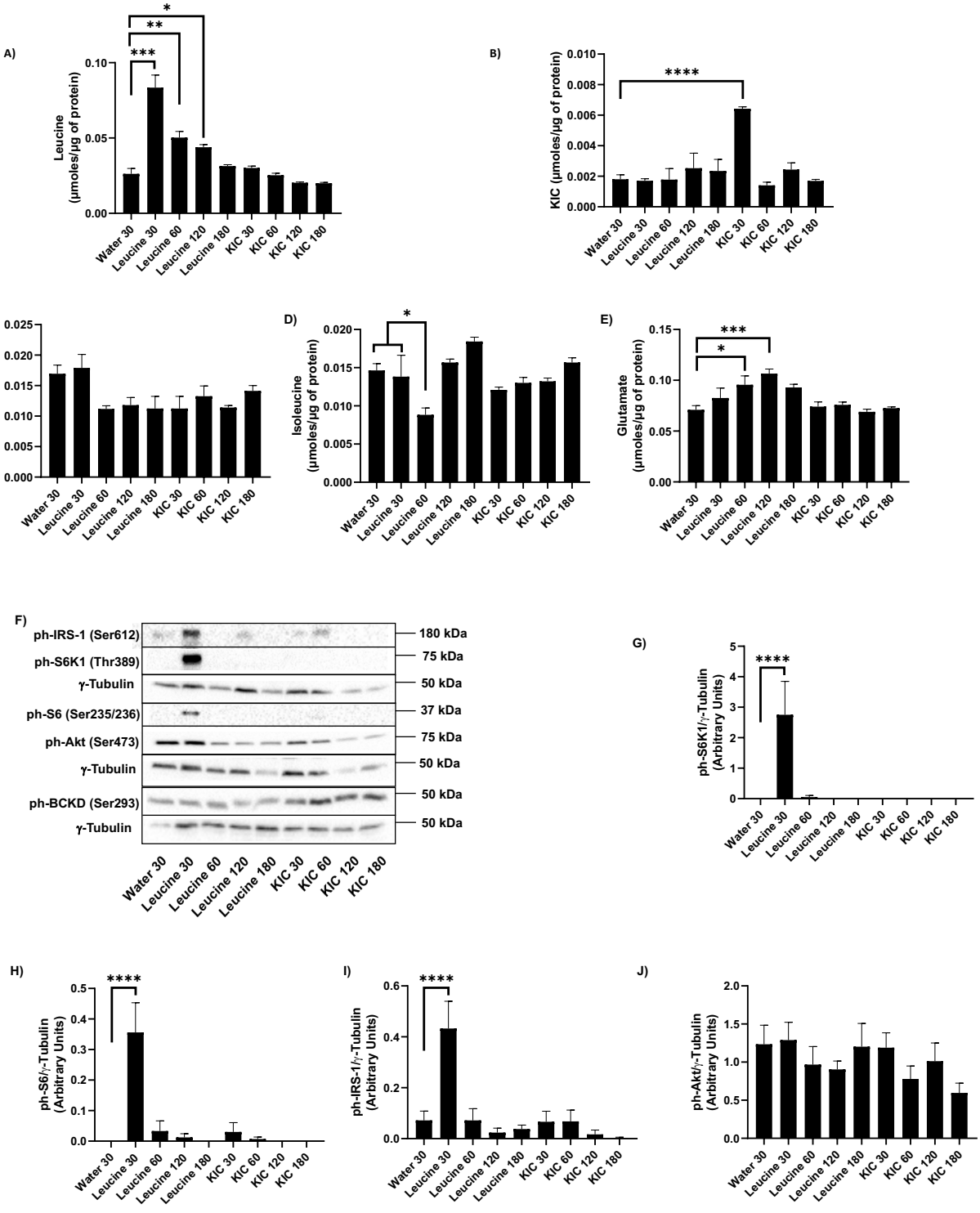
A)
Leucine (µmoles/µg of protein)
0.10
0.05
0.00
*
**
***
Water 30
Leucine 30
Leucine 60
Leucine 120
Leucine 180
KIC 30
KIC 60
KIC 120
KIC 180
B)
KIC (µmoles/µg of protein)
0.010
0.008
0.006
0.004
0.002
0.000
****
C)
Valine (µmoles/µg of protein)
0.025
0.020
0.015
0.010
0.005
0.000
D)
Isoleucine (µmoles/µg of protein)
0.020
0.015
0.010
0.005
0.000
*
E)
Glutamate (µmoles/µg of protein)
0.15
0.10
0.05
0.00
***
*
F)
ph-IRS-1 (Ser612)
ph-S6K1 (Thr389)
γ-Tubulin
ph-S6 (Ser235/236)
ph-Akt (Ser473)
γ-Tubulin
ph-BCKD (Ser293)
γ-Tubulin
180 kDa
75 kDa
50 kDa
37 kDa
75 kDa
50 kDa
50 kDa
50 kDa
G)
ph-S6K1/γ-Tubulin (Arbitrary Units)
5
4
3
2
1
0
****
H)
ph-S6/γ-Tubulin (Arbitrary Units)
0.5
0.4
0.3
0.2
0.1
0.0
****
I)
ph-IRS-1/γ-Tubulin (Arbitrary Units)
0.6
0.4
0.2
0.0
****
J)
ph-Akt/γ-Tubulin (Arbitrary Units)
2.0
1.5
1.0
0.5
0.0

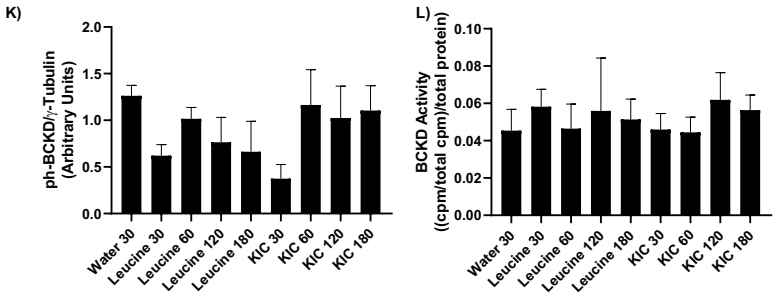

Figure 5.5: Leucine, but not KIC activates S6K1-IRS-1 signalling in the EDL.
Rats were gavaged and euthanized as explained in Fig 5.1. HPLC was then performed to measure leucine (A), KIC (B), valine (C), isoleucine (D), and glutamate (E) concentrations in the EDL. Proteins were immunoblotted against ph-S6K1 (Thr389) (F-G), ph-S6 (Ser235/6) (F, H), ph-IRS-1 (Ser612) (F, I), ph-Akt (Ser473) (F, J), and ph-BCKD (Ser293) (F, K). BCKD activity assay was performed (L). Data are means ± SEM. N=8 each group; * $p<0.05$, ** $p<0.01$, *** $p<0.001$, **** $p<0.0001$.

Leucine levels in the liver were increased 30 min post leucine gavage (Fig 5.6A, $p<0.0001$). There was no effect of KIC gavage on liver leucine levels (Fig 5.6A), but this could be due to the low levels of BCAT2 in the liver (the enzyme responsible for the conversion of KIC back to leucine) (228). KIC gavage significantly increased liver KIC levels 30 minutes post KIC gavage (Fig 5.6B, $p<0.05$). There was no effect of leucine or KIC gavage on valine (Fig 5.6C), isoleucine (Fig 5.6D) or glutamate (Fig 5.6E) levels.

S6 (Ser235/6) phosphorylation was increased 30 min post leucine (Fig 5.6F-G, $p<0.0001$) and KIC gavage (Fig 5.6F-G, $p<0.01$). There was no increase in IRS-1 (Ser612) phosphorylation in response to leucine or KIC (Fig 5.6F, 5.6H). There was no effect of leucine or KIC gavage on BCKD (Ser293) phosphorylation (Fig 5.6F, 5.6I). However, there was a significant increase in liver BCKD activity 30 minutes post leucine ($p<0.0001$) and KIC gavage (Fig 5.6J, $p<0.01$).

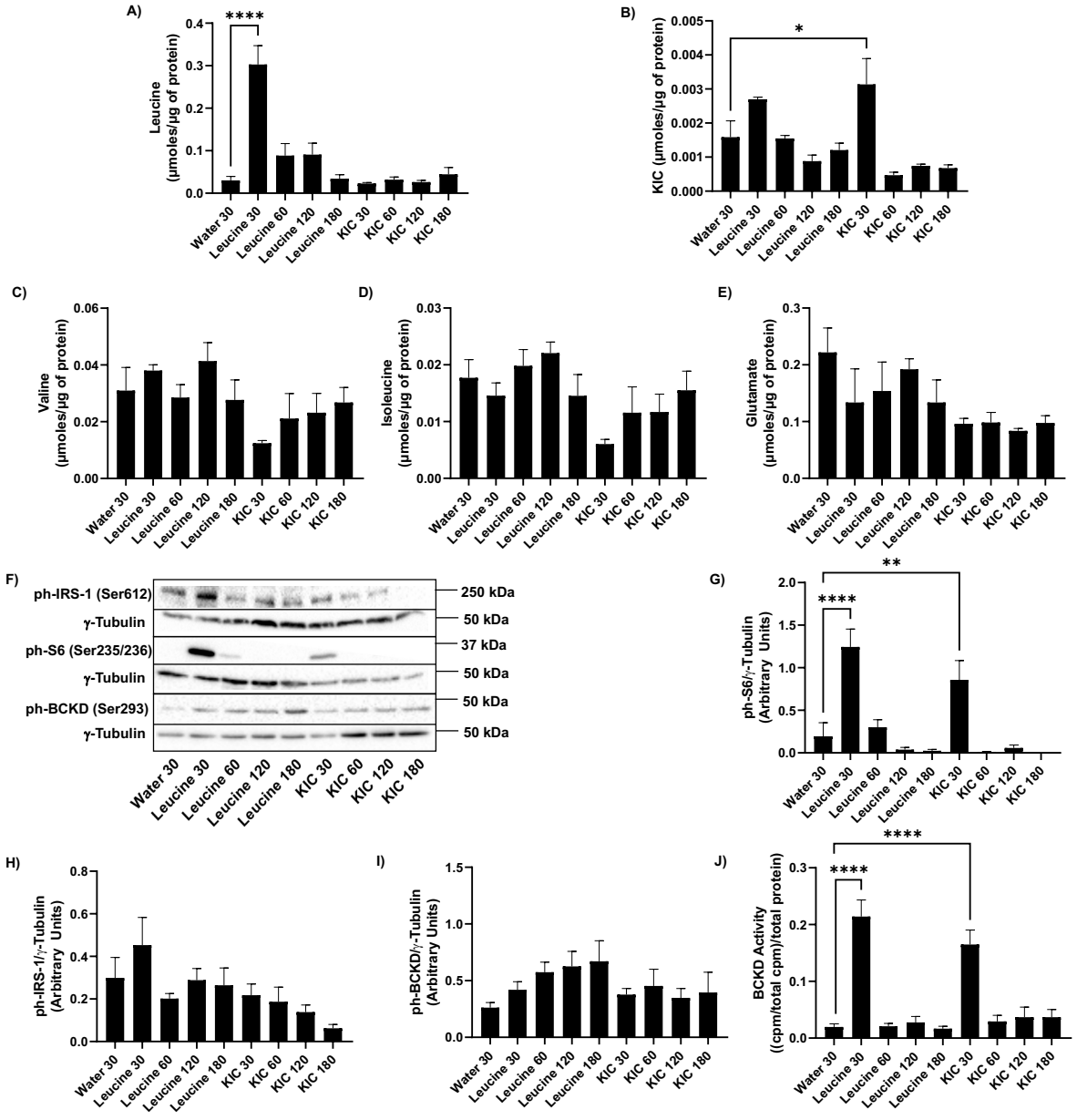

Figure 5.6: Leucine and KIC stimulate liver BCKD activity and S6 phosphorylation. Rats were gavaged and euthanized as explained in Fig 5.1. HPLC was then performed to measure leucine (A), KIC (B), valine (C), isoleucine (D), and glutamate (E) concentrations in the liver. Proteins were immunoblotted against ph-S6 (Ser235/6) (F-G), ph-IRS-1 (Ser612) (F, H), and ph-BCKD (Ser293) (F, I). BCKD activity assay was performed in the liver (J). Data are means ± SEM. N=8 each group; * $p<0.05$, ** $p<0.01$, **** $p<0.0001$.

We next analyzed the effect of KIC gavage in the heart, as myocardial levels of BCAAs and BCKAs are also linked to cardiac insulin resistance (377). There is a strong link between dysregulated BCAA oxidation and contractile dysfunction in heart failure (377). Leucine levels were increased 30-120 min post leucine gavage (Fig 5.7A, $p<0.05$) in the heart. Leucine levels were increased 30- and 60-min post KIC gavage (Fig 5.7A, $p<0.05$). There was no effect of KIC gavage on KIC levels in the heart (Fig 5.7B). There was no effect of leucine or KIC gavage on valine (Fig 5.7C), isoleucine (Fig 5.7D) or glutamate (Fig 5.7E) levels.

In the heart, there was a ~4-fold and ~2-fold increase in ph-S6 (Ser235/6) 30 min post leucine and KIC gavage respectfully, but this was not significant (Fig 5.7F-G). Like in the liver, there was no effect of KIC or leucine on ph-IRS-1 (Ser612) (Fig 5.7F, 5.7H). Neither leucine nor KIC modified Akt (Ser473) phosphorylation (Fig 5.7F, 5.7I). There was no effect of KIC or leucine on phosphorylation of BCKD (Ser293) (Fig 5.7F, 5.7J). There was also no effect of leucine or KIC on BCKD activity in the heart (Fig 5.7K).

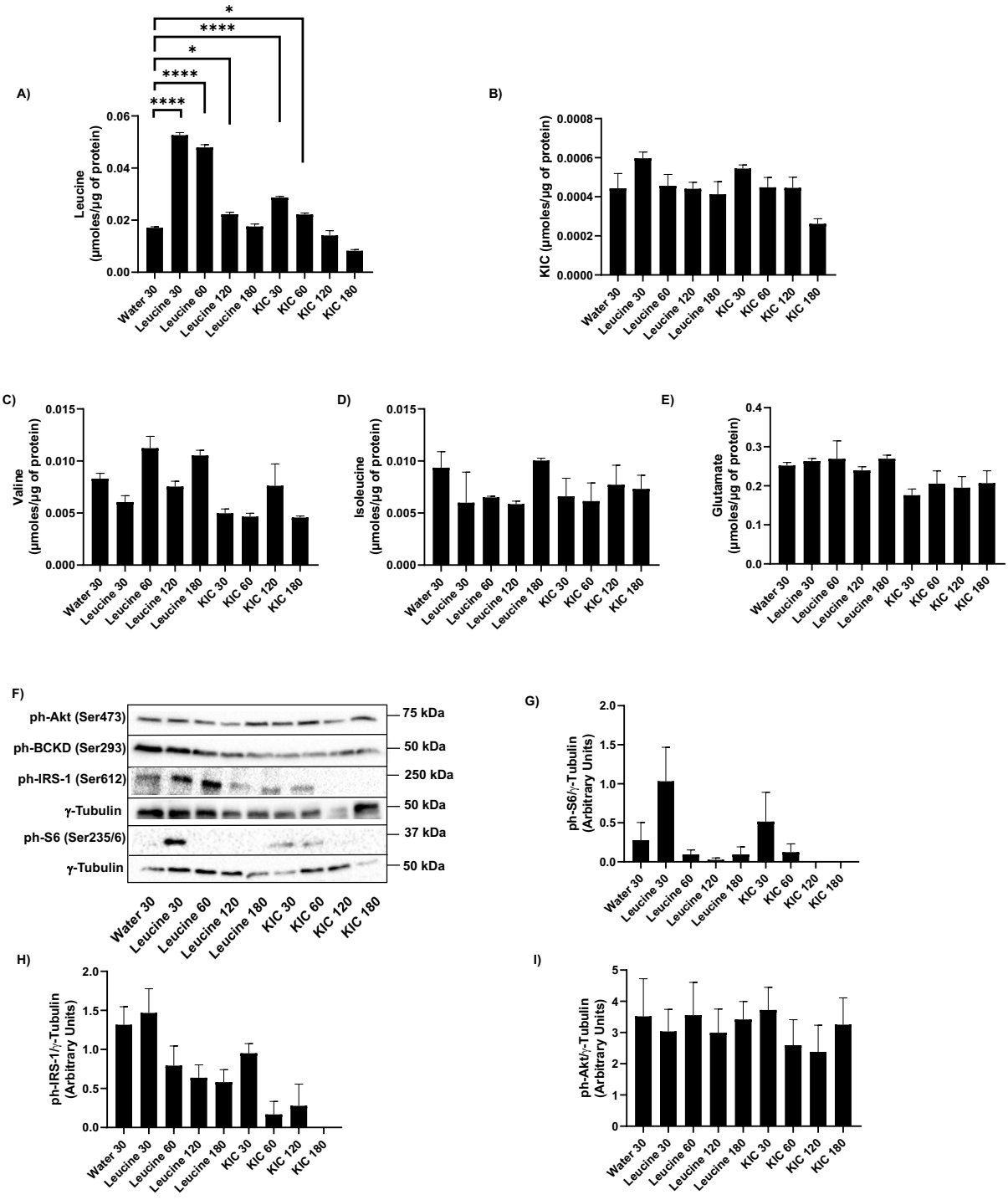
A)
Leucine (µmoles/µg of protein)
B)
KIC (µmoles/µg of protein)
C)
Valine (µmoles/µg of protein)
D)
Isoleucine (µmoles/µg of protein)
E)
Glutamate (µmoles/µg of protein)
Water 30
Leucine 30
Leucine 60
Leucine 120
Leucine 180
KIC 30
KIC 60
KIC 120
KIC 180
F)
ph-Akt (Ser473)
ph-BCKD (Ser293)
ph-IRS-1 (Ser612)
γ-Tubulin
ph-S6 (Ser235/6)
γ-Tubulin
75 kDa
50 kDa
250 kDa
50 kDa
37 kDa
50 kDa
G)
ph-S6/γ-Tubulin (Arbitrary Units)
H)
ph-IRS-1/γ-Tubulin (Arbitrary Units)
I)
ph-Akt/γ-Tubulin (Arbitrary Units)

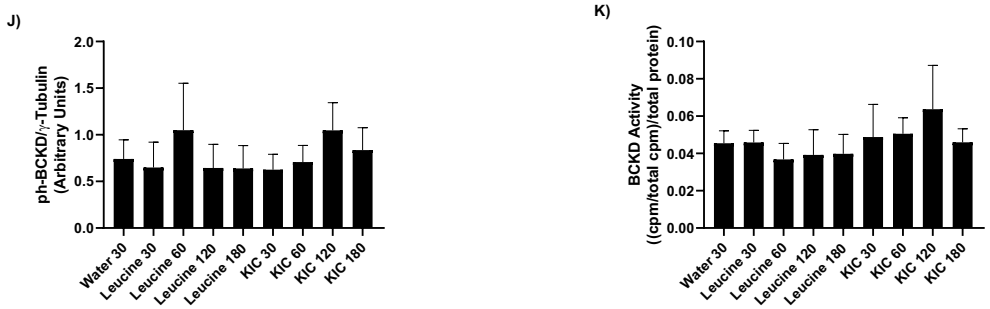

Figure 5.7: Leucine and KIC do not alter insulin signaling in the heart.
Rats were gavaged and euthanized as explained in Fig 5.1. HPLC was then performed to measure leucine (A), KIC (B), valine (C), isoleucine (D), and glutamate (E) concentrations in the heart. Proteins were immunoblotted against ph-S6 (Ser235/6) (F-G), ph-IRS-1 (Ser612) (F, H), ph-Akt (Ser473) (F, I), and ph-BCKD (Ser293) (F, J). BCKD activity assay was performed (K). Data are means ± SEM. N=8 each group; * $p<0.05$, **** $p<0.0001$.

Next, we wanted to analyze how total protein abundance of BCAA catabolic enzymes compared in different muscle fibers and tissues could potentially explain the effect of leucine and KIC in the respective tissue/muscle fiber. Total BCKD protein abundance was greatest in the liver and heart (Fig 5.8A, 5.8B, $p<0.01$), which could explain why KIC only significantly phosphorylated S6 in the liver, as liver is the preferred site for KIC oxidation. Phosphorylation of BCKD (Ser293) was the highest in the gastrocnemius and soleus (Fig 5.8A, 5.8C), although the effect was not significant. BCAT2 levels were not different amongst the groups (Fig 5.8A, 5.8D). Branched chain ketoacid dehydrogenase kinase (BDK), the negative regulator of BCKD, levels were significantly higher in the gastrocnemius compared to heart and liver (Fig 5.8A, 5.8E, $p<0.001$). Finally, protein phosphatase 2Cm (pp2Cm), a positive regulator of BCKD, was greater in the liver and heart compared to the muscles, although not statistically significant (Fig 5.8A, 5.8F).

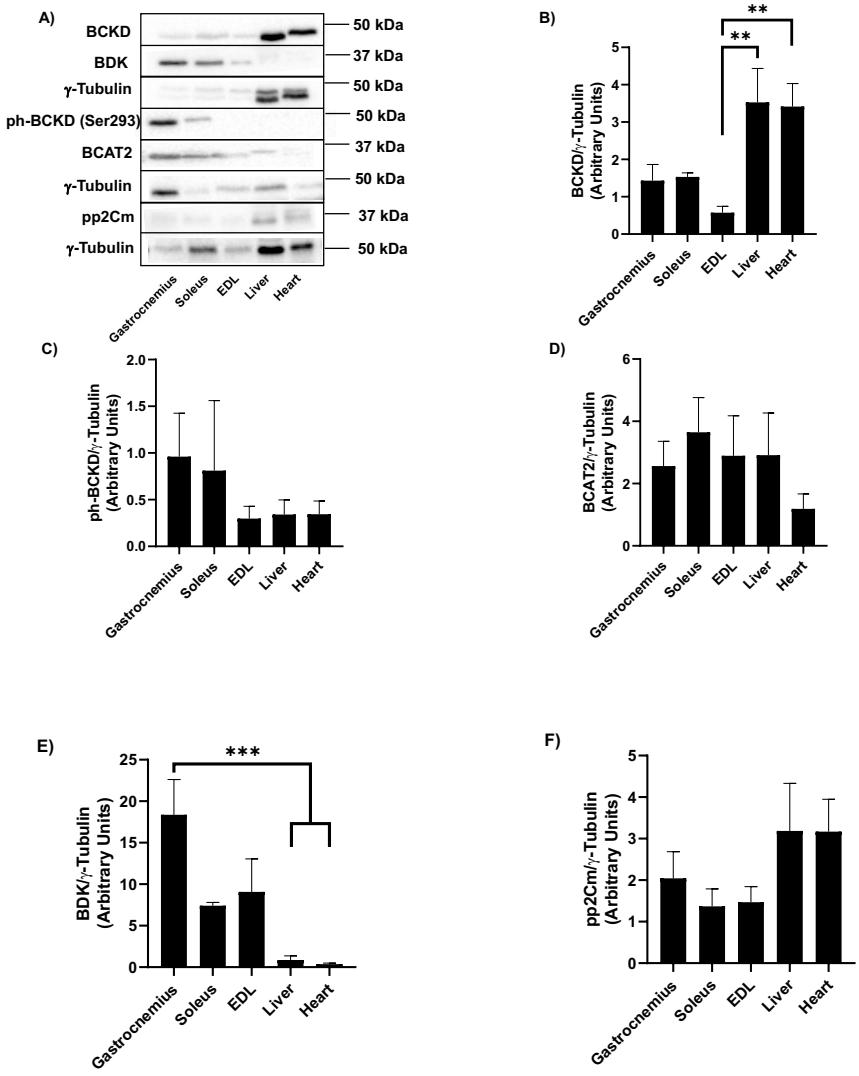

Figure 5.8: Tissues/muscle fiber types have varying levels of BCAA catabolic enzyme abundance.

Gastrocnemius, soleus, EDL, liver, and heart were used from rats euthanized 30 min post water gavage. Proteins were immunoblotted against total BCKD (A-B), ph-BCKD (Ser293) (A, C), BCAT2 (A, D), BDK (A, E), and pp2Cm (A, F). Data are means ± SEM. N=8 each group; ** $p<0.01$, *** $p<0.001$.

5.5 Discussion:

From a clinical perspective it is important to identify biomarkers early that may be implicated in the development of a disease. Elevated levels of plasma BCAAs (13,108,218) and BCKAs (12,108,218) are a common feature of insulin resistance. It is important to determine whether this is correlational or causational. There is controversy in the literature about the role of BCAAs and their metabolites in the development of insulin resistance. Others have shown that BCAAs (especially leucine) (107,113,286) and metabolites of BCAAs (107,309) can induce insulin resistance in skeletal muscle. However, mice lacking BCAT2 the enzyme responsible for BCAA catabolism show greater insulin sensitivity despite increased BCAA levels (214). Also athletes and body builders that consume BCAAs are not insulin resistant (311,312). This complicates the relationship between BCAAs and insulin resistance.

The effect of individual amino acids are relevant due to the increasing prevalence of using single amino acids for anabolic effects (378,379) and overall health (380,381). We have previously shown that leucine both *in vitro* (107) and *in vivo* (18) reduced insulin sensitivity. We have also shown that the metabolite of leucine, KIC reduces insulin-stimulated glucose transport in L6 myotubes (17,107). Due to the contributions of other tissues in whole-body BCAA metabolism, here we examined the effect of KIC *in vivo*. KIC gavage had no effect on insulin tolerance or the S6K1-IRS-1 axis in skeletal muscle and heart but did increase S6 phosphorylation in the liver.

In ob/ob mice and diet-induced obesity (329), KIC concentrations have been reported to be ~15-20 μM. In insulin resistant obese Zucker rats, plasma KIC concentrations increased from ~12 to ~24 μM compared to lean counterparts (382), which are lower than the peak of ~60μM observed in response to leucine or KIC gavage in the current study.

Leucine and KIC had no effect on insulin tolerance, but in our previous work leucine worsened insulin tolerance. This could be due to a higher concentration of leucine administered to the rat in our previous (18) compared to this study. Studies have also shown improved insulin sensitivity with leucine supplementation *in vivo* (20–22), showing the variability of the effect of leucine *in vivo*. Leucine and KIC at supraphysiological concentrations stimulate glucose uptake in soleus muscle, but the effect of leucine is greater (22). Also, supplementation with KIC (383,384) and leucine (385) stimulates insulin secretion *in vivo,* which could in turn reduce blood glucose levels, mitigating the effect of leucine and KIC gavage compared to the water gavage group. However, in past research in our lab, leucine did not stimulate insulin release (18). Interestingly, leucine suppresses the release of glucagon in mice fed a normal chow (386) and high fat diet (387). Since the rise of blood glucose in the insulin tolerance test from minute 30-120 is likely due to a counter regulatory system like glucagon release, we also measured the area under the curve from basal to 60 min and saw no differences between the groups (Appendix J, Supplementary figure 8).

Previous studies have shown that mTORC1 mediates the effects of BCAAs and BCKAs on insulin resistance (79,108,356,357,388). Activated mTORC1/S6K1 phosphorylates inhibitory serine residues of IRS-1 (Ser612) (358), leading to the degradation of IRS-1 (47), and thereby inhibiting insulin signaling downstream (10,15). Here we show that leucine phosphorylates S6K1 and IRS-1, 30 minutes post leucine gavage in all the muscle fibers, but this effect seems to be uncoupled from whole-body insulin tolerance. This shows that perhaps the S6K1-IRS-1 signaling axis cannot solely account for reduced insulin sensitivity in BCAA supplemented treatments *in vivo*. This is emphasized with a study where one group of women consumed a whey-protein drink, while another group consumed a leucine drink. Like our study, the leucine

group showed an increase in mTORC1 activation, but no change in Akt activation or leg glucose uptake. On the other hand, whey-protein increased mTORC1 activation and reduced leg glucose uptake with no change in Akt activation, suggesting that the effect of protein ingestion is not due to inhibition of Akt by leucine-mediated mTORC1 signaling (296).

We also wanted to examine if the effect of leucine or KIC varied in different fiber types. Yamanashi et al. showed that BCAAs increased mTOR (Ser2448) phosphorylation in the EDL, but not the soleus. The soleus is a more oxidative muscle, which has more mitochondria than fast twitch muscles like the EDL (389). Since BCKD is a mitochondrial protein, we expect higher BCKD activity in the soleus. However, since BCKD activity assays for each fiber were not carried out together, we cannot confirm the BCKD activity is higher in the soleus than the EDL. However, in response to leucine there was ~43% increase in BCKD activity in the soleus and a ~22% increase in the EDL (neither statistically significant). This would result in greater catabolism of leucine/KIC and less activation of the S6K1/IRS-1 signaling axis in the soleus compared to the EDL. Despite this, we showed that leucine significantly increased IRS-1, S6K1 and S6 phosphorylation in all muscle fibers. There is greater phosphorylation of BCKD in the soleus and gastrocnemius compared to the EDL (Fig 5.8), but this could be attributed to slightly more total BCKD.

KIC is not activating the S6K1-IRS-1 signaling axis as seen *in vitro* (17,107). In our previous *in vitro* studies we show that KIC is converted back to leucine to elicit its effects on glucose transport and insulin signaling (17,107). Little is known about the absorption of BCKAs by the gut, and how BCKAs are transported into tissues. BCKAs may be transported by non-specific monocarboxylate transporters (390). One study showed that the rate of absorption for BCKAs are lesser than BCAAs in the rat intestines (391). Here we show that KIC gavage does

not result in an increase in leucine levels in the gastrocnemius (Fig 5.3A), soleus (Fig 5.4A) or EDL (Fig 5.5A). Thus, one could speculate that since KIC is largely catabolized in the liver (241), where BCKD, the enzyme responsible for KIC oxidation is most active (241), KIC is oxidized by the liver during its first pass, and does not largely go to the muscle from the liver, whereas for leucine since BCAT2 is low in the liver (228), it would be transported to the muscle to be oxidized. We support this notion, as there is an increase in KIC concentrations in the liver 30 minutes post KIC supplementation. The signaling data supports this as well, as KIC increases phosphorylation of S6 (Ser235/6) in the liver (Fig 5.6G), but not in skeletal muscle. This is consistent with an increase in liver BCKD activity, as KIC has been shown to activate BCKD (280). Also, higher levels of BCKD, and pp2Cm, with lower BDK and phosphorylated BCKD (Ser293) in the liver compared to all three muscle fibers further support the notion of that KIC is largely oxidized in the liver. Delivering KIC intravenously to reduce its first pass extraction by the liver would be a better approach in measuring the effect of KIC on skeletal muscle, however the preferred way of delivering nutrients is orally.

As discussed above, changes in BCAA metabolism and its levels can affect heart function and cardiac insulin sensitivity (377). One study demonstrated major increases in serine phosphorylation of IRS-1 in the hearts of hypertensive rats compared to controls (392). We also demonstrate a trend for increased S6 (Ser235/6) phosphorylation in the heart, but this did not translate to increases in phosphorylation of IRS-1 (Ser612). We did not see increases in IRS-1 phosphorylation like in skeletal muscle, and this is likely due to the fact leucine primarily goes to the muscle to be catabolized, as BCAA transamination largely happens in the skeletal muscle (65% in muscle of rats) (228).

The chronic supplementation of BCAAs and BCKAs are a more real-life applicable approach to studying the effect of BCAAs/BCKAs on insulin sensitivity. It is important to study the acute effects of BCAAs and BCKAs to understand potential mechanisms at work. It is important to ascertain how this study fits with chronic studies. Studies show that chronic leucine supplementation had no effect on insulin sensitivity in mice fed a standard chow diet (20) and protected against high fat diet induced insulin resistance by increasing fatty acid oxidation (20,21,299,300), which is consistent with the lack of effect of leucine on insulin tolerance and Akt (Ser473) phosphorylation in our study.

Dietary restriction of BCAAs improves insulin sensitivity in rodent models (290,292–294). As discussed above, the effect of whey ingestion reduces leg glucose uptake while leucine does not (296). Thus, in recent years studies have focused on valine and isoleucine and their effects on insulin resistance. Valine supplementation worsened the obesogenic effects and insulin sensitivity of a high fat diet, while leucine protected against it (301). This correlated with increased valine induced BCKD inhibition (301), while we show a trend for increased BCKD activation 30 min post leucine supplementation in various muscle fibers and tissues. Another study also shows that valine restriction in lean animals improves insulin sensitivity (303). This suggests that valine specific effects on BCKD activity may be the culprit behind altered insulin sensitivity, as dysregulations of BCAA catabolic enzymes are implicated in insulin resistant states (13,23,24,302). Also since the metabolite of valine 3-HIB induces insulin resistance (12,308–310), more recent studies have focused on the effect of valine instead of leucine on insulin resistance.

Isoleucine restriction results in improved insulin sensitivity in normal chow fed mice (303). Reintroducing isoleucine attenuates the metabolic improvements of a low amino acid diet.

This is supported by a study that shows that isoleucine supplementation in mice fed a high fat diet show increased insulin resistance, along with increased intramuscular lipid droplet accumulation and mitochondrial dysfunction (304). This shows how the adverse effects of BCAAs may be mediated by isoleucine and valine, and not leucine, and our work agrees with this notion.

One limitation of this study was the difficulty in obtaining blots for insulin signaling in the adipose tissue, as adipose tissue is a contributor to BCAA catabolism (393), and KIC gavage could be affecting insulin signaling in adipose tissue. However, BCKD activity is low in the adipose tissue (241), so it is likely that KIC did not affect insulin signaling in adipose tissue like in skeletal muscle. Another limitation was not obtaining a blot for ph-S6K1 (Thr389) in the liver and heart, however, targets of S6K1, S6 (Ser235/6) and IRS-1 (Ser612) can compensate for this. Finally, not being able to get ph-Akt (Ser473) in the liver was a limitation as well.

Only male rats were studied. We did not use female rats as fluctuating hormone levels might make data harder to interpret and results more variable, but including female rats in future studies is required. It is important to study female rats in regards to KIC gavage, as higher BDK activity is seen in female rats (42), which may lead to reduced oxidation of leucine/KIC. This will result in increased leucine/KIC levels in plasma/tissue and thus potentially a greater suppressive effect of leucine/KIC in female rats compared to male rats.

The data show a significant increase in leucine and KIC levels 30 minutes post gavage in plasma and tissues. Also, we see a significant effect of leucine on S6K1, S6 and IRS-1 phosphorylation from leucine gavage in numerous tissues, suggesting an appropriate number of animals were used. None of the figures show a trend for significance for any parameters as well. Power calculations were not done before the start of this study, but using previous research

comparing effect of leucine and water gavage on blood glucose levels post insulin injection (means of ~0.7±0.1 vs ~0.48, power = 80%, and alpha value at 0.05) (18), we calculated that a sample size of 3 rats in each group is enough for significant differences. Here we used 8 animals per group, confirming an appropriate number of animals used.

In conclusion, we demonstrate that KIC gavage has no effect on insulin tolerance or the S6K1-IRS-1 signalling axis in muscle and heart. Additionally, despite the activation of the S6K1-IRS-1 signalling axis in skeletal muscle and liver from leucine gavage, there was no effect on insulin tolerance or Akt phosphorylation in any of the different muscle fiber types. Collectively, our data suggest that leucine affects S6K1-IRS-1 signaling in various tissues, but this is uncoupled from the lack of effect of leucine on insulin tolerance, suggesting that increased levels of plasma BCAAs are a product of insulin resistance and not causative. We also show that KIC does not affect skeletal muscle insulin signaling, but does in the liver, prompting future studies on its effects in the liver specifically.

5.6 Author Contributions

GM and OAJA conceived and designed the experiments. GM and SM performed the experiments. GM drafted the initial version of the manuscript. GM and OAJA reviewed and edited the manuscript. All authors approved the final version of the manuscript.

Acknowledgements

We acknowledge the Muscle Health Research Centre at York University for their help with HPLC.

Funding

This work is supported by funds from the Natural Science and Engineering Research Council

of Canada and from the Faculty of Health, York University.

Disclosure

The authors declare no conflict of interest.

Chapter 6: Effect of Aging and Sex on BCAA Metabolism

Gagandeep Mann, Stephen Mora, Olasunkanmi A J Adegoke*

School of Kinesiology and Health Science and Muscle Health Research Centre, York University, Toronto, ON, Canada M3J 1P3[1]

Corresponding Author: Olasunkanmi A. J. Adegoke Muscle Health Research Centre, School of Kinesiology and Health Science, York University, 4700 Keele Street, Toronto, ON, Canada. Tel: 416-736-2100 ext. 20887 Fax: 416-736-5774. Email: oadegoke@yorku.ca

6.1 Abstract

Increased plasma levels of branched-chain amino acid levels have been implicated in insulin resistance. Insulin resistance worsens with age. Despite this, plasma branched-chain amino acids (BCAAs) levels are downregulated in old men (>75 years). This complicates the link between increased plasma BCAAs and insulin resistance. No studies have examined the effect of aging on BCAA metabolism. Few studies have also looked at sex differences regarding BCAA catabolism. Thus, we wanted to assess the effect of aging and sex on BCAA levels and enzyme activity/abundance responsible for their metabolism.

Male and female young (4-month), and old (18-months) CD2F1 mice were used. BCAA levels in plasma, muscle, liver, adipose tissue, and heart were analyzed. Protein levels of BCAA metabolic enzymes, amino acid transporter LAT1 and mitochondrial marker SDHA, and the activity of branched-chain ketoacid dehydrogenase (BCKD) were analyzed in muscle, liver, adipose tissue, and heart.

Old male mice exhibit greater plasma BCAA concentrations compared to young male counterparts and old female counterparts. There is lower plasma branched chain ketoacid (BCKA) levels in aged mice regardless of sex. Old mice regardless of sex show lower BCAA concentrations compared to younger counterparts in muscle and heart. There is a trend for lower total BCAAs in aging in the liver. In adipose tissue, BCKA concentrations are increased with aging. LAT1 was lower in old female mice compared to young female mice in skeletal muscle. There was also a sex effect of LAT1 in liver, as female mice had higher levels than male mice regardless of age. Total BCKD protein abundance was also lower in old female mice compared to old male mice in liver. There was also an effect of aging on pp2Cm levels in the liver, as old mice had lower levels compared to young counterparts.

Our data showed an increase in plasma BCAAs in old male mice, with lower intramuscular and heart BCAAs in old age. The was also a trend for lower liver BCAA levels in old age. Only few BCAA catabolic enzymes in each tissue were affected by aging or sex differences, which was consistent with minor differences in BCKD activity, but this was not significant. This suggests that protein levels of BCAA catabolic enzymes are preserved in aging in healthy animals and is potentially only dysregulated in disease states.

6.2 Introduction

Branched-chain amino acids (BCAAs; leucine, valine, isoleucine) are essential amino acids required in a human diet. BCAAs stimulate muscle protein synthesis, and regulate body weight and glucose homeostasis (10). BCAAs are catabolized by branched-chain aminotransferase 2 (BCAT2) predominantly in skeletal muscle, producing BCAA metabolites, branched-chain α-ketoacids (BCKAs; alpha-ketoisocaproic acid (KIC), alpha-keto-beta methylvaleric acid (KMV), and alpha-ketoisovaleric acid (KIV)). These BCKAs are predominantly catabolized in the liver as the enzyme responsible for BCKA catabolism, branched-chain ketoacid dehydrogenase (BCKD) is mostly abundant and active in the liver (241).

Despite these benefits, circulating levels of BCAAs are altered in various diseases. In chronic renal failure (236,394) and liver cirrhosis (395,396), there is a reduction in plasma BCAA levels, while in maple syrup urine disease (397,398), and insulin resistant states like obesity and type 2 diabetes mellitus (T2DM), plasma levels are elevated (11–13).

In patients with chronic renal failure there is an increase in BCKD complex abundance (27) and BCAA oxidation (28) in skeletal muscle, which could contribute to reduced BCAA muscle and plasma levels. In liver cirrhosis, decreased BCAA plasma levels may be a product of increased BCKD complex activity (29). In insulin resistant states, the abundance and activity of BCAA catabolic enzymes are altered. *BCAT2* and *BCKDHβ* mRNA levels are significantly decreased in diabetic patients, which could explain the increase in BCAA levels (23). Lian et al. also showed that mice with T2DM or obesity had lower BCKD activity than in control mice (24). Numerous studies have examined how targeting BCAA catabolism can potentially improve insulin sensitivity (23,24,326,327), emphasizing the link between the two pathways.

Additionally, BCAAs and their metabolites have been shown to be causative (17,21,107,113,114) in inducing insulin resistance.

BCAAs and their metabolism implicated in diseases stated above all have age as an important risk factor (34–37). However, there are no studies that have investigated BCAAs and their metabolism in aging. Old men exhibit significantly lower circulating BCAA levels (38,39). This is interesting, as insulin resistance is more prevalent in older individuals (41), and BCAAs are upregulated in insulin resistance (12,13), complicating the link between the two. Amino acid concentrations and protein intake are reduced with aging, which could play a factor, but the activity and the abundance of enzymes involved in BCAA metabolism could play a role in these BCAA levels and ultimately the worsening of insulin sensitivity with age.

Additionally, most studies use male rodents to assess BCAA catabolism, but interestingly, sex hormone estrogen inhibits the BCKD complex by activating BCKD kinase (BDK), a negative regulator of BCKD, decreasing BCAA catabolism (42,43). Previous studies have shown higher plasma BCAA concentrations in males compared to females (266). Also, males have greater leucine oxidation compared to women following endurance exercise (44). However, very little work has been done examining the effect of sex on BCAA levels and BCAA catabolic enzyme activity and abundance in relevant tissues. Thus, since BCAAs are implicated in many disease states, and aging is a risk factor of many diseases, we will analyze how aging affects BCAA levels and enzymes related to their metabolism in various tissues in both sexes.

6.3 Materials and Methods

Ethics Statement:

All animal experiments were approved by the York University Animal Care Committee in accordance with the recommendations of the Canadian Council on Animal Care.

Animals:

Fifteen male and 15 female 8-week-old CD2F1 mice were purchased from Charles River (Senneville, Quebec, Canada) and Envigo Laboratories (Haslett, Michigan, United States). Mice were acclimatized and housed in the vivarium with free access to food and water. Tissues and plasma samples were used from animals following a previous study (399). One set of male and female mice (old) were aged till 16.5 months (n=8 for each). Another set of male and female mice (young) were aged until 10-weeks-old (n=7 for each). For females, because they were cycling, estrous tracking occurred 1-week prior to treatment to ensure that female mice were in the same stage of their estrous cycle. Both young and old, male, and female vehicle mice were injected with vehicle (10% DMSO in saline) for 6 weeks. Animal body weight and food consumption were recorded daily. At the end of the study (4 months for young and 18 months for old) animals were euthanized via cervical dislocation. Following sacrifice, plasma, skeletal muscle, adipose tissue, liver, and heart were collected. Tibialis anterior was used as muscle of choice as it contains both type I and type II fibers.

Insulin Tolerance Test

Following a 6 h food deprivation, glucose readings (basal glucose) and blood was collected through the saphenous vein. Then an intraperitoneal insulin (Humulin R,

DIN#00586714, short acting insulin) injection was administered (0.75 U/kg body weight). Like basal glucose readings, blood glucose post insulin (5-120 min) was measured and collected through the saphenous vein.

BCKD Activity Assay:

We measured BCKD activity using a modified version of a previous assay (21). About ~30 mg of frozen tibialis anterior muscle, adipose tissue, liver, or heart were crushed in liquid nitrogen and homogenized (Bio-Gen PRO200 Homogenizer) in 250 µL of ice-cold buffer 1 (30 mM KPI, 3 mM EDTA, 5 mM DTT, 1 mM valine, 3% FBS, 5% Triton X-100, 1 µM leupeptin) and centrifuged at 10000g for 10 minutes. Then, 50 µL of the supernatant was added to 300 µL of buffer 2 (50 mM HEPES, 30 mM KPI, 0.4 mM CoA, 3 mM NAD+, 5% FBS, 2 mM thiamine, 2 mM magnesium chloride and 7.8 µM ^{14}C-labelled valine (#ARC0678, American Radiolabeled Chemicals (St. Louis, Missouri, United States of America)). This reaction took place in a 1.5 mL Eppendorf tube, which had a 2 M NaOH wick taped to inside surface of the lid. Each Eppendorf tube was capped and sealed tight using tape, before being placed in an incubator at 37°C for 30 min. The radiolabeled $^{14}CO_2$ released from the BCKD reaction reacted with NaOH on the wick. The wick was counted in a liquid scintillation counter to measure BCKD activity. Then 50 µL of the reaction mix was counted in a liquid scintillation counter to measure total radioactivity. Protein levels were also measured, and BCKD activity measured from the wick was adjusted for the total radioactivity and protein levels of the respective sample. We used valine instead of leucine, as valine-derived KIV is the preferred substrate for BCKD (352). Detailed procedure is outlined in Appendix F.

Tissue Homogenization

Tibialis anterior, liver, adipose tissue and heart weighed and homogenized in 7 volumes of homogenization buffer (in mM: 20 mM HEPES pH 7.4, 2 mM EGTA, 50 mM NaF, 100 mM KCl, 0.2 mM EDTA, 50 mM glycerolphosphate) supplemented with 1 mM DTT, 1 mM benzamidine, 0.5 mM sodium vanadate, and protease (10 µl/ml of homogenization buffer (#P8430, Sigma Aldrich (Oakville, Ontario, Canada)) and phosphatase (10 µl/ml of homogenization buffer (#P5726, Sigma Aldrich)) inhibitor cocktails while on ice. This homogenate was then centrifuged 3 min at 1000 *g* and 4°C. The supernatant was collected and centrifuged 30 min at 10000 g and 4°C. These samples were then used for western blotting, and ultra-high-pressure liquid chromatography.

Western Blotting

The Pierce BCA Protein Assay Kit (Thermo Scientific, #23225) was used to determine protein concentration. The KC4 plate reader software (Bio-Tek Instruments Inc., Winooski, Vermont, United States) determined the absorbance reading of each well at a wavelength of 550 nanometers. A standard curve was then used to estimate the volume needed to load 40 µg of protein into one well of a polyacrylamide gel. Proteins were separated on a 10% SDS-polyacrylamide gel electrophoresis (SDS-PAGE). The gel was then transferred overnight onto a 0.2 µm-pore sized polyvinylidene difluoride membranes. Membranes were incubated with a ponceau S dye to check the protein was transferred. Membranes with ponceau were imaged with BioRAD ChemiDoc XRS+ and quantified with Image Lab software (version 8, Bio-RAD, California, United States) as a loading control. Next, the dye was washed off with 3 5-minute washes of Tris Buffered Saline with Tween (TBST). Membranes were then incubated for one

hour in 5% non-fat milk in TBST at room temperature to block non-specific antigen binding. After, they were then rinsed 3 times for 5 minutes each with TBST at room temperature and then incubated with the primary antibody of interest (Table 6.1) overnight at 4°C.

Table 6.1: List of primary antibodies.

Primary Antibody	Dilution	Company Purchased From	Secondary Antibody
BCAT2	1:1000	ProteinTech #16417-1-AP	Anti-rabbit (CST #7074)
BCKD	1:1000	Cell Signaling (CST) #90198	Anti-rabbit (CST #7074)
Ph-BCKD (Ser293)	1:1000	CST #40368	Anti-rabbit (CST #7074)
BDK	1:1000	Thermo Fisher #PA5-31455	Anti-rabbit (CST #7074)
Pp2cm	1:1000	ProteinTech #14573-1-AP	Anti-rabbit (CST #7074)
LAT1	1:500	Invitrogen #PA5-50485	Anti-rabbit (CST #7074)
SDHA	1:1000	CST #11998	Anti-rabbit (CST #7074)

Following the overnight incubation in primary antibody, membranes were rinsed 3 times for 5 minutes each with TBST and then incubated in a secondary antibody (diluted in 5% milk with TBST) for three hours at room temperature. Secondary antibody, anti-rabbit (CST #7074) was diluted in 1:2000-10000. After incubation with the secondary antibody, membranes were washed 3 times for 5 minutes each with TBST before HRP chemical luminescent substrate (Sigma Aldrich, #WBKLS0500) was applied to them. BioRAD ChemiDoc XRS+ was used for signal visualization and the images were quantified with Image Lab software (version 8).

Amino Acid Concentrations

This was done as previously described (17). Tissue was homogenized as described above, and supernatant containing free amino acids were diluted in a 1:2:1:8 ratio (sample: potassium phosphate buffer: 0.1 N hydrochloric acid: HPLC grade water, respectively). Diluted samples were pre-column derivatized with a 1:1 ratio of sample to o-Phthalaldehyde (29.28 mM) (Sigma Aldrich, #P1378). They were injected into a YMC-Triart C18 column (C18, 1.9 µm, 75 × 3.0 mm; YMC America, Allentown, PA, USA) fitted onto an ultra-high-pressure liquid chromatography system (Nexera X2, Shimadzu, Kyoto, Japan) that was connected to a fluorescence detector (Shimadzu, Kyoto, Japan; excitation: 340 nm; emission: 455 nm). Amino acids were eluted with a gradient solution derived from mobile phase A (20 mM potassium phosphate buffer (6.5 pH)) and mobile phase B (45% HPLC-grade acetonitrile, 40% HPLC-grade methanol and 15% HPLC-grade water) at a flow rate of 0.8 ml/min. We used a gradient of 5%–100% of mobile phase B over 21 min. Amino acid concentrations were calculated using amino acid standard (Sigma Aldrich, #AAS18) curves and for muscle, liver, adipose tissue, and heart were normalized to total protein of the respective sample. Detailed procedure is outlined in Appendix G.

BCKA Concentrations

Homogenized muscle, liver, adipose tissue and heart samples, and plasma samples were diluted in a 1:2:1:8 ratio (sample: potassium phosphate buffer: HPLC-grade water/homogenization buffer: HPLC-grade water, respectively). Diluted samples were treated with a 1:1 ratio of a 1,2-diamino-4,5-methylenedioxybenzene (DMB) (Sigma Aldrich, #66807) solution. DMB solution was prepared by adding 1.6 mg of DMB to 1.0 mL of solution, which contained 4.9 mg of

sodium sulfite, 70 μL of 2-mercaptethanol, and 58 μL of concentrated 12 M HCl in 0.87 mL of ddH_2O. Once samples were treated with DMB, this solution was heated at 85ºC for 45 minutes then cooled on ice for at least 5 min. They were injected into an Inertsil ODS-4 (2 μM, 100 × 2.1 mm; GL Sciences, Torrance, CA, USA) fitted onto an ultra-high-pressure liquid chromatography system (Nexera X2, Shimadzu, Kyoto, Japan) that was connected to a fluorescence detector (Shimadzu, Kyoto, Japan; excitation: 367 nm; emission: 446 nm). Mobile phases were (A) HPLC-grade methanol/ddH_2O (30/70, v/v) and (B) HPLC-grade methanol. Gradient elution was performed as follows: 0 min 0% B, 3.33 min 0%B, 5 min 50%B, 17.34 min 50%B. The flow rate was 0.2 mL/min, and the column temperature was maintained at 40ºC. Detailed procedure is outlined in Appendix H.

Statistical Analysis and Data Presentation

All immunoblot analyses were quantified and adjusted to their corresponding ponceau stains, opposed to γ-tubulin in the previous chapters, as microtubules comprising of tubulin proteins are reduced in aging (400). Phosphorylated BCKD was expressed relative to total BCKD in each tissue. BCKD activity data are presented as CPM of the CO_2 released and bound to the wick corrected for total radioactivity and μg of protein of each respective sample. All graphs were drawn using Graph pad prism version 8. Prism software also provided ara under the curve data for the insulin tolerance test. Data are presented as mean ± SEM. Two-way analysis of variance (ANOVA) was used and Tukey's post-hoc tests were done to measure statistically significant differences among means. Significance was determined as $p < 0.05$. Statistical analyses were performed using GraphPad Prism 8 software (GraphPad, Massachusetts, United States).

6.4 Results

There was no sex or aging effect on plasma BCAA (Fig 6.1A-D) or glutamate levels (Fig 6.1E). Old male mice had greater total plasma BCAAs compared to young male mice and old female mice (Fig 6.1A, $p<0.05$). Plasma leucine (Fig 6.1B, $p<0.01$), isoleucine (Fig 6.1C, $p<0.05$) and valine (Fig 6.1D, $p<0.05$) levels were higher in old male mice compared to old female mice. Plasma isoleucine (Fig 6.1C, $p<0.05$) levels and a trend in plasma valine (Fig 6.1D, $p=0.0705$) levels were greater in old male mice compared to young male counterparts. Glutamate is produced in the first step of BCAA oxidation (223). There was no difference in plasma glutamate in old male mice compared to young male mice and old female mice (Fig 6.1E).

In female mice, aging reduced total BCKAs (Fig 6.1F, $p<0.001$), while there was a trend for reduced total BCKAs in aging for male mice ($p=0.0899$). Young female mice showed a trend for higher plasma BCKAs compared to young male mice (Fig 6.1F, $p=0.1060$). Plasma KIV levels were reduced in old female mice compared to young female mice (Fig 6.1G, $p<0.01$). Plasma KIC levels were lower in older mice compared to young mice, but this was not significant (Fig 6.1H). Plasma KMV levels were lower in old males compared to young males (Fig 6.1I, $p<0.01$), and in old females compared to young females (Fig 6.1I, $p<0.0001$). There was an effect of aging in plasma serine and alanine levels. Old male mice had greater plasma serine (Fig 6.1J, $p<0.01$), arginine (Fig 6.1K, $p<0.05$), and alanine (Fig 6.1L, $p<0.0001$) compared to young male mice. Old male mice also had greater plasma serine (Fig 6.1J, $p<0.01$), and alanine (Fig 6.1L, $p<0.001$) compared to old female mice. Old female mice had greater plasma serine (Fig 6.1J, $p<0.05$ and alanine (Fig 6.1L, $p<0.01$) levels compared to young females. There were no sex or aging effect in plasma phenylalanine levels (Fig 6.1M). Since insulin resistance is commonly linked to increased plasma BCAA and BCKA levels (11–

13,221,222), we next looked at the effect of aging and sex on insulin tolerance. Old males and females had worsened insulin tolerance 120 min post insulin injection compared to young counterparts (Fig 6.1N, $p<0.05$), but there was no sex or aging effect on area under the curve of the insulin tolerance test (Fig 6.1O).

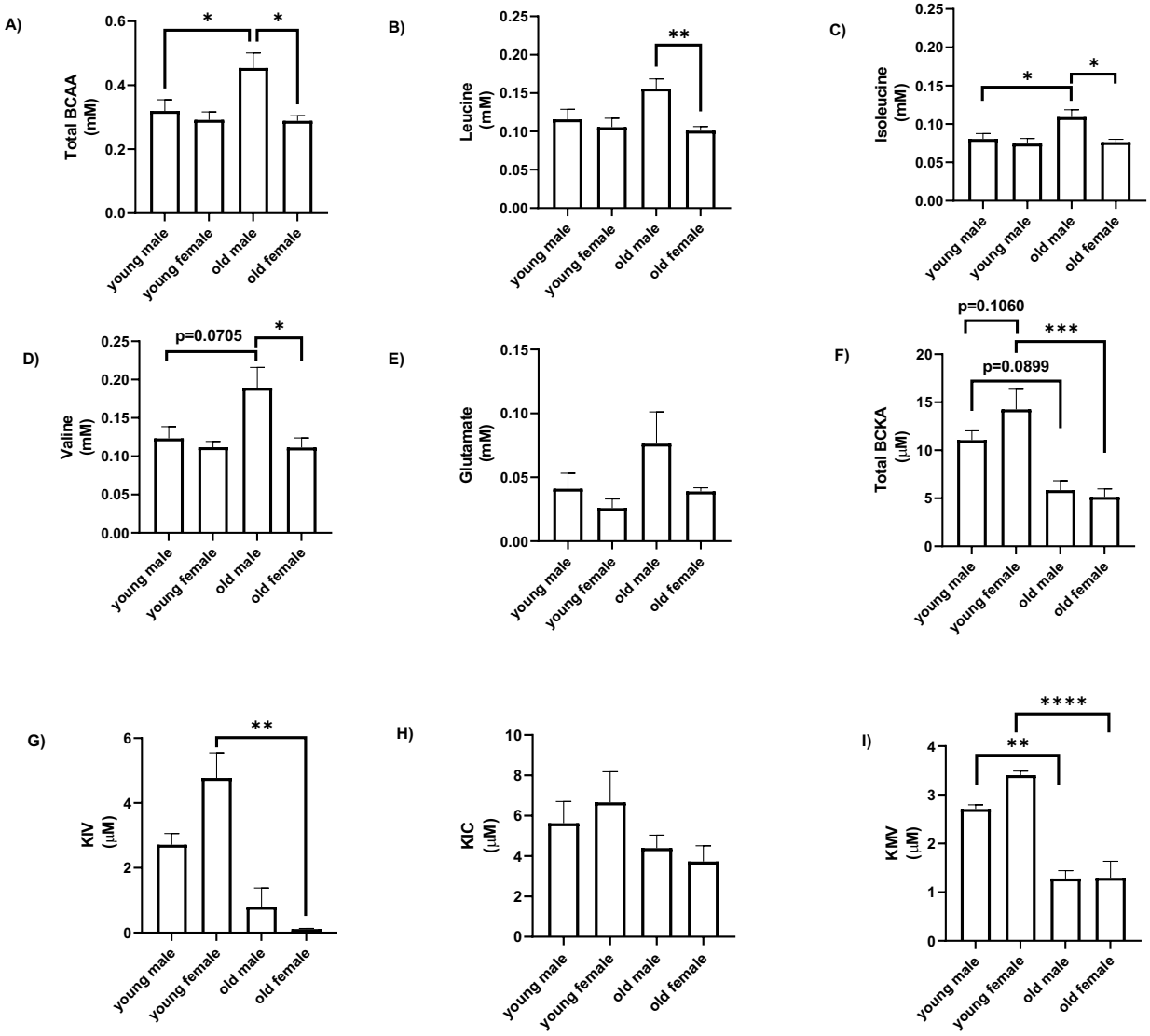

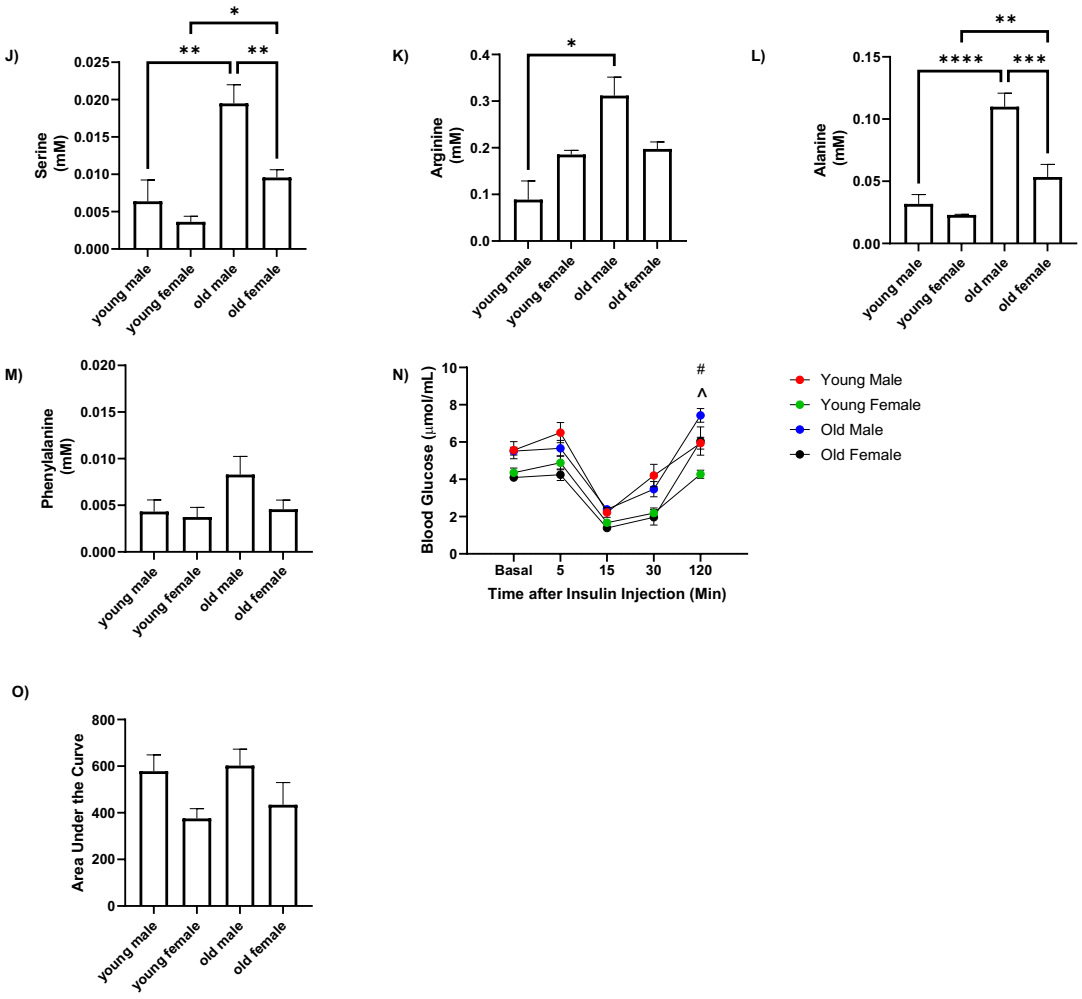

Figure 6.1: Aging affects total BCKA levels, but old male mice exhibit higher plasma BCAA levels.

Male and female young (4-month) (n=7) and old (18-months) (n=8) mice were sacrificed by cervical dislocation. HPLC was performed to measure plasma total BCAA (A), leucine (B), isoleucine (C), valine (D), glutamate (E), total BCKA (F), KIV (G), KIC (H), KMV (I), serine (J), arginine (K), alanine (L), and phenylalanine (M) concentrations. Blood glucose (basal) was taken right before insulin injection. Insulin was injected and then blood glucose was measured at different timepoints (N). Area under the curve of the blood glucose curve was analyzed (O). Data are means ± SEM. * $p<0.05$, ** $p<0.01$, *** $p<0.001$, **** $p<0.0001$. # $p<0.05$, young female vs old female. ^ $p<0.05$, young male vs old male.

Skeletal muscle plays the biggest role in whole-body BCAA oxidation (228). There was a reduced trend or significant effect of aging in intramuscular BCAA levels (Fig 6.2A-D). However, there was no sex effect. There was no effect of aging or sex on BCKA levels (Fig 6.2F-I). Total BCAAs in skeletal muscle of old male mice were reduced compared to young male mice (Fig 6.2A, $p<0.05$), and a trend for reduced total BCAAs in old female mice compared to young female mice (Fig 6.2A, $p=0.0873$). Intramuscular leucine levels in old male mice were reduced compared to young male mice (Fig 6.2B, $p<0.05$), and a trend for reduced intramuscular leucine levels in old female mice compared to young female mice (Fig 6.2B, $p=0.0961$). Old male (Fig 6.2C, $p=0.0852$), and female mice (Fig 6.2C, $p=0.0704$) had a trend for reduced intramuscular isoleucine levels compared to young sex-matched counterparts. Intramuscular valine was reduced in old male mice compared to young male mice (Fig 6.2D, $p<0.01$). There was a trend for reduced glutamate in old female mice compared to young female mice (Fig 6.2E, $p=0.0939$).

There was no difference in BCKA levels across the groups (Fig 6.2F). Intramuscular KIV levels were higher in old female mice compared to old male mice (Fig 6.2G, $p<0.05$) and a trend for increased intramuscular KIV levels in old female mice compared to young females (Fig 6.2G, $p=0.0638$). However, there were no sex or aging effect in intramuscular KIC (Fig 6.2H) or KMV (Fig 6.2I) content. There were no sex or aging effect in intramuscular serine (Fig 6.2J), arginine (Fig 6.2K), alanine (Fig 6.2L), or phenylalanine (Fig 6.2M) levels.

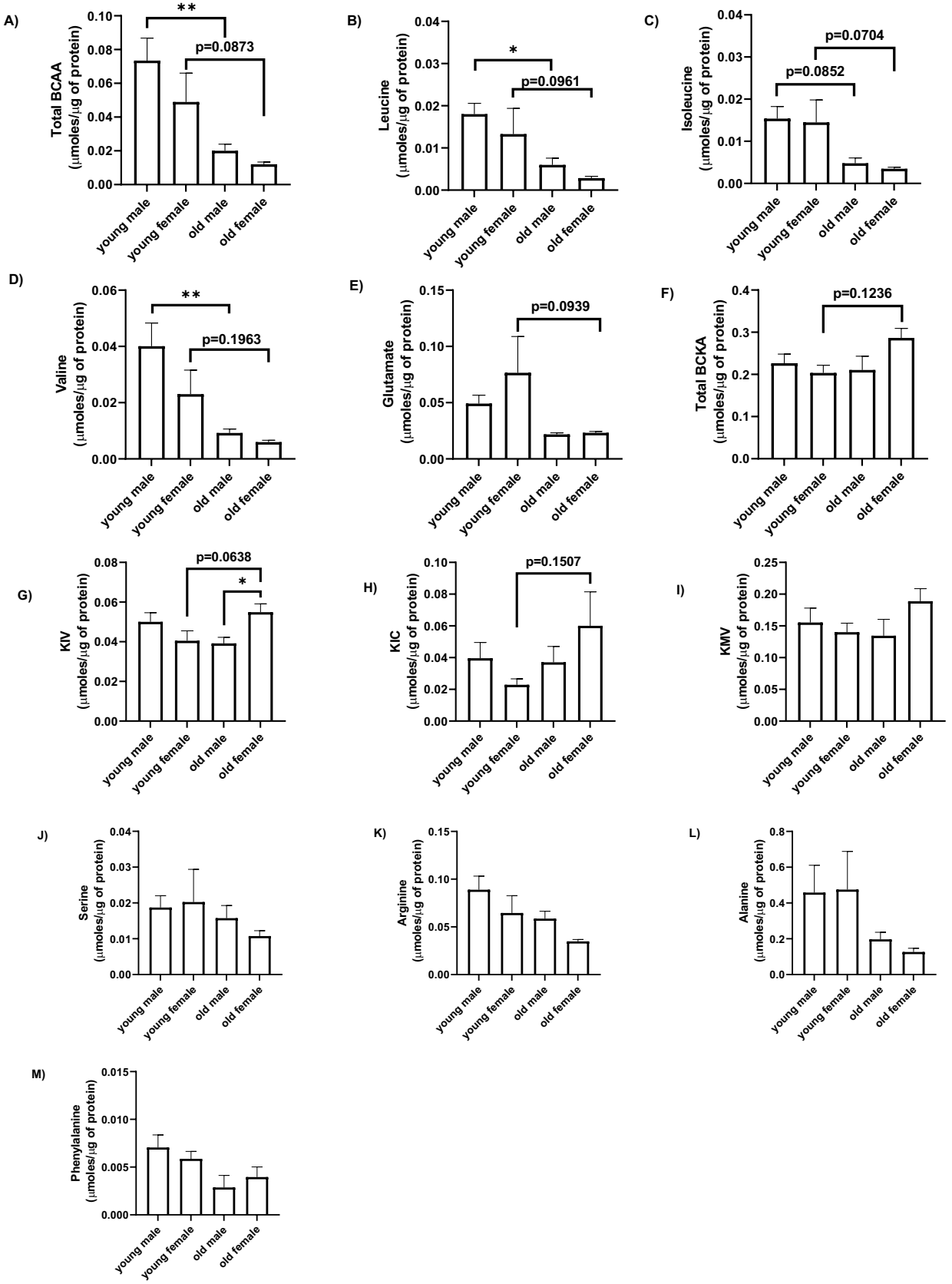
A)
Total BCAA (μmoles/μg of protein)
**
p=0.0873
B)
Leucine (μmoles/μg of protein)
*
p=0.0961
C)
Isoleucine (μmoles/μg of protein)
p=0.0704
p=0.0852
D)
Valine (μmoles/μg of protein)
**
p=0.1963
E)
Glutamate (μmoles/μg of protein)
p=0.0939
F)
Total BCKA (μmoles/μg of protein)
p=0.1236
G)
KIV (μmoles/μg of protein)
p=0.0638
*
H)
KIC (μmoles/μg of protein)
p=0.1507
I)
KMV (μmoles/μg of protein)
J)
Serine (μmoles/μg of protein)
K)
Arginine (μmoles/μg of protein)
L)
Alanine (μmoles/μg of protein)
M)
Phenylalanine (μmoles/μg of protein)
young male
young female
old male
old female

Figure 6.2: BCAAs decline with aging and BCKAs are higher in old females.
Male and female young (4-month) (n=7) and old (18-months) (n=8) mice were sacrificed by cervical dislocation. HPLC was then performed to measure intramuscular total BCAA (A), leucine (B), isoleucine (C), valine (D), glutamate (E), total BCKA (F), KIV (G), KIC (H), KMV (I), serine (J), arginine (K), alanine (L), and phenylalanine (M) concentrations. Data are means ± SEM. * $p<0.05$, ** $p<0.01$.

Changes in plasma and intramuscular BCAA levels could be attributed to changes in BCAA transporters like L-type amino acid transporter (LAT1). LAT1 protein levels were reduced in old female mice compared to young female mice (Fig 6.3A-B, $p<0.01$). There was no effect of sex or aging in protein abundance for total BCKD (Fig 6.3A, 6.3C), phosphorylated BCKD (Ser293) (Fig 6.3A, 6.3D), BCAT2 (Fig 6.3A, 6.3E), branched chain ketoacid dehydrogenase kinase (BDK) (Fig 6.3A, 6.3F), a negative regulator of BCKD, and protein phosphatase 2Cm (pp2Cm), a positive regulator of BCKD (Fig 6.3A, 6.3G) in skeletal muscle. A lack of difference in BCAA catabolic enzymes could be in part due to differences in mitochondrial levels, as many characteristics of mitochondrial health is reduced with aging (271), and these catabolic enzymes are mitochondrial proteins. Thus, we looked at succinate dehydrogenase (SDHA), a mitochondrial complex protein, but there was no effect of aging or sex in SDHA protein levels in skeletal muscle (Fig 6.3A, 6.3H). There was no effect of sex or aging on BCKD activity, but male mice did have a ~35% greater BCKD activity than female mice regardless of age, and old mice had ~30% reduced BCKD activity compared to young mice regardless of sex (Fig 6.3I), although not significant. Since reduced skeletal muscle mass (401) is associated with reduced serum BCAAs, we analyzed tibialis anterior weight. We demonstrated an aging effect on tibialis anterior weight. Tibialis anterior weight of old males ($p<0.0001$) and

old females ($p<0.05$) were reduced compared to younger counterparts (Fig 6.3J). Young female mice tibialis anterior weight was lower compared to young male mice (Fig 6.3J, $p<0.05$).

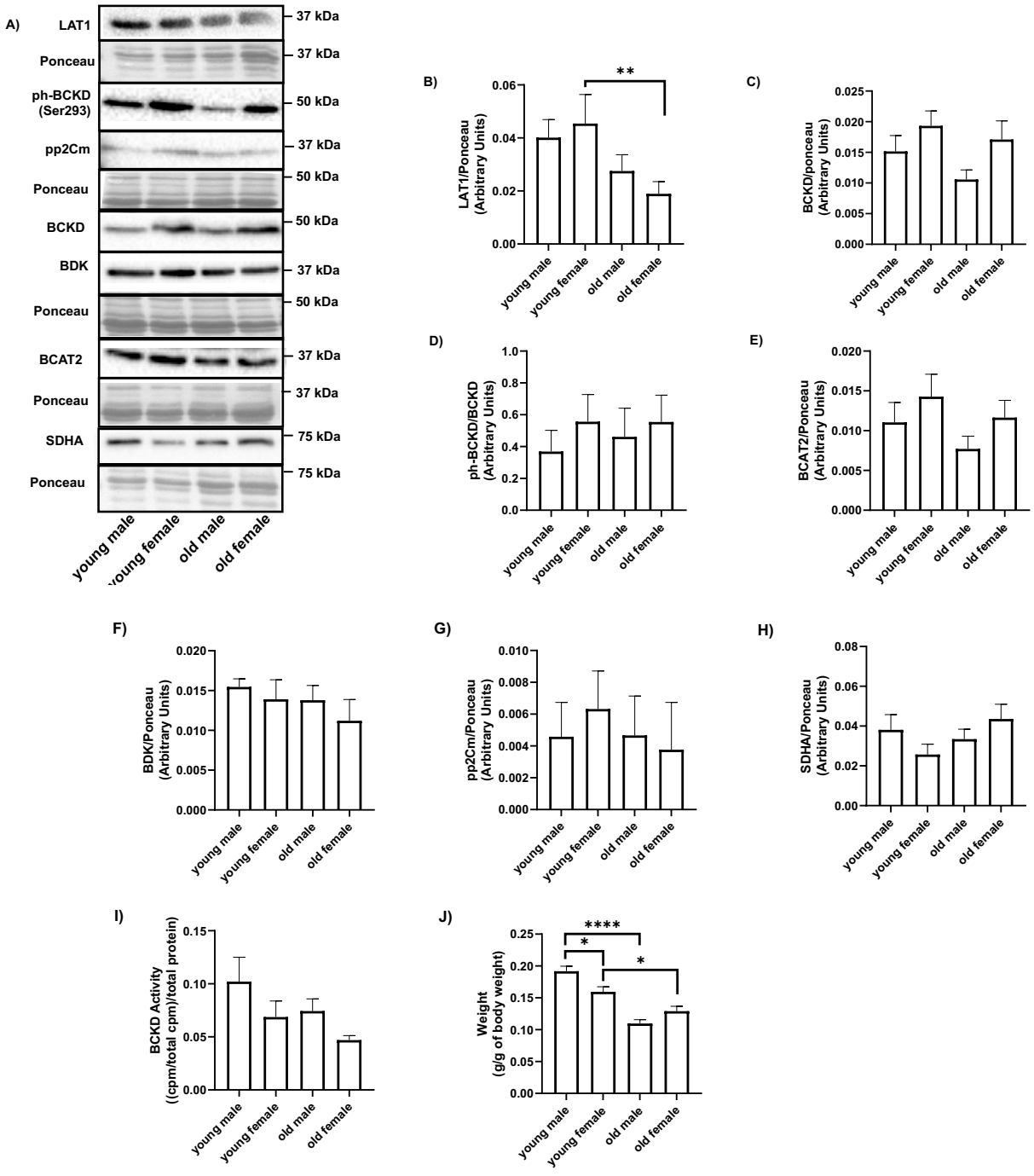

Figure 6.3: BCAA catabolic enzymes in skeletal muscle are not different in aging or sex. Male and female young (4-month) (n=7) and old (18-months) (n=8) mice were sacrificed by cervical dislocation. Proteins were immunoblotted against LAT1 (A-B), BCKD (A, C), phosphorylated (ph)-BCKD (Ser293) (A, D), BCAT2 (A, E), BDK (A, F), pp2Cm (A, G), and SDHA (A, H). BCKD activity assay was performed (I). Weight of the tibialis anterior was measured (J), corrected for body weight. Data are means ± SEM. * $p<0.05$, ** $p<0.01$, **** $p<0.0001$.

The liver is an important tissue to investigate in regard to BCAA catabolism as BCKAs are predominantly catabolized by the liver, where BCKD activity is highest (241). There was a trend for an aging effect in total BCAAs (Fig 6.4A), but no effect of sex on any BCAA levels in the liver (Fig 6.4A-D). Old male mice showed reduced total BCAAs in the liver compared to young males (Fig 6.4A, $p<0.05$), while old female mice showed a trend for reduced total BCAAs compared to young females (Fig 6.4A, $p=0.0909$). Liver leucine showed a trend for reduced levels in old female mice compared to young female mice (Fig 6.4B, $p=0.0674$). There was no effect of sex or aging on liver isoleucine levels (Fig 6.4C). Liver valine levels were reduced in old male mice compared to young male mice (Fig 6.4D, $p<0.05$). There was no effect of sex or aging on liver glutamate levels (Fig 6.4E).

In liver, total BCKAs were higher in old female mice compared to young females (Fig 6.4F, $p<0.05$) and a trend for higher total BCKAs compared to old males (Fig 6.4F, $p=0.0513$). Old female mice had greater KIV levels than old male mice (Fig 6.4G, $p<0.05$). Liver KIC had no differences amongst the groups (Fig 6.4H). Old female mice had greater KMV levels compared to young female mice and old male mice (Fig 6.4I, $p<0.01$). There were no changes in liver serine (Fig 6.4J) or arginine (Fig 6.4K) levels. Liver alanine levels were reduced in old male mice compared to young male mice (Fig 6.4L, $p<0.01$). Liver phenylalanine levels were reduced in old male mice and old female mice compared to young male and young female mice respectively (Fig 6.4M, $p<0.05$).

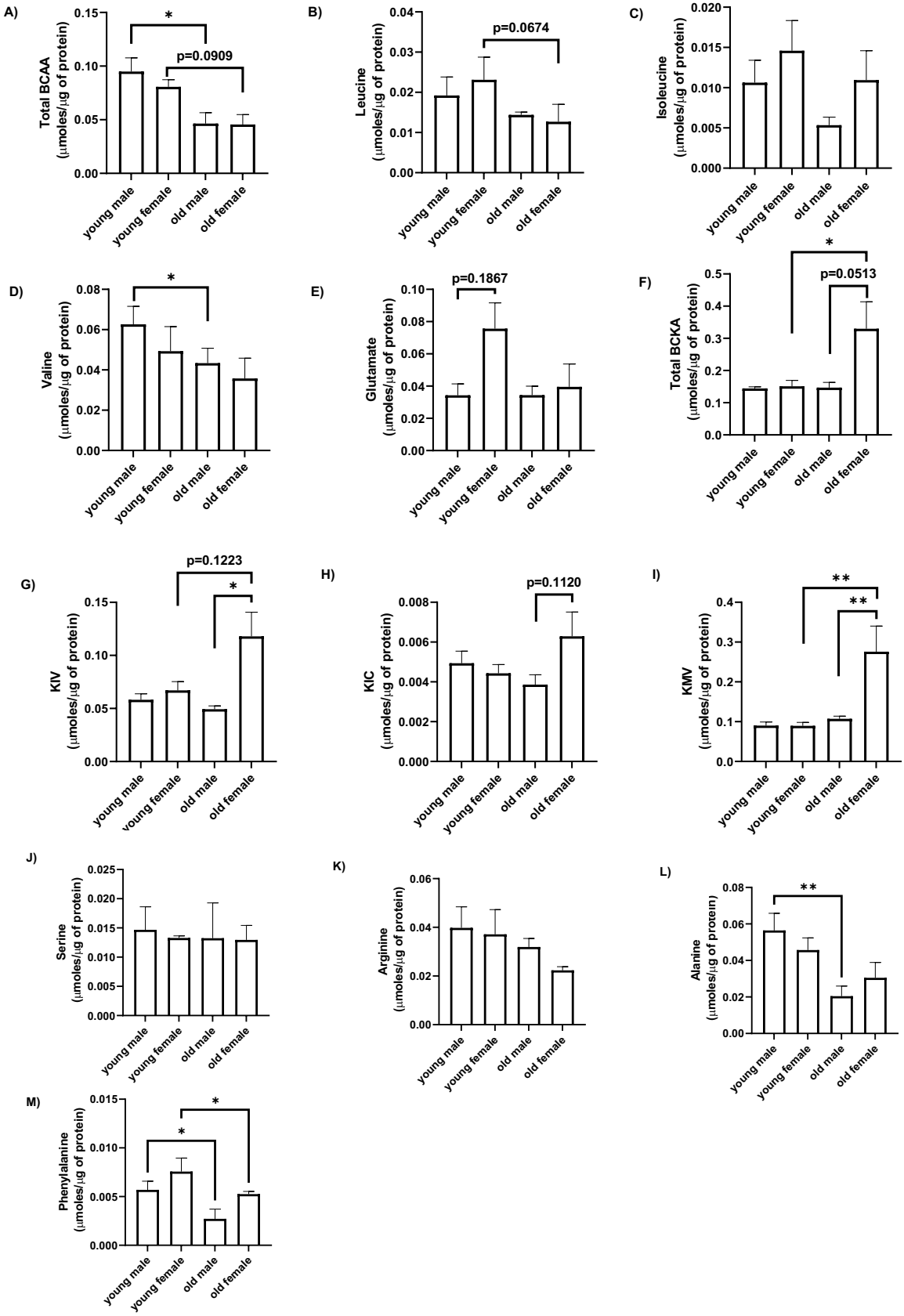
A)
Total BCAA (μmoles/μg of protein)
0.15
0.10
0.05
0.00
*
p=0.0909
young male
young female
old male
old female
B)
Leucine (μmoles/μg of protein)
0.04
0.03
0.02
0.01
0.00
p=0.0674
young male
young female
old male
old female
C)
Isoleucine (μmoles/μg of protein)
0.020
0.015
0.010
0.005
0.000
young male
young female
old male
old female
D)
Valine (μmoles/μg of protein)
0.08
0.06
0.04
0.02
0.00
*
young male
young female
old male
old female
E)
Glutamate (μmoles/μg of protein)
0.10
0.08
0.06
0.04
0.02
0.00
p=0.1867
young male
young female
old male
old female
F)
Total BCKA (μmoles/μg of protein)
0.5
0.4
0.3
0.2
0.1
0.0
*
p=0.0513
young male
young female
old male
old female
G)
KIV (μmoles/μg of protein)
0.15
0.10
0.05
0.00
p=0.1223
*
young male
young female
old male
old female
H)
KIC (μmoles/μg of protein)
0.008
0.006
0.004
0.002
0.000
p=0.1120
young male
young female
old male
old female
I)
KMV (μmoles/μg of protein)
0.4
0.3
0.2
0.1
0.0
**
**
young male
young female
old male
old female
J)
Serine (μmoles/μg of protein)
0.025
0.020
0.015
0.010
0.005
0.000
young male
young female
old male
old female
K)
Arginine (μmoles/μg of protein)
0.06
0.04
0.02
0.00
young male
young female
old male
old female
L)
Alanine (μmoles/μg of protein)
0.08
0.06
0.04
0.02
0.00
**
young male
young female
old male
old female
M)
Phenylalanine (μmoles/μg of protein)
0.015
0.010
0.005
0.000
*
*
young male
young female
old male
old female

Figure 6.4: Total BCAAs are lower in old male mice and total BCKA levels are higher in old female mice
Male and female young (4-month) (n=7) and old (18-months) (n=8) mice were sacrificed by cervical dislocation. HPLC was then performed to measure total BCAA (A), leucine (B), isoleucine (C), valine (D), glutamate (E), total BCKA (F), KIV (G), KIC (H), KMV (I), serine (J), arginine (K), alanine (L), and phenylalanine (M) concentrations. Data are means ± SEM. * $p<0.05$, ** $p<0.01$.

There was an effect of sex on LAT1 protein abundance, as female mice had greater LAT1 protein abundance compared to male age-matched counterparts (Fig 6.5A-B, $p<0.05$). There was no effect of sex or aging on BCAA catabolic enzymes. Female old mice also had reduced total BCKD levels compared to old male mice (Fig 6.5A, 6.5C, $p<0.05$). There was no effect of sex or aging on the phosphorylation of BCKD (Ser293) (Fig 6.5A, 6.5D) or BDK protein abundance (Fig 6.5A, 6.5E). There was an effect of aging in pp2Cm levels, as young mice had greater pp2Cm protein levels compared to sex-matched old mice (Fig 6.5A, 6.4F, $p<0.05$). There was no effect of sex or aging on SDHA protein levels (Fig 6.5A, 6.5G). There was no effect of sex or aging on BCKD activity (Fig 6.5H), but male mice did have ~20% greater BCKD activity than female mice regardless of age, and old mice had ~23% reduced BCKD activity regardless of sex. Liver weight of old males was reduced compared to young males (Fig 6.5I, $p<0.05$).

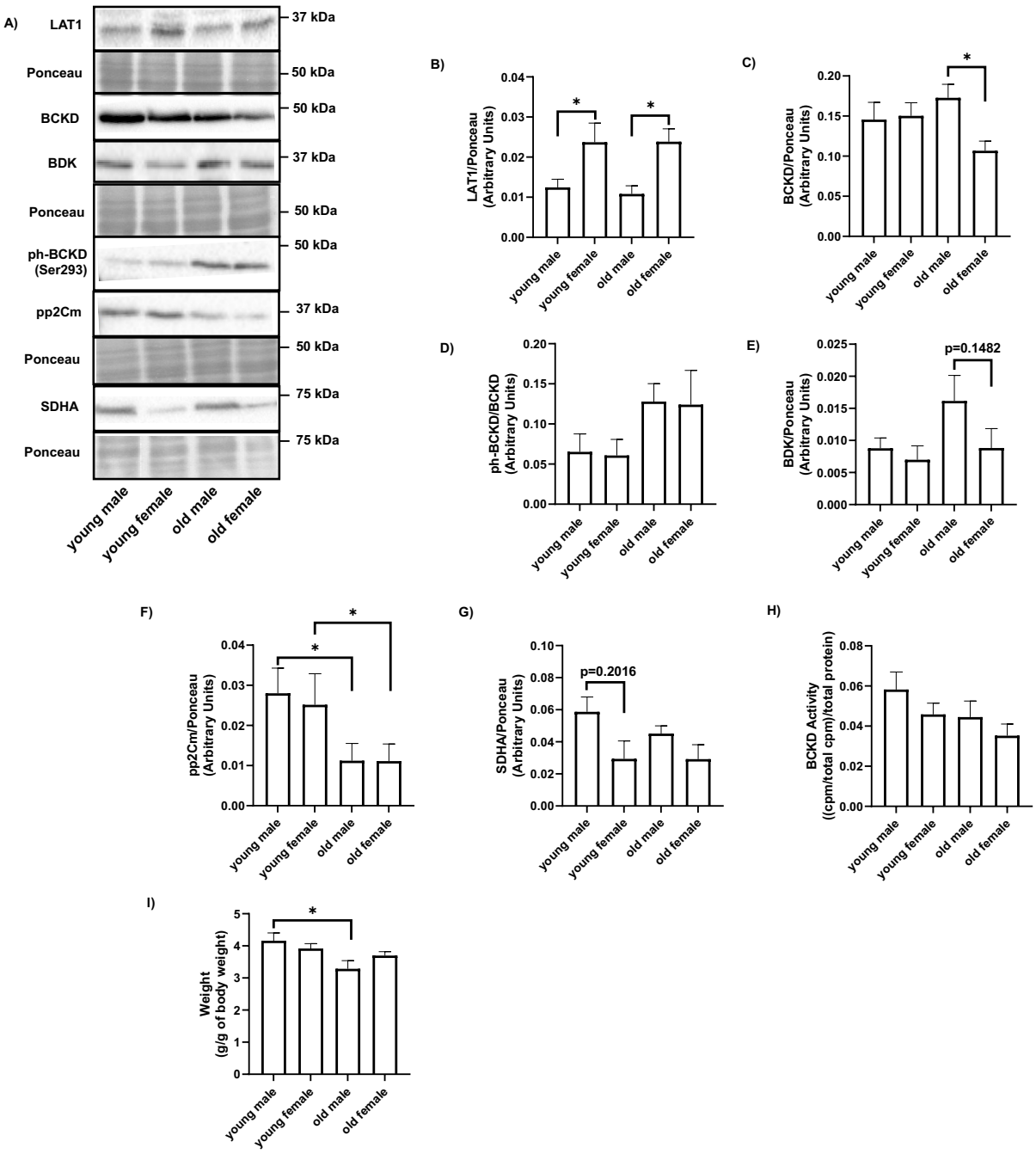

Figure 6.5: LAT1 is higher in females, and pp2Cm is lower in aging in the liver
Male and female young (4-month) (n=7) and old (18-months) (n=8) mice were sacrificed by cervical dislocation. Proteins were immunoblotted against LAT1 (A-B), BCKD (A, C) ph-BCKD (Ser293) (A, D), BDK (A, E), pp2Cm (A, F), and SDHA (A, G). BCKD activity assay was performed (H). Weight of the liver was measured (I), corrected for body weight. Data are means ± SEM. * $p<0.05$, ** $p<0.01$.

Adipose tissue is another site of BCAA catabolism (393). There was no effect of sex or aging on adipose tissue total BCAAs (Fig 6.6A), any of the individual BCAAs (Fig 6.6B-D), or glutamate levels (Fig 6.6E). There was a trend for an aging effect in BCKA levels, as old male mice had greater total BCKAs compared to young male counterparts (Fig 6.6F, $p<0.01$). Old male mice had greater KIV (Fig 6.6G, $p<0.05$) and KMV levels (Fig 6.6I, $p<0.001$) in adipose tissue compared to young males. Young female mice had greater KIC levels compared to young males (Fig 6.6H, $p<0.001$). Old female mice had trend for increased KMV levels compared to young female mice (Fig 6.6I, $p=0.0905$). There was no effect of sex or aging in adipose tissue serine (Fig 6.6J), arginine (Fig 6.6K), alanine (Fig 6.6L), or phenylalanine (Fig 6.6M) levels.

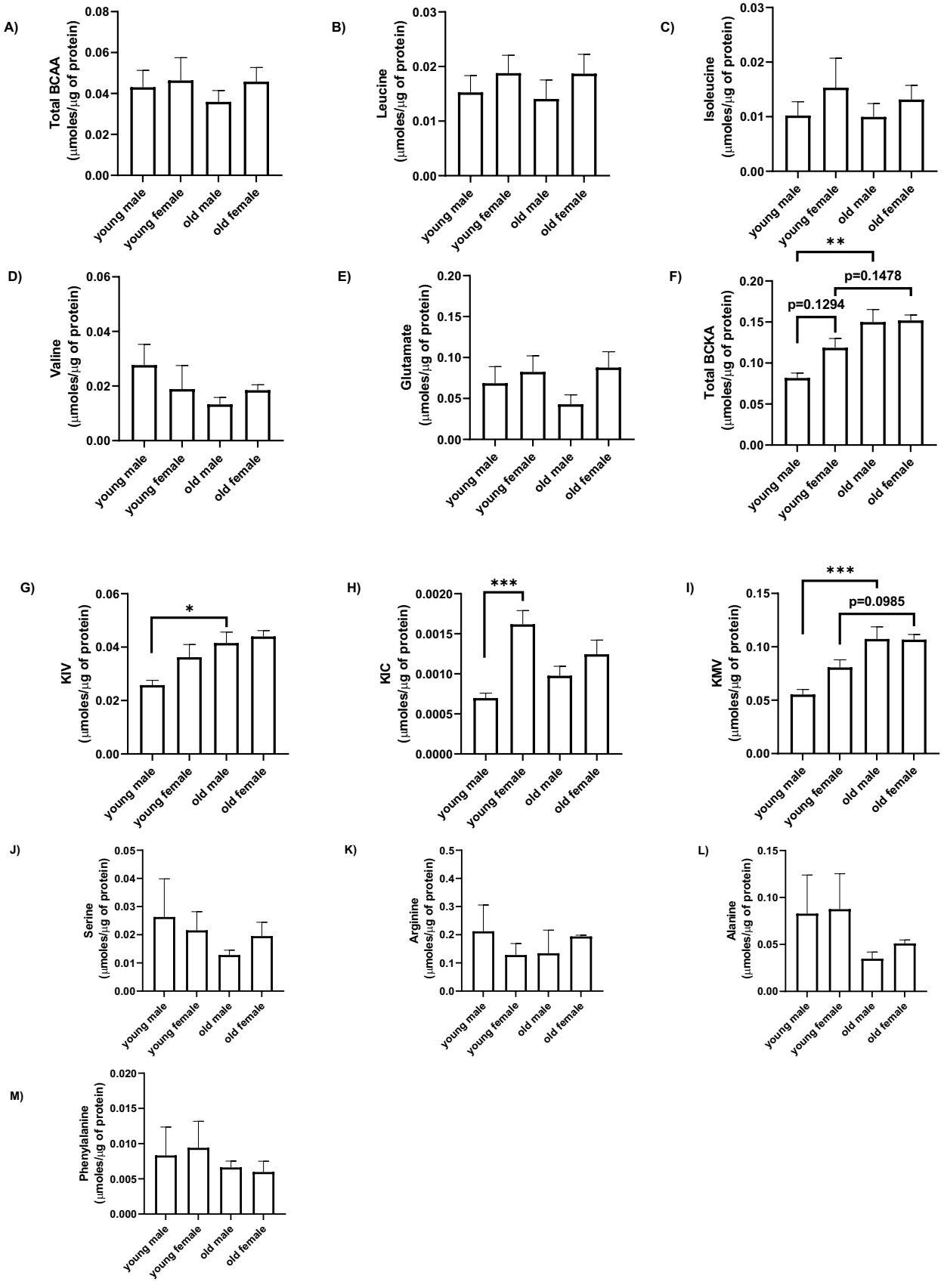
A)
Total BCAA (μmoles/μg of protein)
0.08
0.06
0.04
0.02
0.00
young male
young female
old male
old female
B)
Leucine (μmoles/μg of protein)
0.03
0.02
0.01
0.00
C)
Isoleucine (μmoles/μg of protein)
0.03
0.02
0.01
0.00
**
D)
Valine (μmoles/μg of protein)
0.06
0.04
0.02
0.00
E)
Glutamate (μmoles/μg of protein)
0.20
0.15
0.10
0.05
0.00
F)
Total BCKA (μmoles/μg of protein)
p=0.1294
p=0.1478
0.20
0.15
0.10
0.05
0.00
G)
KIV (μmoles/μg of protein)
*
0.06
0.04
0.02
0.00
H)
KIC (μmoles/μg of protein)
***
0.0020
0.0015
0.0010
0.0005
0.0000
I)
KMV (μmoles/μg of protein)
***
p=0.0985
0.15
0.10
0.05
0.00
J)
Serine (μmoles/μg of protein)
0.05
0.04
0.03
0.02
0.01
0.00
K)
Arginine (μmoles/μg of protein)
0.5
0.4
0.3
0.2
0.1
0.0
L)
Alanine (μmoles/μg of protein)
0.15
0.10
0.05
0.00
M)
Phenylalanine (μmoles/μg of protein)
0.020
0.015
0.010
0.005
0.000

Figure 6.6: Total BCKA levels are higher in aged mice in adipose tissue.
Male and female young (4-month) (n=7) and old (18-months) (n=8) mice were sacrificed by cervical dislocation. HPLC was then performed to measure adipose tissue total BCAA (A), leucine (B), isoleucine (C), valine (D), glutamate (E), total BCKA (F), KIV (G), KIC (H), KMV (I), serine (J), arginine (K), alanine (L), and phenylalanine (M) concentrations. Data are means ± SEM * $p<0.05$, ** $p<0.01$, *** $p<0.001$.

In adipose tissue, there was no effect of sex or aging on LAT1 protein (Fig 6.7A-B). There was no significant effect of sex or aging on total BCKD protein levels (Fig 6.7A, 6.7C), the phosphorylation of BCKD (Ser293, Fig 6.7A, 6.7D) protein, and total BCKD (Fig 6.7A, 6.7C) protein abundance. BCAT2 protein levels were reduced in old female mice compared to young female mice (Fig 6.7A, 6.7E, $p<0.05$). There was no effect of sex or aging on BDK proteins levels (Fig 6.7A, 6.7F). Old male mice had a trend for reduced pp2Cm protein levels in old male mice compared to young male mice (Fig 6.7A, 6.7G, $p=0.1082$). There was no effect of sex or aging on BCKD activity in adipose tissue (Fig 6.7H). Old male mice had 62% and 46% greater BCKD activity compared to young female and old male mice respectively (Fig 6.7I). There was an aging effect on adipose tissue weights, as old animals had greater adipose tissue weights compared to young animals (Fig 6.7I, $p<0.0001$).

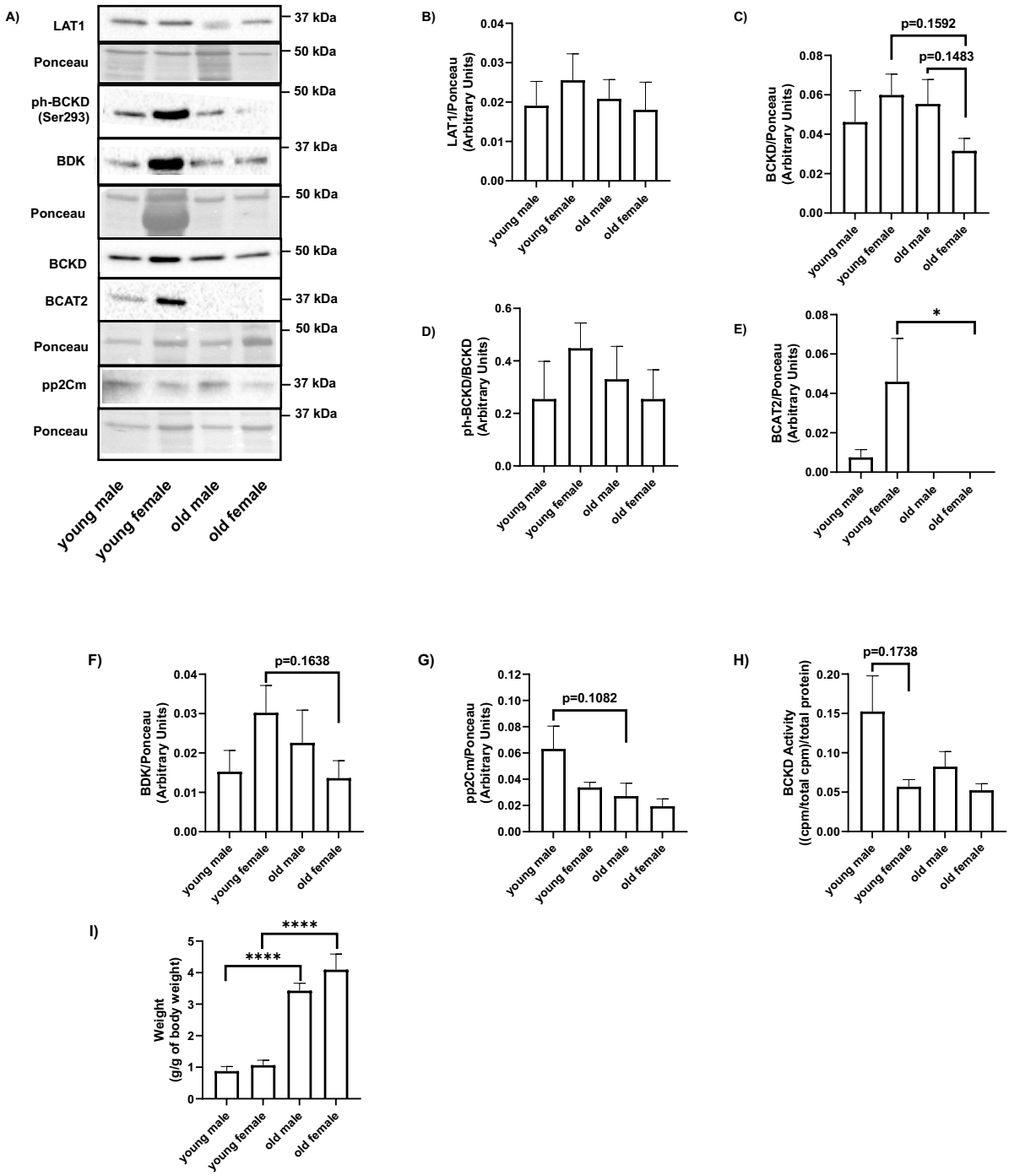

Figure 6.7: BCAT2 protein levels are lower in old female mice in adipose tissue
Male and female young (4-month) (n=7) and old (18-months) (n=8) mice were sacrificed by cervical dislocation. Proteins were immunoblotted against LAT1 (A-B), BCKD (A, C), ph-BCKD (Ser293) (A, D), BCAT2 (A, E), BDK (A, F) and pp2Cm (A, G). BCKD activity assay was performed (H). Weight of the adipose tissue was measured (I), corrected for body weight. Data are means ± SEM * $p<0.05$, **** $p<0.0001$.

Studies have shown how BCAAs and their metabolism are linked to cardiac related diseases (25,377,402), stressing the importance in studying BCAAs and their metabolism in heart tissue with the effect of aging. In the heart, there was an effect of aging on BCAA levels, as old mice had reduced total BCAA (Fig 6.8A, $p<0.0001$), and leucine (Fig 6.8B, $p<0.0001$) levels compared to young counterparts regardless of sex. Young female mice (Fig 6.8A, $p<0.0001$) had reduced total BCAA levels compared to young male mice. Old male mice had reduced isoleucine levels compared to young male mice (Fig 6.8C, $p<0.01$). Old male ($p<0.0001$) and old female ($p<0.01$) mice had reduced valine levels compared to sex-matched young mice (Fig 6.8D). Young male mice also had greater valine levels compared to young female mice (Fig 6.8D, $p<0.0001$). There was an effect of aging, but not sex on glutamate levels (Fig 6.8E, $p<0.0001$). Old female mice also had a trend for reduced glutamate levels compared to old male mice (Fig 6.8E, $p=0.0987$).

There was no effect of sex or aging on total BCKA (Fig 6.8F) or any of the individual BCKAs, KIV (Fig 6.8G), KIC (Fig 6.8H) or KMV (Fig 6.8I) levels in the heart. There was no effect of sex or aging in heart serine levels (Fig 6.8J). Old male mice had reduced heart arginine levels compared to young male mice (Fig 6.8K, $p<0.05$). Old male mice and old female mice had lower heart alanine levels compared to young male mice (Fig 6.8L, $p<0.01$) and young female (Fig 6.8L, $p<0.05$) mice respectively. There was no effect of sex or aging in heart phenylalanine levels (Fig 6.8M).

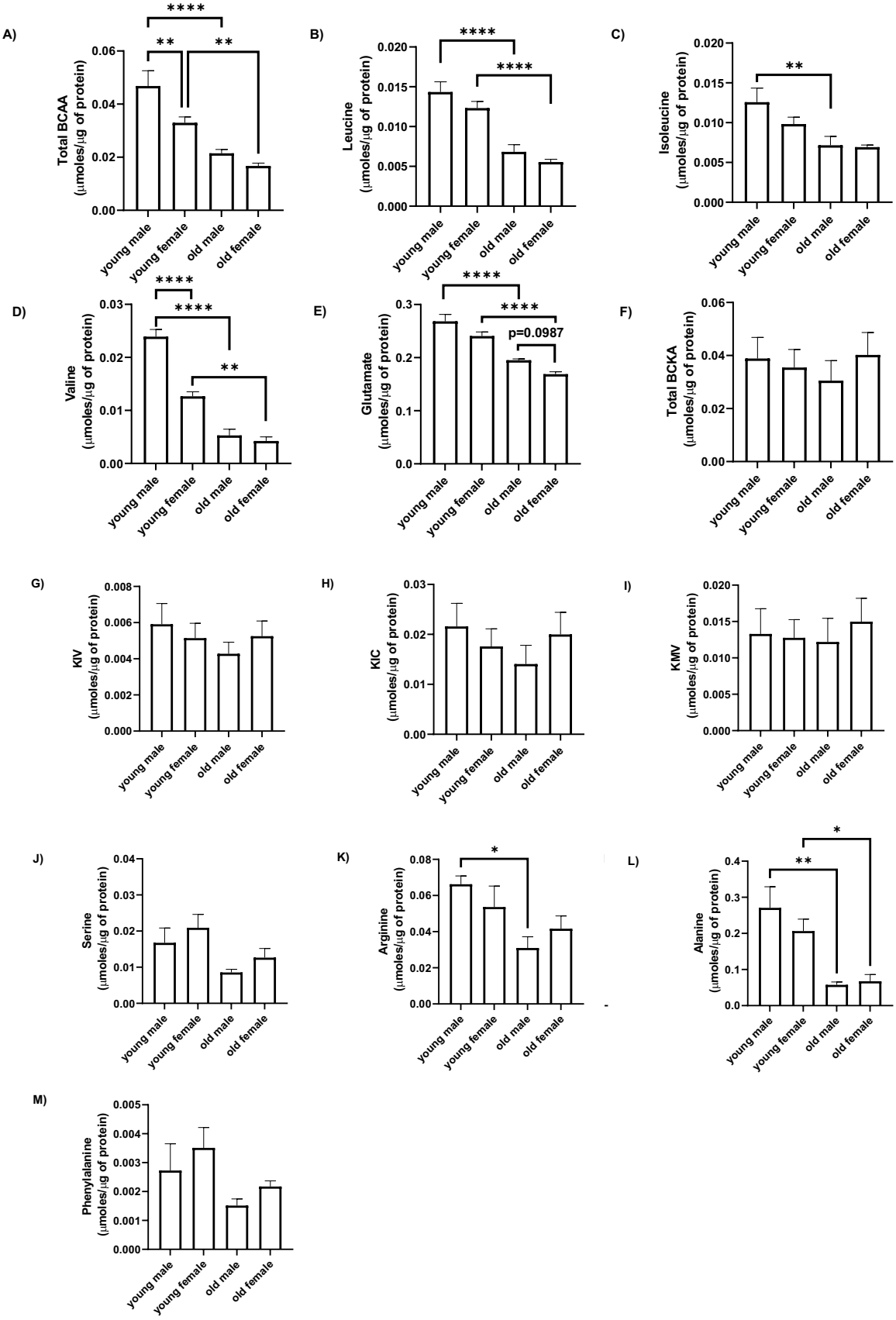
A)
Total BCAA (μmoles/μg of protein)
0.06
0.04
0.02
0.00
****
**
**
young male
young female
old male
old female
B)
Leucine (μmoles/μg of protein)
0.020
0.015
0.010
0.005
0.000
****
****
young male
young female
old male
old female
C)
Isoleucine (μmoles/μg of protein)
0.020
0.015
0.010
0.005
0.000
**
young male
young female
old male
old female
D)
Valine (μmoles/μg of protein)
0.03
0.02
0.01
0.00
****
****
**
young male
young female
old male
old female
E)
Glutamate (μmoles/μg of protein)
0.3
0.2
0.1
0.0
****
****
p=0.0987
young male
young female
old male
old female
F)
Total BCKA (μmoles/μg of protein)
0.06
0.04
0.02
0.00
young male
young female
old male
old female
G)
KIV (μmoles/μg of protein)
0.008
0.006
0.004
0.002
0.000
young male
young female
old male
old female
H)
KIC (μmoles/μg of protein)
0.03
0.02
0.01
0.00
young male
young female
old male
old female
I)
KMV (μmoles/μg of protein)
0.020
0.015
0.010
0.005
0.000
young male
young female
old male
old female
J)
Serine (μmoles/μg of protein)
0.04
0.03
0.02
0.01
0.00
young male
young female
old male
old female
K)
Arginine (μmoles/μg of protein)
0.08
0.06
0.04
0.02
0.00
*
young male
young female
old male
old female
L)
Alanine (μmoles/μg of protein)
0.4
0.3
0.2
0.1
0.0
**
*
young male
young female
old male
old female
M)
Phenylalanine (μmoles/μg of protein)
0.005
0.004
0.003
0.002
0.001
0.000
young male
young female
old male
old female

Figure 6.8: Aging but not sex affects BCAA levels in the heart.
Male and female young (4-month) (n=7) and old (18-months) (n=8) mice were sacrificed by cervical dislocation. HPLC was then performed to measure heart total BCAA (A), leucine (B), isoleucine (C), valine (D), glutamate (E), total BCKA (F), KIV (G), KIC (H), KMV (I), serine (J), arginine (K), alanine (L) and phenylalanine (M) concentrations. Data are means ± SEM. * $p<0.05$, ** $p<0.01$, **** $p<0.0001$.

In the heart, there was no effect of sex or aging on LAT1 (Fig 6.9A-B), BCKD (Fig 6.9A, 6.9C), ph-BCKD (Ser293) (Fig 6.9A, 6.9D), BCAT2 (Fig 6.9A, 6.9E) or BDK (Fig 6.9A, 6.9F) protein levels. Old male mice had reduced pp2Cm (Fig 6.9A, 6.9G, $p<0.01$) and SDHA (Fig 6.9A, 6.9H, $p<0.05$) protein levels compared to young male mice. There was no effect of sex or aging on BCKD activity (Fig 6.9I). There was no effect of aging or sex on heart weight, but old female mice had reduced heart weight compared to young females and old males (Fig 6.9J, $p<0.05$).

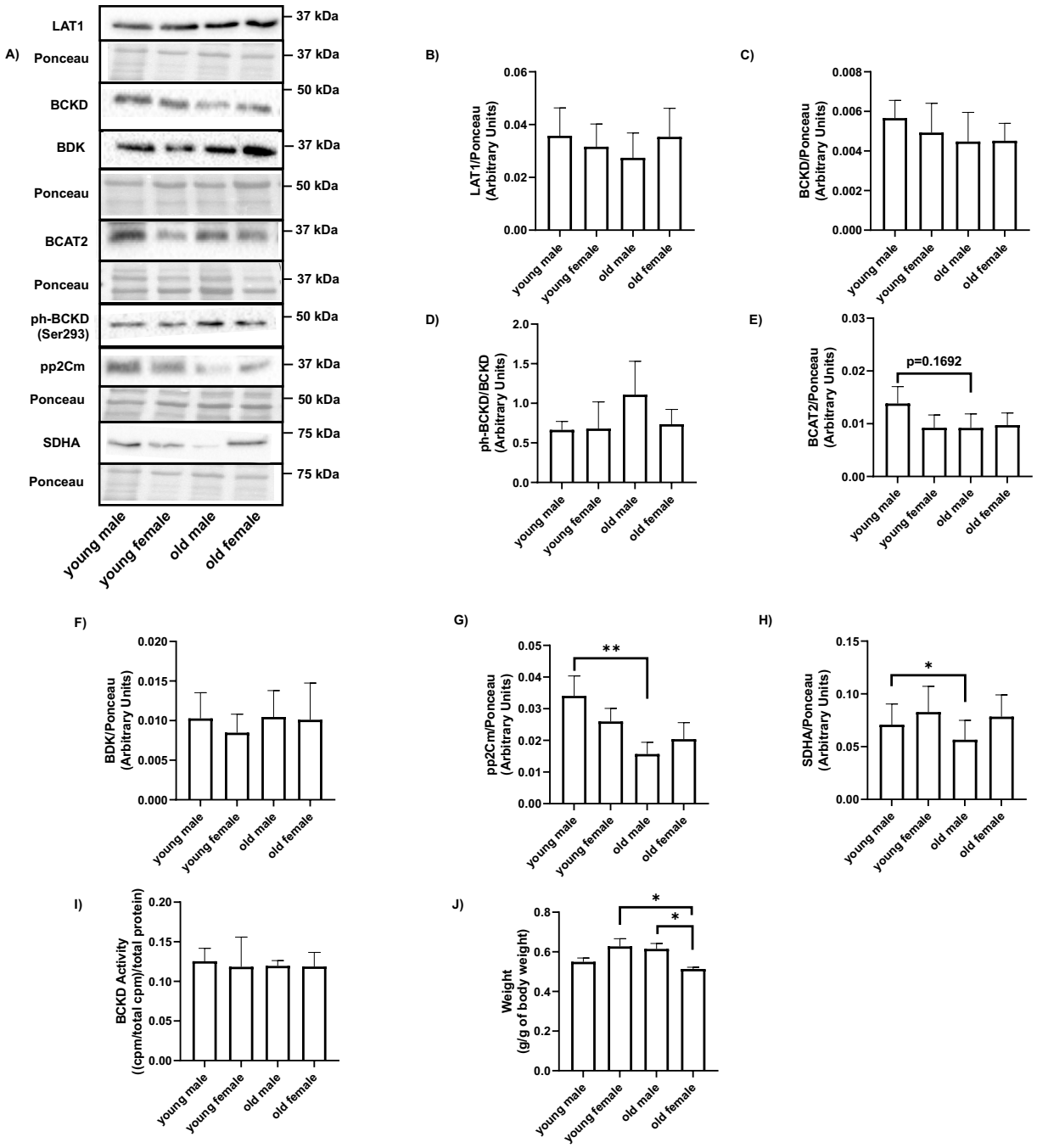

Figure 6.9: Old male mice exhibit lower pp2Cm than young counterparts in the heart
Male and female young (4-month) (n=7) and old (18-months) (n=8) mice were sacrificed by cervical dislocation. Proteins were immunoblotted against LAT1 (A-B), BCKD (A, C) ph-BCKD (Ser293) (A, D), BCAT2 (A, E), BDK (A, F), pp2Cm (A, G) and SDHA (A, H). BCKD activity assay was performed (I). Weight of the heart was measured (J), corrected for body weight. Data are means ± SEM. * $p<0.05$, ** $p<0.01$, **** $p<0.0001$.

6.5 Discussion

BCAAs and their metabolism are linked to a plethora of diseases like insulin resistance, liver cirrhosis, chronic kidney failure and maple syrup urine disease (11–13,236,394–398), and aging is a major risk factor in many of these diseases (34–37). Thus, it is important to analyze the effect of BCAA levels and their metabolic enzyme activity/abundance in relevant tissues in aging, as age related changes in BCAAs and their metabolism may be implicated in the pathogenesis of these diseases. Here we demonstrate that total plasma BCAAs were higher in aging in male mice, but not females, with a trend or significantly lower in plasma BCKAs in aging. We also report a trend for lower intramuscular BCAA levels of old mice compared to young mice regardless of sex, with similar trends in the liver. There was no difference in adipose tissue BCAA levels, but aged mice generally had higher BCKA levels. The heart demonstrated lower BCAA content in aging. However, differences in BCAA/BCKA content could not be attributed to significant differences in BCKD activity in the skeletal muscle, liver, adipose tissue, and heart, but there were still modest differences in BCKD activity. There were no consistent differences of age or sex on catabolic enzymes abundance in these tissues.

Circulating BCAA levels in men is lower compared to young counterparts (38–40). One study showed elderly individuals (average 80 years of age) with lower plasma leucine and isoleucine levels compared to young counterparts (average 29 years of age) (403). Another study showed no age related loss in total serum amino acid levels or serum BCAA levels, and greater serum BCAA levels in males compared to females in young and aged individuals (267). In our study, we see this in old animals, but not young. However, one study did show increased serum BCAAs in an older male population compared to old females, which correlated with reduced energy and protein intake in the female population (268). One study showed a trend for higher

plasma BCAAs in 18-month female mice compared to 2-month young female mice (404), while another study showed no difference in plasma BCAAs in young (3-month) and old (22-month) mice (405). Generally, in aging, protein intake is reduced (406), which could explain the lower BCAAs in old men (38–40). The old male mice from this study consumed more food than old female mice (~18%), but when corrected for body weight the difference was negligible. Young mice did consume more food per day than old mice (~20%), which could also influence intramuscular BCAA content, but this was not consistent with differences in plasma BCAAs.

Higher plasma BCAAs in old male mice might correspond with a compensatory mechanism to increase life span, as endogenous BCAA accumulation has a protective effect on leukocyte telomere length and weakness in an east Asian population (407). Another study showed that BCAA supplementation increased life span of male mice (16 months) by 12% (285), suggesting that perhaps increased plasma BCAAs in old male mice may have protective benefits. However, other studies have shown the opposite. BCAA restriction has increased lifespan in *Drosophila* (408), and this could be by reducing ribosomal protein S6 kinase (S6K1) phosphorylation, as BCAAs are potent activators of S6K1, and downregulation of S6K1 has been shown to prolong lifespan of mammals (409). Despite increased plasma concentrations in old male mice, this was not consistent in increases in intramuscular BCAA content, thus reduced BCAA content in skeletal muscle may result in reduced S6K1 activation leading to prolonged lifespan.

Generally, there was a trend towards or significant difference in intramuscular BCAAs in old age. Lower intramuscular BCAAs in old female mice compared to young female mice could be in part due to lower LAT1 protein in old female mice. There are also higher BCKA levels in old female mice. BCKD activity is ~30-35% lower in females and aged mice, despite no

significance in skeletal muscle. BCKD is tightly regulated, and small differences could contribute to major differences in BCKA levels. The lack of significant differences in BCKD activity in skeletal muscle is consistent with a lack of differences in any catabolic enzymes (ph-BCKD, total BCKD, BCAT2, BDK, and pp2Cm). The trends in BCKD activity with aging and sex seem to be consistent in adipose tissue and liver as well.

Another mechanism that could be affecting BCAA/BCKA levels is muscle wasting, as muscle mass decline is associated with reductions in serum BCAAs (401). There was an effect of aging on the tibialis anterior weight (Fig 6.3J), demonstrating that muscle wasting is occurring. Changes in basal protein degradation/synthesis could affect BCAA/BCKA levels in muscle. Numerous studies have demonstrated no change in basal protein synthesis between young and elderly male individuals (410–412). While some studies have showed a reduction in basal muscle protein synthesis with aging (413,414). One study did see significant increases in skeletal muscle mRNA content of proteolytic enzymes like forkhead box protein O3a (FoxO3a) and Muscle ring-finger protein-1 (MuRF-1) in older women compared to younger women (415). Another study found that mRNA content of MuRF-1 and atrogin-1 are downregulated in skeletal muscle of old female rats (416). Conversely, Welle et al. found no change in these E3 ligases mRNA content in aged male rats (417). The literature is still inconsistent on whether basal protein degradation and synthesis is changed with aging, thus making it hard to speculate if these changes influence BCAA concentrations in plasma and relevant tissues.

Since inflammation is increased with aging (418), depleted levels of intramuscular glutamate in old mice could also be due to their conversion to glutamine, as glutamine inhibits inflammation in muscle (419) and is important for healthy function of the immune system (420). Another potential reason for lower glutamate is our mice were starved for 3 hours prior to

sacrifice, and glutamate is converted to alanine through pyruvate in food deprived conditions for energy production (241,421), although alanine levels are not higher in muscle (Fig 6.2L).

A lack of difference in the abundance of many of the BCAA metabolic enzymes can be linked to mitochondrial content, as these BCAA catabolic enzymes are present in the mitochondria, and mitochondrial DNA volume, integrity and function are reduced with aging (271). However, other studies have shown that changes in mitochondria complex proteins depends on which muscle is being analyzed. The vastus lateralis muscle only showed reductions in aging with complex III, but not complex I, II, IV or V protein abundance (422). Surprisingly, one study shows that in the gastrocnemius and EDL the abundance of mitochondrial complex proteins was increased in aging, while in the soleus, there was a reduction in complex I and IV abundance. Also, in the adductor longus there was no change (423). Another study shows a transient dip in mitochondrial density in old age (24 month rats), but this returns to normal in 35 month rats (424), making it difficult to attribute any differences in BCAA catabolic enzyme activity and abundance to differences in mitochondria in an aging model.

There were no sex related differences between BCAAs in plasma, muscle, liver, adipose tissue, or heart in young animals, but there were significant differences in aged mice. As discussed above, aging seems to alter male mice plasma BCAA content, but female plasma BCAA content is not different. Sex hormone estrogen inhibits the BCKD complex by activating BDK, decreasing BCAA catabolism (42,43), but in old age estrogen is not a factor. We did not see significant differences in BDK in any of the tissues, but the differences in BCKD activity showed greater BCKD activity in male mice compared to female mice in skeletal muscle, liver, and adipose tissue. These differences were somewhat consistent with differences seen in BCKAs in muscle, liver, and adipose tissue. BCKD activity was measured in basal conditions, one study

has shown that males have greater leucine oxidation compared to women following endurance exercise (44), which raises the question if this persists in aging, and how it would be affected in response to BCAAs.

There were no differences in adipose tissue BCAA levels across the groups, and this is consistent with no difference in LAT1 protein abundance. The lack of difference in BCAA levels is surprising given that BCAT2 protein levels in young female mice is greater than in old female mice. Despite higher levels, it is possible that the activity of BCAT2 not different amongst groups. This may also be due to the fact these mice were food deprived for 3 hours, so BCAA oxidation was preserved to combat fasted-state protein degradation. This is supported with no difference in glutamate levels in adipose tissue, which is produced in the transamination of BCAAs to BCKAs. Despite no signal for BCAT2 in adipose tissue for aged mice, BCAT2 protein is not absent in the adipose tissue with aging, as confirmed by another study (425), but the exposure for the membrane was likely not long enough to show a band.

BCAA levels in the heart are consistently lower in old age, but there was no difference in BCKA levels. LAT1 protein levels were not different among any groups, thus it is not responsible for any difference in BCAAs in the heart. BCKD activity and protein levels of the catabolic enzymes were also not different across groups. In old age the heart experiences a decline in diastolic function and left ventricle hypertrophy (426). We did not demonstrate an aging effect on heart weight, but since BCAAs activate mechanistic/mammalian target of rapamycin complex 1 (mTORC1) in the heart (26), which contributes to heart hypertrophy (426), we could see the reduction in the uptake of BCAAs in the heart to compensate for this and preserve heart health in aging. Since LAT1 is largely not different amongst groups across all

tissues, it would be interesting to assess which tissues uptake BCAAs the most in old animals compared to younger counterparts.

In older populations insulin sensitivity is reduced (41). The prevalence of prediabetes in 20- to 39-year old individuals was 17.9%, 34.6% for 40- to 59-year old individuals, 36.8% for 60-to 74-year old individuals and 46.7% for <75-year old individuals (427). Insulin resistance increases with age, but the greatest increase in insulin resistance seems to be around 45-55 years old (428). The reduction in insulin sensitivity with aging could be due to lack of exercise in aging (429), which could also impact BCAA concentrations, as exercise upregulates BCAA oxidation (272–274). We did not measure energy expenditure, and activity, but in this study, females were observationally more active than males in old age, which could contribute to their reduced plasma BCAA levels compared to old male mice.

Studies that are generally carried out in younger cohorts have shown an increase in plasma BCAAs and BCKAs in insulin resistant states (11–13,17,21,107,113,114). Although insulin resistance worsens in aging (430), it is difficult to link of higher plasma BCAAs in old males to differences in insulin sensitivity, especially considering when BCAA catabolic enzyme protein levels were not different, which are downregulated (except for BDK) in insulin resistance in muscle (318), liver (319) and adipose tissue (13). Female mice regardless of age were more insulin sensitive than male mice, although not significant, but this did not lead to differences in catabolic enzyme protein abundance. This suggests that the link between BCAAs and insulin resistance may only be relevant in young male populations. We also show lower plasma BCKAs with age, which contradicts increases in BCKAs in insulin resistant states (12,108,218,220). This suggests that despite worsening of insulin sensitivity with age (430), changes in BCAA levels and BCAA catabolic enzymes are only seen in disease states like chronic renal failure (236,394),

liver cirrhosis (395,396), and T2DM (23,24) and not healthy populations regardless of age. Since the rise of blood glucose in the insulin tolerance test from minute 30-120 is likely due to a counter regulatory system like glucagon release, we also measured the area under the curve from basal to 30 min (Appendix J, Supplementary figure 9) and saw a trend for lower area under the curve for female mice compared to male mice with no effect of aging. Despite females having better insulin sensitivity, this does not correlate with any differences in BCAA levels in plasma or tissue or differences in any metabolic enzyme abundance/activity, suggesting that the link between dysregulated levels of BCAAs and their metabolism is linked to disease states, and age is not a factor in healthy animals.

For many parameters we did not reach significance although we were close. Studies have not looked at change in BCKD activity between sex and aging groups. Power calculations were not done before the start of this study, but using previous research (404) that compared the plasma BCAA levels in young (2-month) vs old (18-month) male mice (means ~7.34±0.98 vs ~8.6, power value was 80%, alpha value was 0.05), we would need 9 mice in each group. This could explain why certain results were not significant, but we did show significant increases in old male mice plasma BCAAs with a sample size of 7-8 mice.

A limitation of this study is using a previous studies' samples that only had 8 mice sacrificed at 18 months, as a greater sample size would have been ideal to reach significance. Additionally, having a group of very old mice (>24 month) may help give greater insight on how BCAA metabolism is changed with old age, as we expect greater insulin resistance (430), worsening muscle atrophy (431), and changes in mitochondrial content (432), which could all contribute to altered levels of BCAA catabolic enzymes.

In conclusion, we see differences in plasma, muscle, liver, and heart BCAAs in aging, but this was not consistent with differences in LAT1 or SDHA. Minor differences in BCKD activity may play a role in altered BCAA and BCKA levels, but cannot account for all of it, especially considering BCAA catabolic enzyme protein abundance was largely not different. This suggests that BCAA catabolic enzymes are largely preserved in aging, and likely are only dysregulated in disease states.

6.6 Author Contributions

GM, SM and OAJA conceived and designed the experiments. GM and SM performed the experiments. GM drafted the initial version of the manuscript. OAJA reviewed and edited the manuscript. All authors approved the final version of the manuscript.

Acknowledgements

We acknowledge the Muscle Health Research Centre at York University for their help with HPLC.

Funding

This work is supported by funds from the Natural Science and Engineering Research Council of Canada and from the Faculty of Health, York University.

Disclosure

The authors declare no conflict of interest.

7.0 Summary of Findings

7.1 General findings and future directions

High protein diets are important in maintaining lean body mass during weight loss, stimulating protein synthesis, enhancing glycemic regulation and increasing intestinal calcium absorption (433). They are often used to combat loss of lean muscle during calorie restriction in weight loss programs (8,9). In particular, branched-chain amino acids (BCAA), can stimulate muscle protein synthesis, and regulate body weight and glucose homeostasis (10). Despite these benefits, branched-chain amino acids (BCAAs), and their metabolites, branched-chain ketoacids (BCKAs), are upregulated in insulin-resistant states (11–13). Whether BCAAs cause insulin resistance is a question that remains to be answered.

In our previous work we showed that depletion of BCKD in L6 myotubes results in reduced insulin-stimulated glucose uptake (17), emphasizing the importance of BCKD in maintaining insulin sensitivity. Thus, we examined the effect of depleting BDK, the inhibitor of BCKD on insulin sensitivity. Here, we demonstrated that BDK depletion/inhibition increased insulin-stimulated glucose uptake in L6 myotubes and rescues the KIC-induced suppression of insulin-stimulated glucose uptake. We also confirmed that KIC suppressed insulin-stimulated glucose transport through the phosphorylation of the S6K1/IRS-1 signalling axis and that BDK depletion/inhibition rescues this likely through the enhanced catabolism of KIC, as BDK inhibition prevented the accumulation of leucine from KIC treatment.

To determine the direct effects of BCAAs/BCKAs on insulin resistance, we conducted the study in starved conditions. Since the presence of other amino acids may have influence our results, a future study would be look at the effect of BCAA/BCKA treatment with BDK

depletion/inhibition in the presence of all the amino acids, as we consume foods with various amino acid profiles.

Although we established the role of S6K1/IRS-1 signalling in BCKA-induced suppression of insulin-stimulated glucose transport, our previous work showed that in starved conditions, BCKD depletion suppressed insulin-stimulated glucose transport, in the absence of the activation of this mechanism (17). On the other hand, BDK depletion improved insulin-stimulated glucose uptake in starved conditions, without changes in the S6K1/IRS-1 mechanism. Thus, a future study would be to explore how BCKD regulation affects insulin-stimulated glucose transport in the absence BCAAs and BCKAs. It would also be interesting to see if the effect of BDK depletion or BT2 treatment can reverse insulin resistance in myotubes that is not induced by BCKAs/BCAAs supplementation.

Another future direction is how BDK depletion/inhibition affects other mechanisms like fatty acid metabolism in an insulin resistant state, as KIC, an endogenous activator of BCKD (280,353), increased fatty acid oxidation in C2C12 myotubes (327). Also, since BDK depletion improved insulin-stimulated glucose transport in starved conditions, independent of mTORC1, it would be interesting to see if the mitochondria plays a role in this, as use of BCKD activators (BT2 and sodium phenylbutyrate) reduced ROS (336,338). It would also be interesting to assess how BDK inhibition/depletion affects AMPK signaling, as AMPK has been shown to negatively regulate BCAA catabolism, but still improve insulin sensitivity (329).

We have previously shown that leucine (16) and ketoisocaproic acid (KIC) (16,17), a metabolite of leucine, suppresses insulin-stimulated glucose uptake in L6 myotubes with an increase in the S6K1/IRS-1 signaling axis (16). Since there are other tissues aside from skeletal muscle that contribute to KIC metabolism, we wanted to demonstrate if KIC gavage *in vivo*

would yield similar results. We see no change in insulin tolerance in rats gavaged with leucine or KIC. We did demonstrate that leucine activated the S6K1-IRS-1 pathway in skeletal muscle of rats as we did L6 myotubes, irrespective of fiber type. However, the activation of this pathway in skeletal muscle seems to be uncoupled with whole-body insulin tolerance.

KIC did not activate the S6K1-IRS-1 pathway in skeletal muscle, as seen in our previous work in L6 myotubes (16,17). This is likely because KIC is being largely catabolized by the liver, where BCKD is most abundant and active (241). Our work supports this, as phosphorylation of S6 and BCKD activity were increased in the liver in response to KIC gavage. The effect of KIC on S6 phosphorylation was higher in the heart as well, but not significant. The effect of KIC on S6 phosphorylation seemed to be the most drastic in the liver and heart, which corresponds with the tissues in which BCKD protein levels were the highest (Fig 5.8). This supports the notion that KIC is likely being oxidized in the liver and lower concentrations of KIC are going to the skeletal muscle from the liver unlike for leucine.

As discussed in the literature review, there is a high degree of variability in studies that supplement BCAAs to rodents. One study showed that mice supplemented BCAAs for 3 months exhibited no change in insulin sensitivity (285), while others showed that chronic leucine supplementation improved insulin sensitivity in rodents fed a high fat diet (20,287,295). Other studies showed improved insulin sensitivity of db/db mice when treated with leucine for 12 weeks (288) or BCAAs for 34 weeks (289). However, one study showed that 12-16 weeks of BCAA supplementation worsened insulin sensitivity in rats fed a high-fat-diet (108), while Zucker-fatty rats restricted of BCAAs show improved insulin sensitivity (290). Thus, since KIC did not affect muscle insulin signaling or whole-body insulin sensitivity in lean animals, it would be interesting to explore how KIC affects insulin sensitivity and relevant signaling in obese

animals. Also, a chronic treatment of KIC may yield different results than an acute, and would be more representative and relevant, as we consume leucine in our diets daily.

Additionally, since KIC did not affect the S6K1/IRS-1 pathway in skeletal muscle of lean rats, and since obesity and insulin resistance is associated with increased fatty acid oxidation (434), it would be interesting to explore how KIC affects lipid metabolism in obese rats, as KIC activates fatty acid oxidation in C2C12 myotubes (327) and leucine improved insulin sensitivity in animals fed a high fat diet by increasing fatty acid oxidation (20,21,299,300).

Since KIC treatment reduced insulin-stimulated glucose transport in our *in vitro* model and not *in vivo* model, it is likely that this could be due to the concentration used in each. Our *in vitro* model received supraphysiological levels of KIC. However, *in vivo*, the liver is metabolizing KIC at first pass, as BCKD is most abundant in the liver. This reduces the amount of KIC being absorbed by the muscle, which may explain the discrepancies of the effect of KIC on insulin signaling in skeletal muscle *in vitro* compared to *in vivo*. Additionally, enhanced BCAA catabolism reversed the effect of KIC *in vitro*, and studies have shown benefits of BT2 in rodent models (326,333,337). Coupled with the fact that BCAA metabolic enzymes are downregulated (except BDK is increased) in insulin resistant states (23,24), it is likely that increased levels of BCAAs are correlated with insulin resistance and are a product of altered enzyme levels/activity in insulin resistant states.

The link between BCAA catabolism and insulin sensitivity is evident. However, this relationship is complicated in aging. Aged men exhibit significantly lower circulating BCAA levels (38,39), which is interesting considering insulin resistance is more prevalent in older individuals (41), and BCAAs are elevated in insulin resistance (12,13). Aging is a major risk factor in many diseases, so understanding BCAA metabolism in aging can help against different

diseases (34–37). No study to our knowledge has examined the effect of aging on BCAA catabolic enzyme abundance and activity, and BCAA levels in relevant tissues. We also examined the effect of sex as a few studies have shown sexual dimorphisms regarding BCAA catabolism and is a field that requires further exploring.

We show an increase in plasma BCAAs in old male mice, compared to young male and old female mice. We also report a reduction of BCAAs in skeletal muscle with aging in both sexes, and reduced BCAAs in aging in male animals in the liver and a trend for female animals. The heart also exhibits reduced BCAAs in aging. There are no changes in BCAA levels in the adipose tissue.

Skeletal muscle, liver and adipose tissue show that BCKD activity is greater in males than females in both age cohorts, but this effect was not significant. However, minor changes may have contributed to increased BCKAs in the tissues of older mice. Changes in BCKD activity or BCAA/BCKA levels were not a result of consistent changes in catabolic enzyme abundance in any of the tissues. Changes in BCAA/BCKA levels were also not consistent with changes in amino acid transporter LAT1 or changes in mitochondrial content seen with SDHA protein levels. Our data suggest that enzymes involved in BCAA catabolism are generally preserved in aging, and that although aging is a risk factor in many diseases, BCAA catabolism is only implicated in disease and not in healthy aged populations. Despite the worsening of insulin resistance in aging (430), it seems that BCAA catabolic enzymes are only dysregulated in insulin resistant states like obesity and T2DM that have major metabolic derangements.

A future direction of this study could be to explore an even older age group (<24 months), as studies showing men with reduced BCAAs in plasma were much older (~80 years of age) (38,39). We showed no effect of aging in SDHA protein levels in any of the tissues

analyzed, but one study did show reduced mitochondrial content in old women compared to young women (432). This could be because the women in this study were prefrail or frail and were also older than the age of our old female mice group. Also insulin sensitivity worsens with age (430), which may have implications on BCKD activity and BCAA catabolic enzyme protein abundance, as they are altered in insulin resistant states (23,227). Finally, muscle mass declines 3-8% after per decade after 30 years of age each decade, and this rate is even higher after 60 years of age (431), emphasizing the importance of studying BCAA metabolism in even older mice.

Ultimately, the future direction of BCAA induced insulin resistance is to analyze the effect of BT2 in clinical applications. In pre-clinical models, BT2 supplementation improves insulin sensitivity (294,326,333,337) and there have been no adverse effects reported in pre-clinical models with chronic dosing (294,333). T2DM patients treated with sodium phenylbutyrate, an activator of BCKD, showed improvements in insulin sensitivity with enhanced carbohydrate oxidation, but no change in fatty acid or triglyceride plasma levels (335). Since recent studies have shown that BT2 improves fatty acid oxidation in the liver (337) and reduces mitochondrial ROS and de novo lipogenesis (338), it may be a better candidate against insulin resistance than sodium phenylbutyrate, and requires further analysis in clinical models. Thus, I would intraperitoneally inject BT2 in patients with insulin resistance and control patients. Firstly, I would measure BCKD phosphorylation to confirm activation of BCKD in skeletal muscle, liver, and adipose tissue mainly, as these tissues are primarily implicated in insulin resistance. Next, I would see how it affects insulin sensitivity by conducting an insulin tolerance test. Next, I would look at insulin signaling pathways in all three tissues, and then also assess

fatty acid levels as BT2 has shown to improve fatty acid oxidation (337). I would also explore how it affects mitochondrial ROS levels in humans.

7.2 Limitations

In this dissertation, despite our best efforts made in the design and execution of these studies, we do acknowledge the presence of limitations.

In chapter 4, we aimed to analyze the effects of BDK depletion/inhibition *in vitro*. It was an important first step to examine the direct effects of enhanced BCAA catabolism on a single tissue, as in *vivo* it would be difficult due to the inputs from other tissues, growth factors, and metabolites. However, this does allow for future studies to explore these effects *in vivo*. Most studies examine the effects of BDK inhibition on the whole-body level, but is important to confirm if depleting/inhibiting BDK in skeletal muscle *in vivo* can improve insulin sensitivity and attenuate insulin resistant states, as skeletal muscle insulin resistance is the primary defect in T2DM (354). It was important to explore the direct effects of BCAA/BCKAs on mTORC1 signalling and insulin-stimulated glucose uptake in amino acid starved conditions, however, the presence of other amino acids may have effects on the results presented. However, this does allow for future studies examining the effect of BDK depletion/inhibition and BCAA/BCKA treatment in the presence of other amino acids. Also, using total proteins instead of a loading control like γ-tubulin is preferred, but the half-life of Akt (36 hours), (435) IRS-1 (20 hours) (436), ribosomes like S6 (300 hour) (437) and tubulin (15-50 hours depending on the cellular model) (438) are longer than our treatment times of KIC and BT2, thus γ-tubulin was a sufficient loading control. We used γ-tubulin as a loading control instead of actin and GAPDH, as the molecular weight of actin is too close to BCKD, while GAPDH may overlap with ph-S6 or the

BCAA catabolic enzymes like BCAT2, BDK, pp2Cm. The molecular weight of γ-tubulin (48 kDa) was above these BCAA metabolic enzymes (37-45 kDa) but also below insulin signaling pathway markers (60-70 kDa).

Another limitation is that we did not measure differentiation markers to confirm myotubes were fully differentiated, which could contribute to some of the variability in the study. We observationally confirmed myotubes were differentiated but did not confirm with the measurement of differentiation markers. On D5 of differentiation, based off previous studies (235), the cells were most likely differentiated.

In chapter 5, a limitation was not being able to obtain blots for the effect of KIC and leucine gavage on insulin signaling in adipose tissue, as adipose tissue is an important site of BCAA catabolism. Since BCKD activity is lowest in skeletal muscle and adipose tissue (241), it is likely that KIC did not activate mTORC1 signalling in adipose tissue like in skeletal muscle. As discussed above since BCKD protein abundance was highest in liver and heart, KIC likely prioritized uptake into these tissues over adipose tissue. Another limitation was not obtaining a blot for ph-S6K1 (Thr389) in the liver and heart. However, we did obtain blots for targets of S6K1, S6 (Ser235/6) and IRS-1 (Ser612), which can compensate for this. Finally, not being able to obtain a blot for ph-Akt (Ser473) in the liver is a limitation as well, but since it was unchanged in other tissues, and whole-body insulin tolerance was unchanged, it is unlikely that ph-Akt was affected by leucine or KIC gavage in the liver. Finally, since supplementation with KIC (383,384) and leucine (385) stimulates insulin secretion *in vivo,* this could explain why blood glucose levels were not increased in our insulin tolerance test, but insulin signaling was changed. We plan on doing this in the future. Like in chapter 4, γ-tubulin was used as a loading control for chapter 5. Use of total proteins as loading control would be ideal, but since KIC and leucine

gavage was an acute treatment (30 min-180 min), and tubulin half-life is much longer, γ-tubulin is a sufficient loading control.

Another limitation is that in the ex vivo BCKD activity assay we were measuring the maximal capacity of the BCKD enzyme, but the gold standard would be to do KIC/leucine tracer experiments *in vivo*. However, maximal enzyme activity is still a valid approach, and still indicates changes in enzyme activity in response to a dose of KIC/leucine.

In chapter 6, a limitation is that despite that all the animals were the same strain, young females were bought from a different company from the rest of the animals due to a bacterial outbreak at one of the companies. My sample size might be underpowered, as unfortunately I only received tissues from 8 animals aged 18-months. Two studies that examined plasma BCAAs in young and old mice used a sample size of 3-4 (404) and 6-10 (405). Additionally, although 18-month mice are considered "old" (439), in future studies, adding an additional very old (<24 month) mouse group would have given more insight on the effects of aging on BCAA metabolism, as reductions in insulin sensitivity (430) and mitochondrial content (432), and increased muscle wasting (431) with aging can all have implications on BCAA metabolism.

Despite doing a protein assay to ensure equal loading of protein, another limitation is the unequal loading for our loading control γ-tubulin in some of the blots for study 1 and 2. This could be due to error in calculating protein concentration values from the protein assay. In the future it is important to ensure γ-tubulin loading is the same, ensuring calculations are done correctly and the protein assay is done with utmost care.

In all three studies, we measured the phosphorylation of Akt at the serine 473 residue, but not the Thr308 residue, and this is a limitation, as Akt requires phosphorylation at both residues for full activation. One study showed that leucine and whey protein increased mTORC1

activation, without affecting Akt phosphorylation of either residue (296), so we decided to measure the Ser473 residue as it is a more reliable antibody according to Cell Signaling Technology, the manufacturer.

7.3 Conclusions

Here we show that the effect of KIC and BCKAs on insulin sensitivity in L6 myotubes was attenuated in conditions where BCAA oxidation was increased like with BDK inhibition and depletion. We also confirmed that in L6 myotubes that mTORC1 signaling is the responsible culprit in reducing insulin-stimulated glucose uptake in response to KIC/BCKA treatment. Despite what we see *in vitro,* KIC gavage in lean healthy rats does not affect whole-body insulin tolerance or insulin signaling in skeletal muscle. However, KIC gavage increased BCKD activity and S6 phosphorylation in the liver, suggesting KIC gavage is predominantly catabolized by the liver in its first pass before reaching the muscle. Since KIC is predominantly catabolized by the liver, a lower concentration of KIC reaches the skeletal muscle, unable to significantly activate S6K1-IRS-1 in skeletal muscle (Fig 5.2-5.4), as seen *in vitro.* It is also important to note that despite increases in the S6K1/IRS-1 signaling axis of skeletal muscle of rats gavaged with leucine, this did not lead to changes in whole-body insulin tolerance.

Finally, we demonstrated changes in plasma BCAAs in old male mice, and reduced BCAAs in skeletal muscle, liver, and heart of old mice. We do see minor changes in BCKD activity between groups, although not significant, which could contribute to some of the significant changes in BCKA levels across groups. There was no consistent change in BCAA catabolic enzymes abundance across the various tissues. Females were more insulin sensitive than males (Fig 6.1N-O), but this did not correlate with any changes on our measures

(BCAA/BCKA plasma/tissue levels and metabolic enzyme levels). Thus, it is likely that although age is a risk factor in diseases that implicate BCAA metabolism, altered BCAA metabolism may only manifest in disease populations, and not in healthy populations regardless of age.

.

8.0 References

1. Savage DB, Petersen KF, Shulman GI. Mechanisms of insulin resistance in humans and possible links with inflammation. Hypertension. 2005.
2. Ormazabal V, Nair S, Elfeky O, Aguayo C, Salomon C, Zuñiga FA. Association between insulin resistance and the development of cardiovascular disease. Cardiovasc Diabetol [Internet]. 2018;17(1):1–14. Available from: https://doi.org/10.1186/s12933-018-0762-4
3. Shanik MH, Xu Y, Skrha J, Dankner R, Zick Y, Roth J. Insulin resistance and hyperinsulinemia: is hyperinsulinemia the cart or the horse? Diabetes Care. 2008;31 Suppl 2.
4. Brown AE, Walker M. Genetics of Insulin Resistance and the Metabolic Syndrome. Curr Cardiol Rep [Internet]. 2016;18(8). Available from: http://dx.doi.org/10.1007/s11886-016-0755-4
5. Hamburg NM, McMackin CJ, Huang AL, Shenouda SM, Widlansky ME, Schulz E, et al. Physical inactivity rapidly induces insulin resistance and microvascular dysfunction in healthy volunteers. Arterioscler Thromb Vasc Biol. 2007;27(12):2650–2656.
6. Yaribeygi H, Maleki M, Sathyapalan T, Jamialahmadi T, Sahebkar A. Pathophysiology of Physical Inactivity-Dependent Insulin Resistance: A Theoretical Mechanistic Review Emphasizing Clinical Evidence. J Diabetes Res. 2021;2021.
7. Yang W, Jiang W, Guo S. Regulation of Macronutrients in Insulin Resistance and Glucose Homeostasis during Type 2 Diabetes Mellitus. Nutrients. 2023;15(21).
8. Astrup A, Raben A, Geiker N. The role of higher protein diets in weight control and obesity-related comorbidities. Int J Obes. 2015;39(5):721–6.
9. Magkos F. Protein-Rich Diets for Weight Loss Maintenance. Curr Obes Rep. 2020;9(3):213–8.
10. Lynch CJ, Adams SH. Branched-chain amino acids in metabolic signalling and insulin resistance. Nat Rev Endocrinol. 2014;10(12):723–36.
11. Andersson-Hall U, Gustavsson C, Pedersen A, Malmodin D, Joelsson L, Holmäng A. Higher concentrations of BCAAs and 3-HIB are associated with insulin resistance in the transition from gestational diabetes to type 2 diabetes. J Diabetes Res. 2018;2018:1–12.
12. Giesbertz P, Padberg I, Rein D, Ecker J, Höfle AS, Spanier B, et al. Metabolite profiling in plasma and tissues of ob/ob and db/db mice identifies novel markers of obesity and type 2 diabetes. Diabetologia. 2015;58(9):2133–43.
13. Lackey DE, Lynch CJ, Olson KC, Mostaedi R, Ali M, Smith WH, et al. Regulation of adipose branched-chain amino acid catabolism enzyme expression and cross-adipose amino acid flux in human obesity. Am J Physiol - Endocrinol Metab. 2013;304(11):1175–87.
14. Crossland H, Smith K, Idris I, Phillips BE, Atherton PJ, Wilkinson DJ. Exploring mechanistic links between extracellular branched-chain amino acids and muscle insulin resistance: an in vitro approach. Am J Physiol - Cell Physiol. 2020;319:C1151–7.
15. Yoon MS. The emerging role of branched-chain amino acids in insulin resistance and metabolism. Nutrients. 2016;8(7):405.
16. Moghei M, Tavajohi-Fini P, Beatty B, Adegoke OAJ. Ketoisocaproic acid, a metabolite of leucine, suppresses insulin-stimulated glucose transport in skeletal muscle cells in a BCAT2-dependent manner. Am J Physiol Physiol. 2016;311(3):C518–27.
17. Mann G, Adegoke OAJ. Effects of ketoisocaproic acid and inflammation on glucose

transport in muscle cells. Physiol Rep. 2021;9(1):e14673.
18. Jeganathan S, Abdullahi A, Zargar S, Maeda N, Riddell MC, Adegoke OAJ. Amino acid-induced impairment of insulin sensitivity in healthy and obese rats is reversible. Physiol Rep. 2014;2(7):e12067.
19. Yamanashi K, Kinugawa S, Fukushima A, Kakutani N, Takada S, Obata Y, et al. Branched-chain amino acid supplementation ameliorates angiotensin II-induced skeletal muscle atrophy. Life Sci [Internet]. 2020;250(March):117593. Available from: https://doi.org/10.1016/j.lfs.2020.117593
20. Binder E, Bermúdez-Silva FJ, André C, Elie M, Romero-Zerbo SY, Leste-Lasserre T, et al. Leucine Supplementation Protects from Insulin Resistance by Regulating Adiposity Levels. PLoS One. 2013;8(9).
21. Macotela Y, Emanuelli B, Bång AM, Espinoza DO, Boucher J, Beebe K, et al. Dietary leucine - an environmental modifier of insulin resistance acting on multiple levels of metabolism. PLoS One. 2011;6(6):e21187.
22. Nishitani S, Matsumura T, Fujitani S, Sonaka I, Miura Y, Yagasaki K. Leucine promotes glucose uptake in skeletal muscles of rats. Biochem Biophys Res Commun. 2002;299(5):693–6.
23. Hernández-Alvarez MI, Díaz-Ramos A, Berdasco M, Cobb J, Planet E, Cooper D, et al. Early-onset and classical forms of type 2 diabetes show impaired expression of genes involved in muscle branched-chain amino acids metabolism. Sci Rep. 2017;7(1):1–12.
24. Lian K, Du C, Liu Y, Zhu D, Yan W, Zhang H, et al. Impaired adiponectin signaling contributes to disturbed catabolism of branched-chain amino acids in diabetic mice. Diabetes. 2015;64(1):49–59.
25. Fillmore N, Wagg CS, Zhang L, Fukushima A, Lopaschuk GD. Cardiac branched-chain amino acid oxidation is reduced during insulin resistance in the heart. Am J Physiol - Endocrinol Metab. 2018;315(5):E1046–52.
26. Huang Y, Zhou M, Sun H, Wang Y. Branched-chain amino acid metabolism in heart disease: An epiphenomenon or a real culprit? Cardiovasc Res. 2011;90(2):220–3.
27. Hara Y, May RC, Kelly RA, Mitch WE. Acidosis, not azotemia, stimulates branched-chain, amino acid catabolism in uremic rats. Kidney Int. 1987;32(6):808–14.
28. Mitch WE, Price SR, May RC, Jurkovitz C, England BK. Metabolic Consequences of Uremia: Extending the Concept of Adaptive Responses to Protein Metabolism. Am J Kidney Dis. 1994 Feb;23(2):224–8.
29. Shimomura Y, Honda T, Shiraki M, Murakami T, Sato J, Kobayashi H, et al. Branched-chain amino acid catabolism in exercise and liver disease. In: Journal of Nutrition. American Institute of Nutrition; 2006. p. S250–3.
30. Holecek M. Branched-chain amino acids and ammonia metabolism in liver disease: Therapeutic implications. Nutrition [Internet]. 2013;29(10):1186–91. Available from: http://dx.doi.org/10.1016/j.nut.2013.01.022
31. Ericksen RE, Lim SL, McDonnell E, Shuen WH, Vadiveloo M, White PJ, et al. Loss of BCAA Catabolism during Carcinogenesis Enhances mTORC1 Activity and Promotes Tumor Development and Progression. Cell Metab [Internet]. 2019;29(5):1151-1165.e6. Available from: https://doi.org/10.1016/j.cmet.2018.12.020
32. Wang P, Wu S, Zeng X, Zhang Y, Zhou Y, Su L, et al. BCAT1 promotes proliferation of endometrial cancer cells through reprogrammed BCAA metabolism. Int J Clin Exp Pathol. 2018;11(12):5536–46.

33. Lee JH, Cho Y ra, Kim JH, Kim J, Nam HY, Kim SW, et al. Branched-chain amino acids sustain pancreatic cancer growth by regulating lipid metabolism. Exp Mol Med. 2019;51(11):1–11.
34. Mullard A. Anti-ageing pipeline starts to mature. Nat Rev Drug Discov. 2018;17:609–12.
35. Hall SS. A trial for the ages. Science (80-). 2015;349(6254):1274–8.
36. Mallappallil M, Friedman EA, Delano BG, Mcfarlane SI, Salifu MO. Chronic kidney disease in the elderly: Evaluation and management. Clin Pract. 2014;11(5):525–35.
37. Kim IH, Kisseleva T, Brenner DA. Aging and liver disease. Curr Opin Gastroenterol. 2015;31(3):184–91.
38. Ribeiro R V., Solon-Biet SM, Pulpitel T, Senior AM, Cogger VC, Clark X, et al. Of older mice and men: Branched-chain amino acids and body composition. Nutrients. 2019;11(8).
39. Sun L, Hu C, Yang R, Lv Y, Yuan H, Liang Q, et al. Association of circulating branched-chain amino acids with cardiometabolic traits differs between adults and the oldest-old. Oncotarget. 2017;8(51):88882–93.
40. Le Couteur DG, Ribeiro R, Senior A, Hsu B, Hirani V, Blyth FM, et al. Branched chain amino acids, cardiometabolic risk factors and outcomes in older men: The concord health and ageing in men project. Journals Gerontol - Ser A Biol Sci Med Sci. 2020;75(10):1805–10.
41. Shou J, Chen PJ, Xiao WH. Mechanism of increased risk of insulin resistance in aging skeletal muscle. Diabetol Metab Syndr [Internet]. 2020;12(1):1–10. Available from: https://doi.org/10.1186/s13098-020-0523-x
42. Obayashi M, Shimomura Y, Nakai N, Jeoung NH, Nagasaki M, Murakami T, et al. Estrogen controls branched-chain amino acid catabolism in female rats. J Nutr. 2004;134(10):2628–33.
43. Kobayashi R, Shimomura Y, Murakami T, Nakai N, Otsuka M, Arakawa N, et al. Hepatic branched-chain α-keto acid dehydrogenase complex in female rats: Activation by exercise and starvation. J Nutr Sci Vitaminol (Tokyo). 1999;45(3):303–9.
44. Mittendorfer B, Horowitz JF, Klein S. Effect of gender on lipid kinetics during endurance exercise of moderate intensity in untrained subjects. Am J Physiol - Endocrinol Metab. 2002;283:E59–65.
45. Kahn CR, White MF. The insulin receptor and the molecular mechanism of insulin action. J Clin Invest. 1988;82(4):1151–6.
46. Boucher J, Kleinridders A, Kahn CR. Insulin Receptor Signaling in Normal and Insulin-Resistant States. Cold Spring Harb Perspect Biol 2014. 2014;6:a009191.
47. Pederson TM, Kramer DL, Rondinone CM. Serine/threonine phosphorylation of IRS-1 triggers its degradation: Possible regulation by tyrosine phosphorylation. Diabetes. 2001;50(1):24–31.
48. Feldhammer M, Uetani N, Miranda-Saavedra D, Tremblay ML. Ptp1b: A simple enzyme for a complex world. Crit Rev Biochem Mol Biol. 2013;48:430–45.
49. Delibegovic M, Bence KK, Mody N, Hong E-G, Ko HJ, Kim JK, et al. Improved Glucose Homeostasis in Mice with Muscle-Specific Deletion of Protein-Tyrosine Phosphatase 1B. Mol Cell Biol. 2007;27(21):7727–34.
50. Huang C, Thirone ACP, Huang X, Klip A. Differential contribution of insulin receptor substrates 1 versus 2 to insulin signaling and glucose uptake in L6 myotubes. J Biol Chem. 2005;280(19):19426–35.
51. Eckstein SS, Weigert C, Lehmann R. Divergent Roles of IRS (Insulin Receptor Substrate)

1 and 2 in Liver and Skeletal Muscle. Curr Med Chem. 2017;24(17):1827–52.
52. Higaki Y, Wojtaszewski JFP, Hirshman MF, Withers DJ, Towery H, White MF, et al. Insulin receptor substrate-2 is not necessary for insulin- and exercise- stimulated glucose transport in skeletal muscle. J Biol Chem. 1999;274(30):20791–5.
53. Fantin VR, Lavan BE, Wang Q, Jenkins NA, Gilbert DJ, Copeland NG, et al. Cloning, tissue expression, and chromosomal location of the mouse insulin receptor substrate 4 gene. Endocrinology. 1999;140(3):1329–37.
54. Cai D, Dhe-Paganon S, Melendez PA, Lee J, Shoelson SE. Two new substrates in insulin signaling, IRS5/DOK4 and IRS6/DOK5. J Biol Chem. 2003;278(28):25323–30.
55. Araki EI, Lipes MA, Patti M, Briinlng JC, Ill BH, Johnson RS, et al. Alternative pathway of insulin signalling in mice with targeted disruption of the IRS-1 gene. Nature [Internet]. 1994;372:186–90. Available from: https://www.nature.com/articles/372186a0
56. Metz HE, Houghton AMG. Insulin receptor substrate regulation of phosphoinositide 3-kinase. Clin Cancer Res. 2011;17(2):206–11.
57. Vadas O, Burke JE, Zhang X, Berndt A, Williams RL. Structural biology structural basis for activation and inhibition of class I phosphoinositide 3-kinases. Sci Signal. 2011;4(195).
58. Carracedo A, Pandolfi PP. The PTEN-PI3K pathway: Of feedbacks and cross-talks. Oncogene. 2008;27:5527–41.
59. Yang J, Nie J, Ma X, Wei Y, Peng Y, Wei X. Targeting PI3K in cancer: Mechanisms and advances in clinical trials. Mol Cancer. 2019;18(1):1–28.
60. Alessi DR, James SR, Downes CP, Holmes AB, Gaffney PRJ, Reese CB, et al. Characterization of a 3-phosphoinositide-dependent protein kinase which phosphorylates and activates protein kinase Bα. Curr Biol. 1997;7(4):261–9.
61. Sarbassov DD, Guertin DA, Ali SM, Sabatini DM. Phosphorylation and regulation of Akt/PKB by the rictor-mTOR complex. Science (80-). 2005;307(5712):1098–101.
62. Schultze SM, Jensen J, Hemmings BA, Tschopp O, Niessen M. Promiscuous affairs of PKB/AKT isoforms in metabolism. Arch Physiol Biochem. 2011;117(2):70–7.
63. Cho H, Mu J, Kim JK, Thorvaldsen JL, Chu Q, Crenshaw EB, et al. Insulin resistance and a diabetes mellitus-like syndrome in mice lacking the protein kinase Akt2 (PKBβ). Science (80-). 2001;292(5522):1728–31.
64. Dugani CB, Klip A. Glucose transporter 4: Cycling, compartments and controversies. EMBO Rep. 2005;6(12):1137–42.
65. Farese R V. Function and dysfunction of aPKC isoforms for glucose transport in insulin-sensitive and insulin-resistant states. American Journal of Physiology - Endocrinology and Metabolism. 2002.
66. Standaert ML, Bandyopadhyay G, Kanoh Y, Sajan MP, Farese R V. Insulin and PIP3 activate PKC-ζ by mechanisms that are both dependent and independent of phosphorylation of activation loop (T410) and autophosphorylation (T560) sites. Biochemistry. 2001;40(1):249–55.
67. Standaert ML, Bandyopadhyay G, Perez L, Price D, Galloway L, Poklepovic A, et al. Insulin activates protein kinases C-ζ and C-λ by an autophosphorylation-dependent mechanism and stimulates their translocation to GLUT4 vesicles and other membrane fractions in rat adipocytes. J Biol Chem. 1999;274(36):25308–16.
68. Kanoh Y, Sajan MP, Bandyopadhyay G, Miura A, Standaert ML, Farese R V. Defective activation of atypical protein kinase C ζ and λ by insulin and phosphatidylinositol-3,4,5-

(PO4)3 in skeletal muscle of rats following high-fat feeding and streptozotocin-induced diabetes. Endocrinology. 2003;144(3):947–54.
69. Beg M, Abdullah N, Thowfeik FS, Altorki NK, McGraw TE. Distinct Akt phosphorylation states are required for insulin regulated Glut4 and Glut1-mediated glucose uptake. Elife. 2017;6:1–22.
70. Kohn AD, Summers SA, Birnbaum MJ, Roth RA. Expression of a constitutively active Akt Ser/Thr kinase in 3T3-L1 adipocytes stimulates glucose uptake and glucose transporter 4 translocation. J Biol Chem. 1996;271(49):31372–8.
71. Hill MM, Clark SF, Tucker DF, Birnbaum MJ, James DE, Macaulay SL. A Role for Protein Kinase Bβ/Akt2 in Insulin-Stimulated GLUT4 Translocation in Adipocytes. Mol Cell Biol. 1999;19(11):7771–81.
72. Wang Q, Somwar R, Bilan PJ, Liu Z, Jin J, Woodgett JR, et al. Protein Kinase B/Akt Participates in GLUT4 Translocation by Insulin in L6 Myoblasts. Mol Cell Biol. 1999;19(6):4008–18.
73. Sakamoto K, Holman GD. Emerging role for AS160/TBC1D4 and TBC1D1 in the regulation of GLUT4 traffic. Am J Physiol - Endocrinol Metab. 2008;295(1).
74. An D, Toyoda T, Taylor EB, Yu H, Fujii N, Hirshman MF, et al. TBC1D1 regulates insulin- and contraction-induced glucose transport in mouse skeletal muscle. Diabetes. 2010;59(6):1358–65.
75. Taylor EB, An D, Kramer HF, Yu H, Fujii NL, Roeckl KSC, et al. Discovery of TBC1D1 as an insulin-, AICAR-, and contraction-stimulated signaling nexus in mouse skeletal muscle. J Biol Chem. 2008;283(15):9787–96.
76. Sano H, Kane S, Sano E, Mîinea CP, Asara JM, Lane WS, et al. Insulin-stimulated phosphorylation of a Rab GTPase-activating protein regulates GLUT4 translocation. J Biol Chem. 2003;278(17):14599–602.
77. Wang HY, Ducommun S, Quan C, Xie B, Li M, Wasserman DH, et al. AS160 deficiency causes whole-body insulin resistance via composite effects in multiple tissues. Biochem J. 2013;2(449):479–89.
78. Yoon MS. The role of mammalian target of rapamycin (mTOR) in insulin signaling. Nutrients. 2017;9(11).
79. Yoon MS, Choi CS. The role of amino acid-induced mammalian target of rapamycin complex 1(mTORC1) signaling in insulin resistance. Exp Mol Med [Internet]. 2016;48(1):e201-6. Available from: http://dx.doi.org/10.1038/emm.2015.93
80. Düvel K, Yecies JL, Menon S, Raman P, Lipovsky AI, Souza AL, et al. Activation of a metabolic gene regulatory network downstream of mTOR complex 1. Mol Cell. 2010;39(2):171–83.
81. Saxton RA, Sabatini DM. mTOR Signaling in Growth, Metabolism, and Disease. Cell. 2017;169(2):361–71.
82. Laplante M, Sabatini DM. mTOR signaling at a glance. J Cell Sci. 2009;122(20):3589–94.
83. Peterson TR, Laplante M, Thoreen CC, Sancak Y, Kang SA, Kuehl WM, et al. DEPTOR is an mTOR Inhibitor Whose Frequent Overexpression in Multiple Myeloma Cells Promotes their Survival Timothy. Cell [Internet]. 2009;137(5):873–86. Available from: http://books.google.com/books?hl=en&lr=&id=xDJoXDOweRwC&oi=fnd&pg=PA85&dq=NF-kB+Signaling+in+Skeletal+Muscle+Health+and+Disease&ots=5evHiNdA6b&sig=rF9rldt8sby9Z4v2PtqR6hqV-l0

84. Liu GY, Sabatini DM. mTOR at the nexus of nutrition, growth, ageing and disease. Nat Rev Mol Cell Biol [Internet]. 2020;21(4):183–203. Available from: http://dx.doi.org/10.1038/s41580-019-0199-y
85. Sancak Y, Thoreen CC, Peterson TR, Lindquist RA, Kang SA, Spooner E, et al. PRAS40 Is an Insulin-Regulated Inhibitor of the mTORC1 Protein Kinase. Mol Cell. 2007;25(6):903–15.
86. Guertin DA, Stevens DM, Thoreen CC, Burds AA, Kalaany NY, Moffat J, et al. Ablation in Mice of the mTORC Components raptor, rictor, or mLST8 Reveals that mTORC2 Is Required for Signaling to Akt-FOXO and PKCα, but Not S6K1. Dev Cell. 2006;11(6):859–71.
87. Long X, Lin Y, Ortiz-Vega S, Yonezawa K, Avruch J. Rheb binds and regulates the mTOR kinase. Curr Biol. 2005;15(8):702–13.
88. Sancak Y, Bar-Peled L, Zoncu R, Markhard AL, Nada S, Sabatini DM. Ragulator-rag complex targets mTORC1 to the lysosomal surface and is necessary for its activation by amino acids. Cell. 2010;141:290–303.
89. Avruch J, Hara K, Lin Y, Liu M, Long X, Ortiz-Vega S, et al. Insulin and amino-acid regulation of mTOR signaling and kinase activity through the Rheb GTPase. Oncogene. 2006;25(48):6361–72.
90. Wang L, Harris TE, Roth RA, Lawrence JC. PRAS40 regulates mTORC1 kinase activity by functioning as a direct inhibitor of substrate binding. J Biol Chem. 2007;282(27):20036–44.
91. Holz MK, Blenis J. Identification of S6 kinase 1 as a novel mammalian target of rapamycin (mTOR)-phosphorylating kinase. J Biol Chem. 2005;280(28):26089–93.
92. Dorrello NV, Peschiaroli A, Guardavaccaro D, Colburn NH, Sherman NE, Pagano M. S6K1- and bTRCP-Mediated Degradation of PDCD4 Promotes Protein Translation and Cell Growth. Science (80-). 2006;314(October):467–72.
93. Yang H-S, Jansen AP, Komar AA, Zheng X, Merrick WC, Costes S, et al. The Transformation Suppressor Pdcd4 Is a Novel Eukaryotic Translation Initiation Factor 4A Binding Protein That Inhibits Translation. Mol Cell Biol. 2003;23:26–37.
94. Biever A, Valjent E, Puighermanal E. Ribosomal protein S6 phosphorylation in the nervous system: From regulation to function. Front Mol Neurosci. 2015;8(DEC):1–14.
95. Ruvinsky I, Meyuhas O. Ribosomal protein S6 phosphorylation: from protein synthesis to cell size. Trends Biochem Sci. 2006;31(6):342–8.
96. Gingras AC, Gygi SP, Raught B, Polakiewicz RD, Abraham RT, Hoekstra MF, et al. Regulation of 4E-BP1 phosphorylation: A novel two step mechanism. Genes Dev. 1999;13(11):1422–37.
97. Qin X, Jiang B, Zhang Y. 4E-BP1, a multifactor regulated multifunctional protein. Cell Cycle [Internet]. 2016;15(6):781–6. Available from: http://dx.doi.org/10.1080/15384101.2016.1151581
98. Lin SC, Hardie DG. AMPK: Sensing Glucose as well as Cellular Energy Status. Cell Metab [Internet]. 2018;27(2):299–313. Available from: https://doi.org/10.1016/j.cmet.2017.10.009
99. Corradetti MN, Inoki K, Bardeesy N, DePinho RA, Guan KL. Regulation of the TSC pathway by LKB1: Evidence of a molecular link between tuberous sclerosis complex and Peutz-Jeghers syndrome. Genes Dev. 2004;18(13):1533–8.
100. Gwinn DM, Shackelford DB, Egan DF, Mihaylova MM, Vasquez DS, Turk BE, et al.

AMPK phosphorylation of raptor mediates a metabolic checkpoint. Mol Cell. 2008;30(2):214–26.
101. Feng Z, Hu W, De Stanchina E, Teresky AK, Jin S, Lowe S, et al. The regulation of AMPK β1, TSC2, and PTEN expression by p53: Stress, cell and tissue specificity, and the role of these gene products in modulating the IGF-1-AKT-mTOR pathways. Cancer Res. 2007;67(7):3043–53.
102. Brugarolas J, Lei K, Hurley RL, Manning BD, Reiling JH, Hafen E, et al. Regulation of mTOR function in response to hypoxia by REDD1 and the TSC1/TSC2 tumor suppressor complex. Genes Dev. 2004;18(23):2893–904.
103. Katiyar S, Liu E, Knutzen CA, Lang ES, Lombardo CR, Sankar S, et al. REDD1, an inhibitor of mTOR signalling, is regulated by the CUL4A-DDB1 ubiquitin ligase. EMBO Rep. 2009;10(8):866–72.
104. Dan HC, Ebbs A, Pasparakis M, Van Dyke T, Basseres DS, Baldwin AS. Akt-dependent activation of mTORC1 complex involves phosphorylation of mTOR (mammalian target of rapamycin) by IκB kinase α (IKKα). J Biol Chem. 2014;289(36):25227–40.
105. Lee DF, Kuo HP, Chen C Te, Hsu JM, Chou CK, Wei Y, et al. IKKβ Suppression of TSC1 Links Inflammation and Tumor Angiogenesis via the mTOR Pathway. Cell. 2007;130(3):440–55.
106. Manifava M, Smith M, Rotondo S, Walker S, Niewczas I, Zoncu R, et al. Dynamics of mTORC1 activation in response to amino acids. Elife. 2016;5(OCTOBER2016):1–21.
107. Moghei M, Tavajohi-Fini P, Beatty B, Adegoke OAJ. Ketoisocaproic acid, a metabolite of leucine, suppresses insulin-stimulated glucose transport in skeletal muscle cells in a BCAT2-dependent manner. Am J Physiol - Cell Physiol. 2016;311(3):C518–27.
108. Newgard CB, An J, Bain JR, Muehlbauer MJ, Stevens RD, Lien LF, et al. A Branched-Chain Amino Acid-Related Metabolic Signature that Differentiates Obese and Lean Humans and Contributes to Insulin Resistance. Cell Metab [Internet]. 2009;9(4):311–26. Available from: http://dx.doi.org/10.1016/j.cmet.2009.02.002
109. Tzatsos A. Raptor binds the SAIN (Shc and IRS-1 NPXY binding) domain of insulin receptor substrate-1 (IRS-1) and regulates thephosphorylation of IRS-1 at Ser-636/639 by mTOR. J Biol Chem. 2009;284(34):22525–34.
110. Shah OJ, Hunter T. Turnover of the Active Fraction of IRS1 Involves Raptor-mTOR- and S6K1-Dependent Serine Phosphorylation in Cell Culture Models of Tuberous Sclerosis. Mol Cell Biol. 2006;26(17):6425–34.
111. Copps KD, White MF. Regulation of insulin sensitivity by serine/threonine phosphorylation of insulin receptor substrate proteins IRS1 and IRS2. Diabetologia. 2012;55(10):2565–82.
112. Haruta T, Uno T, Kawahara J, Takano A, Egawa K, Sharma PM, et al. A rapamycin-sensitive pathway down-regulates insulin signaling via phosphorylation and proteasomal degradation of insulin receptor substrate-1. Mol Endocrinol. 2000;14(6):783–94.
113. Tremblay F, Marette A. Amino acid and insulin signaling via the mTOR/p70 S6 kinase pathway. A negative feedback mechanism leading to insulin resistance in skeletal muscle cells. J Biol Chem. 2001;276(41):38052–60.
114. Tremblay F, Brûlé S, Sung HU, Li Y, Masuda K, Roden M, et al. Identification of IRS-1 Ser-1101 as a target of S6K1 in nutrient- and obesity-induced insulin resistance. Proc Natl Acad Sci U S A. 2007;104(35):14056–61.
115. Sancak Y, Peterson TR, Shaul YD, Lindquist RA, Thoreen CC, Bar-Peled L, et al. The rag

GTPases bind raptor and mediate amino acid signaling to mTORC1. Science (80-). 2008;320:1496–501.
116. Chantranupong L, Wolfson RL, Orozco JM, Saxton RA, Scaria SM, Bar-Peled L, et al. The sestrins interact with gator2 to negatively regulate the amino-acid-sensing pathway upstream of mTORC1. Cell Rep. 2014;9(1):1–8.
117. Parmigiani A, Nourbakhsh A, Ding B, Wang W, Kim YC, Akopiants K, et al. Sestrins Inhibit mTORC1 Kinase Activation through the GATOR Complex. Cell Rep. 2014;9:1281–91.
118. Saxton RA, Knockenhauer KE, Wolfson RL, Chantranupong L, Pacold ME, Wang T, et al. Structural basis for leucine sensing by the Sestrin2-mTORC1 pathway. Science (80-). 2016;351:53–58.
119. Wolfson RL, Chantranupong L, Saxton RA, Shen K, Scaria SM, Cantor JR, et al. Sestrin2 is a leucine sensor for the mTORC1 pathway. Science (80-). 2016;351:43–8.
120. Freeman AM, Pennings N. Insulin Resistance - StatPearls - NCBI Bookshelf. StatPearls Publishing, Treasure Island (FL). 2021.
121. Longo N, Wang Y, Pasquali M. Progressive decline in insulin levels in Rabson-Mendenhall syndrome. J Clin Endocrinol Metab. 1999;84(8):2623–9.
122. Chen YH, Chen QQ, Wang CL. Treatment and five-year follow-up of type A insulin resistance syndrome: A case report. World J Clin Cases. 2022;10(8):2522–8.
123. Yang GQ, Wang BA, Zhao WR, Gu WJ, Lui ZH, Dou JT, et al. Clinical and genetic analysis of the insulin receptor gene in a Chinese patient with extreme insulin resistance. Diabetes Res Clin Pract. 2010;89:e56–8.
124. Kahn CR, Flier JS, Bar RS, Archer JA, Gorden P, Martin MM, et al. The Syndromes of Insulin Resistance and Acanthosis Nigricans: Insulin-Receptor Disorders in Man. N Engl J Med. 1976;294:739–45.
125. Burguete-Garcia AI, Cruz-Lopez M, Madrid-Marina V, Lopez-Ridaura R, Hernández-Ávila M, Cortina B, et al. Association of Gly972Arg polymorphism of IRS1 gene with type 2 diabetes mellitus in lean participants of a national health survey in Mexico: a candidate gene study. Metabolism. 2010;59:38–45.
126. Esposito DL, Li Y, Vanni C, Mammarella S, Veschi S, Della Loggia F, et al. Clinical case seminar: A novel T608R missense mutation in insulin receptor substrate-1 identified in a subject with type 2 diabetes impairs metabolic insulin signaling. In: Journal of Clinical Endocrinology and Metabolism. 2003.
127. Balkau B, Mhamdi L, Oppert JM, Nolan J, Golay A, Porcellati F, et al. Physical activity and insulin sensitivity the RISC study. Diabetes. 2008;57(10):2613–8.
128. Higashida K, Kim SH, Higuchi M, Holloszy JO, Han DH. Normal adaptations to exercise despite protection against oxidative stress. Am J Physiol - Endocrinol Metab. 2011;301(5):779–84.
129. Richter EA, Hargreaves M. Exercise, GLUT4, and skeletal muscle glucose uptake. Physiol Rev. 2013;93:993–1017.
130. Howlett KF, Andrikopoulos S, Proietto J, Hargreaves M. Exercise-induced muscle glucose uptake in mice with graded, muscle-specific GLUT-4 deletion. Physiol Rep. 2013;1(3):e00065.
131. Hussey SE, Mcgee SL, Garnham A, Mcconell GK, Hargreaves M. Exercise increases skeletal muscle GLUT4 gene expression in patients with type 2 diabetes. Diabetes, Obes Metab. 2012;14(8):768–71.

132. Kramer HF, Witczak CA, Taylor EB, Fujii N, Hirshman MF, Goodyear LJ. AS160 regulates insulin- and contraction-stimulated glucose uptake in mouse skeletal muscle. J Biol Chem. 2006;56(12):2854–62.
133. Musi N, Fujii N, Hirshman MF, Ekberg I, Fröberg S, Ljungqvist O, et al. AMP-Activated Protein Kinase (AMPK) Is Activated in Muscle of Subjects With Type 2 Diabetes During Exercise. Diabetes. 2001;50:921–7.
134. Martin IK, Katz A, Wahren J. Splanchnic and muscle metabolism during exercise in NIDDM patients. Am J Physiol - Endocrinol Metab. 1995;269(3 32-3):583–90.
135. Colditz GA, Willett WC, Stampfer MJ, Manson JE, Hennekens CH, Arky RA, et al. Weight as a risk factor for clinical diabetes in women. Am J Epidemiol. 1990;132(3):501–13.
136. Kissebah AH, Krakower GR. Regional adiposity and morbidity. Physiol Rev. 1994;74(4):761–811.
137. Ten Hacken NHT. Physical inactivity and obesity: Relation to asthma and chronic obstructive pulmonary disease? Proc Am Thorac Soc. 2009;6(8):663–7.
138. Hudish LI, Reusch JEB, Sussel L. β Cell dysfunction during progression of metabolic syndrome to type 2 diabetes. J Clin Invest. 2019;129(10):4001–4008.
139. Dela F, Von Linstow ME, Mikines KJ, Galbo H. Physical training may enhance β-cell function in type 2 diabetes. Am J Physiol - Endocrinol Metab. 2004;287(5 50-5):1024–31.
140. Butler AE, Janson J, Bonner-weir S, Ritzel R, Rizza R a, Butler PC. Humans With Type 2 Diabetes. Diabetes [Internet]. 2003;52(January):102–10. Available from: http://www.ncbi.nlm.nih.gov/pubmed/12502499
141. Figueiredo PA, Powers SK, Ferreira RM, Amado F, Appell HJ, Duarte JA. Impact of lifelong sedentary behavior on mitochondrial function of mice skeletal muscle. Journals Gerontol - Ser A Biol Sci Med Sci. 2009;64(9):927–39.
142. Distefano G, Standley RA, Zhang X, Carnero EA, Yi F, Cornnell HH, et al. Physical activity unveils the relationship between mitochondrial energetics, muscle quality, and physical function in older adults. J Cachexia Sarcopenia Muscle. 2018;9(2):279–94.
143. Abadi A, Glover EI, Isfort RJ, Raha S, Safdar A, Yasuda N, et al. Limb immobilization induces a coordinate down-regulation of mitochondrial and other metabolic pathways in men and women. PLoS One. 2009;4(8).
144. Lavie CJ, Ozemek C, Carbone S, Katzmarzyk PT, Blair SN. Sedentary Behavior, Exercise, and Cardiovascular Health. Circ Res. 2019;124(5):799–815.
145. Bilet L, Phielix E, van de Weijer T, Gemmink A, Bosma M, Moonen-Kornips E, et al. One-leg inactivity induces a reduction in mitochondrial oxidative capacity, intramyocellular lipid accumulation and reduced insulin signalling upon lipid infusion: a human study with unilateral limb suspension. Diabetologia. 2020;63(6):1211–22.
146. Laufs U, Wassmann S, Czech T, Münzel T, Eisenhauer M, Böhm M, et al. Physical inactivity increases oxidative stress, endothelial dysfunction, and atherosclerosis. Arterioscler Thromb Vasc Biol. 2005;25(4):809–14.
147. Gracia MC. Inflammatory, autoimmune, chronic diseases: Bad diet and physical inactivity are causes or effects? Med Hypotheses. 2006;66(5):939–944.
148. Burini RC, Anderson E, Durstine JL, Carson JA. Inflammation, physical activity, and chronic disease: An evolutionary perspective. Sport Med Heal Sci. 2020;2(1):1–6.
149. McAuley K, Mann J. Thematic review series: Patient-Oriented Research. Nutritional determinants of insulin resistance. J Lipid Res. 2006;47(8):1668–76.

150. Lombardo GE, Arcidiacono B, De Rose RF, Lepore SM, Costa N, Montalcini T, et al. Normocaloric diet restores weight gain and insulin sensitivity in obese mice. Front Endocrinol (Lausanne). 2016;7(MAY):1–7.
151. Trim W V., Walhin JP, Koumanov F, Turner JE, Shur NF, Simpson EJ, et al. The impact of physical inactivity on glucose homeostasis when diet is adjusted to maintain energy balance in healthy, young males. Clin Nutr [Internet]. 2023;42(4):532–40. Available from: https://doi.org/10.1016/j.clnu.2023.02.006
152. Bray GA, Popkin BM. Dietary fat intake does affect obesity. Am J Clin Nutr. 1998;68(6):1157–73.
153. Curb JD, Marcus EB. Body fat and obesity in Japanese Americans. In: American Journal of Clinical Nutrition. 1991.
154. Astrup A, Buemann B, Western P, Toubro S, Raben A, Christensen NJ. Obesity as an adaptation to a high-fat diet: Evidence from a cross-sectional study. Am J Clin Nutr. 1994;59(2):350–5.
155. Krachler B, Eliasson M, Stenlund H, Johansson I, Hallmans G, Lindahl B. Reported food intake and distribution of body fat: A repeated cross-sectional study. Nutr J. 2006;5(1):1–11.
156. Ruth MR, Port AM, Shah M, Bourland AC, Istfan NW, Nelson KP, et al. Consuming a hypocaloric high fat low carbohydrate diet for 12 weeks lowers C-reactive protein, and raises serum adiponectin and high density lipoprotein-cholesterol in obese subjects. Metabolism. 2013;62(13).
157. Hansen CD, Gram-Kampmann EM, Hansen JK, Hugger MB, Madsen BS, Jensen JM, et al. Effect of Calorie-Unrestricted Low-Carbohydrate, High-Fat Diet Versus High-Carbohydrate, Low-Fat Diet on Type 2 Diabetes and Nonalcoholic Fatty Liver Disease: A Randomized Controlled Trial. Ann Intern Med. 2023;176(1):10–21.
158. Rosholt MN, King PA, Horton ES. High-fat diet reduces glucose transporter responses to both insulin and exercise. Am J Physiol - Regul Integr Comp Physiol. 1994;266:R95-101.
159. Nagy C, Einwallner E. Study of in vivo glucose metabolism in high-fat diet-fed mice using oral glucose tolerance test (OGTT) and insulin tolerance test (ITT). J Vis Exp. 2018;2018(131):1–12.
160. Nakamura S, Takamura T, Matsuzawa-Nagata N, Takayama H, Misu H, Noda H, et al. Palmitate induces insulin resistance in H4IIEC3 hepatocytes through reactive oxygen species produced by mitochondria. J Biol Chem [Internet]. 2009;284(22):14809–18. Available from: http://dx.doi.org/10.1074/jbc.M901488200
161. Pu J, Peng G, Li L, Na H, Liu Y, Liu P. Palmitic acid acutely stimulates glucose uptake via activation of Akt and ERK1/2 in skeletal muscle cells. J Lipid Res. 2011;52(7):1319–27.
162. Aggarwal R, Peng Z, Zeng N, Silva J, He L, Chen J, et al. Chronic Exposure to Palmitic Acid Down-Regulates AKT in Beta-Cells through Activation of mTOR. Am J Pathol [Internet]. 2022;192(1):130–45. Available from: https://doi.org/10.1016/j.ajpath.2021.09.008
163. Clegg DJ, Gotoh K, Kemp C, Wortman MD, Benoit SC, Brown LM, et al. Consumption of a high-fat diet induces central insulin resistance independent of adiposity. Physiol Behav [Internet]. 103(1):10–6. Available from: http://dx.doi.org/10.1016/j.physbeh.2011.01.010
164. von Frankenberg AD, Marina A, Song X, Callahan HS, Kratz M, Utzschneider KM. A

high-fat, high-saturated fat diet decreases insulin sensitivity without changing intra-abdominal fat in weight-stable overweight and obese adults. Eur J Nutr. 2017;56(1):431–43.
165. Speakman JR. Use of high-fat diets to study rodent obesity as a model of human obesity. Int J Obes [Internet]. 2019;43(8):1491–2. Available from: http://dx.doi.org/10.1038/s41366-019-0363-7
166. Zhang XY, Guo CC, Yu YX, Xie L, Chang CQ. Establishment of high-fat diet-induced obesity and insulin resistance model in rats. Beijing Da Xue Xue Bao. 2020;52(3):557–63.
167. Patikorn C, Saidoung P, Pham T, Phisalprapa P, Lee YY, Varady KA, et al. Effects of ketogenic diet on health outcomes: an umbrella review of meta-analyses of randomized clinical trials. BMC Med [Internet]. 2023;21(1):1–12. Available from: https://doi.org/10.1186/s12916-023-02874-y
168. H.M. D, T.C. M, T. H, S.K. A, A. B, M.A. K, et al. Long-term effects of a ketogenic diet in obese patients. Exp Clin Cardiol [Internet]. 2004;9(3):200–5. Available from: http://www.embase.com/search/results?subaction=viewrecord&from=export&id=L39600023
169. Li S, Lin G, Chen J, Chen Z, Xu F, Zhu F, et al. The effect of periodic ketogenic diet on newly diagnosed overweight or obese patients with type 2 diabetes. BMC Endocr Disord [Internet]. 2022;22(1):4–9. Available from: https://doi.org/10.1186/s12902-022-00947-2
170. Bessesen DH. The role of carbohydrates in insulin resistance. J Nutr. 2001;131(10):2782S-2786S.
171. Wolever TMS. Dietary carbohydrates and insulin action in humans. Br J Nutr. 2000;83(SUPPL. 1):97–102.
172. Pérez-Jiménez F, López-Miranda J, Pinillos MD, Gómez P, Paz-Rojas E, Montilla P, et al. A mediterranean and a high-carbohydrate diet improve glucose metabolism in healthy young persons. Diabetologia. 2001;44:2038–43.
173. Fukagawa NK, Anderson JW, Hageman G, Young VR, Minaker KL. High-carbohydrate, high-fiber diets increase peripheral insulin sensitivity in healthy young and old adults. Am J Clin Nutr. 1990;52(3):524–8.
174. Adochio RL, Leitner JW, Gray K, Draznin B, Cornier MA. Early responses of insulin signaling to high-carbohydrate and high-fat overfeeding. Nutr Metab. 2009;6:1–10.
175. Piatti PM, Monti LD, Magni F, Fermo I, Baruffaldi L, Nasser R, et al. Hypocaloric high-protein diet improves glucose oxidation and spares lean body mass: Comparison to hypocaloric high-carbohydrate diet. Metabolism. 1994;43(12):1481–7.
176. Lewis SB, Wallin JD, Kane JP, Gerich JE. Effect of diet composition on metabolic adaptations to hypocaloric nutrition: comparison of high carbohydrate and high fat isocaloric diets. Am J Clin Nutr. 1977;30(2):160–70.
177. Astrup A, Raben A, Geiker N. The role of higher protein diets in weight control and obesity-related comorbidities. Int J Obes. 2015;39(5):721–6.
178. Hamdy O, Horton ES. Protein content in diabetes nutrition plan. Curr Diab Rep. 2011;11(2):111–9.
179. Gannon MC, Nuttall FQ, Neil BJ, Westphal SA. The insulin and glucose responses to meals of glucose plus various proteins in type II diabetic subjects. Metabolism. 1988;37:1081–1088.
180. Gannon MC, Nuttall FQ, Saeed A, Jordan K, Hoover H. An increase in dietary protein improves the blood glucose response in persons with type 2 diabetes. Am J Clin Nutr.

2003;78(4):734–41.
181. Rietman A, Schwarz J, Tomé D, Kok FJ, Mensink M. High dietary protein intake, reducing or eliciting insulin resistance? Eur J Clin Nutr. 2014;68(9):973–9.
182. Weickert MO, Roden M, Isken F, Hoffmann D, Nowotny P, Osterhoff M, et al. Effects of supplemented isoenergetic diets differing in cereal fiber and protein content on insulin sensitivity in overweight humans. Am J Clin Nutr. 2011;94(2):459–71.
183. Salgueiro RB, Gerlinger-Romero F, Guimarães-Ferreira L, de Castro Barbosa T, Nunes MT. Exercise training reverses the negative effects of chronic L-arginine supplementation on insulin sensitivity. Life Sci [Internet]. 2017;191(October):17–23. Available from: https://doi.org/10.1016/j.lfs.2017.10.001
184. De Castro Barbosa T, Jiang LQ, Zierath JR, Nunes MT. L-Arginine enhances glucose and lipid metabolism in rat L6 myotubes via the NO/ c-GMP pathway. Metabolism [Internet]. 2013;62(1):79–89. Available from: http://dx.doi.org/10.1016/j.metabol.2012.06.011
185. Ables GP, Perrone CE, Orentreich D, Orentreich N. Methionine-Restricted C57BL/6J Mice Are Resistant to Diet-Induced Obesity and Insulin Resistance but Have Low Bone Density. PLoS One. 2012;7(12):1–12.
186. Castaño-Martinez T, Schumacher F, Schumacher S, Kochlik B, Weber D, Grune T, et al. Methionine restriction prevents onset of type 2 diabetes in NZO mice. FASEB J. 2019;33(6):7092–7102.
187. Qin LQ, Xun P, Bujnowski D, Daviglus ML, Van Horn L, Stamler J, et al. Higher branched-chain amino acid intake is associated with a lower prevalence of being overweight or obese in middle-aged East Asian and Western adults. J Nutr. 2011;141(2):249–54.
188. De Luis DA, Izaola O, Aller R, De La Fuente B, Bachiller R, Romero E. Effects of a high-protein/low carbohydrate versus a standard hypocaloric diet on adipocytokine levels and insulin resistance in obese patients along 9 months. J Diabetes Complications. 2015;29(7):950–4.
189. Shimobayashi M, Albert V, Woelnerhanssen B, Frei IC, Weissenberger D, Meyer-Gerspach AC, et al. Insulin resistance causes inflammation in adipose tissue. J Clin Invest. 2018;128(4):1538–50.
190. Ellulu MS, Patimah I, Khaza'ai H, Rahmat A, Abed Y. Obesity & inflammation: The linking mechanism & the complications. Arch Med Sci. 2017;13(4):851–63.
191. Shoelson SE, Lee J, Goldfine AB. Inflammation and insulin resistance. JClinInvest. 2006;116(0021-9738 (Print)):1793–801.
192. Sabio G, Davis RJ. CJun NH2-terminal kinase 1 (JNK1): Roles in metabolic regulation of insulin resistance. Trends Biochem Sci. 2010;35(9):490–6.
193. Hotamisligil G, Shargill N, Spiegelman B. Adipose Expression of Tumor Necrosis Factor-α : Direct Role in Obesity-Linked Insulin Resistance Author (s): Gökhan S . Hotamisligil , Narinder S . Shargill and Bruce M . Spiegelman Published by : American Association for the Advancement of Science Stab. Science (80-). 1993;259(5091):87–91.
194. Serrano-Marco L, Barroso E, El Kochairi I, Palomer X, Michalik L, Wahli W, et al. The peroxisome proliferator-activated receptor (PPAR) β/δ agonist GW501516 inhibits IL-6-induced signal transducer and activator of transcription 3 (STAT3) activation and insulin resistance in human liver cells. Diabetologia. 2012;55(3):743–51.
195. Lukic L, Lalic NM, Rajkovic N, Jotic A, Lalic K, Milicic T, et al. Hypertension in obese type 2 diabetes patients is associated with increases in insulin resistance and IL-6 cytokine

levels: Potential targets for an efficient preventive intervention. Int J Environ Res Public Health. 2014;11(4):3586–98.
196. Kolczynska K, Loza-Valdes A, Hawro I, Sumara G. Diacylglycerol-evoked activation of PKC and PKD isoforms in regulation of glucose and lipid metabolism: A review. Lipids Health Dis. 2020;19(113):1–15.
197. Boden G, She P, Mozzoli M, Cheung P, Gumireddy K, Reddy P, et al. Free fatty acids produce insulin resistance and activate the proinflammatory nuclear factor-κb pathway in rat liver. Diabetes. 2005;54:3458–3465.
198. Hotamisligil GS. Role of endoplasmic reticulum stress and c-Jun NH2-terminal kinase pathways in inflammation and origin of obesity and diabetes. Diabetes. 2005;54:S73–S78.
199. Westwick JK, Bielawska AE, Dbaibo G, Hannun YA, Brenner DA. Ceramide activates the stress-activated protein kinases. J Biol Chem. 1995;270:22689–22692.
200. Schenk S, Saberi M, Olefsky JM. Insulin sensitivity: Modulation by nutrients and inflammation. J Clin Invest. 2008;118:2992–3002.
201. Huang S, Huang S, Wang X, Zhang Q, Liu J, Leng Y. Downregulation of lipin-1 induces insulin resistance by increasing intracellular ceramide accumulation in C2C12 myotubes. Int J Biol Sci. 2017;13(1):1–12.
202. Matsuzawa-Nagata N, Takamura T, Ando H, Nakamura S, Kurita S, Misu H, et al. Increased oxidative stress precedes the onset of high-fat diet-induced insulin resistance and obesity. Metabolism. 2008;57(8):1071–7.
203. Kausar S, Wang F, Cui H. The Role of Mitochondria in Reactive Oxygen Species Generation and Its Implications for Neurodegenerative Diseases. Cells. 2018;7(12):274.
204. Rudich A, Tlrosh A, Potashnik R, Hemi R, Kanety H, Bashan N. Prolonged oxidative stress impairs insulin-induced GLUT4 translocation in 3T3-L1 adipocytes. Diabetes. 1998;47:1562–9.
205. Dokken BB, Saengsirisuwan V, Kim JS, Teachey MK, Henriksen EJ. Oxidative stress-induced insulin resistance in rat skeletal muscle: Role of glycogen synthase kinase-3. Am J Physiol - Endocrinol Metab. 2008;294:E615–21.
206. Tiganis T. Reactive oxygen species and insulin resistance: The good, the bad and the ugly. Trends Pharmacol Sci [Internet]. 2011;32(2):82–9. Available from: http://dx.doi.org/10.1016/j.tips.2010.11.006
207. De Figueiredo ASP, Salmon AB, Bruno F, Jimenez F, Martinez HG, Halade G V., et al. Nox2 mediates skeletal muscle insulin resistance induced by a high fat diet. J Biol Chem [Internet]. 2015;290(21):13427–39. Available from: http://dx.doi.org/10.1074/jbc.M114.626077
208. Henríquez-Olguin C, Knudsen JR, Raun SH, Li Z, Dalbram E, Treebak JT, et al. Cytosolic ROS production by NADPH oxidase 2 regulates muscle glucose uptake during exercise. Nat Commun [Internet]. 2019;10(1):1–11. Available from: http://dx.doi.org/10.1038/s41467-019-12523-9
209. Mahadev K, Zilbering A, Zhu L, Goldstein BJ. Insulin-stimulated Hydrogen Peroxide Reversibly Inhibits Protein-tyrosine Phosphatase 1B in Vivo and Enhances the Early Insulin Action Cascade. J Biol Chem. 2001;276:21938–21942.
210. Seo JH, Ahn Y, Lee SR, Yeo CY, Hur KC. The major target of the endogenously generated reactive oxygen species in response to insulin stimulation is Phosphatase and Tensin homolog and not phosphoinositide-3 kinase (PI-3 kinase) in the PI-3 kinase/Akt pathway. Mol Biol Cell. 2005;16:348–357.

211. Kamei Y, Hatazawa Y, Uchitomi R, Yoshimura R, Miura S. Regulation of skeletal muscle function by amino acids. Nutrients. 2020;12(1):261.
212. Yoshizawa F. Regulation of protein synthesis by branched-chain amino acids in vivo. In: Biochemical and Biophysical Research Communications. 2004. p. 417–22.
213. Norton LE, Layman DK. Leucine Regulates Translation Initiation of Protein Synthesis in Skeletal Muscle after Exercise. J Nutr. 2006;136(2):533S-537S.
214. She P, Reid TM, Bronson SK, Vary TC, Hajnal A, Lynch CJ, et al. Disruption of BCATm in mice leads to increased energy expenditure associated with the activation of a futile protein turnover cycle. Cell. 2007;6(3):181–94.
215. Siddik MAB, Shin AC. Recent progress on branched-chain amino acids in obesity, diabetes, and beyond. Vol. 34, Endocrinology and Metabolism. 2019. p. 234–46.
216. Béchet D, Tassa A, Combaret L, Taillandier D, Attaix D. Regulation of skeletal muscle proteolysis by amino acids. In: Journal of Renal Nutrition. 2005. p. 18–22.
217. Lackey DE, Lynch CJ, Olson KC, Mostaedi R, Ali M, Smith WH, et al. Regulation of adipose branched-chain amino acid catabolism enzyme expression and cross-adipose amino acid flux in human obesity. Am J Physiol - Endocrinol Metab. 2013;304(11).
218. Mccormack SE, Shaham O, Mccarthy MA, Deik AA, Wang TJ, Gerszten RE, et al. Circulating branched-chain amino acid concentrations are associated with obesity and future insulin resistance in children and adolescents. Pediatr Obes. 2013;8(1):52–61.
219. Badoud F, Lam KP, Dibattista A, Perreault M, Zulyniak MA, Cattrysse B, et al. Serum and adipose tissue amino acid homeostasis in the metabolically healthy obese. J Proteome Res. 2014;13(7):3455–66.
220. Adams SH. Emerging Perspectives on Essential Amino Acid Metabolism in Obesity and the Insulin-Resistant State. Adv Nutr. 2011;2(6):445–56.
221. Wang TJ, Larson MG, Vasan RS, Cheng S, Rhee EP, McCabe E, et al. Metabolite profiles and the risk of developing diabetes. Nat Med. 2011;17(4):448–53.
222. Wurtz P, Soininen P, Kangas AJ, Rönnemaa T, Lehtimäki T, Kähönen M, et al. Branched-chain and aromatic amino acidsare predictors of insulinresistance in young adults. Diabetes Care. 2013;36(3):648–55.
223. Goto M, Miyahara I, Hirotsu K, Conway M, Yennawar N, Islam MM, et al. Structural determinants for branched-chain aminotransferase isozyme-specific inhibition by the anticonvulsant drug gabapentin. J Biol Chem. 2005;280(44):37246–56.
224. Adeva-Andany MM, López-Maside L, Donapetry-García C, Fernández-Fernández C, Sixto-Leal C. Enzymes involved in branched-chain amino acid metabolism in humans. Amino Acids. 2017;49(6):1005–28.
225. Tetrick MA, Odle J. What Constitutes a Gluconeogenic Precursor? J Nutr. 2020;150(9):2239–41.
226. Green MH. Are Fatty Acids Gluconeogenic Precursors? J Nutr. 2020;150(9):2235–8.
227. Neinast MD, Jang C, Hui S, Anthony TG, Rabinowitz JD, Correspondence ZA, et al. Quantitative Analysis of the Whole-Body Metabolic Fate of Branched-Chain Amino Acids Cell Metabolism Quanti. Cell Metab [Internet]. 2018;29:1–13. Available from: https://doi.org/10.1016/j.cmet.2018.10.013
228. Suryawan A, Hawes JW, Harris RA, Shimomura Y, Jenkins AE, Hutson SM. A molecular model of human branched-chain amino acid metabolism. Am J Clin Nutr. 1998;68(1):72–81.
229. Bledsoe RK, Dawson PA, Hutson SM. Cloning of the rat and human mitochondrial

branched chain aminotransferases (BCAT(m)). Biochim Biophys Acta - Protein Struct Mol Enzymol. 1997;1339(1):9–13.
230. Davoodi J, Drown PM, Bledsoe RK, Wallin R, Reinhart GD, Hutson SM. Overexpression and characterization of the human mitochondrial and cytosolic branched-chain aminotransferases. J Biol Chem. 1998;273(9):4982–9.
231. Wallin R, Hall TR, Hutson SM. Purification of branched chain aminotransferase from rat heart mitochondria. J Biol Chem. 1990;265(11):6019–24.
232. Hall TR, Wallin R, Reinhart GD, Hutson SM. Branched chain aminotransferase isoenzymes. Purification and characterization of the rat brain isoenzyme. J Biol Chem. 1993;268(5):3092–8.
233. She P, Zhou Y, Zhang Z, Griffin K, Gowda K, Lynch CJ. Disruption of BCAA metabolism in mice impairs exercise metabolism and endurance. J Appl Physiol. 2010;108(4):941–9.
234. Lynch CJ, Kimball SR, Xu Y, Salzberg AC, Kawasawa YI. Global deletion of BCATm increases expression of skeletal muscle genes associated with protein turnover. Physiol Genomics. 2015;47(11):569–80.
235. Dhanani ZN, Mann G, Adegoke OAJ. Depletion of branched-chain aminotransferase 2 (BCAT2) enzyme impairs myoblast survival and myotube formation. Physiol Rep. 2019;7(23):1–15.
236. Indo Y, Kitano A, Endo F, Akaboshi I, Matsuda I. Altered kinetic properties of the branched-chain α-keto acid dehydrogenase complex due to mutation of the β-subunit of the branched-chain α-keto acid decarboxylase (E1) component in lymphoblastoid cells derived from patients with maple syrup urine disease. J Clin Invest. 1987;80(1):63–70.
237. Conway M., Hutson SM. BCAA Metabolism and NH3 Homeostasis. In: The Glutamate/GABA-Glutamine Cycle [Internet]. 2016. p. 99–132. Available from: http://link.springer.com/10.1007/978-3-319-45096-4
238. Ananieva EA, Conway ME. Branched-Chain Amino Metabolism. In: Reference Module in Life Sciences. Elsevier; 2020.
239. Chuang DT, Chuang JL, Wynn RM. Branched-Chain Amino Acids : Metabolism , Physiological Function , and Application Lessons from Genetic Disorders of Branched-Chain Amino. J Nutr. 2006;(March):243–9.
240. Litwer S, Herring WJ, Danner DJ. Reversion of the maple syrup urine disease phenotype of impaired branched chain α-ketoacid dehydrogenase complex activity in fibroblasts from an affected child. J Biol Chem. 1989;264(25):14597–600.
241. Harper a E, Miller RH, Block KP. Branched-Chain Amino Acid Metabolism. Metabolism. 1984;30(6):409–54.
242. Beatty B. Branched-Chain Keto Acid Dehydrogenase Kinase Depletion Affects Branched-Chain Alpha-Keto Acid Dehydrogenase Activity and Muscle Cell Differentiation. York Univ. 2018;
243. Van Koevering M, Nissen S. Oxidation of leucine and α-ketoisocaproate to β-hydroxy-β-methylbutyrate in vivo. Am J Physiol - Endocrinol Metab. 1992;262(1 25-1):27–31.
244. Nissen S, Sharp R, Ray M, Rathmacher JA, Rice D, Fuller JC, et al. Effect of leucine metabolite β-hydroxy-β-methylbutyrate on muscle metabolism during resistance-exercise training. J Appl Physiol. 1996;81(5):2095–104.
245. Wilson GJ, Wilson JM, Manninen AH. Effects of beta-hydroxy-beta-methylbutyrate (HMB) on exercise performance and body composition across varying levels of age, sex,

and training experience: A review. Nutr Metab. 2008;5(1):1–17.
246. Kimura K, Cheng XW, Inoue A, Hu L, Koike T, Kuzuya M. β-Hydroxy-β-methylbutyrate facilitates PI3K/Akt-dependent mammalian target of rapamycin and FoxO1/3a phosphorylations and alleviates tumor necrosis factor α/interferon γ-induced MuRF-1 expression in C2C12 cells. Nutr Res [Internet]. 2014;34(4):368–74. Available from: http://dx.doi.org/10.1016/j.nutres.2014.02.003
247. Suryawan A, Rudar M, Fiorotto ML, Davis TA. Differential regulation of mTORC1 activation by leucine and β-hydroxy-β-methylbutyrate in skeletal muscle of neonatal pigs. J Appl Physiol. 2020;128(2):286–95.
248. Wilkinson DJ, Hossain T, Hill DS, Phillips BE, Crossland H, Williams J, et al. Effects of leucine and its metabolite β-hydroxy-β-methylbutyrate on human skeletal muscle protein metabolism. J Physiol. 2013;591(11):2911–23.
249. Liebich HM, Först C. Hydroxycarboxylic and oxocarboxylic acids in urine:products from branched-chain amino acid degradation and from ketogenesis. J Chromatogr B Biomed Sci Appl. 1984;309(C):225–42.
250. Anderson KA, Huynh FK, Fisher-Wellman K, Stuart JD, Peterson BS, Douros JD, et al. SIRT4 Is a Lysine Deacylase that Controls Leucine Metabolism and Insulin Secretion. Cell Metab [Internet]. 2017;25(4):838-855.e15. Available from: http://dx.doi.org/10.1016/j.cmet.2017.03.003
251. Wynn RM, Chuang JL, Cote CD, Chuang DT. Tetrameric assembly and conservation in the ATP-binding domain of rat branched-chain α-ketoacid dehydrogenase kinase. J Biol Chem. 2000;275(39):30512–9.
252. Shimomura Y, Nanaumi N, Suzuki M, Popov KM, Harris RA. Purification and partial characterization of branched-chain α-ketoacid dehydrogenase kinase from rat liver and rat heart. Arch Biochem Biophys. 1990;283(2):293–289.
253. Popov KM, Zhao Y, Shimomuras Y, Kuntz MJ, Harris R a. Branched-chain a-ketoacid dehydrogenase kinase: molecular cloning, expression, and sequence similarity with histidine protein kinases. 1992;267:13127–30.
254. Popov KM, Shimomura Y, Harris RA. Purification and comparative study of the kinases specific for branched chain α-ketoacid dehydrogenase and pyruvate dehydrogenase. Protein Expr Purif. 1991;2(4):278–86.
255. Damuni Z, Merryfield M, Humphreys J, Reed L. Purification and properties of the catalytic subunit of the branched-chain alpha-keto acid dehydrogenase phosphatase from bovine kidney mitochondria. Proc Natl Acad Sci U S A. 1984;81:4335–8.
256. Damuni Z, Reed LJ. Purification and properties of the catalytic subunit of the branched-chain alpha-keto acid dehydrogenase phosphatase from bovine kidney mitochondria. J Biol Chem. 1987;262(11):5129–32.
257. Machius M, Chuang JL, Wynn RM, Tomchick DR, Chuang DT. Structure of rat BCKD kinase: Nucleotide-induced domain communication in a mitochondrial protein kinase. Proc Natl Acad Sci U S A. 2001 Sep;98(20):11218–23.
258. Obayashi M, Sato Y, Harris RA, Shimomura Y. Regulation of the activity of branched-chain 2-oxo acid dehydrogenase (BCODH) complex by binding BCODH kinase. FEBS Lett. 2001;491(1–2):50–4.
259. Harris RA, Zhang B, Goodwin GW, Kuntz MJ, Shimomura Y, Rougraff P, et al. Regulation Branched-Chain and Elucidation of a Molecular Basis for Maple Syrup Urine. Adv Enz Reg. 1990;30:245–63.

260. Ishikawa T, Kitaura Y, Kadota Y, Morishita Y, Ota M, Yamanaka F, et al. Muscle-specific deletion of BDK amplifies loss of myofibrillar protein during protein undernutrition. Sci Rep. 2017;7:1–11.
261. Dolatabad MR, Guo L lu, Xiao P, Zhu Z, He Q tao, Yang D xiao, et al. Crystal structure and catalytic activity of the PPM1K N94K mutant. J Neurochem. 2019;148(4):550–60.
262. Lu G, Sun H, She P, Youn JY, Warburton S, Ping P, et al. Protein phosphatase 2Cm is a critical regulator of branched-chain amino acid catabolism in mice and cultured cells. J Clin Invest. 2009;
263. Zhou M, Lu G, Gao C, Wang Y, Sun H. Tissue-specific and nutrient regulation of the branched-chain α-keto acid dehydrogenase phosphatase, protein phosphatase 2Cm (PP2Cm). J Biol Chem. 2012;287(28):23397–406.
264. Abell LE. Defective branched chain amino acid catabolism impairs exercise capacity and glucose homeostasis in the mouse. Univ Washingt. 2019;1–96.
265. Perng W, Gillman MW, Fleisch AF, Michalek RD, Watkins SM, Isganaitis E, et al. Metabolomic profiles and childhood obesity. Obesity. 2014;22(12):2570–8.
266. Costanzo M, Caterino M, Sotgiu G, Ruoppolo M, Franconi F, Campesi I. Sex differences in the human metabolome. Biol Sex Differ. 2022;13(30):1–18.
267. Kouchiwa T, Wada K, Uchiyama M, Kasezawa N, Niisato M, Murakami H, et al. Age-related changes in serum amino acids concentrations in healthy individuals. Clin Chem Lab Med. 2012;50(5):861–70.
268. Pitkänen HT, Oja SS, Kemppainen K, Seppä JM, Mero AA. Serum amino acid concentrations in aging men and women. Amino Acids. 2003;24(4):413–21.
269. Nair KS, Ford GC, Ekberg K, Fernqvist-Forbes E, Wahren J. Protein dynamics in whole body and in splanchnic and leg tissues in type I diabetic patients. J Clin Invest. 1995;95(6):2926–37.
270. Felig P, Marliss E, Cahill GF. Plasma Amino Acid Levels and Insulin Secretion in Obesity. N Engl J Med. 1969;281:811–6.
271. Chistiakov DA, Sobenin IA, Revin V V., Orekhov AN, Bobryshev Y V. Mitochondrial aging and age-related dysfunction of mitochondria. Biomed Res Int. 2014;2014:1–7.
272. Fujii H, Shimomura Y, Murakami T, Nakai N, Sato T, Suzuki M, et al. Branched-chain α-keto acid dehydrogenase kinase content in rat skeletal muscle is decreased by endurance training. Biochem Mol Biol Int. 1998;44(6):1211–6.
273. Wagenmakers AJM, Brookes JH, Coakley JH, Reilly T, Edwards RHT. Exercise-induced activation of the branched-chain 2-oxo acid dehydrogenase in human muscle. Eur J Appl Physiol Occup Physiol. 1989;59:159–67.
274. Shimomura Y, Fujii H, Suzuki M, Murakami T, Fujitsuka N, Nakai N. Branched-chain α-keto acid dehydrogenase complex in rat skeletal muscle: Regulation of the activity and gene expression by nutrition and physical exercise. J Nutr. 1995;125(Suppl):1762S–5S.
275. Xu M, Nagasaki M, Obayashi M, Sato Y, Tamura T, Shimomura Y. Mechanism of activation of branched-chain α-keto acid dehydrogenase complex by exercise. Biochem Biophys Res Commun. 2001 Sep;287(3):752–6.
276. Shimomura Y, Murakami T, Nakai N, Nagasaki M, Harris RA. Exercise promotes BCAA catabolism: Effects of BCAA supplementation on skeletal muscle during exercise. In: Journal of Nutrition. 2004.
277. Groennebaek T, Vissing K. Impact of resistance training on skeletal muscle mitochondrial biogenesis, content, and function. Front Physiol. 2017;8(SEP).

278. Knapik J, Meredith C, Jones B, Fielding R, Young V, Evans W. Leucine metabolism during fasting and exercise. J Appl Physiol. 1991;70(1):43–7.
279. Shimomura Y, Fujii H, Suzuki M, Fujitsuka N, Naoi M, Sugiyama S, et al. Branched-chain 2-oxo acid dehydrogenase complex activation by tetanic contractions in rat skeletal muscle. BBA - Gen Subj. 1993;1157(2):290–6.
280. Paxton R, Harris RA. Regulation of branched-chain α-ketoacid dehydrogenase kinase. Arch Biochem Biophys. 1984 May;231(1):48–57.
281. Chen S, Minegishi Y, Hasumura T, Shimotoyodome A, Ota N. Involvement of ammonia metabolism in the improvement of endurance performance by tea catechins in mice. Sci Rep. 2020;10(1):1–13.
282. Yin Q, Brameld JM, Parr T, Murton AJ. Leucine and mTORc1 act independently to regulate 2-deoxyglucose uptake in L6 myotubes. Amino Acids [Internet]. 2020;52(3):477–86. Available from: https://doi.org/10.1007/s00726-020-02829-0
283. Liu H, Liu R, Xiong Y, Li X, Wang X, Ma Y, et al. Leucine facilitates the insulin-stimulated glucose uptake and insulin signaling in skeletal muscle cells: Involving mTORC1 and mTORC2. Amino Acids. 2014;46(8):1971–9.
284. She P, Van Horn C, Reid T, Hutson SM, Cooney RN, Lynch CJ. Obesity-related elevations in plasma leucine are associated with alterations in enzymes involved in branched-chain amino acid metabolism. Am J Physiol - Endocrinol Metab. 2007;293(6):1552–63.
285. D'Antona G, Ragni M, Cardile A, Tedesco L, Dossena M, Bruttini F, et al. Branched-chain amino acid supplementation promotes survival and supports cardiac and skeletal muscle mitochondrial biogenesis in middle-aged mice. Cell Metab [Internet]. 2010;12(4):362–72. Available from: http://dx.doi.org/10.1016/j.cmet.2010.08.016
286. Baum JI, O'Connor JC, Seyler JE, Anthony TG, Freund GG, Layman DK. Leucine reduces the duration of insulin-induced PI 3-kinase activity in rat skeletal muscle. Am J Physiol - Endocrinol Metab. 2005;288(1 51-1):86–91.
287. Li X, Wang X, Liu R, Ma Y, Guo H, Hao L, et al. Chronic leucine supplementation increases body weight and insulin sensitivity in rats on high-fat diet likely by promoting insulin signaling in insulin-target tissues. Mol Nutr Food Res. 2013;57(6):1067–79.
288. Chen KH, Chen YL, Tang HY, Hung CC, Yen TH, Cheng ML, et al. Dietary leucine supplement ameliorates hepatic steatosis and diabetic nephropathy in db/db mice. Int J Mol Sci. 2018;19(7):1921.
289. Iwasa J, Shimizu M, Shiraki M, Shirakami Y, Sakai H, Terakura Y, et al. Dietary supplementation with branched-chain amino acids suppresses diethylnitrosamine-induced liver tumorigenesis in obese and diabetic C57BL/KsJ-db/db mice. Cancer Sci. 2010;101(2):460–7.
290. White PJ, Lapworth AL, An J, Wang L, McGarrah RW, Stevens RD, et al. Branched-chain amino acid restriction in Zucker-fatty rats improves muscle insulin sensitivity by enhancing efficiency of fatty acid oxidation and acyl-glycine export. Mol Metab [Internet]. 2016;5(7):538–51. Available from: http://dx.doi.org/10.1016/j.molmet.2016.04.006
291. Sun Y, Sun B, Wang Z, Lv Y, Ma Q. Short-Term Decreasing and Increasing Dietary BCAA Have Similar, but Not Identical Effects on Lipid and Glucose Metabolism in Lean Mice. Int J Mol Sci. 2023;24(6).
292. Maida A, Chan JSK, Sjøberg KA, Zota A, Schmoll D, Kiens B, et al. Repletion of

branched chain amino acids reverses mTORC1 signaling but not improved metabolism during dietary protein dilution. Mol Metab [Internet]. 2017;6(8):873–81. Available from: http://dx.doi.org/10.1016/j.molmet.2017.06.009
293. Fontana L, Cummings NE, Arriola Apelo SI, Neuman JC, Kasza I, Schmidt BA, et al. Decreased Consumption of Branched-Chain Amino Acids Improves Metabolic Health. Cell Rep [Internet]. 2016;16(2):520–30. Available from: http://dx.doi.org/10.1016/j.celrep.2016.05.092
294. Zhou M, Shao J, Wu CY, Shu L, Dong W, Liu Y, et al. Targeting BCAA catabolism to treat obesity-associated insulin resistance. Diabetes. 2019;68(9):1730–46.
295. Liu R, Li H, Fan W, Jin Q, Chao T, Wu Y, et al. Leucine supplementation differently modulates branched-chain amino acid catabolism, mitochondrial function and metabolic profiles at the different stage of insulin resistance in rats on high-fat diet. Nutrients. 2017;9(565):1–20.
296. Smith GI, Yoshino J, Stromsdorfer KL, Klein SJ, Magkos F, Reeds DN, et al. Protein ingestion induces muscle insulin resistance independent of leucine-mediated mTOR activation. Diabetes. 2015;64(5):1555–63.
297. Blomstrand E, Saltin B. BCAA intake affects protein metabolism in muscle after but not during exercise in humans. Am J Physiol - Endocrinol Metab. 2001;281(2 44-2):365–74.
298. Zhang Y, Kobayashi H, Mawatari K, Sato J, Bajotto G, Kitaura Y, et al. Effects of branched-chain amino acid supplementation on plasma concentrations of free amino acids, insulin, and energy substrates in young men. J Nutr Sci Vitaminol (Tokyo). 2011;57(1):114–7.
299. Zhang Y, Guo K, LeBlanc RE, Loh D, Schwartz GJ, Yu YH. Increasing dietary leucine intake reduces diet-induced obesity and improves glucose and cholesterol metabolism in mice via multimechanisms. Diabetes. 2007;56(6):1647–54.
300. Li H, Xu M, Lee J, He C, Xie Z. Leucine supplementation increases SIRT1 expression and prevents mitochondrial dysfunction and metabolic disorders in high-fat diet-induced obese mice. Am J Physiol - Endocrinol Metab. 2012;303(10):1234–44.
301. Bishop CA, Machate T, Henning T, Henkel J, Püschel G, Weber D, et al. Detrimental effects of branched-chain amino acids in glucose tolerance can be attributed to valine induced glucotoxicity in skeletal muscle. Nutr Diabetes. 2022;12(1):1–9.
302. Kuzuya T, Katano Y, Nakano I, Hirooka Y, Itoh A, Ishigami M, et al. Regulation of branched-chain amino acid catabolism in rat models for spontaneous type 2 diabetes mellitus. Biochem Biophys Res Commun. 2008;373(1):94–8.
303. Yu D, Richardson NE, Green CL, Spicer AB, Murphy ME, Flores V, et al. The adverse metabolic effects of branched-chain amino acids are mediated by isoleucine and valine. Cell Metab [Internet]. 2021;33(5):905-922.e6. Available from: https://doi.org/10.1016/j.cmet.2021.03.025
304. Liu S, Sun Y, Zhao R, Wang Y, Zhang W, Pang W. Isoleucine increases muscle mass through promoting myogenesis and intramyocellular fat deposition. Food Funct. 2021;12(1):144–53.
305. Essén-Gustavsson B, Blomstrand E. Effect of exercise on concentrations of free amino acids in pools of type I and type II fibres in human muscle with reduced glycogen stores. Acta Physiol Scand. 2002;174(3):275–81.
306. Xu G, Kwon G, Cruz WS, Marshall CA, McDaniel ML. Metabolic regulation by leucine of translation initiation through the mTOR-signaling pathway by pancreatic β-cells.

Diabetes. 2001;50(2):353–60.
307. Biswas D, Dao KT, Mercer A, Cowie AM, Duffley L, El Hiani Y, et al. Branched-chain ketoacid overload inhibits insulin action in the muscle. J Biol Chem [Internet]. 2020;295(46):15597–621. Available from: http://dx.doi.org/10.1074/jbc.RA120.013121
308. Avogaro A, Bier DM. Contribution of 3-hydroxyisobutyrate to the measurement of 3-hydroxybutyrate in human plasma: Comparison of enzymatic and gas-liquid chromatography-mass spectrometry assays in normal and in diabetic subjects. J Lipid Res. 1989;30(11):1811–7.
309. Jang C, Oh SF, Wada S, Rowe GC, Liu L, Chan C, et al. A branched chain amino acid metabolite drives vascular transport of fat and causes insulin resistance. Nat Med. 2016;22(4):421–6.
310. Mullen E, Ohlendieck K. Proteomic profiling of non-obese type 2 diabetic skeletal muscle. Int J Mol Med. 2010;25:445–58.
311. Helms ER, Aragon AA, Fitschen PJ. Evidence-based recommendations for natural bodybuilding contest preparation: nutrition and supplementation. J Int Soc Sports Nutr. 2014;11(20):1–20.
312. Shou J, Chen PJ, Xiao WH. The effects of BCAAs on insulin resistance in athletes. J Nutr Sci Vitaminol (Tokyo). 2019;65(5):383–9.
313. Biolo G, Tipton KD, Klein S, Wolfe RR. An abundant supply of amino acids enhances the metabolic effect of exercise on muscle protein. Am J Physiol - Endocrinol Metab. 1997;273:E122-129.
314. Fujita S, Dreyer HC, Drummond MJ, Glynn EL, Cadenas JG, Yoshizawa F, et al. Nutrient signalling in the regulation of human muscle protein synthesis. J Physiol. 2007;582:813–23.
315. Churchward-Venne TA, Burd NA, Phillips SM. Nutritional regulation of muscle protein synthesis with resistance exercise: Strategies to enhance anabolism. Nutr Metab. 2012;9(40).
316. Moore DR, Robinson MJ, Fry JL, Tang JE, Glover EI, Wilkinson SB, et al. Ingested protein dose response of muscle and albumin protein synthesis after resistance exercise in young men. Am J Clin Nutr [Internet]. 2009;89(1):161–8. Available from: http://dx.doi.org/10.3945/ajcn.2008.26401
317. Roberts LD, Boström P, O'Sullivan JF, Schinzel RT, Lewis GD, Dejam A, et al. β-Aminoisobutyric acid induces browning of white fat and hepatic β-oxidation and is inversely correlated with cardiometabolic risk factors. Vol. 19, Cell Metabolism. 2014. 96–108 p.
318. Lefort N, Glancy B, Bowen B, Willis WT, Bailowitz Z, De Filippis EA, et al. Increased reactive oxygen species production and lower abundance of complex I subunits and carnitine palmitoyltransferase 1B protein despite normal mitochondrial respiration in insulin-resistant human skeletal muscle. Diabetes. 2010;59:2444–52.
319. Shin AC, Fasshauer M, Zielinski E, Lindtner C, Scherer T, O'Hare J, et al. Brain insulin regulates systemic branch-chain amino acid levels. Diabetes. 2012;20:898–909.
320. Lotta LA, Scott RA, Sharp SJ, Burgess S, Luan J, Tillin T, et al. Genetic Predisposition to an Impaired Metabolism of the Branched-Chain Amino Acids and Risk of Type 2 Diabetes: A Mendelian Randomisation Analysis. PLoS Med. 2016;13(11):1–22.
321. Aguillard AM, Tzeng J, Ferrer I, Tam BT, Lorenzo DN. A cell-autonomous mechanism regulates BCAA catabolism in white adipocytes and systemic metabolic balance. BioRxiv.

2023;(Preprint).
322. David J, Dardevet D, Mosoni L, Savary-Auzeloux I, Polakof S. Impaired skeletal muscle branched-chain amino acids catabolism contributes to their increased circulating levels in a non-obese insulin-resistant fructose-fed rat model. Nutrients. 2019;11(2):1–13.
323. Lian K, Guo X, Wang Q, Liu Y, Wang RT, Gao C, et al. PP2Cm overexpression alleviates MI/R injury mediated by a BCAA catabolism defect and oxidative stress in diabetic mice. Eur J Pharmacol. 2020 Jan;866.
324. Burrill JS, Long EK, Reilly B, Deng Y, Armitage IM, Scherer PE, et al. Inflammation and ER stress regulate branched-chain amino acid uptake and metabolism in adipocytes. Mol Endocrinol. 2015;29(3):411–20.
325. Softic S, Stanhope KL, Boucher J, Divanovic S, Lanaspa MA, Johnson RJ, et al. Fructose and hepatic insulin resistance. Crit Rev Clin Lab Sci. 2020;57(5):308–322.
326. White PJ, McGarrah RW, Grimsrud PA, Tso SC, Yang WH, Haldeman JM, et al. The BCKDH Kinase and Phosphatase Integrate BCAA and Lipid Metabolism via Regulation of ATP-Citrate Lyase. Cell Metab [Internet]. 2018;27(6):1281-1293.e7. Available from: https://doi.org/10.1016/j.cmet.2018.04.015
327. Lerin C, Goldfine AB, Boes T, Liu M, Kasif S, Dreyfuss JM, et al. Defects in muscle branched-chain amino acid oxidation contribute to impaired lipid metabolism. Mol Metab. 2016;5(10):926–36.
328. Adams SH, Hoppel CL, Lok KH, Zhao L, Wong SW, Minkler PE, et al. Plasma acylcarnitine profiles suggest incomplete long-chain fatty acid β-oxidation and altered tricarboxylic acid cycle activity in type 2 diabetic African-American women. J Nutr. 2009;139(6):1073–81.
329. Zhao X, Zhang X, Pei J, Liu Y, Niu W, Sun H. Targeting BCAA metabolism to potentiate metformin's therapeutic efficacy in the treatment of diabetes in mice. Diabetologia [Internet]. 2023;(0123456789). Available from: https://doi.org/10.1007/s00125-023-05985-6
330. Sears B, Perry M. The role of fatty acids in insulin resistance. Lipids Health Dis [Internet]. 2015;14(1):1–9. Available from: http://dx.doi.org/10.1186/s12944-015-0123-1
331. Corkey BE, Martin-Requero A, Walajtys-Rode E, Williams RJ, Williamson JR. Regulation of the branched chain α-ketoacid pathway in liver. J Biol Chem. 1982;257(16):9668–76.
332. Hu H, Jaskiewicz JA, Harris RA. Ethanol and oleate inhibition of α-ketoisovalerate and 3-hydroxyisobutyrate metabolism by isolated hepatocytes. Arch Biochem Biophys. 1992;299:57–62.
333. Blair MC, Neinast MD, Jang C, Chu Q, Jung JW, Axsom J, et al. Branched-chain amino acid catabolism in muscle affects systemic BCAA levels but not insulin resistance. Nat Metab. 2023;5(4):589–606.
334. Nishi K, Yoshii A, Abell L, Zhou B, Frausto R, Ritterhoff J, et al. Branched-chain keto acids inhibit mitochondrial pyruvate carrier and suppress gluconeogenesis in hepatocytes. Cell Rep. 2023;42(6):112641.
335. Vanweert F, Neinast M, Tapia EE, van de Weijer T, Hoeks J, Schrauwen-Hinderling VB, et al. A randomized placebo-controlled clinical trial for pharmacological activation of BCAA catabolism in patients with type 2 diabetes. Nat Commun. 2022;13(1):1–9.
336. Rivera CN, Smith CE, Draper L V, Watne RM, Wommack AJ, Vaughan RA. Physiological 4-phenylbutyrate promotes mitochondrial biogenesis and metabolism in

C2C12 myotubes. Biochimie. 2023 Nov;(Preprint).
337. Bollinger E, Peloquin M, Libera J, Albuquerque B, Pashos E, Shipstone A, et al. BDK inhibition acts as a catabolic switch to mimic fasting and improve metabolism in mice. Mol Metab. 2022;66(October):1–17.
338. Acevedo A, Jones AE, Danna BT, Turner R, Montales KP, Reue K, et al. The BCKDK inhibitor BT2 is a chemical uncoupler that lowers mitochondrial ROS production and de novo lipogenesis. BioRxiv. 2023;(Preprint).
339. Rivera ME, Lyon ES, Vaughan RA. Effect of metformin on myotube BCAA catabolism. J Cell Biochem. 2020;121(1):816–27.
340. Shimomuras Y, Yamamoto Y, Bajotto G, Sato J, Murakami T, Shimomura N, et al. Nutraceutical Effects of Branched-Chain Amino Acids on Skeletal Muscle. J Nutr. 2006;136:525–8.
341. Shimomura Y, Murakami T, Nakai N, Nagasaki M, Harris RA. Exercise promotes BCAA catabolism: Effects of BCAA supplementation on skeletal muscle during exercise. J Nutr. 2004;134(6 SUPPL.):1583–7.
342. Dela F, Larsen JJ, Mikines KJ, Ploug T, Petersen LN. Effects of One-Legged Physical Training. 1995;44(September).
343. Houmard JA, Egan PC, Neufer PD, Friedman JE, Wheeler WS, Israel RG, et al. Elevated skeletal muscle glucose transporter levels in exercise-trained middle-aged men. Am J Physiol - Endocrinol Metab. 1991;261(4 24-4).
344. Hughes VA, Fiatarone MA, Fielding RA, Kahn BB, Ferrara CM, Shepherd P, et al. Exercise increases muscle GLUT-4 levels and insulin action in subjects with impaired glucose tolerance. Am J Physiol - Endocrinol Metab. 1993;264(6 27-6):855–62.
345. Holecek M. Branched-chain amino acids in health and disease: metabolism, alterations in blood plasma, and as supplements. Nutr Metab (Lond). 2018;15(33):1–12.
346. Xu M, Kitaura Y, Ishikawa T, Kadota Y, Terai C, Shindo D, et al. Endurance performance and energy metabolism during exercise in mice with a muscle-specific defect in the control of branched-chain amino acid catabolism. PLoS One. 2017;12(7):1–19.
347. Tso SC, Gui WJ, Wu CY, Chuang JL, Qi X, Skvorak KJ, et al. Benzothiophene carboxylate derivatives as novel allosteric inhibitors of branched-chain α-ketoacid dehydrogenase kinase. J Biol Chem. 2014;289(30):20583–93.
348. Avelar-Freitas BA, Almeida VG, Pinto MCX, Mourão FAG, Massensini AR, Martins-Filho OA, et al. Trypan blue exclusion assay by flow cytometry. Brazilian J Med Biol Res. 2014;47(4):307–15.
349. Choi YJ, Park YJ, Park JY, Jeong HO, Kim DH, Ha YM, et al. Inhibitory effect of mTOR activator MHY1485 on autophagy: Suppression of lysosomal fusion. PLoS One. 2012;7(8):e43418.
350. Lamming DW. Inhibition of the mechanistic target of rapamycin (mTOR)–Rapamycin and beyond. Cold Spring Harb Perspect Med. 2016;6(5):1–14.
351. Somwar R, Sweeney G, Ramlal T, Klip A. Stimulation of glucose and amino acid transport and activation of the insulin signaling pathways by insulin lispro in L6 skeletal muscle cells. Clin Ther. 1998;20(1):125–40.
352. Yoshida I, Sweetman L, Nyhan WL. Metabolism of branched-chain amino acids in fibroblasts from patients with maple syrup urine disease and other abnormalities of branched-chain ketoacid dehydrogenase activity. Pediatr Res. 1986;20(2):169–74.
353. Voronova V, Sokolov V, Morias Y, Boezelman MJ, Wågberg M, Henricsson M, et al.

Evaluation of therapeutic strategies targeting BCAA catabolism using a systems pharmacology model. Front Pharmacol. 2022;13(November):1–11.
354. DeFronzo RA, Tripathy D. Skeletal muscle insulin resistance is the primary defect in type 2 diabetes. Diabetes Care. 2009;32(2):S157–63.
355. Agarwal S, Bell CM, Rothbart SB, Moran RG. AMP-activated Protein Kinase (AMPK) Control of mTORC1 Is p53- and TSC2-independent in Pemetrexed-treated Carcinoma Cells. J Biol Chem. 2015;290(46):27476–86.
356. Newgard CB. Interplay between lipids and branched-chain amino acids in development of insulin resistance. Cell Metab. 2012;15(5):606–14.
357. Um SH, D'Alessio D, Thomas G. Nutrient overload, insulin resistance, and ribosomal protein S6 kinase 1, S6K1. Cell Metab. 2006;3(6):393–402.
358. Gual P, Le Marchand-Brustel Y, Tanti JF. Positive and negative regulation of insulin signaling through IRS-1 phosphorylation. Biochimie. 2005;87(1 SPEC. ISS.):99–109.
359. Ishikawa T, Kitaura Y, Kadota Y, Morishita Y, Ota M, Yamanaka F, et al. Muscle-specific deletion of BDK amplifies loss of myofibrillar protein during protein undernutrition. Sci Rep. 2017;7(November 2016):1–11.
360. Bentzinger CF, Romanino K, Cloëtta D, Lin S, Mascarenhas JB, Oliveri F, et al. Skeletal Muscle-Specific Ablation of raptor, but Not of rictor, Causes Metabolic Changes and Results in Muscle Dystrophy. Cell Metab. 2008;8(5):411–24.
361. Guridi M, Kupr B, Romanino K, Lin S, Falcetta D, Tintignac L, et al. Alterations to mTORC1 signaling in the skeletal muscle differentially affect whole-body metabolism. Skelet Muscle [Internet]. 2016;6(1):1–14. Available from: http://dx.doi.org/10.1186/s13395-016-0084-8
362. Deblon N, Bourgoin L, Veyrat-Durebex C, Peyrou M, Vinciguerra M, Caillon A, et al. Chronic mTOR inhibition by rapamycin induces muscle insulin resistance despite weight loss in rats. Br J Pharmacol. 2012;165(7):2325–40.
363. Gonano LA, Jones PP. FK506-binding proteins 12 and 12.6 (FKBPs) as regulators of cardiac Ryanodine Receptors: Insights from new functional and structural knowledge. Channels [Internet]. 2017;11(5):415–25. Available from: https://doi.org/10.1080/19336950.2017.1344799
364. Andersson DC, Marks AR. Fixing ryanodine receptor Ca2+ leak - A novel therapeutic strategy for contractile failure in heart and skeletal muscle. Drug Discov Today Dis Mech. 2010;7(2):e151–e157.
365. Uryash A, Mijares A, Lopez CE, Adams JA, Lopez JR. Chronic Elevation of Skeletal Muscle [Ca2+]i Impairs Glucose Uptake. An in Vivo and in Vitro Study. Front Physiol. 2022;13(April):1–13.
366. Liu HY, Hong T, Wen GB, Han J, Zuo D, Liu Z, et al. Increased basal level of Akt-dependent insulin signaling may be responsible for the development of insulin resistance. Am J Physiol - Endocrinol Metab. 2009;297(4):E898–E906.
367. Thong FSL, Derave W, Kiens B, Graham TE, Ursø B, Wojtaszewski JFP, et al. Caffeine-induced impairment of insulin action but not insulin signaling in human skeletal muscle is reduced by exercise. Diabetes. 2002;51(3):583–90.
368. Adegoke OAJ, Bates HE, Kiraly MA, Vranic M, Riddell MC, Marliss EB. Exercise in ZDF rats does not attenuate weight gain, but prevents hyperglycemia concurrent with modulation of amino acid metabolism and AKT/mTOR activation in skeletal muscle. Eur J Nutr [Internet]. 2015;54(5):751–9. Available from: http://dx.doi.org/10.1007/s00394-

014-0754-4
369. Op Den Kamp CM, Langen RC, Snepvangers FJ, De Theije CC, Schellekens JM, Laugs F, et al. Nuclear transcription factor κB activation and protein turnover adaptations in skeletal muscle of patients with progressive stages of lung cancer cachexia. Am J Clin Nutr. 2013;98:738–48.
370. Zheng L, Wei H, He P, Zhao S, Xiang Q, Pang J, et al. Effects of supplementation of branched-chain amino acids to reduced-protein diet on skeletal muscle protein synthesis and degradation in the fed and fasted states in a piglet model. Nutrients. 2017;9(1):1–18.
371. Blachier F, Blais A, Elango R, Saito K, Shimomura Y, Kadowaki M, et al. Tolerable amounts of amino acids for human supplementation: summary and lessons from published peer-reviewed studies. Amino Acids [Internet]. 2021;53(9):1313–28. Available from: https://doi.org/10.1007/s00726-021-03054-z
372. Dubuisson C, Lioret S, Touvier M, Dufour A, Calamassi-Tran G, Volatier JL, et al. Trends in food and nutritional intakes of French adults from 1999 to 2007: Results from the INCA surveys. Br J Nutr. 2010;103(7):1035–48.
373. Pasiakos SM, Agarwal S, Lieberman HR, Fulgoni VL. Sources and amounts of animal, dairy, and plant protein intake of US adults in 2007–2010. Nutrients. 2015;7(8):7058–69.
374. Hutson SM, Sweatt AJ, Lanoue KF. Branched-Chain Amino Acid Metabolism: Implications for Establishing Safe Intakes. J Nutr. 2005;135(5):1557–64.
375. Serino AS, Adegoke OA, Zargar S, Gordon CS, Szigiato AA, Hawke TJ, et al. Voluntary physical activity and leucine correct impairments in muscle protein synthesis in partially pancreatectomised rats. Diabetologia. 2011;54(12):3111–20.
376. Mann G, Mora S, Madu G, Adegoke OAJ. Branched-chain Amino Acids: Catabolism in Skeletal Muscle and Implications for Muscle and Whole-body Metabolism. Front Physiol. 2021;12:1–25.
377. Karwi QG, Lopaschuk GD. Branched-Chain Amino Acid Metabolism in the Failing Heart. Cardiovasc Drugs Ther. 2023;37(2):413–20.
378. Churchward-Venne TA, Breen L, Di Donato DM, Hector AJ, Mitchell CJ, Moore DR, et al. Leucine supplementation of a low-protein mixed macronutrient beverage enhances myofibrillar protein synthesis in young men: A double-blind, randomized trial1-3. Am J Clin Nutr. 2014;99(2):276–86.
379. Rowlands DS, Nelson AR, Phillips SM, Faulkner JA, Clarke J, Burd NA, et al. Protein-leucine fed dose effects on muscle protein synthesis after endurance exercise. Med Sci Sports Exerc. 2014;47(3):547–55.
380. Steinert RE, Landrock MF, Ullrich SS, Standfield S, Otto B, Horowitz M, et al. Effects of intraduodenal infusion of the branched-chain amino acid leucine on ad libitum eating, gut motor and hormone functions, and glycemia in healthy men. Am J Clin Nutr. 2015;102(4):820–7.
381. Monti LD, Galluccio E, Fontana B, Spadoni S, Comola M, Marrocco Trischitta MM, et al. Pharmacogenetic influence of eNOS gene variant on endothelial and glucose metabolism responses to L-arginine supplementation: Post hoc analysis of the L-arginine trial. Metabolism. 2015;64:1582–91.
382. She P, Olson KC, Kadota Y, Inukai A, Shimomura Y, Hoppel CL, et al. Leucine and Protein Metabolism in Obese Zucker Rats. PLoS One. 2013;8(3).
383. Zhou Y, Jetton TL, Goshorn S, Lynch CJ, She P. Transamination is required for α-ketoisocaproate but not leucine to stimulate insulin secretion. J Biol Chem.

2010;285(44):33718–26.
384. Meredith M, Rabaglia ME, Metz SA. Evidence of a role for GTP in the potentiation of Ca2+-induced insulin secretion by glucose in intact rat islets. J Clin Invest. 1995;96(2):811–21.
385. Yang J, Dolinger M, Ritaccio G, Mazurkiewicz J, Conti D, Zhu X, et al. Leucine stimulates insulin secretion via down-regulation of surface expression of adrenergic α2A receptor through the mTOR (mammalian target of rapamycin) pathway: Implication in new-onset diabetes in renal transplantation. J Biol Chem. 2012;287(29):24795–806.
386. Knuth ER, Foster HR, Jin E, Merrins MJ. Leucine suppresses glucagon secretion from pancreatic islets by directly modulating α-cell cAMP. bioRxiv. 2023;preprint.
387. Zhang Y, Guo K, LeBlanc RE, Loh D, Schwartz GJ, Yu YH. Increasing dietary leucine intake reduces diet-induced obesity and improves glucose and cholesterol metabolism in mice via multimechanisms. Diabetes. 2007;56(6):1647–54.
388. Um SH, Frigerio F, Watanabe M, Picard F, Joaquin M, Sticker M, et al. Absence of S6K1 protects against age- and diet-induced obesity while enhancing insulin sensitivity. Nature. 2004;431(7005):200–5.
389. Sanchez B, Li J, Bragos R, Rutkove SB. Differentiation of the intracellular structure of slow- versus fast-twitch muscle fibers through evaluation of the dielectric properties of tissue. Phys Med Biol. 2014;59(10):2369–238.
390. Silva LS, Poschet G, Nonnenmacher Y, Becker HM, Sapcariu S, Gaupel A, et al. Branched-chain ketoacids secreted by glioblastoma cells via MCT 1 modulate macrophage phenotype . EMBO Rep. 2017;18(12):2172–85.
391. Weber FL, Deak SB, Laine RA. Absorption of Keto-Analogues of Branched-Chain Amino Acids from Rat Small Intestine. Gastroenterology. 1979;76(1):62–70.
392. Sugita M, Sugita H, Kaneki M. Increased insulin receptor substrate 1 serine phosphorylation and stress-activated protein kinase/c-Jun N-terminal kinase activation associated with vascular insulin resistance in spontaneously hypertensive rats. Hypertension. 2004;44(4):484–9.
393. Herman MA, She P, Peroni OD, Lynch CJ, Kahn BB. Adipose tissue Branched Chain Amino Acid (BCAA) metabolism modulates circulating BCAA levels. J Biol Chem. 2010;285(15):11348–56.
394. Cano NJM, Fouque D, Leverve XM. Application of branched-chain amino acids in human pathological states: Renal failure. J Nutr. 2006;136(1):299–307.
395. Holecek M, Kandar R, Sispera L, Kovarik M. Acute hyperammonemia activates branched-chain amino acid catabolism and decreases their extracellular concentrations: Different sensitivity of red and white muscle. Amino Acids. 2011;40(2):575–84.
396. Tajiri K, Shimizu Y. Branched-chain amino acids in liver diseases. Vol. 3, World Journal of Gastroenterology. 2018. p. 47.
397. Blackburn PR, Gass JM, Pinto e Vairo F, Farnham KM, Atwal HK, Macklin S, et al. Maple syrup urine disease: Mechanisms and management. Appl Clin Genet. 2017;10:57–66.
398. Xu J, Jakher Y, Ahrens-Nicklas RC. Brain branched-chain amino acids in maple syrup urine disease: Implications for neurological disorders. Int J Mol Sci. 2020;21(20):1–18.
399. Mora S, Mann G, Adegoke OAJ. Sex-related Differences in Cachexia Outcomes and Branched-Chain Amino Acid Metabolism following Chemotherapy in Old Animals. 2023;
400. Cash AD, Aliev G, Siedlak SL, Nunomura A, Fujioka H, Zhu X, et al. Microtubule

reduction in Alzheimer's disease and aging is independent of τ filament formation. Am J Pathol. 2003;162(5):1623–7.
401. Tsuji S, Koyama S, Taniguchi R, Fujiwara T, Fujiwara H, Sato Y. Association of Serum Amino Acid Concentration With Loss of Skeletal Muscle Mass After 1 Year in Cardiac Rehabilitation Center Patients. Circ Reports. 2019;1(10):456–61.
402. Uddin GM, Zhang L, Shah S, Fukushima A, Wagg CS, Gopal K, et al. Impaired Branched Chain Amino Acid Oxidation Contributes to Cardiac Insulin Resistance in Heart Failure. Cardiovasc Diabetol [Internet]. 2019;1–12. Available from: https://doi.org/10.1186/s12933-019-0892-3
403. Chaleckis R, Murakami I, Takada J, Kondoh H, Yanagida M. Individual variability in human blood Metabolites identifies age-related differences. Proc Natl Acad Sci U S A. 2016;113(16):4252–9.
404. Seo C, Hwang YH, Kim Y, Joo BS, Yee ST, Kim CM, et al. Metabolomic study of aging in mouse plasma by gas chromatography-mass spectrometry. J Chromatogr B Anal Technol Biomed Life Sci [Internet]. 2016;1025:1–6. Available from: http://dx.doi.org/10.1016/j.jchromb.2016.04.052
405. Houtkooper RH, Argmann C, Houten SM, Canto C, Jeninga EH, Andreux Ṕeńelope A., et al. The metabolic footprint of aging in mice. Sci Rep. 2011;1.
406. Wysokiński A, Sobów T, Kłoszewska I, Kostka T. Mechanisms of the anorexia of aging—a review. Age (Omaha). 2015;37(4).
407. Zhang Y, Zhou Q, Yang R, Hu C, Huang Z, Zheng C, et al. Serum branched-chain amino acids are associated with leukocyte telomere length and frailty based on residents from Guangxi longevity county. Sci Rep [Internet]. 2020;10(1):1–8. Available from: http://dx.doi.org/10.1038/s41598-020-67010-9
408. Juricic P, Grönke S, Partridge L. Branched-chain amino acids have equivalent effects to other essential amino acids on lifespan and aging-related traits in drosophila. Journals Gerontol - Ser A Biol Sci Med Sci. 2020;75(1):24–31.
409. Selman C, Tullet JMA, Wieser D, Irvine E, Lingard SJ, Choudhury AI, et al. Ribosomal protein S6 kinase 1 signaling regulates mammalian life span. Science (80-). 2009;326(5949):140–4.
410. Cuthbertson D, Smith K, Babraj J, Leese G, Waddell T, Atherton P, et al. Anabolic signaling deficits underlie amino acid resistance of wasting, aging muscle. FASEB J. 2005;19(3):1–20.
411. Volpi E, Sheffield-Moore M, Rasmussen BB, Wolfe RR. Basal muscle amino acid kinetics and protein synthesis in healthy young and older men. JAMA. 2001;286(10):1206–12.
412. Volpi E, Mittendorfer B, Wolf SE, Wolfe RR. Oral amino acids stimulate muscle protein anabolism in the elderly despite higher first-pass splanchnic extraction. Am J Physiol - Endocrinol Metab. 1999;277(3 40-3):513–20.
413. Balagopal P, Rooyackers OE, Adey DB, Ades PA, Nair KS. Effects of aging on in vivo synthesis of skeletal muscle myosin heavy- chain and sarcoplasmic protein in humans. Am J Physiol - Endocrinol Metab. 1997;273(4):E790-800.
414. Welle S, Thornton C, Jozefowicz R, Statt M. Myofibrillar protein synthesis in young and old men. Am J Physiol - Endocrinol Metab. 1993;264:E693-8.
415. Raue U, Slivka D, Jemiolo B, Hollon C, Trappe S. Proteolytic gene expression differs at rest and after resistance exercise between young and old women. Journals Gerontol - Ser

A Biol Sci Med Sci. 2007;62(12):1407–12.
416. Edström E, Altun M, Hägglund M, Ulfhake B. Atrogin-1/MAFbx and MuRF1 are downregulated in aging-related loss of skeletal muscle. Journals Gerontol - Ser A Biol Sci Med Sci. 2006;61(7):663–74.
417. Welle S, Brooks AI, Delehanty JM, Needler N, Thornton CA. Gene expression profile of aging in human muscle. Physiol Genomics. 2003;14:149–59.
418. Ferrucci L, Fabbri E. Inflammageing: chronic inflammation in ageing, cardiovascular disease, and frailty. Physiol Behav. 2018;15(9):505–22.
419. Petry ÉR, Dresch D de F, Carvalho C, Medeiros PC, Rosa TG, de Oliveira CM, et al. Oral glutamine supplementation attenuates inflammation and oxidative stress-mediated skeletal muscle protein content degradation in immobilized rats: Role of 70 kDa heat shock protein. Free Radic Biol Med [Internet]. 2019;145(September):87–102. Available from: https://doi.org/10.1016/j.freeradbiomed.2019.08.033
420. Rogeri PS, Gasparini SO, Martins GL, Costa LKF, Araujo CC, Lugaresi R, et al. Crosstalk Between Skeletal Muscle and Immune System: Which Roles Do IL-6 and Glutamine Play? Front Physiol. 2020;11(October):1–11.
421. Nicastro H, Da Luz CR, Chaves DFS, Bechara LRG, Voltarelli VA, Rogero MME, et al. Does branched-chain amino acids supplementation modulate skeletal muscle remodeling through inflammation modulation? Possible mechanisms of action. J Nutr Metab. 2012;2012:136937.
422. Spendiff S, Vuda M, Gouspillou G, Aare S, Perez A, Morais JA, et al. Denervation drives mitochondrial dysfunction in skeletal muscle of octogenarians. J Physiol. 2016;594(24):7361–79.
423. Picard M, Ritchie D, Thomas MM, Wright KJ, Hepple RT. Alterations in intrinsic mitochondrial function with aging are fiber type-specific and do not explain differential atrophy between muscles. Aging Cell. 2011;10(6):1047–55.
424. Mathieu-Costello O, Ju Y, Trejo-Morales M, Cui L. Greater capillary-fiber interface per fiber mitochondrial volume in skeletal muscles of old rats. J Appl Physiol. 2005;99(1):281–9.
425. Han HS, Ahn E, Park ES, Huh T, Choi S, Kwon Y, et al. Impaired BCAA catabolism in adipose tissues promotes age-associated metabolic derangement. Nat Aging. 2023;3:982–1000.
426. Obas V, Vasan RS. The aging heart. Clin Sci. 2018;132(13):1367–82.
427. Cowie CC, Rust KF, Ford ES, Eberhardt MS, Byrd-Holt DD, Li C, et al. Full accounting of diabetes and pre-diabetes in the U.S. population in 1988-1994 and 2005-2006. Diabetes Care. 2009;32(2):287–94.
428. Chambers J, Elliott P, Scott J, Kooner J. Physical activity and risk of type 2 diabetes in UK Indian Asian and Northern European subjects in the London Life Sciences Population (LOLIPOP) study. In: 79th Annual Scientific Session of the American-Heart-Association. 2006. p. 894–5.
429. Amati F, Dubé JJ, Coen PM, Stefanovic-Racic M, Toledo FGS, Goodpaster BH. Physical inactivity and obesity underlie the insulin resistance of aging. Diabetes Care. 2009;32(8):1547–9.
430. Short KR, Vittone JL, Bigelow ML, Proctor DN, Rizza RA, Coenen-Schimke JM, et al. Impact of aerobic exercise training on age-related changes in insulin sensitivity and muscle oxidative capacity. Diabetes. 2003;52(8):1888–96.

431. Volpi E, Nazemi R, Fujita S. Muscle tissue changes with aging. Curr Opin Clin Nutr Metab Care. 2004;7(4):405–10.
432. Sonjak V, Jacob KJ, Spendiff S, Vuda M, Perez A, Miguez K, et al. Reduced Mitochondrial Content, Elevated Reactive Oxygen Species, and Modulation by Denervation in Skeletal Muscle of Prefrail or Frail Elderly Women. Journals Gerontol - Ser A Biol Sci Med Sci. 2019;74(12):1887–95.
433. Pasiakos SM. Metabolic advantages of higher protein diets and benefits of dairy foods on weight management, glycemic regulation, and bone. J Food Sci. 2015;80(S1):A2–7.
434. Lopaschuk GD. Fatty Acid Oxidation and Its Relation with Insulin Resistance and Associated Disorders. Ann Nutr Metab. 2016;68:15–20.
435. Basso AD, Solit DB, Chiosis G, Giri B, Tsichlis P, Rosen N. Akt forms an intracellular complex with heat shock protein 90 (Hsp90) and Cdc37 and is destabilized by inhibitors of Hsp90 function. J Biol Chem [Internet]. 2002;277(42):39858–66. Available from: http://dx.doi.org/10.1074/jbc.M206322200
436. Potashnik R, Bloch-Damti A, Bashan N, Rudich A. IRS1 degradation and increased serine phosphorylation cannot predict the degree of metabolic insulin resistance induced by oxidative stress. Diabetologia. 2003;46(5):639–48.
437. Nikolov EN, Dabeva MD, Nikolov TK. Turnover of ribosomes in regenerating rat liver. Int J Biochem. 1983;15(10):1255–60.
438. Voelzmann A, Hahn I, Pearce SP, Sánchez-Soriano N, Prokop A. A conceptual view at microtubule plus end dynamics in neuronal axons. Brain Res Bull [Internet]. 2016;126:226–37. Available from: http://dx.doi.org/10.1016/j.brainresbull.2016.08.006
439. Flurkey K, Currer JM, Harrison DE. Mouse Models in Aging Research. In: The Mouse in Biomedical Research. 2007. p. 637–672.
440. Mann G, Riddell MC, Adegoke OAJ. Effects of Acute Muscle Contraction on the Key Molecules in Insulin and Akt Signaling in Skeletal Muscle in Health and in Insulin Resistant States. Diabetology. 2022;3(3):423–46.

Appendix A) Cell Treatment: BT2 experiments

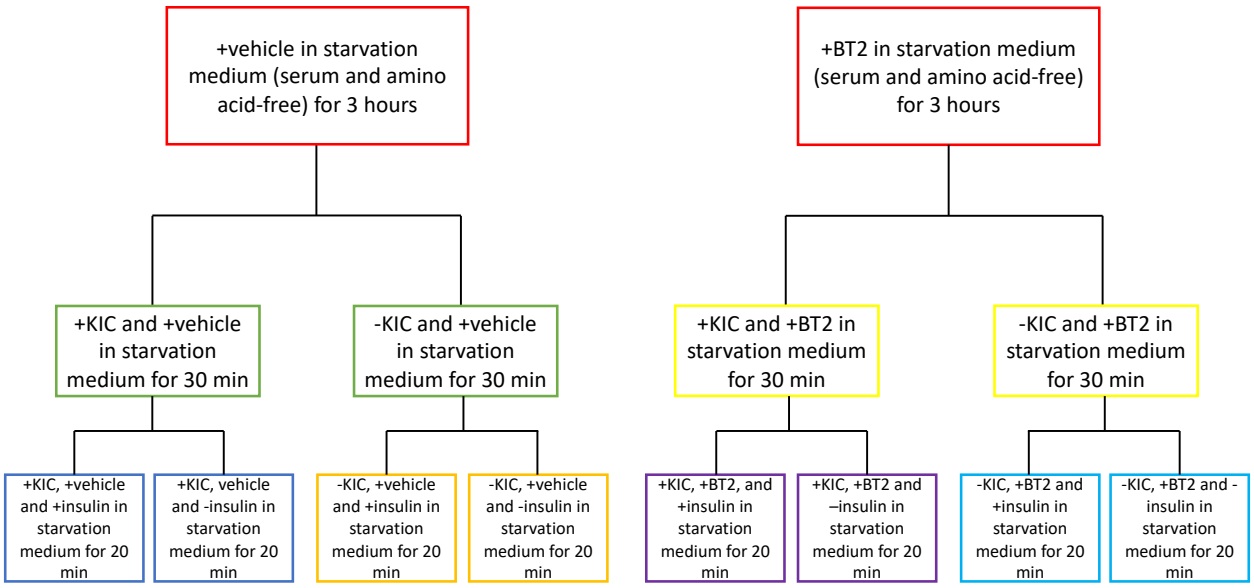

Supplementary Figure 1: Experimental design of experiments with BT2, KIC and insulin On day 5 of differentiation, myotubes were incubated with or without BT2 for three hours in starvation medium (serum and amino acid-free medium). They were then incubated in starvation medium with or without KIC for 30 minutes. Following this, myotubes were incubated with or without insulin for 20 minutes.

Appendix B) Cell Treatment: mTORC1 activation experiments (Fig 4.9)

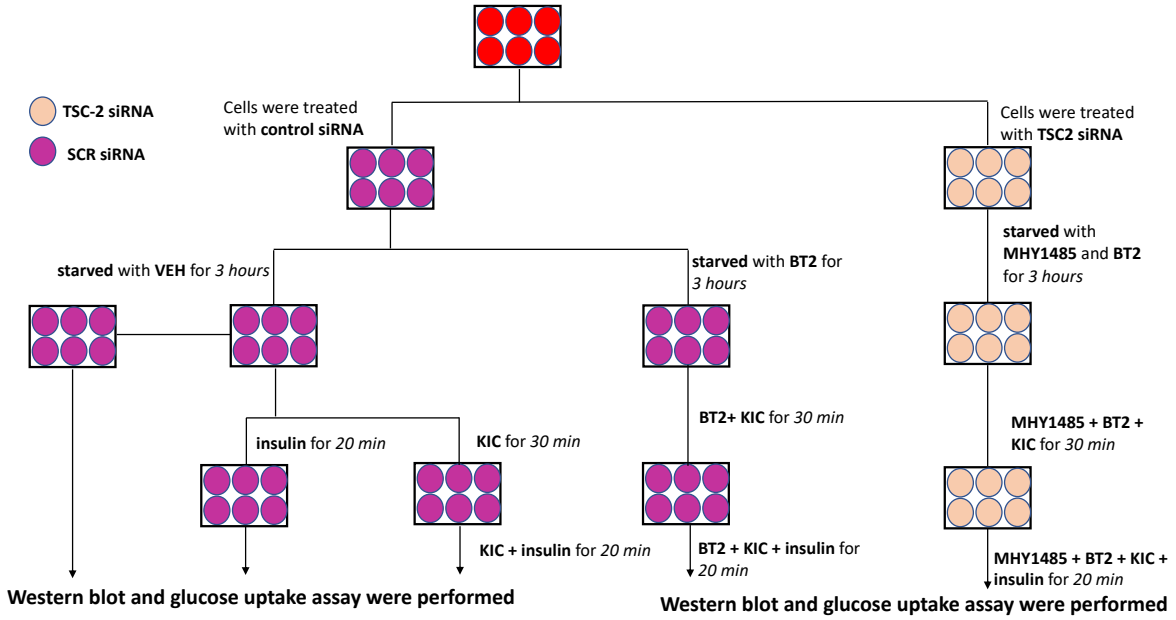

Supplementary Figure 2: mTORC1 reactivation experimental design.
On day 3 of differentiation, myotubes were transfected with SCR (control) or TSC-2 siRNA oligonucleotides. On day 5 of differentiation, myotubes were incubated with or without MHY1485 and BT2 for three hours in starvation medium (serum and amino acid-free medium). They were then incubated in starvation medium with or without KIC for 30 minutes. Following this, myotubes were incubated with or without insulin for 20 minutes.

Appendix C) Cell Treatment: Rapamycin experiments (Fig 4.10)

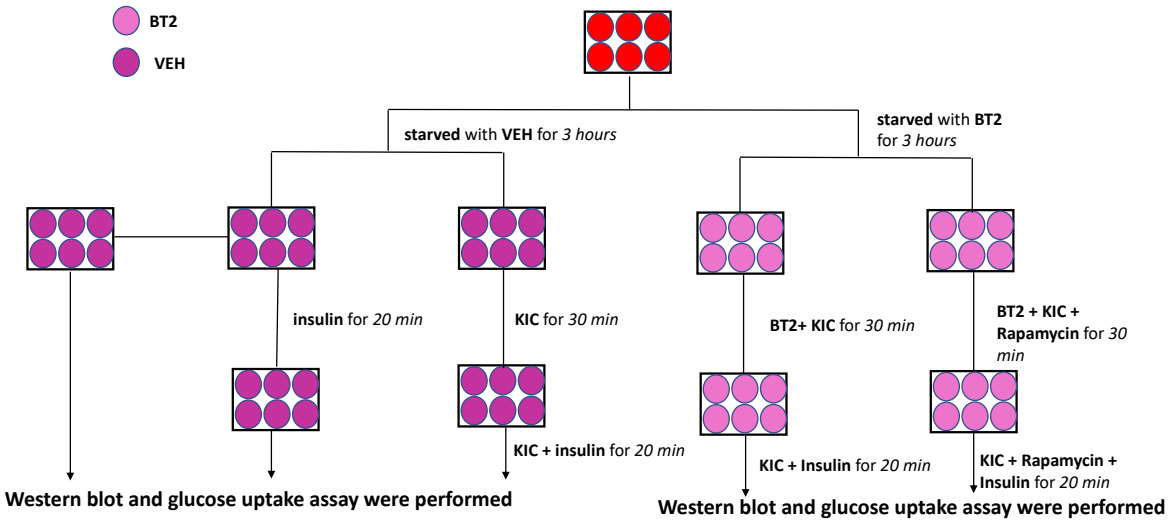

Supplementary Figure 3: mTORC1 inhibition experimental design.
On day 5 of differentiation, myotubes were incubated with or without BT2 for three hours in starvation medium (serum and amino acid-free medium). They were then incubated in starvation medium with or without KIC and rapamycin for 30 minutes. Following this, myotubes were incubated with or without insulin for 20 minutes.

Appendix D) Glucose Transport Assay

Materials and Methods

HEPES Buffer Saline:
• 140 mM NaCl (Wisent, #600-082-LG)
• 20 mM HEPES-Na, pH 7.4 (Research Organics, #6003H)
• 5mM KCl (Fisher Scientific, #M-12445)
• 2.5 mM MgSO4 (Bioshop, #10034-99-8)
• 1.0 mM CaCl2 (Bioshop, #10035-04-8)

Stop Solution:
• 0.9% NaCl (Saline) (Wisent, #600-082-LG)

2-DG Stock Solution:
• 10 mM 2-Deoxy-D-Glucose (Sigma Aldrich, #D8375) in HEPES buffer

Transport Solution:
Prepare in HEPES buffer
10 μM 2-Deoxy-Glucose (Sigma Aldrich, #D8375)
0.5 μCi/mL H3 2-Deoxy-Glucose (Perkin Elmer, #NET549250UCI)

Glucose Uptake Procedure

1. On the designated radioactive bench in the lab, wash L6 myotubes in 12 well plates two times with 400 μL of 37^{o}C HEPES buffer and aspirate any remaining buffer.
2. Add 300 μL of room temperature Transport Solution per well for a 12-well plate.
3. Incubate the plates for 5 minutes at 37°. Be sure to not exceed this time.
4. Aspirate away the Transport Solution quickly and wash the wells thoroughly three times with 1 mL of ice-cold Stop Solution (0.9% Saline) while on ice. Aspirate to dryness.
5. While on ice, add 1 mL of ice-cold 0.05 M NaOH to each well in the plate.
6. Scrape the cells and transfer 0.8 mL of the contents into scintillation vials already filled with 3.5 mL of scintillation fluid.
7. Transfer the remaining contents into 1.5 mL Eppendorf tubes (to be used for protein assay).
8. Count the amount of radioactivity in each vial using the scintillation counter.
9. Adjust amount of radioactivity in each vial to respective sample's protein content.

Appendix E) *In Vitro* BCKD Activity Assay

Materials and Methods

- 6-well culture plate (Greiner Bio-one, #657165)
- Clear tape
- Filter paper wicks (1.3cm x 2cm) (VWR, #28298-020)
- 2 M NaOH
- Heat Incubator-Shaker
    - Differentiation Medium (DM) (AMEM (Wisent Inc. Cat #310-010-CL) supplemented with 2% horse serum (Gibco, 26050-088) and 1% Ab-Am (Wisent Inc., #450-115-EL))
- Krebs Ringer Phosphate Buffer (KRB)
    - 0.018M $NaHPO_4$ (made from sodium phosphate dibasic (BioShop, #SPD307) and sodium phosphate monobasic (BioShop, #SPM306)).
    - 0.68% (w/v) NaCl (BioShop, #SOD004)
    - 0.045% (w/v) KCl (BioShop, #POC999)
    - 0.03% (w/v) $MgSO_4$ (BioShop, #MAG513)
- 1 mg of thiamine hydrochloride/well (working dilution: 1 mg per 856µl of KRB = 14mg per 12ml of KRB). Thiamine pyrophosphate binding to BCKD is required for the oxidative decarboxylation reaction to take place (376).

- Reaction Mixture (working volume, 1ml (936.65 µL PBS, 43.35 µL valine (50 mg/mL stock), 20 µL 1-^{14}C labelled valine). We used valine instead of leucine, as valine-derived KIV is the preferred substrate for BCKD (352).
    - Phosphate Buffer Saline (Wisent, #311-010-CL)
    - Valine 50 mg/mL mixture (Sigma Aldrich, #V0513)
    - U-^{14}C labelled valine (American radiolabelled chemicals, #ARC0678)
- Lysis Buffer

BCKD Activity Assay Procedure

1. Inside the sterile hood aspirate medium from all the wells (6-well plate) and replenish with 200 µL/well of starvation medium. The starvation media contains vitamin B6, an important cofactor in the BCAT2 reaction, as valine needs to be transaminated to KIV, so it can be oxidatively decarboxylated by BCKD.
2. Add 1 mg of thiamine hydrochloride (Sigma Aldrich, #T1270) per 856 µL of **KRB.**
3. Move to radioactive bench in lab, immediately add 856 µL of KRB to each well
4. Add 61 µL (0.12 µCi) of **Reaction Mixture**/well.
5. Administer 60 µL of 2M NaOH to each filter paper wick, while they are anchored in place to the clear strip of tape.
6. Place clear tape (mounted with filter paper wicks) across desired wells, ensuring wicks are centralized on all wells (Supplementary Figure 4A-D).
7. Start to apply additional strips of clear tape, covering the remaining gaps and ensuring that each well is sealed.

8. Place 6-well plate lid over top of the taped plate and tape the lid down.
9. Place plate in heat incubator-shaker for 1 hour at 50 rpm and at 37.1°C.
10. After 1 hour incubation, remove plate from heat incubator-shaker and bring to radiation bench. Using a small set of scissors, make an incision in the clear tape, just along the inside perimeter of the plate, and cut along the perimeter line along three sides (Supplementary Figure 5A-C).
11. Peel back the tape, and using clean tweezers grab the wicks (Supplementary Figure 5D) and put them in the respective labelled scintillation vials filled with 3.5 mL of scintillation fluid.
12. Aspirate the contents of each well, then rinse with PBS.
13. Then add 100ul/well of lysis buffer.
14. Harvest cells following typical cell harvesting protocol.

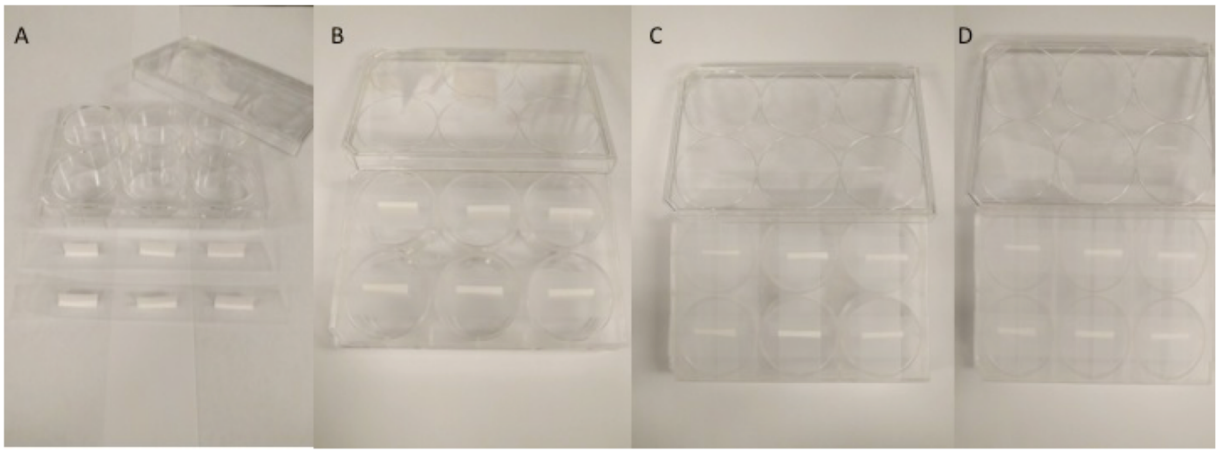

Supplementary Figure 4: Images of *In Vitro* BCKD Assay Set Up

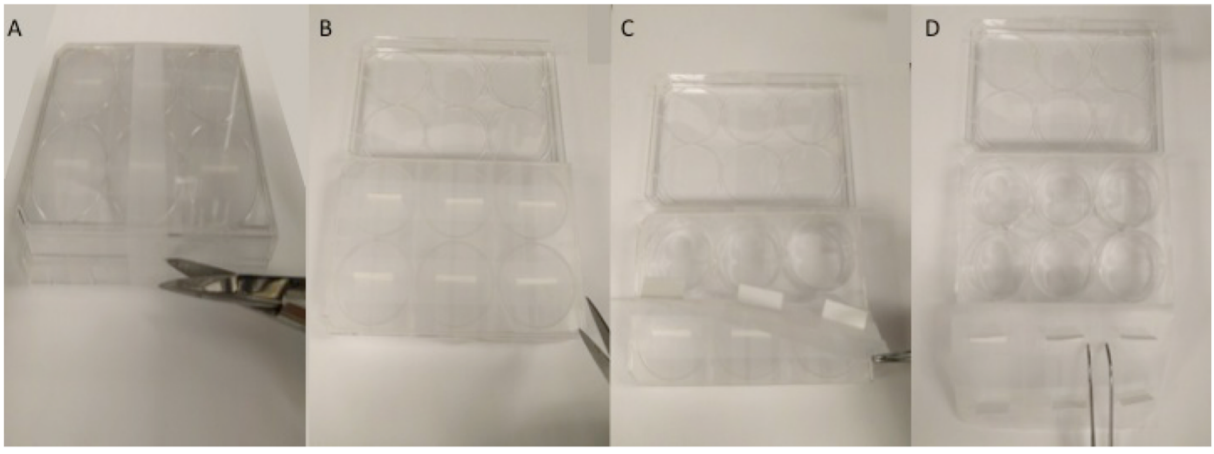

Supplementary Figure 5: Images of *In Vitro* BCKD Assay wick removal

Supplementary Figures 4 and 5 were taken from reference (242).

Appendix F) Ex Vivo BCKD Activity Assay

Materials

- Buffer 1
    - Potassium phosphate buffer (KPi) (30mM, pH 7.5). KPi is made from potassium phosphate dibasic (K_2HPO_4 salt) (BioShop, PPD555.1) and potassium phosphate monobasic (KH_2PO_4 salt) (BioShop, PPM302.1)
    - EDTA (3mM)
    - DTT (5mM) (Research Organics, #2190D-A101X)
    - Valine (1mM) (Sigma Aldrich, V0513)
    - FBS (3%) (Gibco, #12483-020)
    - Triton X-100 (5%) (MP Biomedicals, LLC, #M2528)
    - Leupeptin (1 μM) (Sigma Aldrich, #L2884)

- Buffer 2
    - HEPES (50 mM) (Research Organics, #6003H)
    - KPi (30 mM)
    - CoA (0.4 mM) (Sigma Aldrich, #4282)
    - NAD+ (3 mM) (Sigma Aldrich, #N0632)
    - FBS (5%)
    - Thiamine (2 mM) (Sigma Aldrich, #T1270)
    - Magnesium $Chloride_2$ (2 mM) (Sigma Aldrich, 7786-30-3)
    - Radiolabeled U-^{14}C-Valine (7.8 μM) (American radiolabelled chemicals, #ARC0678)

Procedure

Potassium Phosphate Buffer (KPi)

1. Make KPI Buffer (Making 100 mL) – 30 mM
    i. Start with 80 mL of ddH_2O in the 200 mL sized beaker.
    ii. Add 107.96 mg of m potassium phosphate monobasic.
    iii. Add 384.37 6mg of potassium phosphate dibasic.
    iv. pH to 7.5
2. Make the Buffer 1 (Make 25 mL)
3. Add 15mL of the newly made KPI buffer into a new 50 mL tube.
4. Add 150 μL of 0.5 M EDTA into the solution (3 mM)
5. Add 125 μL of 1 M DTT into the solution (5 mM)
6. In the -20 freezer, there is a valine stock that is 169014uM (25mg of valine per 1ml of ddH_2O). Grab that and add 147.92uL into the solution (1 mM)
7. Add 750uL of FBS into the solution (3%)
8. Add 1250uL of Triton X-100 into the solution (5%)

9. In the -20°C freezer grab the leupeptin, there is a main stock of 10 mM and an Eppendorf tube that is diluted to 2.1 mM. Using the Eppendorf tube (2.1 mM), add 11.9uL into the solution (1 μM).
10. Now top off the rest of the solution to make it 25 mL. Add 7565 μL of the KPI buffer we made **(remember this is made in ddH_2O. But remember we used 40uL of acid to pH, so we really add 7525 μL of KPI buffer)**
11. Store at 4°C fridge.

Buffer 2

1. Now Make Buffer 2 (Make 30 mL)
2. Add 15 mL of KPi buffer made above.
3. Add 357.5 mg of HEPES into the solution (50 mM)
4. Add 9.2 mg of Coenzyme A into the solution (0.4 mM)
5. Add 1.5 mL of Fetal bovine serum into the solution (5%)
6. Add 20.24 mg of Thiamine into the solution (2mM)
7. Add 12.2 mg of $MgCl_2$ into the solution (3mM)
8. Add 61.75 mg of NAD+ into the solution (3mM)
9. Top up the solution to 20mLs for now. The day you use this buffer, you must add radioactivate valine (7.8 μM) and the remaining KPI buffer. This equated to 0.16 μL per sample.

Once Buffer 1 and 2 are made.

12. Homogenize ~35mg of tissue sample with homogenizer (PRO200) at max speed in 250μL of ice-cold Buffer 1 for 30 seconds in 15mL homogenization tubes bought from stores (these are too long for the homogenizer, must cut some off at the top).
13. Centrifuge the homogenized sample for 10 minutes at 10000 g at 4°C.
14. Remove 50 μL of supernatant and add to 300μL of Buffer 2 in a 1.5mL Eppendorf tube.
15. Administer 60 μl of 2 M NaOH to each filter paper wick (VWR, 28298-020).
16. Tape the raised 2 M NaOH wick (blotting paper, VWR, 28298-020) attached to the inside of the lid of the Eppendorf tube, cap the tube, and tightly tape the seal shut to ensure no CO_2 escapes.
17. Place samples in a non-shaking incubator at 37.1°C for 30 minutes.
18. The $^{14}CO_2$ released from the BCKD reaction binds to the NaOH on the wick, forming $NaHCO_3$ (Supplementary Figure 6). This wick is then placed in a scintillation vial with 3.5 mL of scintillation fluid. This is read by a scintillation counter.
19. 50 μL of the solution from the Eppendorf tube is added to a scintillation vial with 3.5 mL of scintillation fluid. This is read by a scintillation counter (total radioactivity)
20. The remaining solution in the Eppendorf tube is used to determine protein concentration.

21. The radioactivity reading from the wick is divided by the radioactivity reading of the solution (total radioactivity) and the protein concentration.

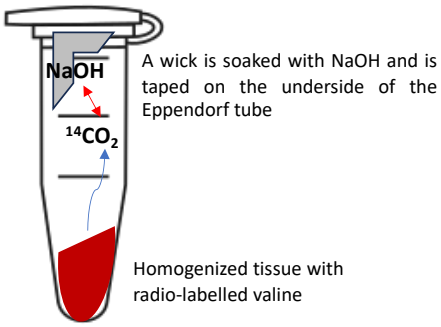

Supplementary Figure 6: Depiction of Ex Vivo BCKD Assay Set up

Appendix G) High Pressure Liquid Chromatography (HPLC) BCAA Protocol

1.0 Materials:

- Column (YMC-Triart 75 mm x 3.0 mm OD x 1.9 μm particle size)
- Metal Ferrule (IDEX health & science, #VHP-321)
- Metal tubing (IDEX Health & Science, #U-154)
- Vials and lids (Supelco, #27080-U)
- Vial Inserts (Supelco, #24716)
- Phthaldialdehyde solution (**OPA**) – keep on ice.
    - Phthaldialdehyde salt (Sigma Aldrich, #P1378)
    - HPLC grade methanol (Fisher Chemical, #A-4524)
    - Brij 35 (Sigma Aldrich, #B4184)
    - 2-mercaptoethanol (Sigma Aldrich, #M6250)
    - 0.04 M sodium borate buffer
- Micropipette (20-200μL) and tips (20-200μL)
- Samples (keep on ice)
- Saturated Potassium Borate Buffer (30 g of potassium borate into 800 mL of ddH_2O, bring up to 1L, then add potassium borate until no more will dissolve)
- Standards (made from Sigma Aldrich, #AAS18)
- Phosphate buffered saline (PBS, Wisent Inc, #311-010-CL))
- 10% Trichloroacetic Acid (TCA)
- 0.1N hydrochloric acid (HCl)
- Sodium hydroxide (NaOH)
- Buffer A (made in 1 L glass bottles in lab)
    - Potassium phosphate dibasic (K_2HPO_4 salt) (BioShop, PPD555.1)
    - Potassium phosphate monobasic (KH_2PO_4 salt) (BioShop, PPM302.1)
    - ddH_2O
- Buffer B (made in 1 L glass bottles in lab)
    - HPLC grade methanol (Fisher Chemical, #A-4524)
    - HPLC grade acetonitrile (Sigma, Aldrich, #34998)
    - ddH_2O

OPA (would recommend using it in the same week it was made):
To make 5 mL (only need 20ul per sample) – ***make it in a 15mL test tube wrapped with aluminum foil as OPA is sensitive to light.***
1. Add 0.02g of OPA in 500 μL methanol (HPLC grade, found at stores)
2. Add 120ul of Brij 35
3. Add 20μL of 2-mercaptoethanol
4. Add 4.48mL of 0.04M Sodium borate buffer (15.234g of sodium borate in 900mL of ddH_2O, and then adjust to pH 9.5 with sodium hydroxide (NaOH)/hydrochloric acid (HCl) with pH reading machine in the lab and bring up to 1L).

Buffer A: 20mmol/L (potassium) phosphate buffer (pH 6.5)

Required components.

Component	Mass	Molarity
K_2HPO_4 (mw: 174.2 g/mol)	1.175 g	0.0067 M
KH_2PO_4 (mw: 136.086 g/mol)	1.804 g	0.0133 M

1. Prepare 800 mL of ddH_2O in a suitable container.
2. Add 1.175 g of K_2HPO_4 to the solution.
3. Add 1.804 g of KH_2PO_4 to the solution.
4. Add ddH_2O until volume is 1 L.

Buffer B: HPLC-grade Acetonitrile/HPLC-grade Methanol/Water = 45%/40%/15%(v/v/v)

2.0 Sample/Standard Preparation:

1. **Cell Harvesting**
   - Wash myotubes in 6-well plates twice with 2 mL PBS
   - Harvest cells with 250 µL of 10% TCA (dilute from stock: #196057 from Millipore)
   - Mix up and down with micropipette to break down cell suspension.

2. **Sample Preparation**
   - Centrifuge lysate at 2.3g for 15 minutes in 4°C
   - Next take lysate supernatant and neutralize in another set of test tubes as shown below.

3. **Sample Dilution**

Prepare sample/standard in 1:2:1:8 ratio.
1: Sample/Standard (Standard: #AAS18, purchased from Sigma)
2: Saturated Potassium Borate Buffer
1: *0.1N HCl/10% TCA**
8: ddH_2O

**Amino acid standard is made in 0.1 N HCl so add 10% TCA into standards, while samples are harvested with 10% TCA, so add 0.1N HCl into samples*.*

Make sure to have 4 standard curve points (0, 0.25, 0.5, 1.0)
For 0 standard curve point: 1 part: ddH_2O **2 part:** saturated potassium buffer **1 part:** 0.1N TCA **8 part:** ddH_2O
For 0.25 standard curve point: first dilute amino acid standard 1-part amino acid standard, 3-part ddH_2O. Then **1 part:** diluted amino acid standard **2 part:** saturated potassium buffer **1 part:** 0.1N TCA **8 part:** ddH_2O
For 0.5 standard curve point: first dilute amino acid standard 1-part amino acid standard, 1-part ddH_2O. Then **1 part:** diluted amino acid standard **2 part:** saturated potassium buffer **1 part:** 0.1N TCA **8 part:** ddH_2O
For 1.0 standard curve point: 1 part: undiluted amino acid standard **2 part:** saturated potassium buffer **1 part:** 0.1N TCA **8 part:** ddH_2O

Ensure that samples are filtered before ran through the column. They can be filtered using a 0.2 μM 1ml syringe filter (#83.1826.001 from Sarstedt). In the filtering process you lose a lot of sample, so prepare for this (dilute more sample to begin with).

3.0 Protocol Parameters:

Gradient Elution
Flow rate: 0.8 ml/min
Column temp: 35°C
Sample Temp: 4°C
Excitation-Emission: 350-450 nm
Maximum Pressure: 18000 psi
Injection volume: 1 μL
Preferred Column: YMC-Triart 75 mm x 3.0 mm OD x 1.9 μm particle size
Pretreatment: Go to Reagent and add 20μL (this is the OPA that'll be put into sample in each vial – 1*:1 ratio of OPA to sample, so add 20* μL of sample into each vial as well)

4.0 Procedure

1. Turn on all the machines on the HPLC except the UV detector.
2. Turn on the computer and choose the software "lab solutions", go to instruments and pick "HPLC RF", as we are running a fluorescent detection protocol not UV.
3. Next set the gradient as shown in Supplementary Figure 7.

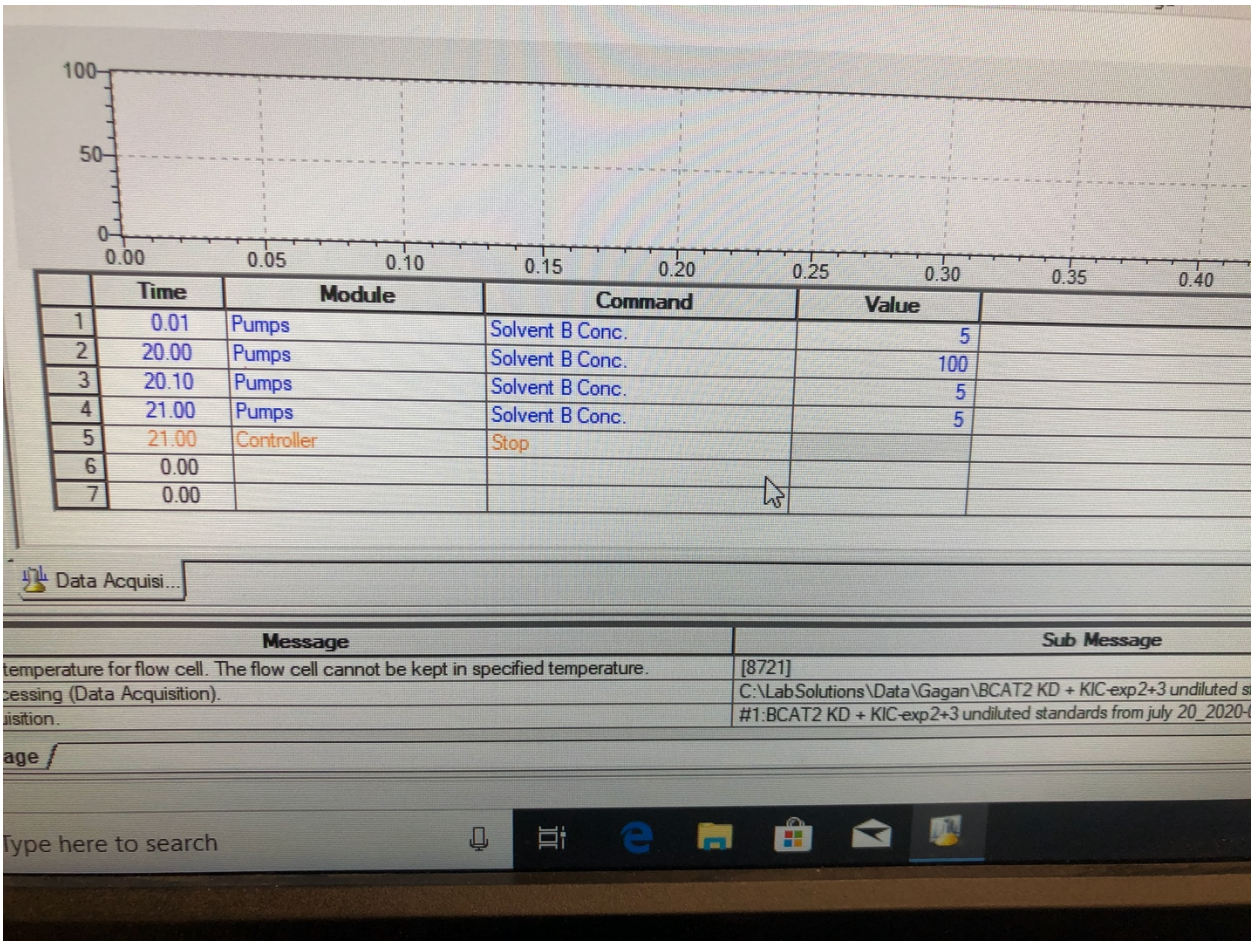

Supplementary Figure 7: Gradient Set up

4. Set the temperature under the "column oven" subheading to 35°C.
5. Next under the "detector A" subheading put 350 for excitation and 450 for emission.
6. Under the "autosampler" subheading, click "pre-treatment" and click on "reagent". Tick the box "Reagent 1" and make the volume 20 µL, then press "apply to pre-treatment program". Also choose the vial number you want to keep the OPA vial in. This will mix the OPA with each sample before it runs through the machine.
7. Next you want to purge the line with your mobile phases (Buffer A + B).
    a. Under the subsection "pump" set solvent B to 100% in the computer, solvent C and D are 0%. Open the pump on the liquid chromatograph machine and press purge on this machine. Lift line B from the solution it was kept in, when you see an air-bubble in the solvent B line you put the line in your desired Buffer B.
    b. Then purge line A. Make solvent B value to 0%, solvent C and D to 0% on the computer (this means A is 100%). Open the pump on the liquid chromatograph machine and press purge, then lift line A from the solution it was kept in, when you see an air-bubble in the solvent A line, put the line in your desired Buffer A.

    c. While the machine is purging your buffers, attach the metal ferrules on both ends of metal tubing that you have. Put one end into place holder connecting the tubing

from the autosampler into the oven. Put the other end into our column (use a wrench and tighten ferrules into column/place holder).

d. Into other end of the column put the plastic ferrule and the red tubing that comes from the fluorescence detector (above the oven) down to the oven.
e. Once column is in place and both lines are purged, put 5% solvent B on the computer, and close the pump on the machine. Then press pump on the machine so it runs through the whole machine and your column now. Once the pressure is stabilized (usually around 6500-7000psi), your samples are ready to load.

8. Put OPA (20 μL per sample and with a bit of safety) into a vial with no insert and put it in the autosampler vial container (put it in the same vial number as chosen in step 6).
9. Put inserts into vials for sample vials.
10. Put in standards and samples (20 μL) into the respective sample vials and insert into vial container. Put this vial container in the autosampler unit, you should hear a click noise if inserted correctly.
11. Then on the computer, go to “data acquisition” on the left side panel and choose “quick batch” and add your samples to the queue.
12. Name your samples by your conditions and ensure the injection volume is set to 1 μL for each sample.
13. Save the data file to the computer to access once the run is done.
14. Now press run.

Appendix H) High Pressure Liquid Chromatography (HPLC) BCKA Protocol

1.0 Materials:

- Column (Intersil ODS-4 100mm x 2.1mmOD x 2um particle size (Gl Sciences, #IN5020-81204)
- Metal Ferrule (IDEX Health & Science, #VHP-321)
- Metal tubing (IDEX Health & Science #U-154)
- Vials and lids (Supelco, #27080-U)
- Vial Inserts (Supelco, #24716)
- 1,2-diamino-4,5-methylenedioxybenzene (DMB) (Sigma Aldrich, #66807) – keep on ice.
    - Sodium sulfite (BioBasic, #7757-83-7)
    - 2-mercaptoethanol (Sigma Aldrich, #M6250)
    - Concentrated HCl (Sigma, Aldrich, 258148-2.5L-GL)
    - Double distilled water
- Micropipette (20-200µL) and tips (yellow: 20-200µL)
- Samples kept on ice
- 0.1N hydrochloric acid (HCl)
- Sodium hydroxide (NaOH)
- Buffer A (made in 1 L glass bottles in lab)
    - HPLC grade methanol (30%) (Fisher Chemical, #A-4524)
    - ddH_2O (70%)
- Buffer B (made in 1 L glass bottles in lab)
    - 100 % HPLC grade methanol (Fisher Chemical, #A-4524)

DMB solution was prepared by adding 1.6 mg of DMB to 1.0 mL of solution, which contained 4.9 mg of sodium sulfite, 70 µL of 2-mercaptethanol, and 58 µL of concentrated HCl in 0.87 mL of double distilled H_2O. This is made in a 15 mL tube that is covered in aluminum foil as it is light sensitive.

Buffer A: 30% methanol/70% ddH20 (v/v)
Buffer B: 100% methanol

2.0 Sample/Standard Preparation:

Sample Neutralization
Prepare sample/standard in 1:2:1:8 ratio.
1: Sample/Standard
2: Saturated Potassium Borate Buffer
1: ddH_2O/*homogenization buffer**
8: ddH_2O

*Sample was tissue homogenized in homogenization buffer, so the standard receives 1 part homogenization buffer, while standard was made in ddH_2O, so sample receives 1 extra part ddH_2O instead of homogenization buffer

Standards are made using KIC (Sigma Aldrich, #K0629), KIV (Sigma Aldrich, #198994), and KMV (Sigma Aldrich, #K7125) salts in the lab.
Dissolved each BCKA with 25mg/ml. Then did a 1:10000 dilution (equivalent to about 19.2uM for KIC and KMV, and 21.53uM for KIV). If not diluted, then the peaks are oversaturated. To create a standard curve, dilute further 2-fold (0.5) and 4-fold (0.25). Just HPLC-grade water is used as the 0 point in the standard curve.

Ensure that samples are filtered before ran through the column. They can be filtered using a 0.2 μM 1 ml syringe filter (#83.1826.001 from sarstedt). In the filtering process you lose a lot of sample, so prepare for this.

3.0 Protocol Parameters:

Gradient elution was performed as follows: 0 min 0% B, 3.33 min 0% B, 5 min 50% B, 17.34 min 50% B (The remaining % is automatically buffer A in the software, for example 50% B is also 50% A, 0% B is 100% A)
Flow rate: 0.2 ml/min
Column Temp: 40^{o}C
Sample Temp: 4^{o}C
Excitation-Emission: 367-446
Maximum Pressure: 18000psi
Injection volume: 5 μL
Preferred Column: Intersil ODS-4 100mm x 2.1mmOD x 2 μm particle size
Pretreatment: 40 μL of DMB solution is added to 40μL of standard/sample and then heated at 85^{o}C for 45 minutes on the heating block in the lab then cooled on ice for at least 5 minutes.

Appendix I) Cell Culture Transfection

RNAi Gene Silencing Materials

- Opti-MEM (Life technologies, #31985070)
- Lipofectamine RNAiMAX reagent (Life technologies, #13778-150)
- siRNA scramble (Sigma Aldrich, #SIC001) and BDK (Sigma Aldrich, #NM019244) or siRNA of choice.
- Differentiation Medium (DM) without antibiotics - AMEM (Wisent Inc., #310-010- CL) supplemented with 2% horse serum (Gibco, 26050-088)
- Differentiation Medium (DM) with antibiotics (AMEM (Wisent Inc. Cat # 310-010-CL) supplemented with 2% horse serum (Gibco, 26050-088) and 1% Ab-Am (Wisent Inc., #450-115-EL))
- 15 ml polypropylene conical tubes (BD Falcon, #372096)
- 6 well plates (Cellstar, #657160) or 12 well plates (Falcon, #353043)

Procedures:

On day 3 of differentiation, L6 myotubes (in 6 well and 12 wells) transfection was carried out below.

1. In the cell culture hood, prepare three 15 ml tubes and label as “A”, “B” and “C”

Test Tube A: Lipofectamine + Opti-MEM

Test Tube B: Scramble siRNA + Opti-MEM

Test Tube C: BDK (or siRNA of choice) siRNA + Opti-MEM

2. Add 118 µL of Opti-MEM and 7 µL of Lipofectamine to tube “A”.
3. Add 3 µL of scramble siRNA and 122 µL of Opti-MEM to tube “B”.
4. Add 3 µL of BDK siRNA and 122 µL of Opti-MEM to tube “C”.
5. Add equal amounts of test tube A to test tube B and C in 1:1 ratio. (For example, 125 µL of test tube A into 125 µl of test tube B and 125 µl of test tube C).
6. Wait at least 5 minutes.
7. While waiting, add 1 mL/well of GM without antibiotics to each well of a 6 well plate (would be 500 µL for a 12 well plate).
8. Add 250 µL/well of test tube B or C into respective wells of 6 well plate (125 µL /well for 12 well plate).
9. Following 24 hours (day 4 of differentiation), add 1 mL/well of GM (with antibiotics) to each well of a 6 well plate (would be 500uL for a 12 well plate).
10. On day 5 of differentiation 6 wells were harvested for immunoblotting and HPLC, and 12 wells were used for glucose transport assay.

Appendix J) Area Under the Curve Analysis

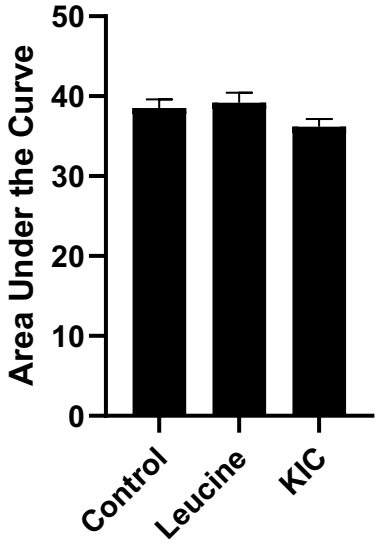

Supplementary Figure 8: Area under the curve for figure 5.2A for only timepoints 0-60min.

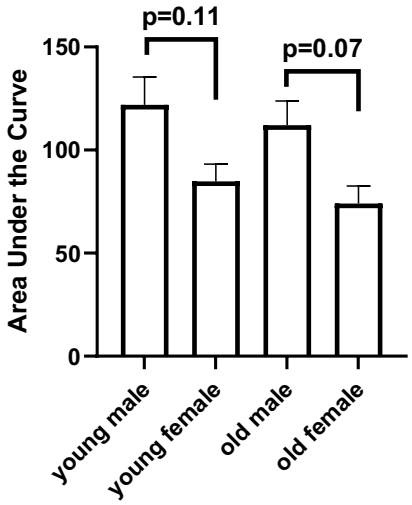

Supplementary Figure 9: Area under the curve for figure 6.1N for only timepoints 0-30min.